FOR REFERENCE ONLY

ProQuest LLC.
789 East Eisenhower Parkway
P.O. Box 1346
Ann Arbor, MI 48106 – 1346

AN INVESTIGATION INTO THE CRITICAL OPERATING PARAMETERS AFFECTING HIGH THROUGHPUT LC ANALYSIS WITHIN THE PHARMACEUTICAL INDUSTRY

By

Julie Woodward

A thesis submitted to the Nottingham Trent University for the degree of Master of Philosophy

This research programme was carried out in collaboration with AstraZeneca R&D Charnwood

September 2003

ABSTRACT

Optimisation of liquid chromatography (LC) and mass spectrometry (MS) parameters has enabled rapid methodologies to be developed which significantly increase sample throughput. Stationary phase characterisation highlighted the importance of selecting a column with minimum acidic silanol content for high efficiencies for the analysis of basic analytes. DryLab optimisation software can be used to accurately predict separations on short, narrow i.d. columns packed with small particles running at high flow rates. The need to select appropriate detector flow cells, optimise response times, and extra column volumes for rapid analysis has been shown. To ensure that the rate limiting step in rapid analysis is not the injection timing, rapid injections, or an overlap injection mode which buries the injection time in the run time of the method can be used.

The sensitivity of an LC/MS analysis can be enhanced by selecting an appropriate buffer and buffer concentration. The choice of organic modifier was shown to have less of an impact on sensitivity although the use of a low viscosity organic solvent gave rise to low column pressures allowing analysis at higher flow rates than would otherwise be used. The electrospray source was shown to exhibit concentration dependent sensitivity whilst the APCI source exhibited mass flow sensitivity. A comparison between APCI and ESI showed little drift in response over a 16 hour run. Using an analogue output from the MSD a single SIM trace was taken from the MSD into a chromatography data system for processing. The analogue output allowed the processing of data for a typical overnight run to be cut from 3 hours to under 30 minutes.

Using the optimised LC and MS parameters rapid LC/MS methods were developed. Using MS as a detection technique allowed the increased speed of analysis compared with UV detection due to complete separation of the analyte from its impurities not being necessary. MS detection can increase the sensitivity of the method by as much as 100 times over that of UV detection which makes it suitable for the analysis of low concentration samples. Combine this with the use of column switching approaches to remove non-volatile materials and LC/MS becomes a very important technique for pharmaceutical analysis.

ACKNOWLEDGEMENTS

I would like to thank my supervisor at AstraZeneca R&D Charnwood, Dr Mel Euerby for his help and guidance with my research.
I would also like to thank my supervisor at Nottingham Trent University, Dr Alan Braithwaite.

CONTENTS

LIST OF ABBREVIATIONS

A2B	Apical to Basolateral
AC	Alternating Current
APCI	Atmospheric Pressure Chemical Ionisation
API	Atmospheric Pressure Ionisation
API-ES	Atmospheric Pressure Electrospray Ionisation
A_s	Assymetry Factor
B2A	Basolateral to Apical
BDS	Base Deactivated Silica
BSA	Bovine Serum Albumin
CDS	Chromatography Data System
CE	Capillary Electrophoresis
DAD	Diode Array Detector
DC	Direct Current
ER	Efflux Ratio
ESI	Electrospray Ionisation
ESI-TOF	Electrospray Ionisation – Time of Flight
FDA	Food and Drug Administration
FFD	Formoterol Fumerate Dihydrate
FIA	Flow Injection Analysis
FT/MS	Fourier Tranformed Mass Spectrometry
HBSS	Hank's Balanced Salt Solution
H_2O	Water
HPLC	High Performance Liquid Chromatography
i.d.	Internal Diameter
LAN	Local Area Network
LC	Liquid Chromatography
LOD	Limit of Detection
LOQ	Limit of Quantification
MeCN	Acetonitrile
MeOH	Methanol
MS	Mass Spectrometry

MSD	Mass Selective Detector
MW	Molecular Weight
$[M+H]^+$	Molecular ion (monomer) analysed in the positive mode
m/z	Mass-to-charge ratio
N	Column Efficiency
N_2	Nitrogen
ODS	Octadecylsilane
Papp	Apparent Permeability
PEEK	Polyetheretherketone
pMDI	Pressurised Metered Dose Inhaler
psig	Pounds per square inch gauge
QA	Quality Assurance
QC	Quality Control
QTOF	Quadrupole Time of Flight
RF	Radio Frequency
RP	Reverse Phase
R_s	Resolution
RSD	Relative Standard Deviation
RT	Retention Time
SIDE	Sprite Information Data Extender
SIM	Selected Ion Monitoring
TFA	Trifluoro-acetic Acid
TOF	Time of Flight
USP	United States Pharmacoepia
UV	Ultra Violet
Vcap	Capillary Voltage
ZDV	Zero Dead Volume

LIST OF FIGURES

LIST OF TABLES

1. INTRODUCTION

The race to speed up the development of new drugs and get them to the market quickly continues to be the focus of the pharmaceutical industry. There is an increased pressure to 'do more with less' – this can be translated into performing more samples per unit time. As a consequence of this there is a need to increase the knowledge base of analysts so that rapid LC/MS methodologies may be implemented in quality control departments. This study will investigate the critical operating parameters affecting high throughput LC/MS analysis within the pharmaceutical industry.

2. AIMS

This project has been split into three phases.

2.1 Phase 1

Initially the investigation will look at the age-old problem of peak tailing of basic analytes on silica based reverse phase columns. A common belief is that residual silanol groups are responsible for this phenomena; however, it is possible that silanol groups *per se* are not the problem. An alternative view is that it is the heterogeneity of the silanol distribution profile that is vital to understanding the problem. What is meant by this is that if you have a homogenous distribution of silanol groups then the "on-off rate" of the analyte onto the stationary phase will be constant so a Gaussian peak would be produced irrespective of the number of silanol groups. In contrast it is possible that a phase may have a small number of a highly heterogeneous population which would yield a highly distorted peak due to different "on-off rates". Preliminary investigations for this research have shown that by producing a chromatographic pH titration using a range of test analytes, the distribution profile of commercially available stationary phases can be studied. The theory to be studied is that given a certain knowledge of the basic analytes pK_a and the database of the chromatographic pH titration of a range of materials, a suitable stationary phase could be chosen which would require minimal

ionic strength to suppress unwanted secondary silanol interactions. The study aims to compare the performance of a range of columns over the pH range 2.7 - 7.6 with the same set of basic compounds which cover a range of pK_a and stereochemistry, to determine whether significant variation in column performance is obtained and to establish if the column rankings are the same over the entire pH range.

2.2 Phase 2

The second phase will involve the optimisation of the LC and MS operational and hardware parameters. For LC this will include the use of computer optimisation software, LC hardware e.g. PEEK tubing dimensions and detector flow cell volumes, column lifetime studies and high throughput autosamplers. For MS ionisation modes, flow rates and mobile phase composition (organic type, ionic strength, pH and counterion types) requirements will have profound influences on the choice of column dimensions and chromatography performed. As the MS and chromatographic conditions are independent on one another the optimisation may be iterative in nature.

2.3 Phase 3

Once phases 1 and 2 have been completed, we will put our knowledge to the test by developing rapid and highly specific and sensitive LC/MS methods for the analysis of a range of structurally diverse analytes from AstraZeneca R&D Charnwood's drug portfolio. This may involve investigating the use of peak focusing large injection volumes of dilute solutions on small i.d. columns and various novel column switching approaches.

3. THEORY

3.1 HPLC

High Performance Liquid Chromatography (HPLC) is a separation technique in which a mixture of analytes are separated based on their affinity for either a moving mobile phase or a stationary phase. The majority of HPLC performed in the pharmaceutical industry uses alkyl C18 stationary phases in reversed phase, where reversed phase chromatography uses a polar mobile phase and a non-polar stationary phase, separating analytes based primarily on differences in hydrophobicity.

3.1.1 HPLC Instrumentation

HPLC instrumentation includes a pump, injector, column, detector and recorder or data system, connected as shown in Figure 1. The heart of the system is the column where separation of the analytes occurs. Since the stationary phase is composed of micrometre size porous particles, a high pressure pump is required to move the mobile phase through the column. The chromatographic process begins by injecting the solute onto the top of the column. Separation of the components occurs as the analytes and mobile phase are pumped through the column. Eventually, each component elutes from the column as a narrow band (or peak) on the recorder. Detection of the eluting components can be either selective or universal, depending upon the detector used. The response of the detector to each component is displayed as a chromatogram on a chart recorder or computer screen. To collect, store and analyze the chromatographic data, computers, integrators, and other data processing equipment are frequently used.

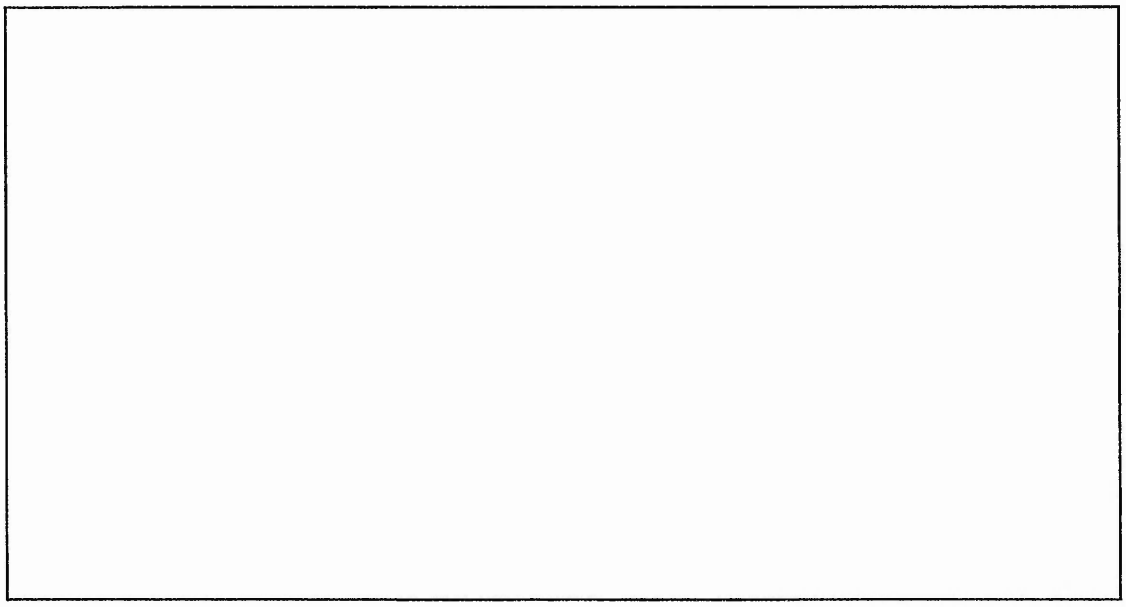

Figure 1. Components of a HPLC system

3.1.1.1 Pumps

High pressure pumps are needed to force the mobile phases through packed stationary phase beds, smaller bed particles requiring higher pressures. Modern pumps have the following parameters:

- Flow rate range: 0.05 to 5 ml/min
- Flow rate precision: greater than 99%
- Maximum pressure: up to 400 bar

It is desirable to have an integrated degassing system, either helium purging, or better vacuum degassing to remove any dissolved gases from the mobile phase. The three common types of pump from Agilent Technologies are isocratic, binary and quaternary. The isocratic pump has a virtually pulse-free and stable solvent flow, with dual floating pistons in series. It is suitable for the analysis of simple mixtures and is the HPLC workhorse for demanding QA/QC laboratories. The binary pump is designed for top performance high-pressure mixing giving reproducible gradients at low flow rates. The binary pump has an optional programmable solvent selection valve which combines two out of four solvents for flexibility. It has low volume capillary connections of 180 - 480 µl internal volume (without mixer), and consists of a dual-piston in series

design. The design of the quaternary pump ensures virtually pulse-free and stable solvent flow, with dual floating pistons in series. It has a high-speed proportioning valve for low-pressure mixing of up to four solvents for isocratic or gradient programming giving great flexibility in solvent choices.

3.1.1.2 Autosamplers

In liquid chromatography, samples are injected into the HPLC via an injection port. The injection port of a HPLC commonly consists of an injection valve and the sample loop. The sample is dissolved in a suitable solvent before injection into the sample loop. The solvent need not be the mobile phase, but often it is chosen to avoid detector interference, column/component interference, loss in efficiency or all of these. The sample is then drawn into a syringe and injected into the loop via the injection valve. A rotation of the valve rotor closes the valve and opens the loop in order to inject the sample into the stream of the mobile phase. Loop volumes can range between 10 µl to over 900 µl. In modern HPLC systems, the sample injection is typically automated. The autosamplers used in this study were the Agilent Technologies standard and well plate autosamplers and the CTC Analytics HTC PAL autosampler.

3.1.1.3 Agilent Technologies standard and well plate autosamplers

The Agilent Technologies standard autosampler has an arm that picks up the sample vial from its position in the sample tray and takes it to the needle for injection. A needle wash can be used which dips the needle in a solvent of choice to wash the exterior surfaces to prevent any carryover. It has a sample capacity of 100 x 2 ml vials and a low internal volume of 300 µl for minimum contribution to the system's total internal volume. With the Agilent Technologies well-plate sampler, the needle moves to the vial to make the injection which speeds up the injection process over the standard autosampler for high sample throughput. It has a sample capacity of 110 x 2 ml vials or two well plates (96 or 384).

The Agilent Technologies standard autosampler and well plate sampler are shown in Figure 2. Both of the Agilent Technologies autosamplers can be used in overlap injection mode which buries the injection time in the run time of the method to reduce cycle times and increase productivity. This is shown in Figure 3. Both autosamplers have a minimal delay volume for rapid gradients and fast equilibration when bypassing the autosampler after injecting the sample onto the column. This is shown in Figure 4.

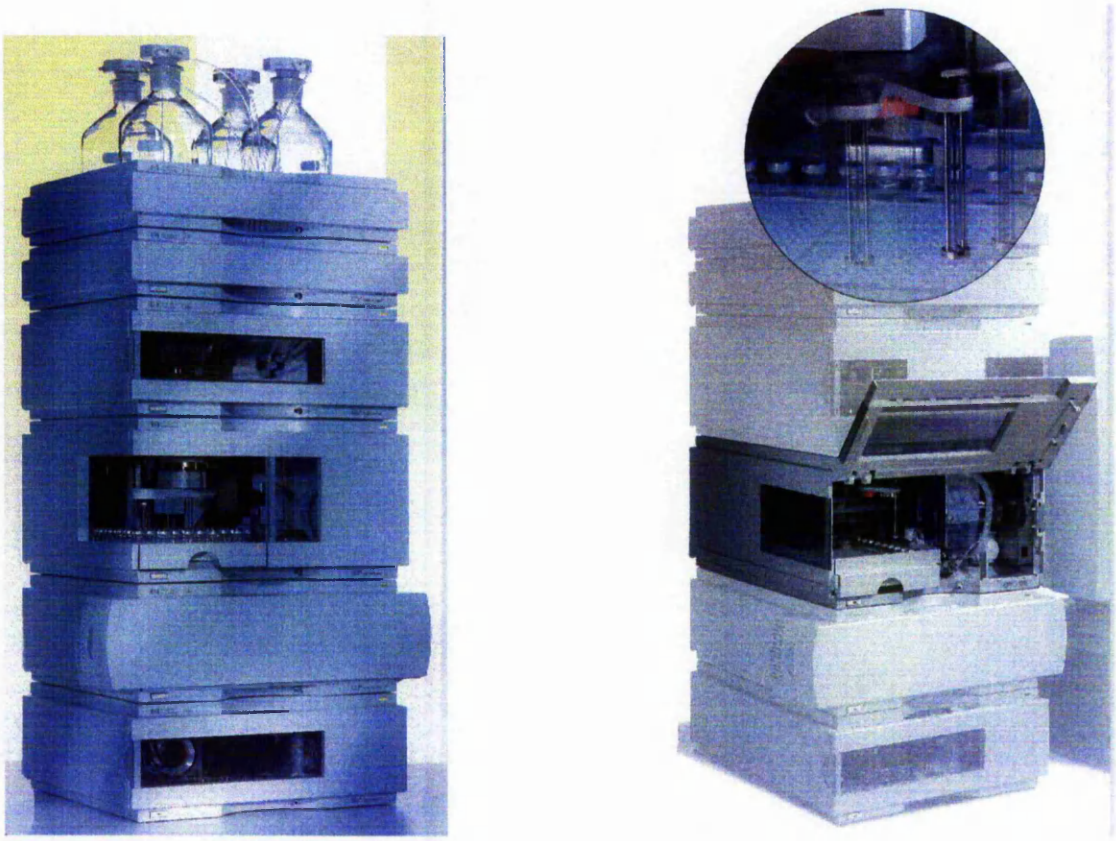

Figure 2. **Agilent Technologies standard and well plate autosamplers**

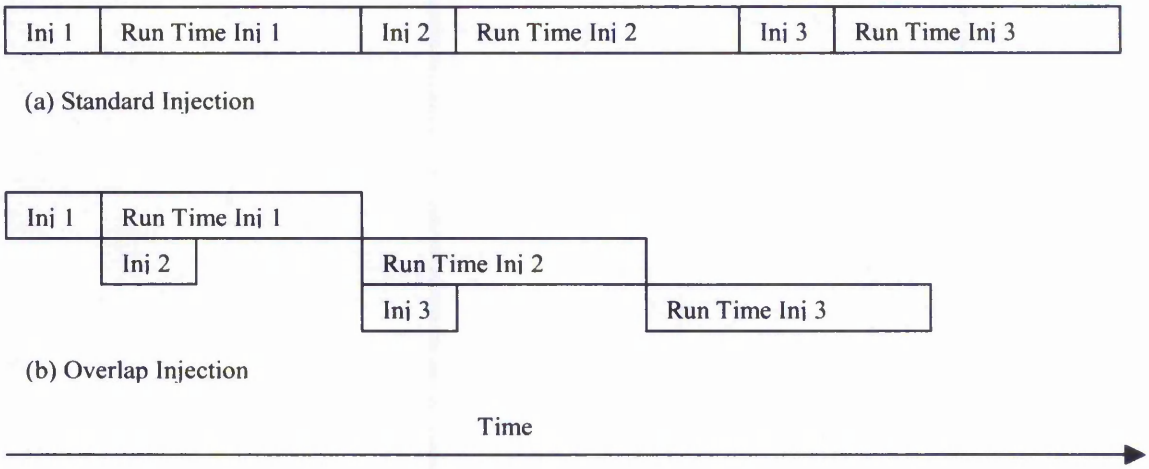

Figure 3. Comparison of overlap and standard injection cycle times

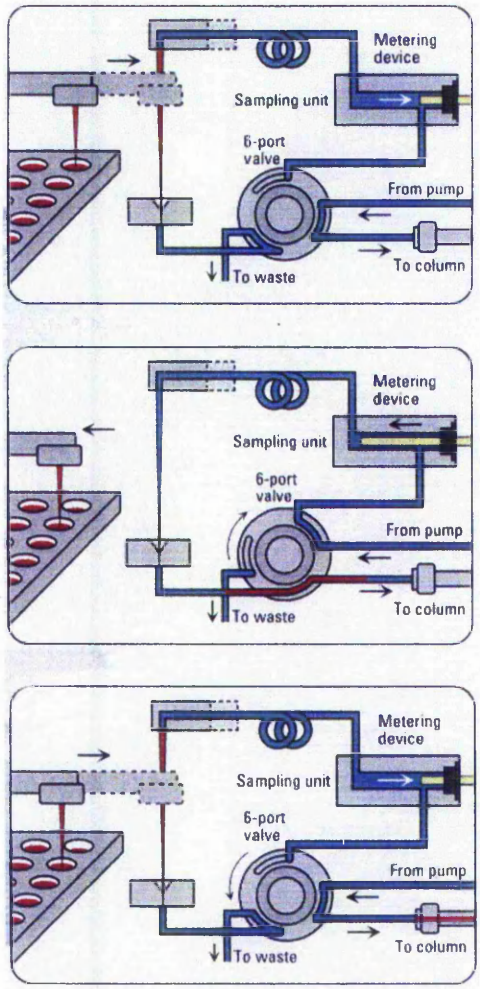

Figure 4. Agilent Technologies autosampler injection flow path

3.1.1.4 CTC Analytics HTC PAL autosampler

The CTC Analytics HTC PAL autosampler was designed for high throughput applications. It has a fast speed of injection due to the use of syringe only technology. Samples are aspirated with a conventional syringe and are transferred directly into the sample loop. It has a high sample capacity, capable of holding up to 324 x 2 ml vials or 576 vials in deep well plates. A wash station allows for needle, syringe and valve washes from two different solvents to prevent carryover. The autosampler can be operated through Chemstation, allowing simple installation on an Agilent Technologies 1100 HPLC system. The CTC Analytics HTC PAL autosampler is shown in Figure 5 with the injection flow path shown in Figure 6.

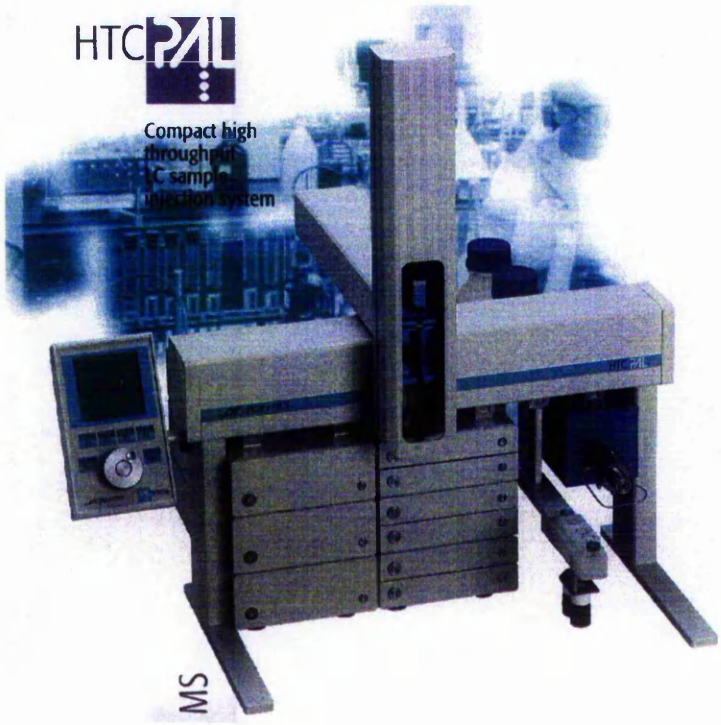

Figure 5. CTC PAL autosampler

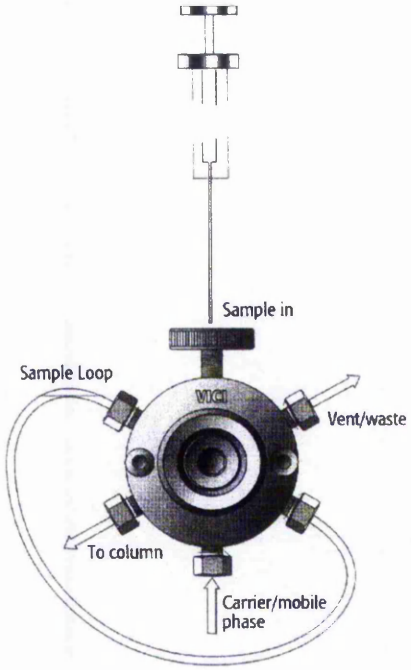

Figure 6. CTC PAL injection flow path

3.1.1.5 Stationary Phases

The stationary phase in HPLC refers to the solid support contained within the column over which the mobile phase continuously flows. The sample solution is injected into the mobile phase of the analysis through the injector port. As the sample solution flows with the mobile phase through the stationary phase, the components of the solution will migrate according to the non-covalent interactions of the compounds with the stationary phase. The chemical interactions of the stationary phase and the sample with the mobile phase, determines the degree of migration and separation of the components contained in the sample. For example, those samples which have stronger interactions with the stationary phase than with the mobile phase will elute from the column less quickly, and thus have a longer retention time. Columns containing various types of stationary phases are commercially available. Some of the more common stationary phases include: liquid-liquid, liquid-solid (adsorption), size exclusion, normal phase, reverse phase, ion exchange, and affinity, the most common being reverse phase columns.

Reverse Phase (RP) operates on the basis of hydrophilicity and lipophilicity. The stationary phase consists of silica based packing with n-alkyl chains covalently bound. For example, C8 signifies an octyl chain and C18 an octadecyl ligand in the matrix. The more hydrophobic the matrix on each ligand, the greater the tendancy of the column to retain hydrophobic moieties. Thus hydrophilic compounds elute more quickly than hydrophobic compounds.

Historically HPLC columns were typically 250 x 4.6 mm i.d. and were packed with 10 µm irregular particles. Today technology has advanced to allow commercially available columns for analytical separations with lengths ranging from 10 to 250 mm and internal diameters of 1.0, 2.1 and 3.0 mm, which are packed with spherical particles of diameters 1.8, 3 or 5 µm. This allows for improvements in peak efficiency, sensitivity and time. In general, LC columns are fairly durable and have a long service life unless they are used in some manner which is intrinsically destructive, for example, with highly acidic or basic eluents, or with continual injections of 'dirty' biological or crude samples.

3.1.1.6 Detectors

The detector for a HPLC is the component that emits a response due to the eluting compound and subsequently signals a peak on the chromatogram. It is positioned immediately after the stationary phase in order to detect the compounds as they elute from the column. There are many types of detectors that can be used. Some of the more common detectors include: Refractive Index (RI), Ultra-Violet (UV), Fluorescent, Radiochemical, Electrochemical, Near-Infra Red (Near-IR), Mass Spectroscopy (MS), Nuclear Magnetic Resonance (NMR), and Light Scattering (LS). Of these detectors UV is the most widely used, accounting for over 80% of all applications [1].

Ultra-Violet (UV) detectors measure the ability of a sample to absorb light. This can be accomplished at one or several wavelengths:

- Fixed Wavelength measures at one wavelength, usually 254 nm
- Variable Wavelength measures at one wavelength at a time, but can detect over a wide range of wavelengths
- Diode Array measures a spectrum of wavelengths simultaneously

A feature of diode array detectors is the ability to perform spectroscopic scanning and precise absorbance readings at a variety of wavelengths while the peak is passing through the flowcell. The diode array can give qualitative information beyond simple identification by retention time.

There are two major advantages of diode array detection. In the first, it allows for the most appropriate wavelength(s) to be selected for the analysis. The second major advantage is related to the problem of peak purity. Often, the peak shape in itself does not reveal that it actually corresponds to two (or even more) components. In such a case, absorbance rationing at several wavelengths can be helpful in deciding whether the peak represents a single compound or, is in fact, a composite peak. A schematic of the diode array detector is shown in Figure 7.

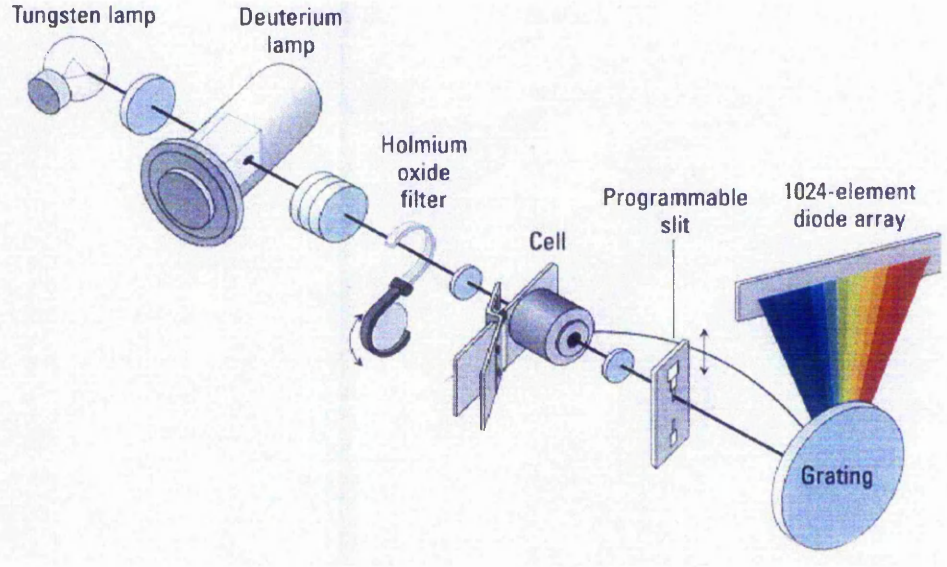

Figure 7. Schematic of the Agilent Technologies diode array detector

One of the limitations of UV detection is that the molecule has to absorb in the UV-Visible wavelength range. This can be a problem if some of the components of the sample do not absorb in this region due to the lack of a chromophore (part of the molecule that produces a particular absorption band in the absorbance spectrum). To overcome this problem an orthogonal detection method such as mass spectrometry can be used.

3.1.1.7 Chromatography Data Systems

Since the detector signal is electronic, use of modern data acquisition techniques can aid in the signal analysis. In addition, some systems can store data in a retrievable form for sophisticated data processing at a later time. The main goal in using electronic data systems is to increase analysis accuracy and precision, while reducing operator attention. The electronic storage of data aids compliance with Good Laboratory Practice and Good Manufacturing Practice controls. There are several types of data systems, each differing in terms of available features. In routine analysis, where no automation (in terms of data management or process control) is needed, a pre-programmed computing integrator may be sufficient. If higher control levels are desired, a more intelligent device is necessary, such as a data station or computer. The advantages of intelligent processors in chromatographs are found in several areas. First, additional automation options become easier to implement. Secondly, complex data analysis becomes more feasible. These analysis options include such features as run parameter optimisation and deconvolution (i.e. resolution) of overlapping peaks.

3.1.2 Resolution Equation

The factors influencing resolution are given in the equation below:

$$R_s = \underbrace{\left(\frac{1}{4}\right)N^{0.5}}_{\text{(efficiency)}} \quad \underbrace{\left(\frac{\alpha-1}{\alpha}\right)}_{\text{(selectivity factor)}} \quad \underbrace{\left(\frac{k}{1+k}\right)}_{\text{(retention factor)}}$$

where α is measure of selectivity of the solute, k is the rate of movement of the solutes through the column and N is the column efficiency.

Hence increasing N, α or k will give better resolution. However, because resolution is a function of the square root of N, relatively large increases in N are required to make small improvements in resolution. For example a two fold increase in N gives a 1.44 fold increase in resolution. The easiest way to increase resolution is to increase k. This can be achieved by decreasing the organic content in the mobile phase. For small molecules, a 10% reduction in organic content will increase k three fold. This relationship is called the 'rule of three' [2]. Decreasing the organic content has the disadvantage of increasing the retention time of the last peak in the separation and hence the run time of the method. Where k is large, increasing k further will have little effect on the resolution. Increasing k can give rise to increased band broadening and so limits its use in increasing resolution. Small changes in selectivity can have a large effect on resolution. Selectivity is changed by altering the mobile phase composition (type of organic and pH) and the type of stationary phase.

3.1.3 Rapid Analysis

Reducing analysis times has become a major importance in pharmaceutical analysis with the need to perform more samples per unit time. There are a number of ways this can be achieved including increasing the flow rate, reducing the gradient time and reducing the column length. Each of the options has its own limitations including high pressures, loss of resolution and loss of efficiency. These limitations can be overcome by using short columns with a small particle size, fast gradients and fast linear velocities which gives rise to an increase in peak capacity, which is a measure of separation power for gradient analyses [3, 4]. The use of short columns gives rise to faster method development times, faster routine analysis times, lower sample and solvent consumption and faster re-equilibration times. With rapid analysis there is often a compromise between analysis time, peak capacity and resolution.

Peak capacity defines the resolving power of a column and is the theoretical number of peaks that can be baseline resolved for a given separation [5]. Limited peak capacity

can result in poor resolution between peaks, or unresolved peaks which can not be detected by UV detection.

Peak capacity (P) is defined as the theoretical number of peaks with a peak width (w) that can be separated in a given gradient duration time (t_g):

Equation 1. $$P = 1 + \frac{t_g}{w}$$

The peak width (w) is a function of the plate count (N) and the retention factor (k_e) at the point of elution.

Equation 2. $$w = 4 \cdot \frac{t_0 \cdot (k_e + 1)}{\sqrt{N}}$$

Substitute Equation 2 for the peak width (w) in Equation 1 gives the following equation:

Equation 3. $$P = 1 + \frac{\sqrt{N}}{4} \cdot \frac{t_g}{t_0} \cdot \frac{1}{k_e + 1}$$

Using the theory of reversed phase gradient chromatography to calculate the retention factor (k_e) at elution results in:

Equation 4. $$k_e = \frac{t_g}{B \cdot \Delta c \cdot t_0}$$

Equation 4 assumes that the analyte is well retained at the start of the gradient. The retention factor at elution (k_e) depends on the compound specific parameter B, which is the slope of a plot of log retention factor versus % organic, (Δc), the difference in solvent composition between the start and end of the gradient and the gradient time (t_g). The most important point for the speed of analysis is the ratio of gradient time (t_g) to the time for an unretained peak (t_0). Substituting Equation 4 into Equation 3 gives the following:

Equation 5. $$P=1+\frac{\sqrt{N}}{4}\cdot\frac{B\cdot\Delta c}{B\cdot\Delta c\frac{t_0}{t_g}+1}$$

The peak capacity (P) depends primarily on the difference in solvent composition (Δc), and the ratio of gradient time (t_g) to the time for an unretained peak (t_0). The peak capacity increases as the gradient time (t_g) increases. The van Deemter equation is shown in Equation 6.

Equation 6. $$h=A+\frac{B}{\mu}+C\cdot\mu$$

where $h=\frac{L}{N}$

The A term represents eddy diffusion and is a characteristic of the column packing. The B term represents longitudinal diffusion of sample components in the mobile phase and C is the mass transfer term is influenced by the partition coefficient and solubility of the sample in the mobile phase and is dependent on flow rate. Substituting the van Deemter equation into Equation 5 shows that peak capacity depends not only on the parameters above but also the column length (L) and the particle size (d_p) as shown in Equation 7.

Equation 7. $$P=1+\frac{\sqrt{\frac{L}{a\cdot d_p+b\cdot D_M\cdot\frac{t_0}{L}+\frac{d_p^{\,2}}{c\cdot D_M}\cdot\frac{L}{t_0}}}}{4}\cdot\frac{B\cdot\Delta c}{B\cdot\Delta c\cdot\frac{t_0}{t_g}+1}$$

3.1.4 Narrow-bore Chromatography

In recent years there has been a growing interest in columns with a reduced internal diameter, reduced length and are packed with smaller particles. Narrow-bore technology employs columns with an internal diameter of typically 3 mm or less, but greater than micro-bore (1 mm and below). Narrow-bore HPLC has many advantages

over standard-bore HPLC, such as reduced solvent consumption, reduced stationary phase consumption, increased sensitivity and increased peak height and peak area [6, 7]. Narrow-bore columns are compatible with most modern HPLC systems, although they often perform poorly due to extra-column volume, as this results in peak dispersion. To obtain the best performance from narrow-bore columns, the HPLC system must be optimised by reducing the amount of extra column volume.

3.1.4.1 Advantages of using narrow-bore columns

The major advantage of using narrow-bore columns is an increase in sensitivity. When the internal diameter of the column is reduced, the dilution of the analyte in the column is lowered resulting in an increased sensitivity of detection [8]. The height of the analyte peak is larger when using narrow-bore columns. This is related to the UV detector signal being proportional to the concentration of the analyte in the flow cell. As the band elutes, the concentration changes, giving rise to the peak shape. The apex of the peak corresponds to the maximum concentration, and as components eluting from a narrow-bore column are more concentrated, the maximum concentration is greater resulting in a larger peak height.

This is useful for trace analysis as it enhances minimum detectable mass. Narrow-bore columns are 4 to 6 times more sensitive than standard-bore columns when using the same injection volume. This increase in sensitivity is important where samples are from a limited source e.g. biological samples, as the increase in detection signal means samples can be prepared from less material or a smaller injection volume can be used to give the same response.

The reduction in injection volume required to give the same peak height for a change in the column internal diameter is given by the equation below:

$$\frac{(\text{i.d. of column 2})^2}{(\text{i.d. of column 1})^2} \times \text{Injection volume on column 1} = \text{Injection volume on column 2}$$

For example, if you change from using a 4.6 mm i.d. column with a 100 µl injection volume, to a 2.1 mm i.d. column, you can reduce the injection volume by 80% whilst maintaining the same peak height.

i.e. $\frac{(2.1\ mm)^2}{(4.6\ mm)^2} \times 100\ \mu l = 20\ \mu l$

Another advantage of using narrow-bore columns is the reduction in mobile phase consumption and reduced waste. As the cost of solvents can be expensive, and with more demanding disposal procedures for hazardous waste, this had led to higher disposal costs and an increased pressure to avoid the generation of such waste. As solvent consumption is directly related to column flow rate, to maintain the same linear velocities (and therefore retention times) a lower flow rate must be applied, reducing solvent consumption. The reduction in flow rate makes narrow-bore chromatography more convenient for direct coupling with mass spectrometry.

The equation below is used to calculate the flow rate required to maintain the same relative separation for a change in the column internal diameter:

$$\frac{(\text{i.d. of column 2})^2}{(\text{i.d. of column 1})^2} \times \text{Flow rate of column 1} = \text{Flow rate of column 2}$$

For example, if you change from using a 4.6 mm i.d. column at 1 ml/min, to a 2.1 mm i.d. column you can reduce the flow rate by 80% whilst maintaining the same linear velocity.

i.e. $\frac{(2.1\ mm)^2}{(4.6\ mm)^2} \times 1\ ml/min = 0.2\ ml/min$

A final advantage is a reduction in the amount of stationary phase material required to pack the column due to the reduced column volume. This should give rise to reduction in the cost of purchasing the column, therefore facilitating the use of valuable and expensive packing materials or the use of longer columns. However, in practice it is often harder to pack narrow-bore columns which can increase the purchase cost.

3.1.4.2 Disadvantages of narrow-bore columns

Narrow-bore columns often perform poorly in typical HPLC systems due to extra column dispersion. This is an effect of the extra column volume in the HPLC system between and including the injector and the detector, but not including the column volume, i.e. sample volume, connecting tubing volume, fitting volume and detector cell volume. Sources of extra column volume include long lengths of tubing or large diameter tubing. This can create sufficient system volume resulting in peak broadening, which can give rise to a significant loss in resolution. An increase in extra column volume dramatically decreases column efficiency for narrow-bore columns.

The HPLC system must be optimised to minimise extra column volume to maintain the best chromatographic performance. This can be achieved by ensuring connecting tubing is as short as possible between the injector and the column and the column and the detector, and that this connecting tubing has an internal diameter of ideally no more than 0.1 mm. Only low dead volume fittings should be used. It is also necessary to use a low volume detector flow cell (preferably 2 µl or less) to maintain detector sensitivity with the narrow sample bandwidths that the smaller internal diameter columns produce. Column efficiency should not be deteriorated during the detection process. The design of the detector flow cell can be just as important as the cell volume.

An optimum flow cell for narrow bore chromatography has a low extra column volume. To increase sensitivity the path length needs to be large which in turn leads to a small cell diameter. A small cell diameter limits the intensity of light through the cell, which gives rise to an increase in noise and hence reduces the sensitivity. Therefore the optimum flow cell dimensions are a compromise between minimising the contribution to peak dispersion and maximising sensitivity. Low volume flow cells manufactured by Agilent Technologies have a volume of 1.7 µl and a reduced path length of 6 mm (compared to the standard flow cell of 13 µl volume and 10 mm path length). These are found to be a compromise between sensitivity and efficiency, as a 6 mm path length only gives 60% of the response obtained for 10 mm path length, but gives improved efficiency due to its low volume.

A HPLC system that is affected by extra column volume will show a significant reduction in the number of theoretical plates than that reported by the column manufacturer. Early eluting peaks in an isocratic separation are more susceptible to extra column dispersion than later eluting peaks due to having a lower peak volume. The smaller the peak volume the more likely the peak will broaden due to extra column volume.

Narrow-bore HPLC can be applied to any analytical method (isocratic and gradient) performed by the equivalent standard bore column assuming the HPLC systems performance is comparable.

Ye *et al* [9] compared the column performance of narrow-bore (2.1 mm i.d.) and standard bore (4.6 mm i.d.) columns for the determination of alpha-, beta-, gamma- and delta-tocopherol. HPLC equipment with minimum extra column volume was used with analytical silica columns of identical length. The narrow bore column gave a seven fold increase in sensitivity compared to the standard bore column at equivalent running times for the analytes. With the narrow bore column one third solvent savings were achieved.

3.1.5 Stationary Phase Characterisation

The analysis of basic pharmaceuticals can be problematic and lead to severe peak tailing, low efficiencies and changes in separation as the column ages. These problems can be more pronounced with one column than another and can vary with the structure of the analyte. This can be attributed to ionic interactions of basic pharmaceuticals with residual silanols and other active sites of the stationary phase [10, 11]. The ionic interactions comprise of a number of stationary phase-solute interactions including ion-ion (ion exchange), ion-dipole, dipole-dipole (e.g. hydrogen bonding), dipole-induced dipole and induced dipole-induced dipole and shows the importance of selecting an appropriate column for the analyte under test. Developments in manufacturing of stationary phases have led to a large number of commercially available phases with differences in peak shape and selectivity which has made it increasingly difficult to ensure that the optimum column has been selected for a particular application.

Examples of the different phases available are high purity silica, end-capped, polymer encapsulated, polar embedded and bidentate phases.

Numerous attempts have been made to classify and characterise reverse phase HPLC columns [12-19]. These use a variety of tests including the following [12]:

Hydrophobicity (K_{BB}): A measure of the retentivity of a phase based upon hydrophobic interactions with a neutral analyte, determined from the k-value of butylbenzene or amylbenzene

Selectivity (α_{CH2}): The ability of a compound to distinguish between two compounds based upon a single methylene (-CH_2-) unit substitution, determined by injecting a series of alkylbenzene homologues e.g. amylbenzene and butylbenzene. The slope of a log k versus number of methylene units gives the methylene selectivity value.

Hydrogen bonding capacity ($\alpha_{C/P}$): A measure of the amount of accessible hydrogen bonding sites (from silanol groups) on the silica surface after bonding and is determined from the selectivity (α) between caffeine and phenol.

Ion-exchange capacity at pH 2.5 ($\alpha_{B/P\ pH\ 2.5}$): The extent of silanophilic interactions with basic analytes under conditions in which the majority of the residual silanol groups are protonated, determined from the selectivity of benzylamine and phenol using a pH 2.5 mobile phase.

Ion-exchange capacity at pH 7 ($\alpha_{B/P\ pH\ 7}$): The total ion-exchange capacity under conditions in which a large proportion of residual silanols are deprotonated and ionised, determined from the selectivity of benzylamine and phenol using a pH 7 mobile phase.

Layne [12] used the above tests to compare the behaviour of conventional C18, polar-embedded and polar endcapped phases. Polar endcapped phases showed similar hydrophobic retention characteristics as conventional C18 columns but had higher hydrogen bonding capacities and silanol activity. The polar embedded phases displayed the opposite behaviour with reduced hydrophobic nature and reduced silanol activity.

Euerby *et al* [13] used the stationary phase characterisation tests to compare 135 commercially available alkyl, cyano, phenyl, perfluorinated, polar embedded, polar endcapped, aqua and novel phases. Principle component analysis was used to provide a simple graphical comparison of the differences/similarities between the columns. This enabled the identification of equivalent phases, determination of columns of widely differing characteristics to exploit selectivity differences in method development, the rational selection of suitable stationary phases and provided a greater understanding of retention mechanisms and bonding chemistries used by the column manufacturers.

McCalley [14, 15] compared the performance of eight different silica based columns with a variety of basic test probes using mobile phases buffered at pH 3.0 and at pH 7.0. Considerable differences in column performance (measured by column efficiency and asymmetry factor) were observed at pH 7.0 but were less apparent at pH 3.0, which led to a difference in column ranking at the two pH values studied, and emphasises the need to perform column evaluations at the pH of intended use.

3.1.6 Column Switching

The use of column switching in HPLC allows the separation of the analyte from any endogenous material present in the sample. A column switching system consists of a switching valve and a pre-concentration cartridge and is shown in Figure 8.

Following injection in the load position, pump A which delivers the weak organic solution, loads the sample on the clean-up column. The solvent front from the clean-up column which contains the majority of the endogenous components of the sample is directed to waste. This prevents fouling of the mass spectrometer when used as a detector. A second pump, pump B delivers the mobile phase using a gradient through the analytical column and into the detector. At this time the valve is switched back to the inject position and the analytes are backflushed on to the analytical column for separation and detection. The valve is then switched back to the load position for equilibrium of the clean-up column and preparation for the next sample.

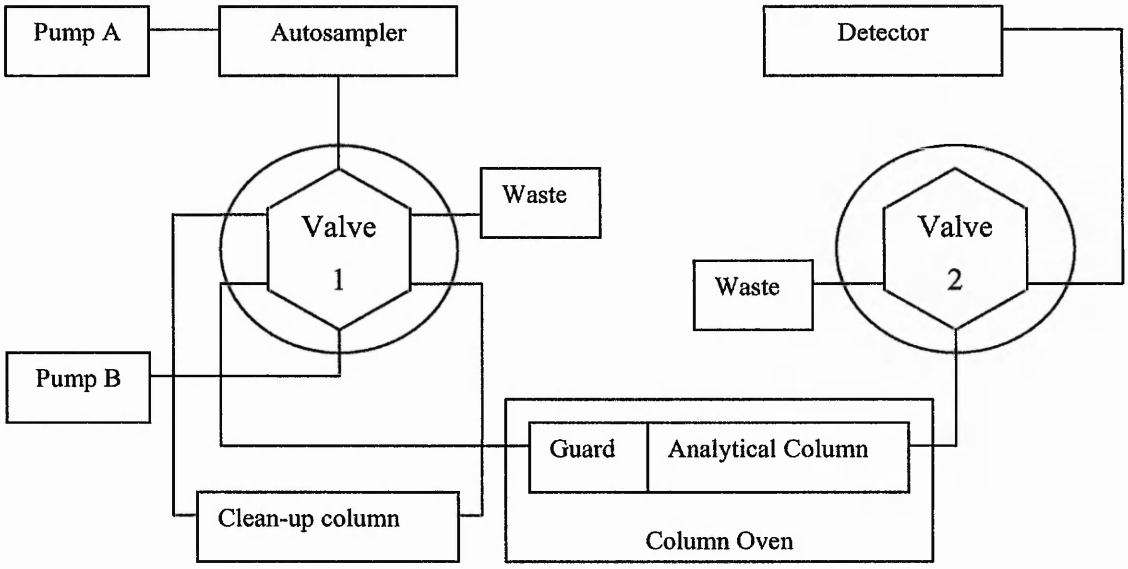

Figure 8. Column switching HPLC system

The column switching method can also be used to minimise any sample carryover by using parallel processing.

The column switching approach for separation with short columns allows the use of rapid gradients with short equilibrium times thus increasing sample throughput. Using narrow bore columns will allow analyses to be performed at lower flow rates, thus avoiding splitting of the LC eluent into the mass spectrometer. However, the disadvantage of using low flow rates is the increase in cycle times.

This approach to separation was performed by Gao *et al* [20] for high throughput preclinical pharmacokinetic studies. They showed that the method was suitable for the determination of multiple compounds in dog and rat plasma. The analytes were ionised using the Sciex TurboIon Spray ionisation source in a positive mode, and detected by multiple reaction monitoring. Using a column switching system allowed the separation of multiple analytes in just 4 minutes. Calibration curves were linear over the range 0.5 to 1000 ng/ml with the accuracy of QC samples in rat plasma estimated to be 95.4 to 109%. The method was found to be fast, precise, accurate and rugged, and suitable for the routine bioanalysis of drugs and metabolites.

Motoyama *et al* [21] used column switching in the determination of bisphenol A (BPA) and nonylphenol (NP) in river water, by liquid chromatography with electrospray mass spectrometry detection. BPA is widely used in the manufacture of plastics and NP is a biodegrative product of alkylphenol ethoxylates which are used as non-ionic detergents. Guidelines for limiting the level of these chemicals in the environment have been introduced. A sensitive analytical method was developed using a Capcellpak MF-PH 10 x 2 mm precolumn for sample cleanup and enrichment with a Capcellpak C18 150 x 1.5 mm analytical column. The method was capable of concentrating sample solutions which allowed the direct handling of dilute solutions. A reduced flow rate of 100 µl/min was optimised for the narrow bore column. The method produced detection limits of 0.5 ng/ml for BPA and 10 ng/ml for NP, with a RSD ranging from 2.2 – 9.7%. The role of the column switching process in this method was to concentrate the analytes of interest, and to remove polar substances which are undesirable for the mass spectrometer.

Schmeer *et al* [22] demonstrated a rapid pharmacokinetic screen for salbutamol in plasma by column switching high performance chromatography-electrospray mass spectrometry. Requiring a sensitive and selective assay for pharmacokinetic studies an assay was developed with pre-column enrichment using internal standard calibration. The column switching approach required only minimum efforts for sample preparation whilst showing a low quantification limit of 0.2 ng/ml. Accuracy and imprecision were found to be less than 7%. Carryover was investigated and found to be less than 0.61%.

Column switching has also been employed with fluorescence detection. Iwata *et al* [23] showed that it could be used to overcome tedious and often poorly reproducible solid phase extraction for estriol metabolites in biological fluids whilst maintaining sensitivity and reliability.

Column switching does not have to be performed with only two columns as in the above examples. Jeong *et al* [24] demonstrated the use of a triple column approach with microbore chromatography. The use of a micro-column with an internal diameter of 1.5 mm had the advantage of being able to use smaller plasma volumes with increased sensitivity, high column efficiency and lower solvent consumption. The intermediate

column in the triple column system was used to protect the main column and save analysis time by reducing the time taken to transfer the sample from the pre-column to the analytical column. It also protected the pre-column from high pressure. The disadvantage of this system was that the precolumn required replacing after 40 injections of plasma samples. Triple column systems have been used without showing any loss in sensitivity increase and chromatographic efficiency obtained by using micro-columns [25].

An alternative use for column switching is for the selection of an optimum column for a particular separation. Using a column oven which can connect typically six columns in parallel, this process of column screening can be performed in one automated sequence. Another approach is the Sepiatec Sepmatrix system [26] which can perform up to eight HPLC runs at the same time. The flow control provides constant flow to eight separate columns with parallel injections into a multiplex eight channel diode array detector allowing for high throughput analysis of up to 900 unattended runs. The advantages of the system are that it has the same output as eight separate HPLCs with a 30% reduction in cost and an 80% reduction in space. The Sepiatec Sepmatrix system with flow diagram outlining the main constituents of the system are shown in Figure 9.

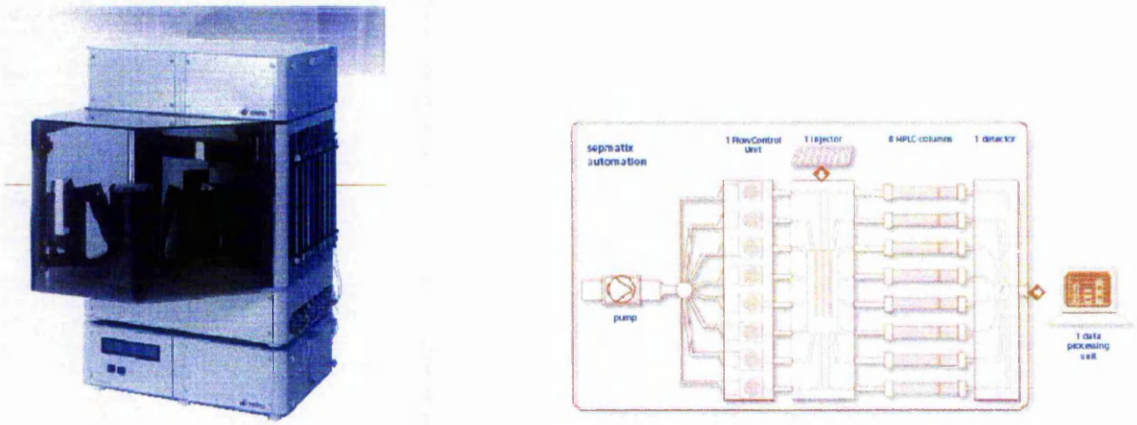

Figure 9. **Sepiatec Sepmatrix system with flow diagram**

3.1.7 Flow Injection Analysis

Flow Injection Analysis (FIA) is a technique that uses the HPLC to inject a sample into the HPLC system towards the detector by the pump without any separation taking place. Instead of using a stationary phase column to separate out the sample components a Zero Dead Volume (ZDV) connector can be used. The ZDV can be made of PEEK or stainless steel and contains no stationary phase packing material. As no separation is taking place the analysis time is greatly reduced. This technique works best with single component samples where separation is not required, or where the resolving power of the detector will be used to separate out components of the sample. It can be used in LC/MS to rapidly optimise the mass spectrometry conditions for a particular analyte. However, its use in LC/MS analysis may be limited due to the need to retain the analyte from the solvent front to avoid signal suppression effects during the ionisation/volatilisation process.

Chong *et al* [27] used flow injection analysis as a process control in the synthesis of an LTD_4 antagonist. In a key step of the synthesis, a prochiral diester intermediate undergoes an enantioselective enzymatic hydrolysis (in the presence of the surfactant Triton X-100). Analytical methods using flow injection analysis were developed for the determination of enzymatic activity and for the determination of Triton X-100. The method for enzymatic activity showed comparable results to those of batch experiments. The method for the determination of Triton X-100 provided rapid and accurate results with good correlation with standard addition and calibration curve methods.

Flow injection analysis with UV detection was used by Altiokka *et al* [28] for the determination of doxazosin mesylate in pharmaceutical preparations. The developed FIA method had an RSD of 1.16% at the LOQ. The results showed a good agreement with those obtained by UV spectrophotometry.

Aboul-Enein *et al* [29] developed and validated a flow injection analysis method with UV detection for the determination of ketoprofen in tablets. The developed method was simple, selective, fast and had been optimised to give sensitive and reproducible results with recoveries of 102.75% for peak area and 98.42% for peak height.

3.1.8 DryLab

3.1.8.1 Overview

The development of a rugged HPLC method requires the selection of experimental conditions for adequate separation, e.g. baseline resolution of all peaks or resolution > 1.5. The following factors are also important:

1. Reasonable run time
2. Acceptable operating pressures
3. Minimum peak volume for maximum signal-to-noise ratio
4. Rugged method, insensitive to minor changes in separation conditions
5. Minimum time and effort spent on method development

The importance of these criteria is dependant on the intended use of the method. The need for efficient HPLC method development has led to a number a computer optimisation programmes, e.g. HIPAC (no longer commercially available), DryLab and ACD LC Simulator.

The use of computer simulation is summarised as follows:
Rank the various separation variables that affect retention and resolution, e.g. mobile phase solvent type and concentration, mobile phase pH, concentration and type of mobile phase additives, stationary phase. Perform a small number (two or three) of experimental runs in which only one mobile phase variable is changed. The data are entered into the optimisation program and simulations with a computer are made giving simulated chromatograms and tabulated data. The best separation based on the simulation is selected and confirmed in the laboratory. For further improvements in the separation, perform additional experiments for a new separation variable and repeat the computer simulation.

The procedure is continued until adequate separation is achieved, with the possibility of simulating and studying a number of variables. Computer simulation emphasises those experimental variables that have a large effect on retention and resolution. It also allows simulation of column parameters e.g. dimensions, particle size and flow rate

without any further experimental data. The column plate number can be optimised to give a good compromise among different separation goals such as resolution, run time, pressure and peak volume.

3.1.8.2 Theory

Computer simulation (DryLab, LC Resources, Lafayette, CA, USA) is based on simple theory for the following relationships:

dependence of retention on mobile phase composition
dependence of column plate number on experimental conditions
interrelationship of isocratic and gradient retention
predictability of gradient retention as a function of gradient conditions.

There is no precise theory that allows absolute predictions of HPLC retention as a function in the change in mobile phase. Numerous studies have established that the following relationship [30]

$$\log k = \log k_w - S\varphi$$

is relatively accurate for the variation of strong solvent concentration (%B or φ) in reversed phase separations. k refers to the retention factor of the solute, φ is the volume fraction or organic solvent in the mobile phase and k_w and S are constants that are characteristic of the solvent and solute.

This can be generalised in the form $\log k = A - Bx$

where x is any of the common variables used to adjust retention, e.g. temperature, pH, additive or fraction of one mobile phase in a mixture of two mobile phases. This equation assumes that log k varies linearly with x as shown in Figure 10 for a homologous series differing by CH_2 units. Where the analytes have different physicochemical properties the slopes obtained for plots of log k versus % organic can be very different as shown in Figure 11.

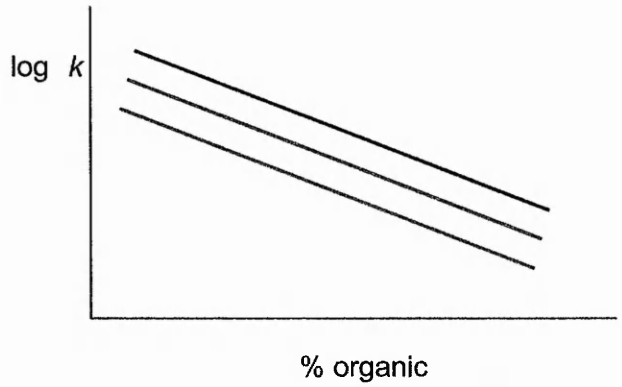

Figure 10. **Plot of log *k* versus % organic for a homologous series differing by CH_2 units**

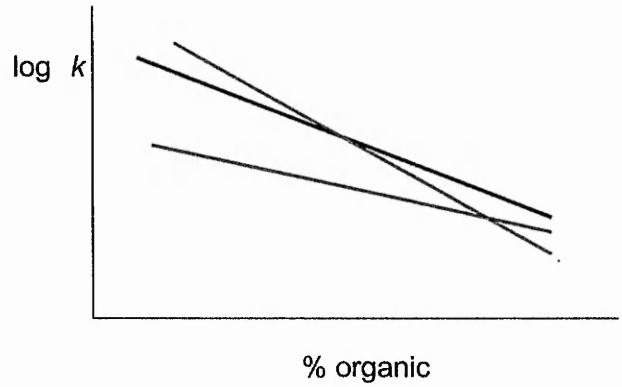

Figure 11. **Plot of log *k* versus % organic for analytes of different physicochemical properties**

DryLab can be used to aid the development of isocratic [31, 32] and gradient [33, 34] HPLC methods. To determine the gradient profile required to separate a mixture of components in a sample, two linear gradient runs 5 – 100 %B are performed with a run time of a factor of three difference, e.g. 20 and 60 minutes. The data are imported into DryLab and computer simulation performed to study how separation varies with the percentage of organic solvent in the mobile phase (%B). A resolution map can be displayed which shows a plot of resolution R_s for the poorest peak separation versus %B. The map allows the chromatographer to select the required %B for optimum separation of the critical pair or to edit a gradient profile and view the simulated

chromatograms. The mobile phase that gives maximum resolution is not always the best choice. A suitable retention time (e.g. $1 < k < 20$) and method ruggedness are equally important considerations. Small changes in mobile phase composition should not give rise to large changes in retention time or separation.

Dolan *et al* [33] found that for a broad range of samples, retention times can generally be predicted to an accuracy of ± 1-3% and resolution is predictable to ± 5 - 10%.

3.1.8.3 Advantages

Many hours of analyst and instrument time and solvents can be saved through the use of computer simulation. The optimised method usually gives a much better separation than would otherwise be achieved. Computer simulation has the ability to use changes in column conditions to improve the separation further or speed up analysis after retention optimisation has been performed. The use of DryLab enables HPLC methods to be easily transferred between instruments or laboratories by allowing for changes in dwell volumes and extra column band broadening.

3.1.8.4 Limitations

The major sources of error in computer simulation [34] are due to:

1. Equipment
2. Column processes
3. Change in column
4. Errors in interpreting the chromatogram
5. Non-linear plots of log k versus %B
6. Human error

Problems can arise from gradient or pumping errors, inaccurately measured dwell volumes or excessive rounding of the gradient due to dispersion effects. Errors can be caused by demixing of the mobile phase within the column. Loss of bonded phase or column deactivation during use (especially at high or low pH) can give rise to changes

in retention. This can be overcome by performing all computer simulated runs within a short space of time.

A major problem with computer assisted method development procedures is the necessity to match peaks between the two runs. It is usually possible to track peaks by comparison of peak area. However, it is possible that peaks of similar size may switch places in the chromatogram from one run to the next without being noticed. In this situation performing a third intermediate run and comparing the predicted with the actual chromatogram is usually sufficient. Overlapping peaks can cause errors in measured retention times. Non-linear retention plots of log k versus %B can lead to errors in predicted retention. One of the largest sources of error is often due to errors in mobile phase preparation. Inaccurate measuring of solvent volumes can give rise to very different separations than those predicted.

3.1.8.5 Applications

Wristley [35] has demonstrated the use of DryLab in the development of gradient and isocratic HPLC methods for the analysis of drug compounds and synthetic intermediates. DryLab was shown to be effective in method development and optimisation of gradient purity methods for two drug substances (Zalospirone and WY-47 384) and two synthetic intermediates (2-methylcarboxybenzaldehyde and cyclooctatetraene). It was also shown to be accurate in predicting isocratic retention for the separation of impurities in cyclooctatetraene, both in scaling down to small columns for fast analysis and scaling up for a semi-preparative separation for isolation of impurities.

Bonfichi [36] showed that DryLab was an invaluable tool for the development of a HPLC method for the analysis of a glycopeptide antibiotic. Glycopeptide antibiotics naturally occur as mixtures. Due to the intrinsic structural complexity and the large number of components normally constituting these mixtures, the development of a reliable and robust analytical method is normally challenging and time consuming. Two linear gradients were performed over the range 0-100 %B in 20 and 60 minutes. The same peak sequence was shown in both chromatograms which aided identification

of the twelve peaks. DryLab was used to simulate an optimised gradient method for the separation of the twelve components. Retention times obtained from a simulated gradient method showed good agreement with those obtained experimentally.

Dolan *et al* [37] optimised reverse-phase HPLC separations of 14 different samples based on simultaneous changes in temperature and gradient steepness. Four experimental runs were required for each sample. Linear gradients with a factor of three difference in run time, were each performed at two different temperatures. For example a sample containing nine corticosteroids was analysed with gradient times of 20 and 60 minutes at 30 and 60°C. The resolution map generated showed the resolution between the most overlapped pair of peaks in the chromatogram as a function of both temperature and gradient time. Predicted conditions for maximum resolution used a 52.5 minute gradient and a temperature of 30°C to achieve a resolution of 1.06 for the critical pair. Experimental retention times showed an average deviation of 0.03 min.

3.1.8.6 Conclusions

DryLab represents an efficient, practical technique for facilitating HPLC method development. It allows the user to perform equivalent trial and error separations with much less effort and in a much shorter time than the corresponding experimental runs. The final optimised separation is usually much better than would otherwise be achieved.

3.2 Liquid Chromatography/Mass Spectrometry

Liquid Chromatography/Mass Spectrometry (LC/MS) is fast becoming the preferred tool of liquid chromatographers. It is a powerful analytical technique that combines the resolving power of high pressure liquid chromatography with the detection specificity of mass spectrometry. The components of the sample are separated using liquid chromatography and introduced into the mass spectrometer where they are ionised for detection.

The mass spectrometer consists of the following components:
- sample inlet
- ion source
- mass analyser
- detector

3.2.1 Atmospheric Pressure Ionisation

Detection by mass spectrometry requires the analyte to be able to generate ions in the gas phase from the sample being analysed. According to the ionisation mode chosen, positive or negative ions will be generated in the ion source (spray chamber). Reactions of the molecular ion (ion that is produced from the ionisation of the analyte), such as adducts or fragmentation may also occur. Atmospheric pressure ionisation (API) techniques are soft ionisation processes occurring at atmospheric pressure which are suitable for the analysis of small and large, polar and non-polar, labile compounds. The two main atmospheric pressure ionisation techniques are atmospheric pressure chemical ionisation (APCI) and atmospheric pressure electrospray ionisation (API-ES).

3.2.1.1 Atmospheric Pressure Chemical Ionisation

Atmospheric Pressure Chemical Ionisation (APCI) is a well-known ionisation mode. It is based on a gas-phase ionisation and is applicable for the analysis of polar and non-

polar compounds of moderate molecular weights. It is a soft ionisation technique that primarily yields singly charged molecular ions and adduct ions.

Ionisation of the analyte can occur by either charge transfer or adduct formation. With charge transfer a proton is transferred in the positive mode and removed in the negative mode. Adduct formation can occur with ions in the mobile phase or sample solvent e.g. sodium and potassium adducts. The ionisation process can make APCI an aggressive technique. A schematic of the ionisation process in APCI is shown in Figure 12 [38].

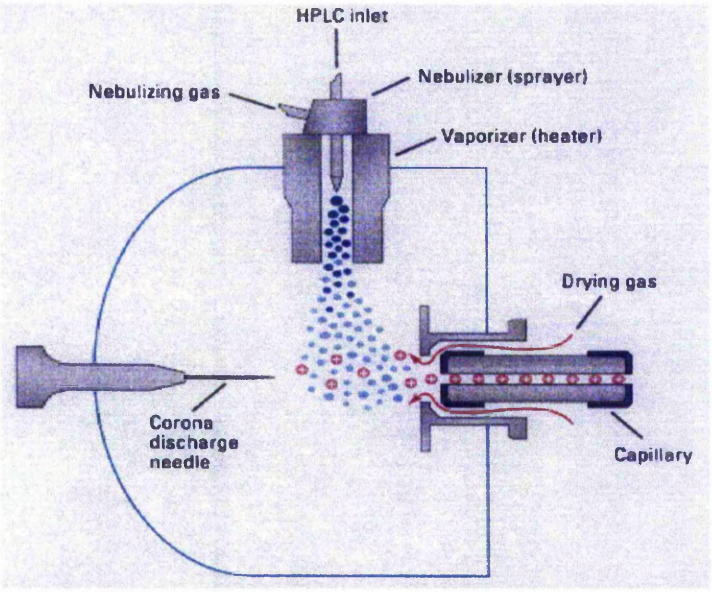

Figure 12. Schematic of the APCI ionisation source

The sample solution typically enters the ionisation source via the HPLC inlet (up to 1.5 ml/min). The solution is first nebulised due to the presence of a high temperature nebuliser gas (N_2) that pushes the solution into the spray chamber. At the end of the needle a mist of droplets is produced and the solvent starts to evaporate due to the high temperature gas flow through the vaporisation chamber. The nebuliser gas carries the resulting gas-phase solvent towards the corona needle. A high voltage is applied to the corona needle which produces an electron discharge that interacts with the flow into the spray chamber to form different ionised solvent molecules. These ions will then ionise

the analyte by charge transfer through ion-molecule reactions, which is the main ionisation phenomenon that occurs in APCI, while the molecules are drifting towards an orthogonal capillary, where a voltage is applied.

Depending on the analyte and solvent system, other reactions may occur such as charge exchange or electron capture. A high voltage (typically 2000-3000 V) is applied to the orthogonal capillary. This attracts the produced ions and focuses them into the mass analyser (less than 10^{-5} Torr) via a chamber which is at an intermediate vacuum level (about 10^{-2} Torr).

By altering the potential of the capillary, positively or negatively charged ions can be produced. Analytes that are more basic in character are preferably analysed in the positive mode where the ionisation occurs by picking up a proton from the solvent to generate the positive molecular ion $[M+H]^+$. Analytes that are more acidic in character are preferably analysed in the negative mode where the ionisation occurs by losing a proton to generate the negative molecular ion $[M-H]^-$. In both ionisation modes the possibility of generating adduct ions occurs.

Horning and co-workers were early pioneers of the technique, applying it to GC/MS [39] and LC/MS [40, 41]. APCI gained popularity and acceptance in the late 1970s for trace gas analysis in environmental and industrial applications [42, 43]. It was introduced commercially by both Sciex and Extranuclear Corporation and used as a very sensitive technique for detecting polar compounds in the gas phase. APCI is now in widespread use.

3.2.1.2 Atmospheric Pressure Electrospray Ionisation

Atmospheric Pressure Electrospray Ionisation (API-ES) is one of the most used and well-known ionisation modes. Electrospray is another example of a soft ionisation technique and it is useful at analysing samples that become multiply charged such as proteins and peptides as well as analysing samples that are singly charged.

Electrospray ionisation is based on solution chemistry ionisation and requires the analyte to have an ionisable group that can easily pick up a charge from the solvent chemistry composition. A schematic of the ionisation process in ESI is shown in Figure 13 [38].

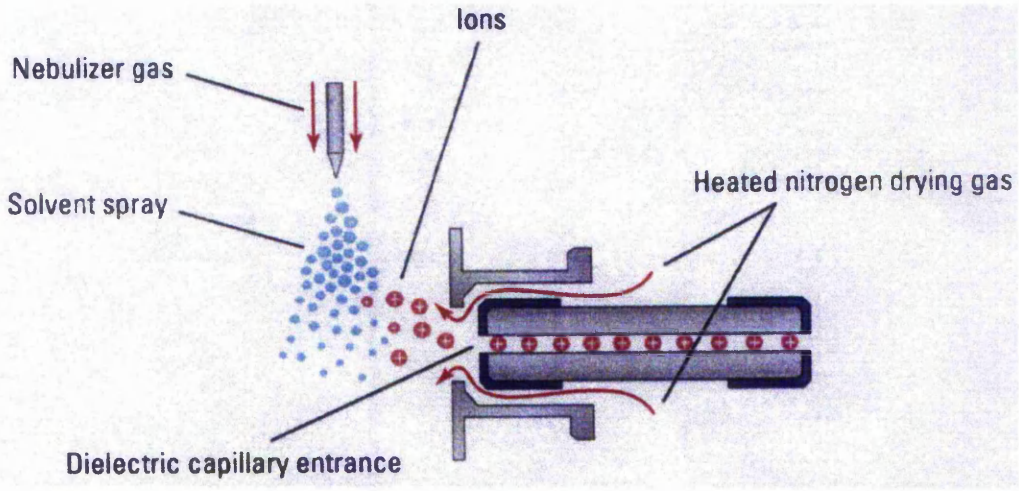

Figure 13. Schematic of the ESI ionisation source

The sample solution typically enters the ionisation source via the HPLC inlet (up to 1.0 ml/min without splitting). The HPLC eluent is pumped through a nebulising needle which is at ground potential. The spray goes through a semi-cylindrical electrode which is at high potential. The potential difference between the needle and the electrode (3 to 6 kV) produces a strong electric field. This field charges the surface of the liquid and forms a spray of charged droplets. The charged droplets are attracted towards the capillary sampling orifice. Along their migration, the multi-charged droplets are first desolvated due to the presence of a heated nitrogen drying gas flowing into the spray chamber, which makes the droplets shrink as shown in Figure 14 and carries away the uncharged material. As the droplets shrink, their charge/mass ratio increases until this ratio reaches the Rayleigh limit, where the droplets are mechanically deformed and become unstable and explode, a phenomenon called Coulomb explosion. This process continues until single charged ions are generated. However, the exact mechanism by which the ions present in the charged droplets are converted into gas phase ions is not

known [44]. The gas phase ions pass through the capillary sampling orifice into the low pressure region of the ion source and the mass analyser.

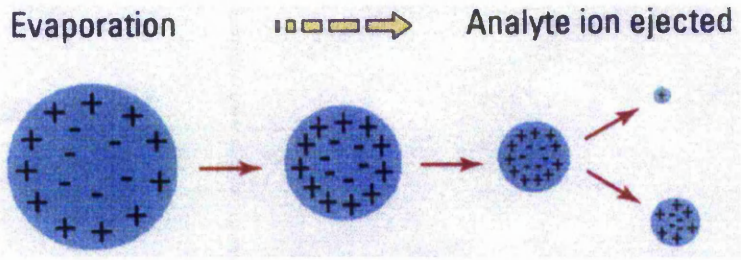

Figure 14. Desorption of ions from solution in the ESI ionisation mode

Electrospray was developed as a mass spectrometry ionisation technique by John Fenn and his group at Yale University during the early to mid 1980s [45]. The technique was largely ignored until its application to the ionisation and detection of large molecules was demonstrated in 1988 [46]. Fenn, Whitehouse and co-workers recognised the application of electrospray as an LC/MS interface [45] and focused their interest on molecular weight measurements of biopolymers. However, it was Henion's lab at Cornell which led the way in developing a practical LC/MC interface from electrospray and ion evaporation. As API mass spectrometers began to come onto the market from 1989 onward, electrospray and APCI became the dominant LC/MS methods [47].

3.2.2 Mass Analyser

The aim of the mass analyser is to separate the gas-phase ions generated from the ionisation source on the basis of their *m/z* ratios. There are many types of mass analyser available, including quadrupoles, ion traps, magnetic sector and time of flight. The Agilent Technologies 1100 MSD (formally known as Hewlett Packard) contains a quadrupole mass analyser which operates at high vacuum to prevent fragmentation of the ions by collisions during their separation.

The problem of coupling an atmospheric pressure ionisation source with a high vacuum mass analyser is overcome by the use of staged pressure reduction and an ion optic system with focusing lenses which have very small openings. The ions travel through three stages of continuously decreasing pressure until they reach the detector. Stage 1 is the spray chamber which is at atmospheric pressure. A rough pump generates the stage 2 vacuum where the pressure reaches about 3 Torr. The final stage is high vacuum and is obtained by the use of two turbomolecular pumps which maintain the quadrupole region at less than 10^{-5} Torr. Skimmers are used to focus the ions towards the octopole which guides the ions towards the quadrupole for separation.

The quadrupole mass filter consists of four parallel rods as shown in Figure 15.

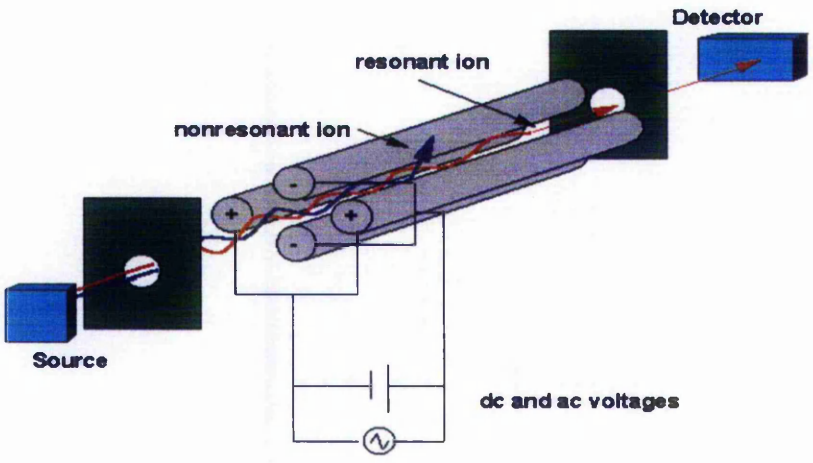

Figure 15. Schematic of the Quadrupole Mass Analyser

One pair of opposite rods has a Direct Current (DC) voltage applied, the other pair has a Radio Frequency (RF) voltage applied. Ions which are introduced along the central axis of the rods will oscillate about that axis. At a particular amplitude of the DC and the RF potential, only one ion will have a stable oscillation according to its mass to charge ratio and will drift down to the rods towards the detector, while all other ions will collide with the rods. Varying the RF voltage will enable ions of different mass to charge ratio

to be brought to the detector. The detector consists of an electron multiplier which amplifies the ions to produce a detectable signal.

The resolution R_s ($R_s=m/\Delta m$) of a quadrupole mass analyser is not very high at around 1000, enabling a mass of 1000 Da to be distinguished from a mass at 1001 Da.

Two different modes can be used to record the response of the MS. These are the mass scan mode or the Selected Ion Monitoring (SIM) mode. In scan mode the instrument will detect signals over a selected mass range. The MS can only measure a given *m/z* at a time and therefore the larger the *m/z* range the less time is spent on recording the response for each particular ion which leads to a reduction in sensitivity. A complete mass scan lasts about 0.6 sec. Hence when scanning over the range 150 – 1000, a particular ion is only recorded for approximately $0.6/(1000-150) = 7 \times 10^{-4}$ sec, which is 0.12% of the total time it is produced from the ion source. The sensitivity can be improved by reducing the *m/z* range or by increasing the mass scan time.

Where detection of a single *m/z* or a series of known *m/z* are required, SIM is preferred over scan. In SIM, for the detection of a single *m/z* the quadrupole spends 100% of its time sampling that ion. Where a series of ions are selected the sampling time will be split between those ions, i.e. for four selected ions 25% of the sampling time will be spent sampling each ion which gives a vast improvement in sensitivity compared to the mass scan mode.

SIM is typically used for quantitative analysis where the analyte mass is known. The scan mode is typically used for qualitative analyses or for quantitative analyses where the analyte mass is not known in advance.

The main advantages of this instrument are that it is reasonably robust, cheap, and simple to use. The mass scanning is fast, which allows combination with a separation technique such as HPLC or Capillary Electrophoresis (CE).

3.2.3 Agilent Technologies 1100 MSD

The original 'A' model MSD was subsequently upgraded to the 'B' and more recently enhanced to the 'D' model and is now known as the Agilent Technologies 1100 MSD SL. Models 'A' and 'D' of the MSD are shown in Figures 16 and 17.

The 'B' model upgrade contains an analogue output which allows the output of MS SIM data into a chromatography data system. The enhanced 'D' model MSD gives an increase in sensitivity of 10 fold (determined for reserpine). This is achieved by a series of modifications to the hardware. These include the following:

- removal of one of the skimmers and an increase in octopole length to give a decrease in distance between the capillary and the octopole which optimises the transmission of the ions and reduces the role of the fragmentor voltage in ion transmission
- raise in nebuliser height by 8 mm to give an increase in ion migration into the capillary
- larger bore capillary (0.6 mm) which allows a higher ion transmission and reduces chances of clogging
- new desolvation assembly to precisely align with the ion optics
- skimmer angle is flatter which reduces the amount of gas required to generate the same number of ions.

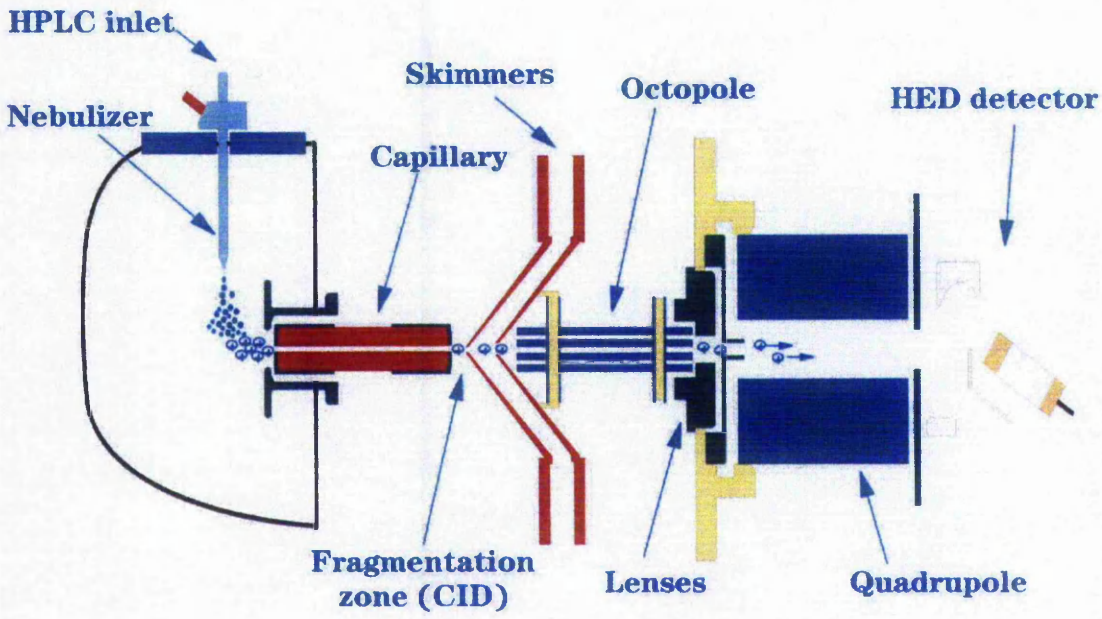

Figure 16. **Agilent Technologies electrospray source and 'A' model analyser design**

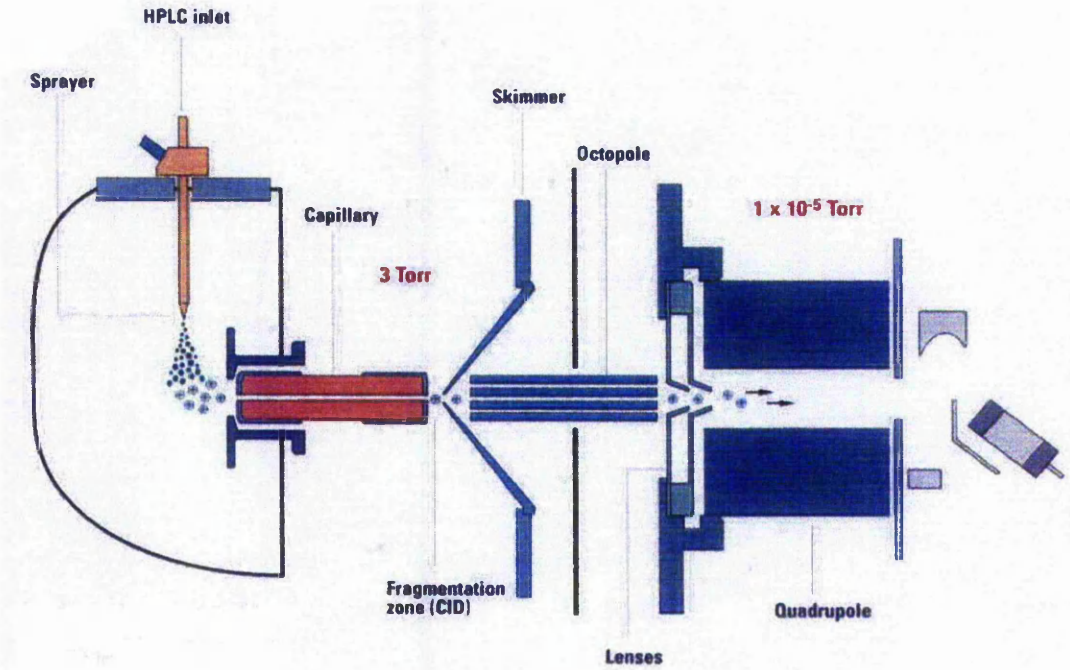

Figure 17. **Agilent Technologies electrospray source and 'D' model analyser design**

LC/MS has been extensively used in the pharmaceutical industry for drug and degradant identification [48, 49], metabolite profiling and identification [50-52] as well as screening and quantification [53-58]. Traditionally LC/MS conditions are based on a compromise between those which are optimum for chromatography and those which are optimum for mass spectrometry. In the former a sufficient ionic strength is necessary to minimise the unwanted secondary interactions of analytes with silanol groups on reverse phase stationary materials such as octadecylsilane bonded silicas. In the absence of a sufficient ionic strength the resultant peak can show severe tailing which reduces the sensitivity of the method. In contrast mass spectrometry ideally favours a mobile phase of low ionic strength as this enhances analyte ionisation. Therefore we have conflicting requirements and hence a compromise is frequently made.

3.3 Quantitative LC/MS Applications

Due to its capability of achieving extremely low detection limits in SIM, and the enhanced specificity achieved with MS detection, LC/MS has been widely used for quantitative applications. Where low level detection is required it is often not possible to perform analyses by LC/UV.

Olah *et al* [53] reported the use of LC/MS with APCI for the quantitative analysis of timolol in plasma. Timolol is a non-selective β-adrenoreceptor antagonist designed for the treatment of both cardiovascular disease and glaucoma. Linearity was achieved over the concentration range 0.2 – 20 ng/ml. Acceptable accuracy, intra- and inter-day precision were demonstrated in the assay range 0.5-20 ng/ml. The RSD at 0.2 ng/ml was 14.1% and an accuracy of 102.5% was achieved. Detection at such limits was unobtainable with either LC/UV or GC/MS.

The determination of ZD9583, a thromboxane receptor antagonist, in human plasma by LC/MS with APCI was described by Goa *et al* [54]. MS detection was required to increase the sensitivity over that previously achieved with HPLC with fluorescence detection, in order to be able to analyse clinical samples at low concentrations. Using a column switching approach to divert the solvent front from entering the mass spectrometer, a run time of less than 2 minutes was achieved. A linear calibration curve

with a range of 1-500 ng/ml was obtained with an intra- and inter-day precision of less than 10% over the calibration range.

Kleinschnitz *et al* [55] developed a sensitive and selective method for the determination of 1,4-benzodiazepines: diazepam, N-desmethyldiazepam, flunitrazepam and medazepam in human serum and urine using solid-phase extraction and LC/MS with ESI. Using diazepam-d_5 and N-desmethyldiazepam-d_5 as internal standards, recoveries of between 90.4 and 109.7% were determined. The routine quantification limit was set at 2 ng/ml at a signal to noise ratio of 10:1.

Hammes *et al* [56] described a quantitative LC/MS method using positive ion electrospray for the determination of α-cyclodextrin in human plasma. The method used β-cyclodextrin as an internal standard. The analytes were isolated using protein precipitation and solid phase extraction with analysis on a narrow-bore aminopropyl column (5 μm 125 x 2 mm) and detection in electrospray MS of the positive ion $[M+NH_4]^+$. Adequate isocratic chromatography was required to eliminate any matrix effects. The limit of quantification was 5 ng/ml with linearity achieved over the concentration range 5-1000 ng/ml. The intra- and inter-assay precisions were less than 18% with an accuracy of less than 10.5% over the entire concentration range.

Whilst the majority of LC/MS methods reported use reversed phase (RP) chromatography, normal phase LC/MS [59] is also possible as a complimentary method to RPLC/MS for those compounds which are not readily analysed by RPLC/MS.

3.4 Rapid LC/MS Analysis

The use of nonporous silica stationary phase for reversed-phase fast LC applications was examined by Jenke [60]. Comparisons between conventional columns (5 μm Adsorbosphere C18 150 x 4.6 mm) and 'fast columns' (1.5 μm nonporous silica chemically bonded C18 microspheres 33 x 4.6 mm) showed that fast LC columns produced workable separations in shorter time periods and required mobile phases that contain proportionally less organic modifier. However, the use of nonporous silica

requires control of the dead volume and the use of small injection volumes for good efficiencies and symmetrical peak shapes.

Eichhold *et al* [61] developed a sensitive and selective LC/MS method for the analysis of fluprostenol in rat plasma. Using a 10 mm HPLC column in conjunction with MS detection allowed the development of a rapid, selective and rugged method for the analysis of trace levels of fluprostenol. The retention time was around 40 seconds, with a cycle time of 1.2 minutes. The short columns proved to be fairly rugged, allowing at least 100 injections before column performance degraded.

Bayliss *et al* [62] described a high throughput method using parallel ultra-high flow rate liquid chromatography with mass spectrometric detection using a multiplex (MUX) electrospray source for the determination of pharmaceuticals in plasma. The method described used four columns in parallel with a four-way multiple sprayer interface into the mass spectrometer allowing the simultaneous quantification of drugs from four plasma samples at ng/ml concentrations. The method enabled up to 120 samples to be analysed per hour.

Pereira *et al* [63] transferred a method for three anabolic steroids and metabolites from a 5 µm HyPURITY ADVANCE C18 150 x 4.6 mm column, to a 3 µm 30 x 2.1 mm column of the same stationary phase with no change in selectivity and with added speed of analysis, shortening the analysis time from 5.5 to 1.2 minutes. They also demonstrated a reduction in analysis time of six triazines from 24 to 6.5 minutes with a change in column/geometry from 5 µm 150 x 4.6 mm column to a 3 µm 30 x 2.1 mm column. Short 4.6 mm i.d. columns provide low back pressures which allow analysis to be performed at a high flow rates. The separation of eight β-blockers was obtained in 65 seconds using a 3 µm HyPURITY C18 30 x 4.6 mm, column with a flow rate of 2 ml/min combined with a fast gradient (20 to 75% organic in 1.5 minutes).

A generic ultra high flow rate LC/MS method for the direct on-line analysis of pharmaceuticals in plasma was reported by Ayrton *et al* [64]. Using a flow rate of 4 ml/min with a large particle size stationary phase the direct analysis of a plasma sample spiked with isoquinoline was performed without the need for time consuming

sample preparation. Due to the large flow rate it was necessary to split the flow to enable only 400 μl/min to enter the MS. The generic method used a rapid gradient from 100% formic acid (0.1%) to acetonitrile-formic acid (0.1%) (95:5) with a total cycle time of 1.2 mins. This enabled the analysis of up to 50 samples per hour. The method was validated over the range 5-1000 ng/ml with weighted 1/x linear regression and showed the method to be accurate and precise.

4. MATERIALS AND METHODS

4.1 Chemicals

All buffer chemicals and solvents ethanol and acetone were of HPLC grade (Fisher Scientific, Loughborough, UK). Solvents methanol and acetonitrile were of HPLC grade and were supplied by Romil (Cambridgeshire, UK). Water was purified by means of a Milli-Q-plus 185 ultra pure water system (Molsheim, France). Basic test analytes were obtained from Sigma-Aldrich (Dorset, UK) and in-house from AstraZeneca R&D Charnwood (Loughborough, UK).

A hydrophilic base mix solution contained the following chemicals at 27.27 µg/ml: nicotine, benzylamine hydrochloride, procainamide hydrochloride, terbutaline sulphate, salbutamol and phenol as the neutral marker. A lipophilic base mix solution contained the following chemicals at 27.27 µg/ml: AR-R12495AA, AR-C68397AA, diphenhydramine hydrochloride, remacemide hydrochloride, nortriptyline hydrochloride and phenol as the neutral marker. A 10 base mix solution contained all hydrophilic and lipophilic bases above plus phenol as the neutral marker at 27.27 µg/ml.

4.2 pH measurement

The pH of buffer solutions used was measured using a Mettler Toledo MP 225 standard pH meter with combined glass and reference electrode which was calibrated prior to use with standard solutions of pH 2, 7 and 9.2.

4.3 Chromatography

4.3.1 Stationary phase characterisation

Analyses were performed using a Hewlett Packard 1090M HPLC system with diode array detection. Data acquisition and integration were controlled by Multichrom.

All analyses were performed using a flow rate of 1.0 ml/min and a temperature of 40°C with a thermostatted column heater (Model CS 7266, Jones Chromatography). A column switching device was employed (Mistral, model 880, Spark Holland). A selection of C18 columns were used as detailed in section 5.1.1.

Mobile phase A contained 0.02 M potassium dihydrogen orthophosphate, pH 2.7 in methanol-water (30:70 v/v). Mobile phase B contained 0.02 M potassium dihydrogen orthophosphate, pH 7.6 in methanol-water (30:70 v/v). Mobile phase composition was varied in thirteen stages between pH 2.7 and 7.6. The pH of each of these points was measured prior to addition of organic modifier.

20 µl of the test solution which contained the basic analyte under test (nicotine 0.3 mg/ml, codeine 0.6 mg/ml, pyridine 0.1 mg/ml, procainamide hydrochloride 0.14 mg/ml, benzylamine hydrochloride 0.6 mg/ml) and phenol (0.6 mg/ml) in mobile phase A was injected.

4.3.2 LC Optimisation

Analyses were performed using an Agilent Technologies 1100 liquid chromatograph system with diode array detection at wavelength 214 nm. Data acquisition and integration were controlled by Chemstation software. A selection of Hypersil HyPURITY C18 columns of differing dimensions and particle sizes were used.

Mobile phase A contained 0.02 M potassium dihydrogen orthophosphate, pH 2.7 in water. Mobile phase B contained 0.02 M potassium dihydrogen orthophosphate, pH 2.7 in methanol-water (65:35 v/v).

4.3.3 LC/MS Analysis

LC/MS was performed using an Agilent Technologies (formerly Hewlett Packard) 1100 liquid chromatograph with an Agilent Technologies MSD mass selective detector. 'A' and 'D' model MSDs were used as detailed in section 3.2.3.

4.4 Test Analytes for Stationary Phase Assessment

The structures of the 5 bases analysed for stationary phase assessment are shown below in Figure 18.

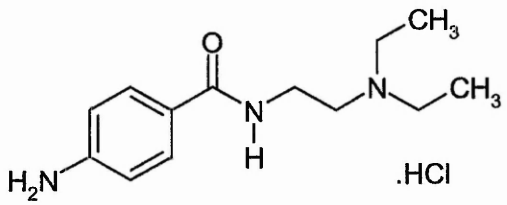

Procainamide pK_a 2.63 and 9.86

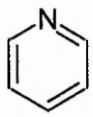

Pyridine pK_a 5.32

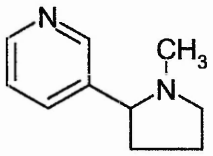

Nicotine pK_a 4.23 and 9.13

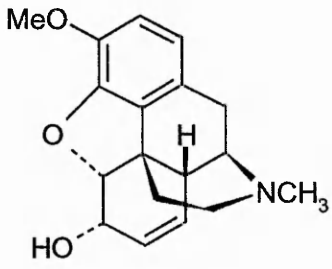

Codeine pK_a 8.19

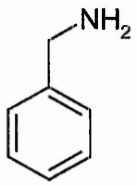

Benzylamine pK_a 9.40

pK_a data taken from ACD prediction software

Figure 18. Structures of basic pharmaceutical compounds

4.5 Test Analytes for LC Optimisation

The structures of the 10 bases and phenol analysed for LC optimisation are shown below in Figure 19.

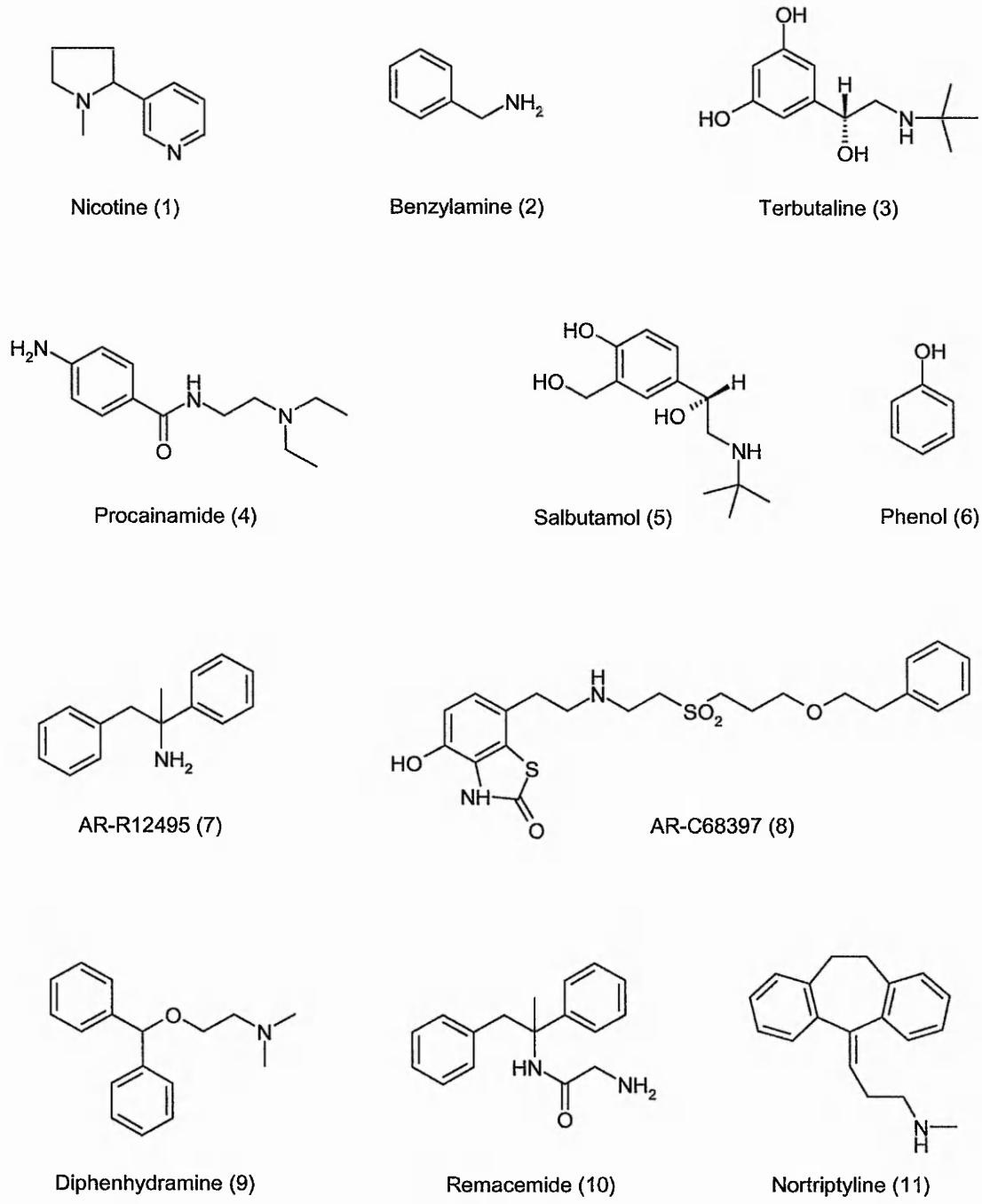

Figure 19. Basic test analytes for LC optimisation

The physicochemical properties of the test analytes in Figure 19 are shown in Table 1 below.

Table 1. Physicochemical properties of test analytes

Compound	log P	pK_a of basic functionality	log D at pH 2.7
1. Nicotine	0.72 ± 0.26	9.13 ± 0.40 4.23 ± 0.12	-2.88
2. Benzylamine	1.09 ± 0.21	9.40 ± 0.10	-2.01
3. Terbutaline	1.22 ± 0.29	9.45 ± 0.50	-2.62
4. Procainamide	1.23 ± 0.37	9.86 ± 0.25 2.63 ± 0.10	-2.23
5. Salbutamol	0.36 ± 0.31	9.22 ± 0.50	-3.08
6. Phenol	1.48 ± 0.19	NA	1.48
7. AR-D12495	3.47 ± 0.23	9.97 ± 0.50	0.37
8. AR-C68397	4.00 ± 0.82	9.19 ± 0.19	0.92
9. Diphenhydramine	3.66 ± 0.37	8.76 ± 0.28	0.56
10. Remacemide	2.54 ± 0.43	7.76 ± 0.29	-0.62
11. Nortriptyline	5.65 ± 0.32	10.08 ± 0.10	2.55

Data taken from ACD prediction software

5. RESULTS

5.1 LC Optimisation

5.1.1 Stationary Phase Assessment

The ion exchange capacity was determined for six different columns over the pH range 2.7 to 7.6 by determining the quotient of the corrected retention factor for benzylamine with respect to phenol.

The columns used for the analysis were as follows:

5µm Hypersil EXCEL 5ODS C18 250 x 4.6 mm
5µm Shandon Hypersil 100 C18 250 x 4.6 mm
5µm Hypersil BDS C18 150 x 4.6 mm
5µm Shandon Elite C18 150 x 4.6 mm
5µm Hypersil HyPURITY C18 150 x 4.6 mm
5µm Phenomenex Prodogy OSD(3) C18 150 x 4.6 mm

The results at pH 2.7 and 7.6 are shown in Table 2.

Table 2. Ion Exchange Capacity of benzylamine at pH 2.7 and 7.6

Column	pH 2.7	pH 7.6
Hypersil 5ODS	0.611	0.944
Hypersil 100	0.106*	0.477
Hypersil BDS	0.115	0.367
Hypersil Elite	0.099	0.361
Hypersil HyPURITY	0.059	0.391
Phenomenex Prodigy ODS(3)	0.062	0.311

*pH 2.9

The values at pH 2.7 represent the acidic silanols on the stationary phase. The values at pH 7.6 represent the total isolated silanol content. The results are shown graphically in

Figure 20. This experiment was repeated using the following basic compounds: pyridine, procainamide, codeine and nicotine. The structures of these compounds are shown in Figure 18. Plots of the ratio of corrected retention factor *k* of the test compound with respect to phenol, versus pH are shown in Figures 21-24. Results showing the effect the pH on peak symmetry and efficiency are shown in Tables 1-10 in the appendix.

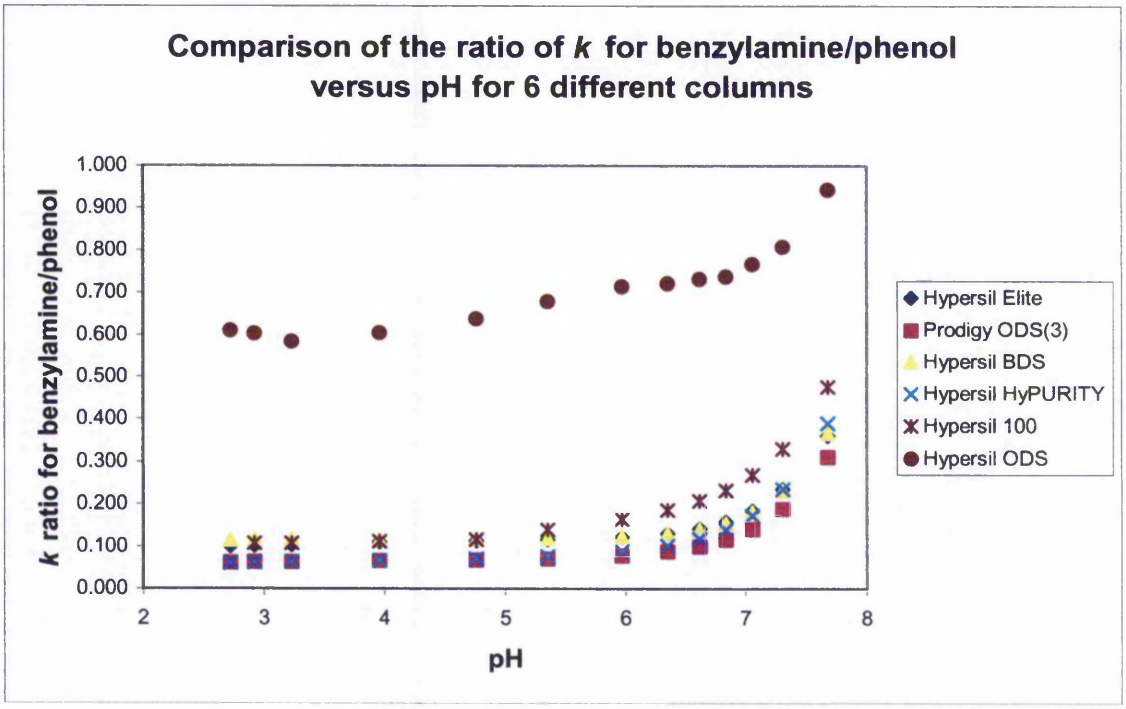

Figure 20. Comparison of the ratio of *k* for benzylamine/phenol

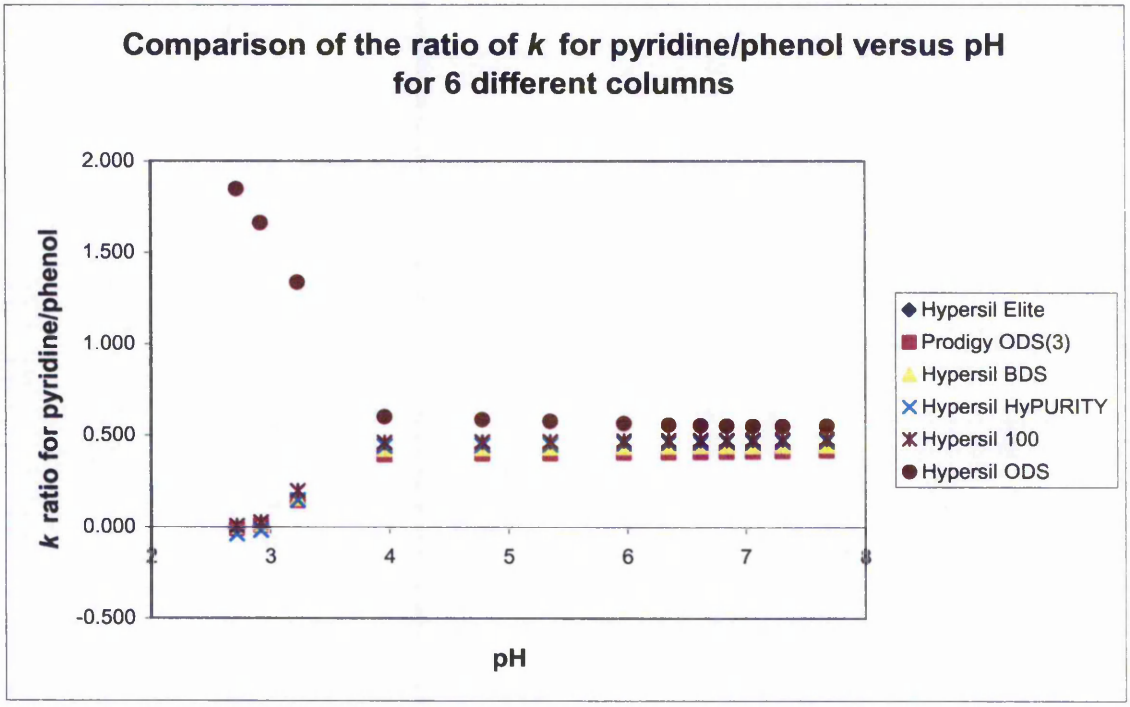

Figure 21. **Comparison of the ratio of *k* for pyridine/phenol**

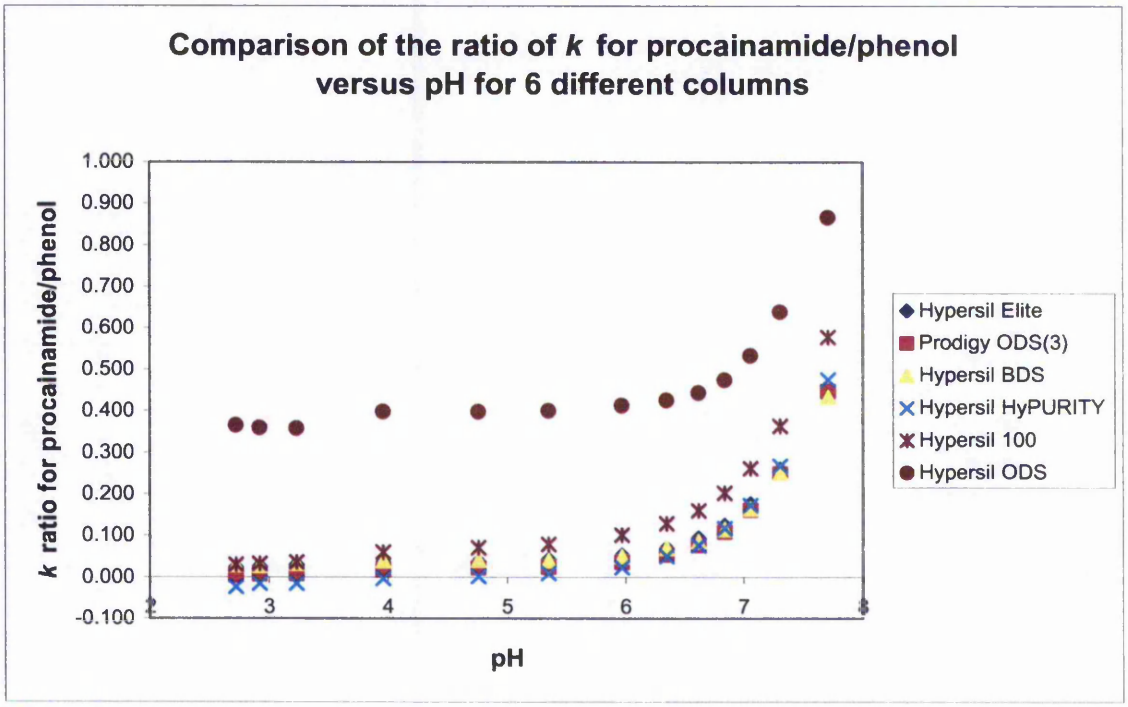

Figure 22. **Comparison of the ratio of *k* for procainamide/phenol**

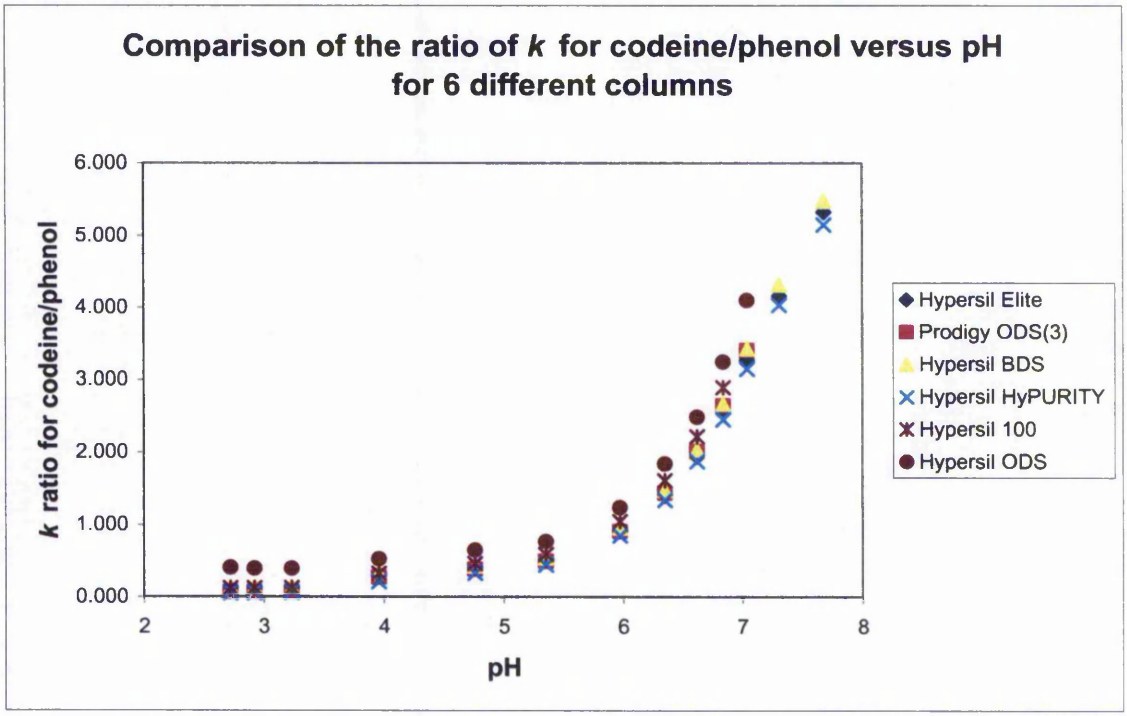

Figure 23. **Comparison of the ratio of *k* for codeine/phenol**

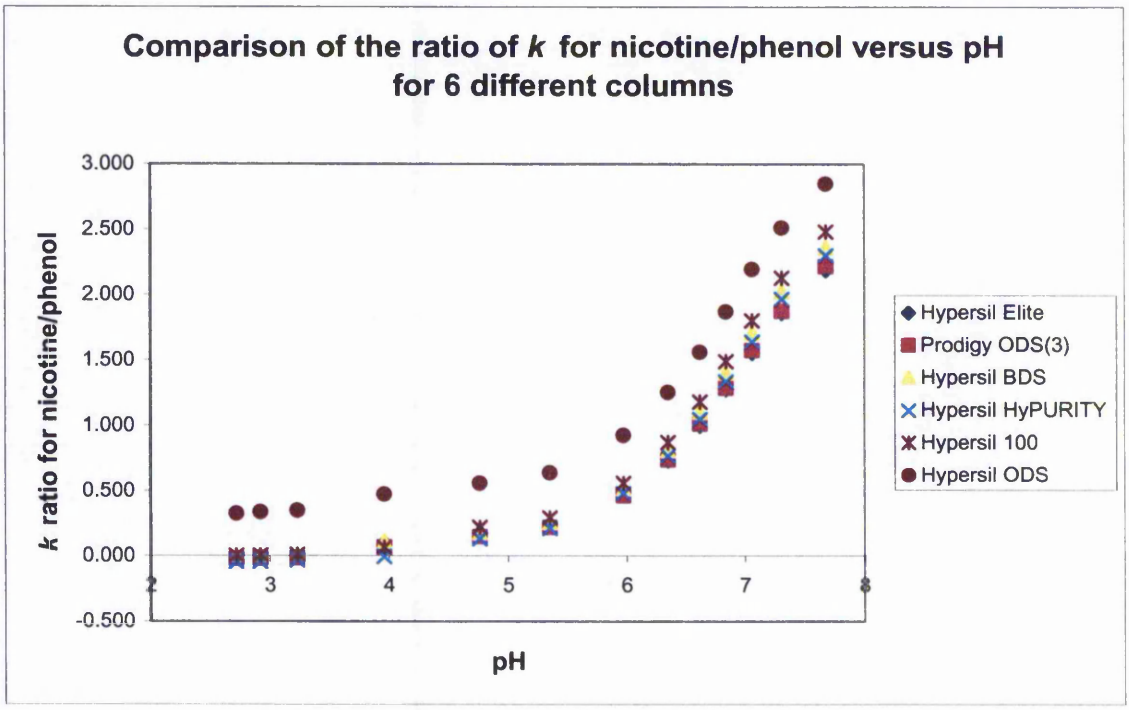

Figure 24. **Comparison of the ratio of *k* for nicotine/phenol**

The pH titration results for benzylamine show that the ODS column had the largest number of isolated silanol groups. The Hypersil 100 column showed reduced acidic and total isolated silanols. The BDS column had a reduced total silanol content, although a large proportion of these were acidic. The Elite had reduced acidic silanols over the BDS column. The Hypersil HyPURITY is one of a new generation of columns and showed that the acidic silanols was lower than the Elite, although the total number of silanols was about the same. The Prodigy column was expected to show similar results to the HyPURITY, although the total silanol content was found to be lower.

Some of the analytes were chosen as they have been used previously to show differences in the performance of reverse phase columns [14, 15]. The compounds were also chosen on the basis that they could all be eluted using the same concentration of organic solvent in the mobile phase and as such could be directly compared. Column performance is usually measured by asymmetry factor (A_S) and column effiency (N); however, these parameters are not consistent for unrelated analytes.

All compounds showed that the ODS column performed the worst as the ratios of corrected retention factor *k* at both pH 2.7 and 7.6 were the greatest of all the columns tested. Peak shape was also very poor. This would suggest that the silanol groups present were not all of the same type (i.e. geminal, vicinal, acidic).

Most of the test compounds followed the same pattern i.e. as the pH increased, the compound became less ionised and therefore stayed on the column for longer giving rise to broader peaks. However, pyridine on the ODS column followed a different pattern. As the pH approached the pK_a of the compound the *k* ratio reduced. Thereafter it was only the hydrogen bonding ability between the analyte and the silica surface which was seen. The results for codeine suggest that the molecule was not getting down to the silica surface i.e. there were no silanol interactions. This was probably due to the size and shape of the analyte.

Strong retention of protonated bases on isolated silanols with subsequent overloading of the small number of these sites is a major contributor to band broadening and peak tailing [65]. Analytes with a pK_a of 8 or higher behave rather similar at low pH for a

given column. This may be because the basic group responsible for tailing would be expected to be fully protonated at low pH.

Apart from pyridine, all analytes showed improved peak shape at low pH. Pyridine gave similar or worse results at low pH. Pyridine is unprotonated at pH 7 whereas all other analytes are at least partially protonated. Thus compounds of low pK_a may be able to be analysed in the unprotonated state. In general, protonation of silanols at low pH discourages ion-exchange interactions for strong bases. Unlike other analytes in this study, pyridine is largely unprotonated at pH 7, resulting in fewer ion-exchange interactions.

For benzylamine, the majority of the columns showed that efficiency was constant over the pH range 2.7 - 6. Between pH 6 and 7 an increase in efficiency was seen. Above pH 7 the efficiency was seen to decrease. The columns not conforming to this pattern were Hypersil ODS which showed poor efficiencies at all pHs, and the Hypersil 100 which showed a decrease in efficiency between pH 4.8 and 7, with a slight increase above pH 7. An increase in efficiency at pH 7 for some compounds may be explained by the number of dissociated silanols which exist at pH 7 in comparison to pH 3. Around pH 7 support silanols and basic analytes become partially ionised. This pH presents the greatest challenge in obtaining good peak shape and high column efficiency. At low pH the peak shape can be improved due to reduced dissociation of silanols, whereas at a higher pH, protonation of the base is reduced which may improve peak symmetry. An increase in the accessible silanol concentration could lead to improved peak shape for basic compounds due to reduced silanol overloading effects. Others [66, 67] suggests that the optimum pH for analysis is dependant on the analyte, and that it is not simply the pK_a of the analyte which affects its interaction with the stationary phase, but that the size, shape and bonding chemistry of the analyte are also important.

5.1.2 Predictive nature of DryLab

20 and 60 min linear gradients (5 to 100% mobile phase B followed by a 5 minute hold) of the 10 base mix were performed at 30 and 80°C on a 5 µm HyPURITY C18 150 x 4.6 mm column using a flow rate of 1.0 ml/min. The chromatograms obtained are shown below in Figures 25-28.

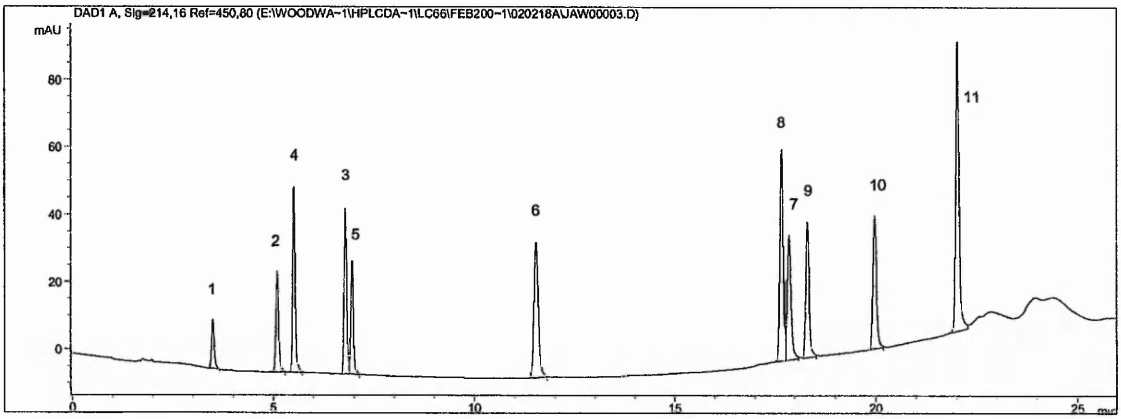

Figure 25. 20 minute linear gradient with hold at 30°C

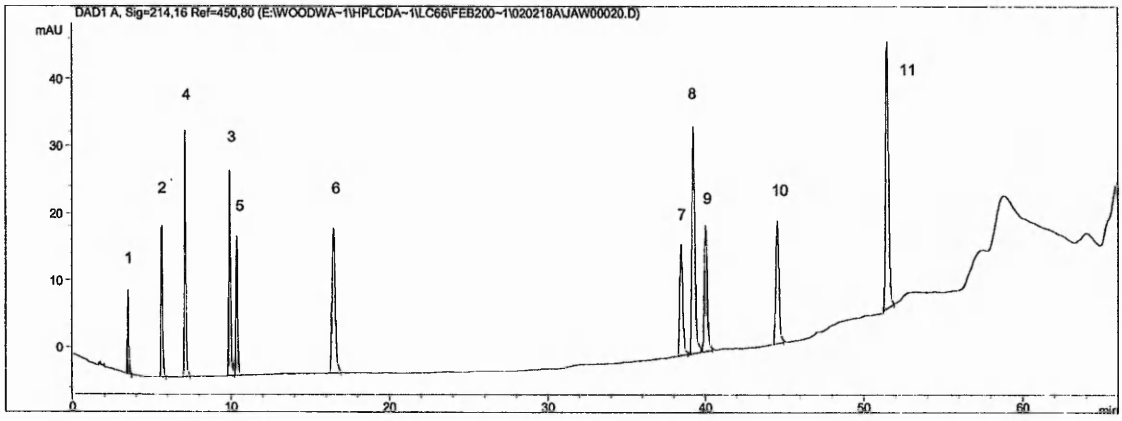

Figure 26. 60 minute linear gradient with hold at 30°C

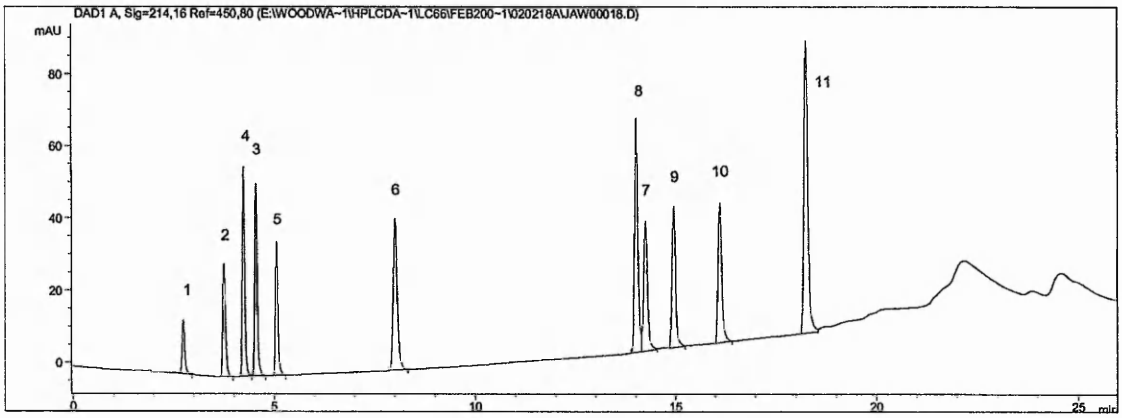

Figure 27. 20 minute linear gradient with hold at 80°C

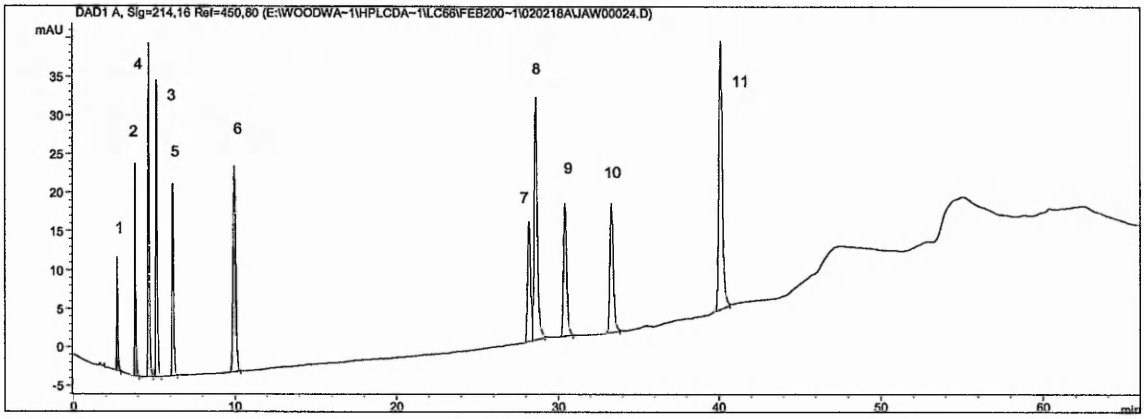

Figure 28. 60 minute linear gradient with hold at 80°C

The data show that peaks 8 and 7 reverse position when the gradient time is increased from 20 to 60 minutes. This occurs at both 30 and 80°C. The data were imported into DryLab with appropriate column efficiency, t_0, delay volume and extra column volume entered. The data were used to predict the separation and peak shape obtained when using a column of reduced dimensions and particle size operating at a higher linear velocity. Using the DryLab resolution map shown in Figure 29, the optimum temperature for separation of the critical pair can be selected.

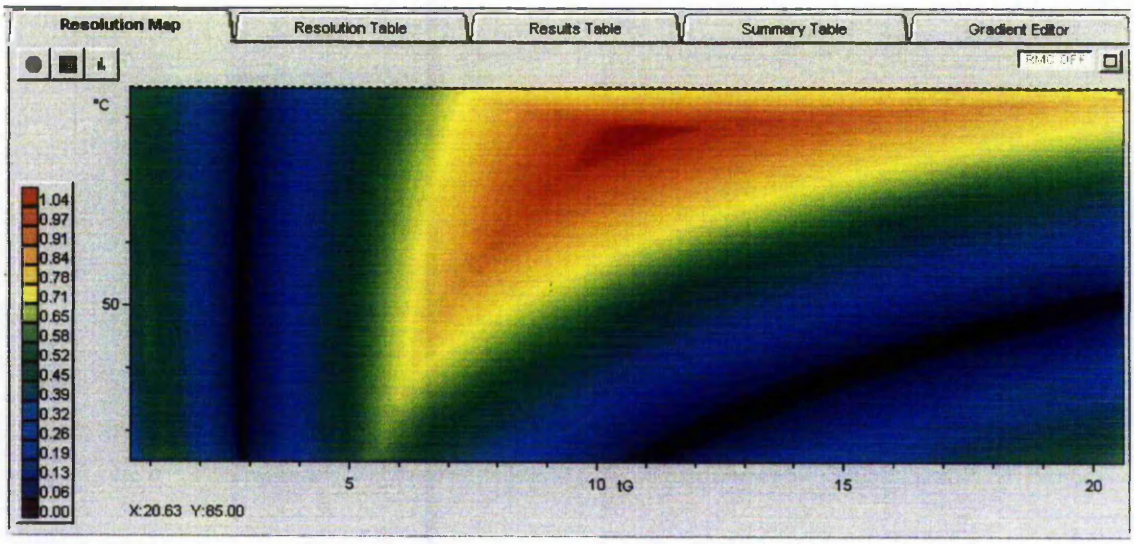

Figure 29. **DryLab resolution map for 10 base mix with phenol on a 5 µm HyPURITY C18 150 x 4.6 mm column**

As indicated above, areas on the resolution map which are blue represent poor resolution between the critical pair, whilst areas which are red represent optimum separation. Optimum separation for the critical pair within the 10 base mix with phenol is achieved at 75°C over a 10 minute linear gradient. This is predicted to give a minimum resolution of 1.04 between any two components. The gradient can be modified to be user defined using the gradient editor shown in Figure 30. The gradient is displayed numerically in a status dialogue box shown in Figure 31. Using the gradient editor may further improve the resolution.

The status box displays the gradient from the gradient editor and shows the predicted resolution of the critical pair. This has been shown to increase from 1.04 to 1.45 using the gradient editor.

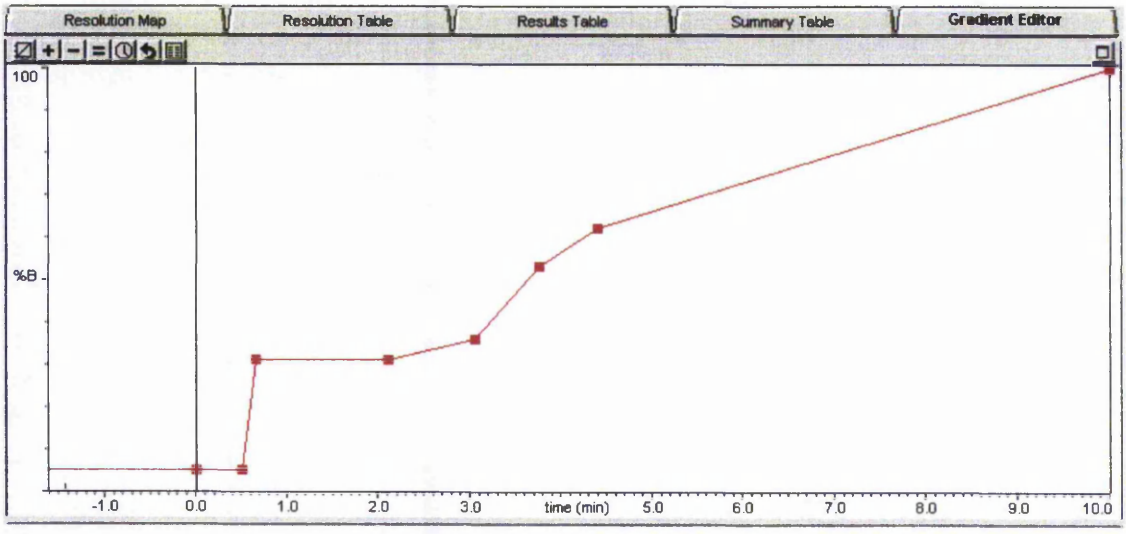

Figure 30. DryLab gradient editor

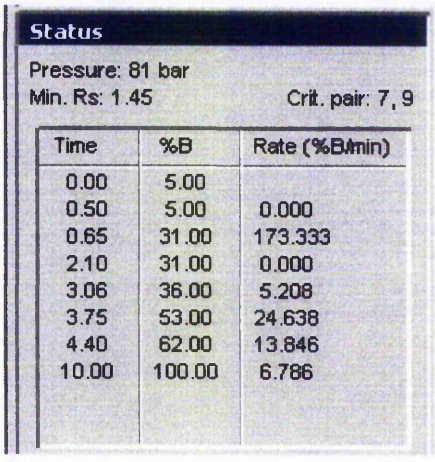

Time	%B	Rate (%B/min)
0.00	5.00	
0.50	5.00	0.000
0.65	31.00	173.333
2.10	31.00	0.000
3.06	36.00	5.208
3.75	53.00	24.638
4.40	62.00	13.846
10.00	100.00	6.786

Figure 31. Status box for gradient editor

To accurately predict the separation experimentally determined values for column efficiency, t_0, delay volume and extra column volume were required. A solution of salbutamol at 27 µg/ml was analysed on an isocratic method using 10% mobile phase B on a 5 µm HyPURITY C18 150 x 4.6 mm column. The column efficiency achieved was 13100 plates per column. A solution of thiourea, an unretained analyte, at 27 µg/ml was analysed on the 20 minute linear gradient to determine the value of t_0 as 1.91 minutes. A delay volume of 1.0 ml was determined for the Agilent Technologies 1100

HPLC by performing a linear gradient test with water, containing 0.5% acetone in mobile phase B. This is calculated according to Figure 32. If the delay volume is inaccurately calculated this will result in retention time offsets for all peaks. The extra column volume was determined by combining the detector flow cell volume of 1.7 µl with the post injector tubing volume of 15 µl.

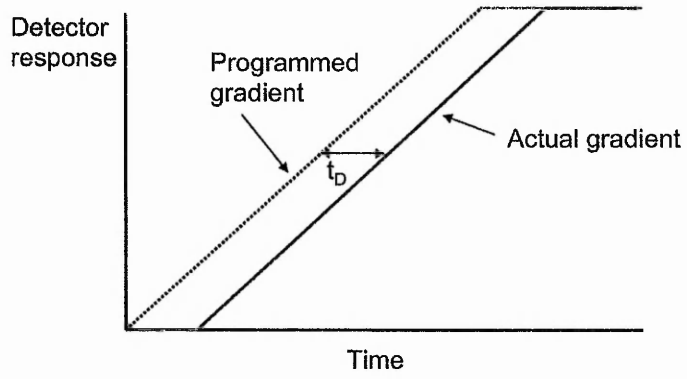

Figure 32. Calculation of system delay volume (t_D)

Using the gradient editor the optimum predicted separation for the 10 base mix with phenol was obtained for HyPURITY C18 50 x 2.1 mm columns of particle sizes 3 and 5 µm, operating at a flow rate of 0.7 ml/min. A flow rate of 0.2 ml/min on a 2.1 mm i.d. column represents the same linear velocity as 1.0 ml/min on a 4.6 mm i.d. column. A flow rate of 0.7 ml/min is considered to be rapid analysis as the flow rate is 3 ½ times the linear velocity. The predicted separations were performed in the laboratory to assess the ability of DryLab to predict separations on reduced column dimensions with high linear velocities. The chromatograms for predicted and obtained separations are shown in Figures 33-36.

Peak 1, nicotine does not fit the DryLab model due to its early elution in the dwell volume and hence does not appear on the predicted chromatograms. The chromatograms show that DryLab is excellent at predicting separations for reduced column dimensions operating at high flow rates. However, it is critical that the appropriate column efficiency, t_0, delay volume and extra column volume are inputted

as this can greatly affect peak shape. This is due to the equation used in the DryLab predictions $\log k = A - Bx$ (section 3.1.8.2), where

$k = \frac{t_r - t_0}{t_0}$ and t_r is the retention time of the analyte.

This is shown for analytes 2-5, where sharp, well separated peaks were predicted, where as broader, less well resolved peaks were obtained. This can either be attributed to an incorrectly determined value for efficiency or it demonstrates the presence of extra column band broadening, which occurs as the solute is carried through the PEEK tubing which connects the different modules of the HPLC system. Broadening arises from differences in flow rates between layers of liquid adjacent to the wall and centre of the tubing. As a consequence the centre part of the solute band moves more rapidly than the peripheral part. Extra column effects are more significant when microbore columns are used [68].

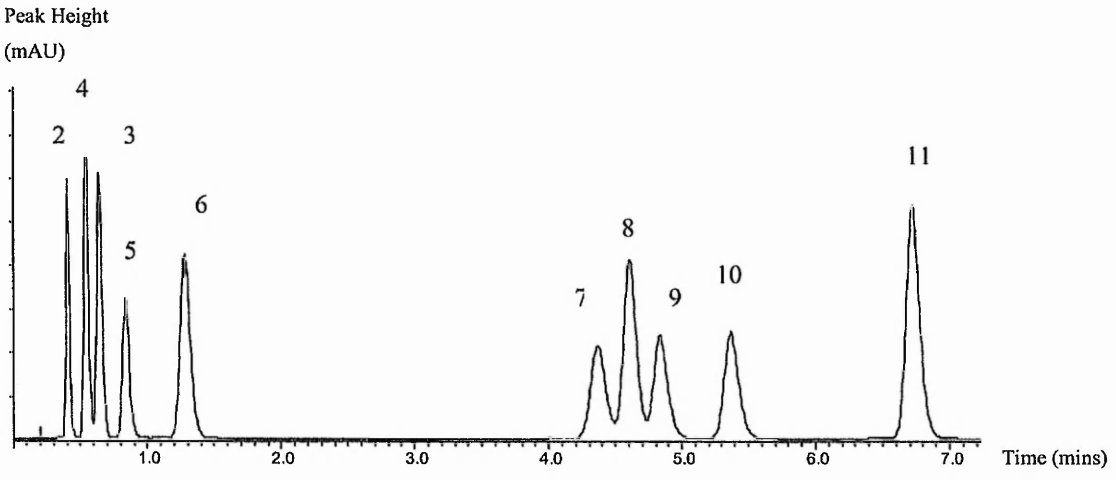

Figure 33. **DryLab predicted chromatogram for 5 µm HyPURITY C18 50 x 2.1 mm column at 0.7 ml/min**

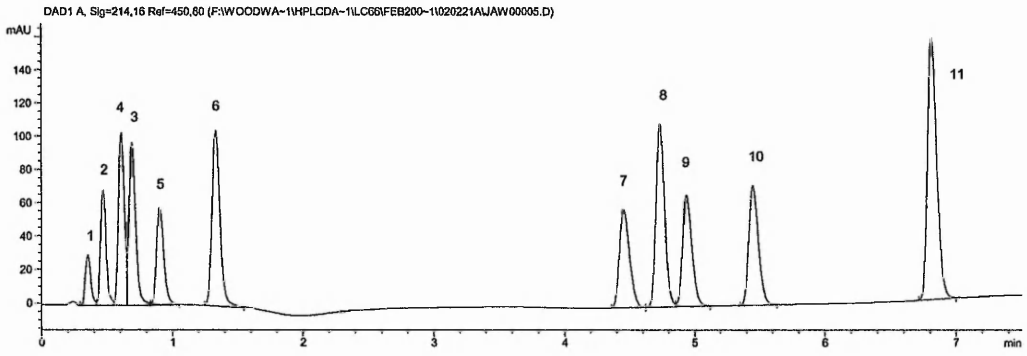

Figure 34. **Obtained chromatogram for 5 µm HyPURITY C18 50 x 2.1 mm column at 0.7 ml/min**

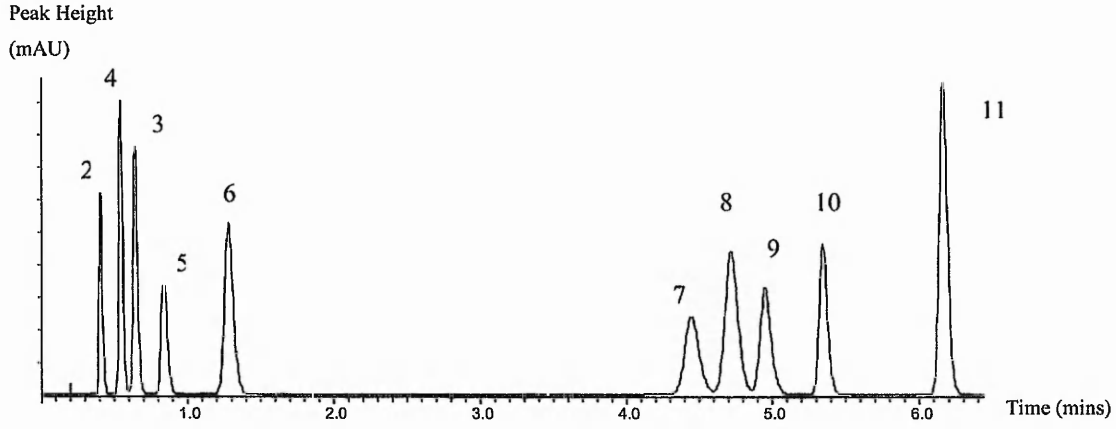

Figure 35. **DryLab predicted chromatogram for 3 µm HyPURITY C18 50 x 2.1 mm column at 0.7 ml/min**

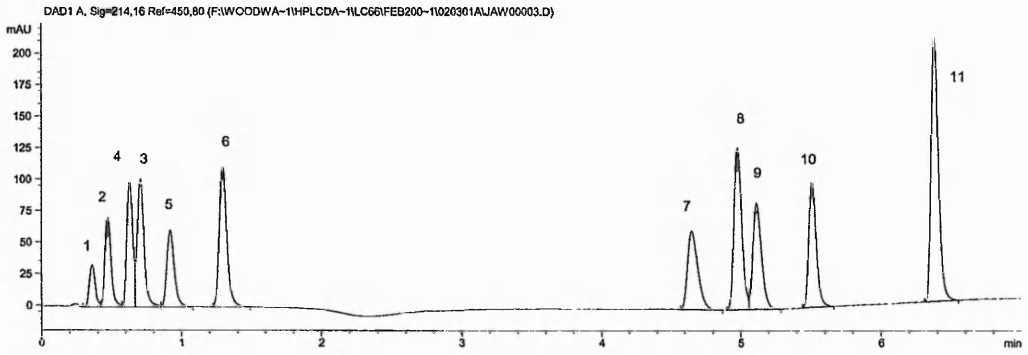

Figure 36. **Obtained chromatogram for 3 µm HyPURITY C18 50 x 2.1 mm column at 0.7 ml/min**

Pressure profiles obtained during 20 minute linear gradients at 30, 60 and 80°C on a 5 µm HyPURITY C18 150 x 4.6 mm column are shown in Figures 37-39.

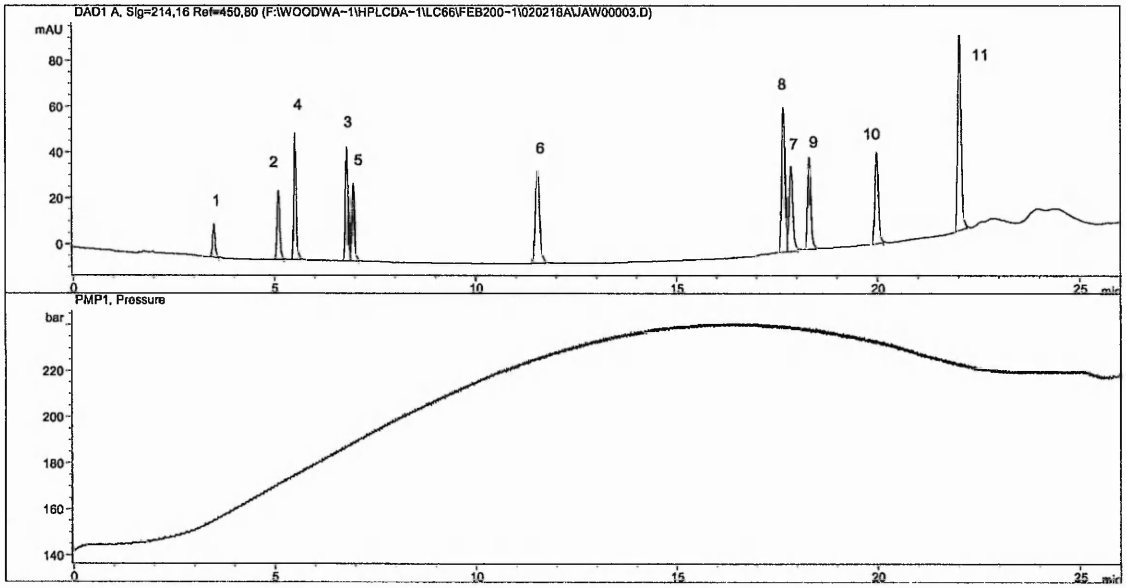

Figure 37. Pressure profile at 30°C

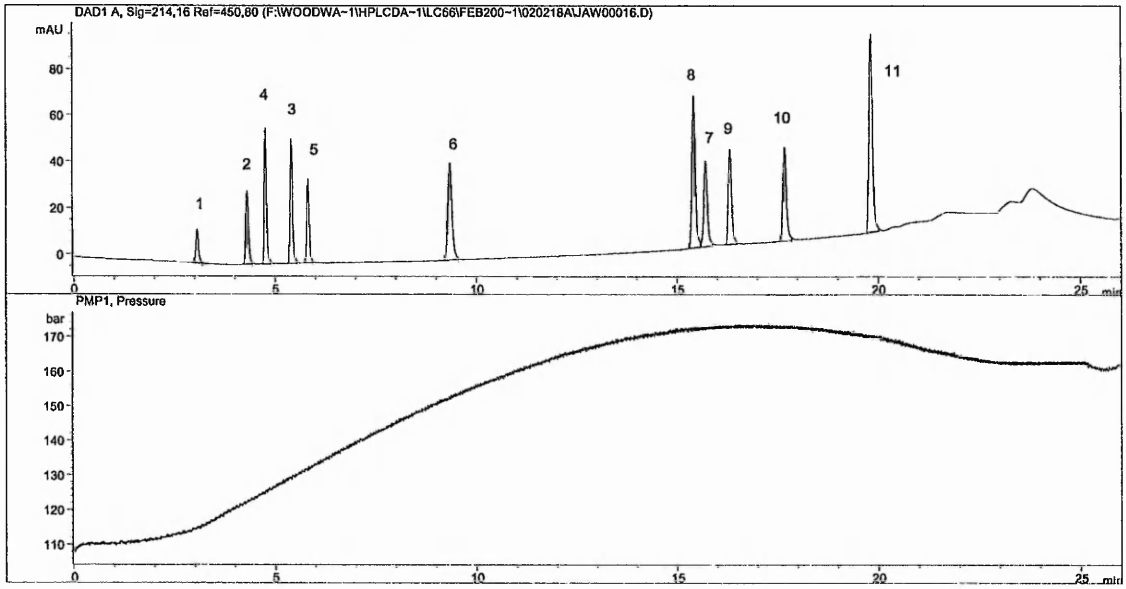

Figure 38. Pressure profile at 60°C

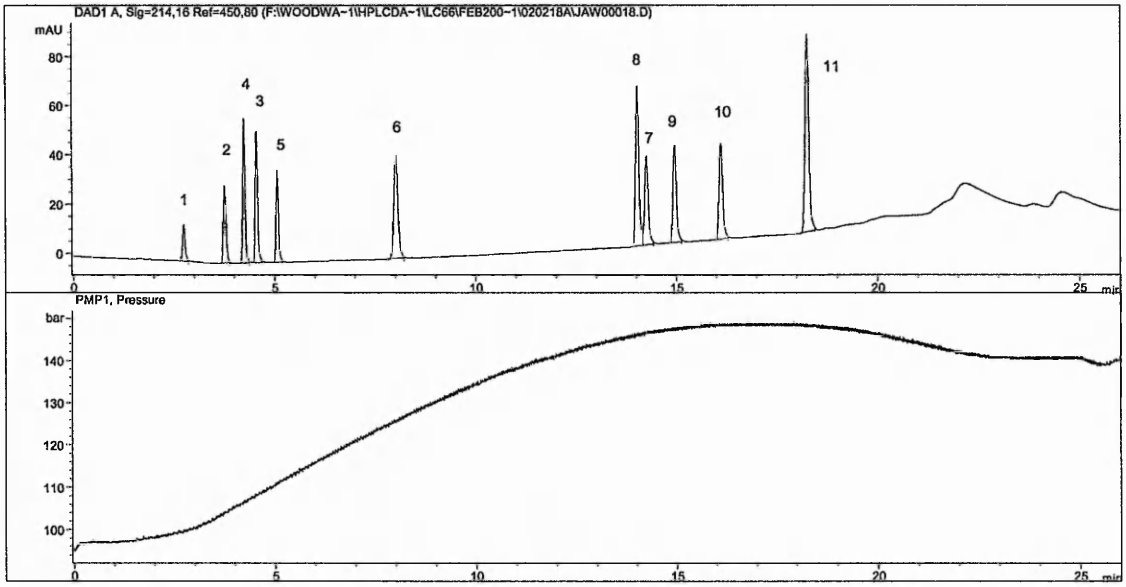

Figure 39. Pressure profile at 80°C

The change in pressure with increasing temperature is summarised in Table 3.

Table 3. Pressure change with increasing temperature

Temperature (°C)	Pressure (Bar) 5% Mobile Phase B	Pressure (Bar) 100% Mobile Phase B
30	142	240
60	108	172
80	95	149

These results show that a significant drop in column pressure can be obtained when operating at high temperature. This is due to a decrease in viscosity of the mobile phase. The importance of the drop in pressure is that when transferring methods on to a column of smaller dimensions but with the same packing material, it is possible to operate these short columns at high flow rates when using high temperatures. The DryLab data for the 5 µm HyPURITY C18 50 x 2.1 mm column showed that the optimum separation was achieved at 75°C. To obtain the same separation on a reduced internal diameter column as that obtained on the 4.6 mm internal diameter column would require using a linear velocity. For a 2.1 mm internal diameter column this equates to a flow rate of 0.208 ml/min. The use of short columns allows for an increase

in flow rate before the column achieves a higher pressure. Figures 40 and 41 below show the pressure profiles obtained using the 5 µm HyPURITY C18 50 x 2.1 mm column at 75°C at flow rates of 0.7 and 1.0 ml/min over a 10 minute linear gradient.

It was not possible to operate the 3 µm column at as high a flow rate as the 5 µm packing material due to the increase in pressure associated with reduced particle size packing material. Pressure profiles were obtained at 0.5 and 0.7 ml/min for the 3 µm HyPURITY C18 50 x 2.1 mm column at 75°C. These are shown in Figures 42 and 43. The change in pressure with increasing flow rate for the 3 µm and 5 µm HyPURITY 50 x 2.1 mm C18 column at 75°C is summarised in Table 4.

Table 4. Pressure change with increasing flow rate

Particle Size (µm)	Flow Rate (ml/min)	Pressure (Bar) 5% Mobile Phase B	Pressure (Bar) 100% Mobile Phase B
3	0.5	106	160
3	0.7	145	218
5	0.7	84	130
5	1.0	117	181

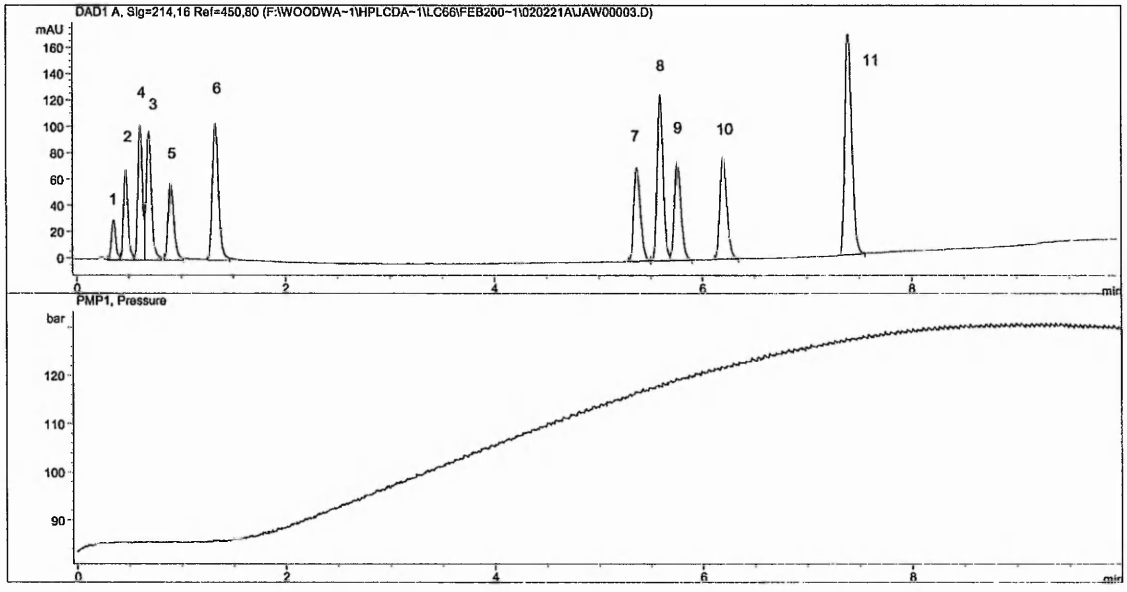

Figure 40. Pressure profile for 5 µm HyPURITY C18 50 x 2.1 mm column at 75°C at flow rate of 0.7 ml/min

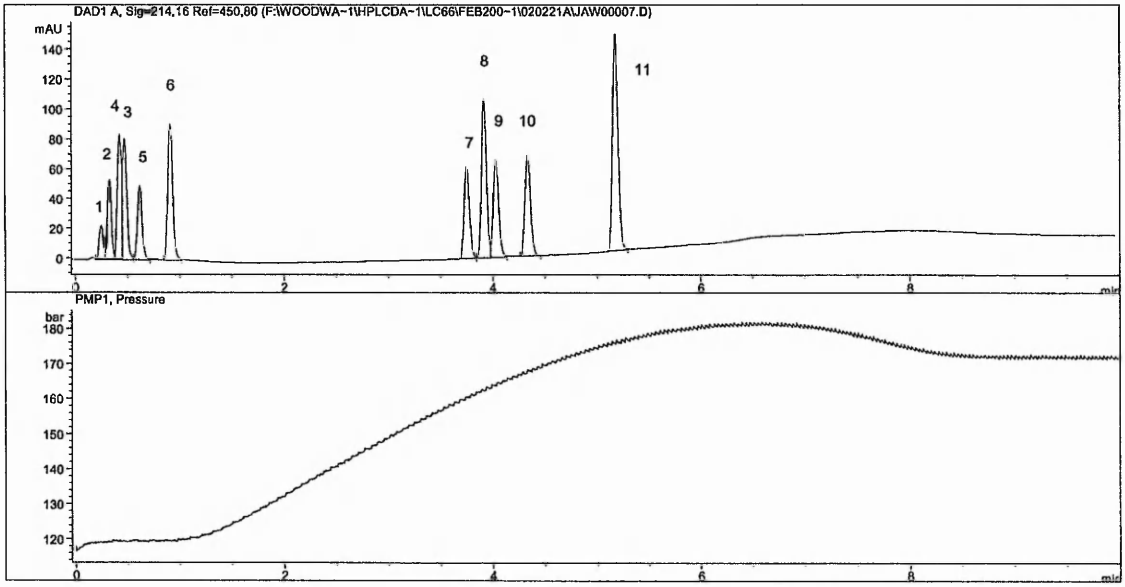

Figure 41. **Pressure profile for 5 µm HyPURITY C18 50 x 2.1 mm column at 75°C at flow rate of 1.0 ml/min**

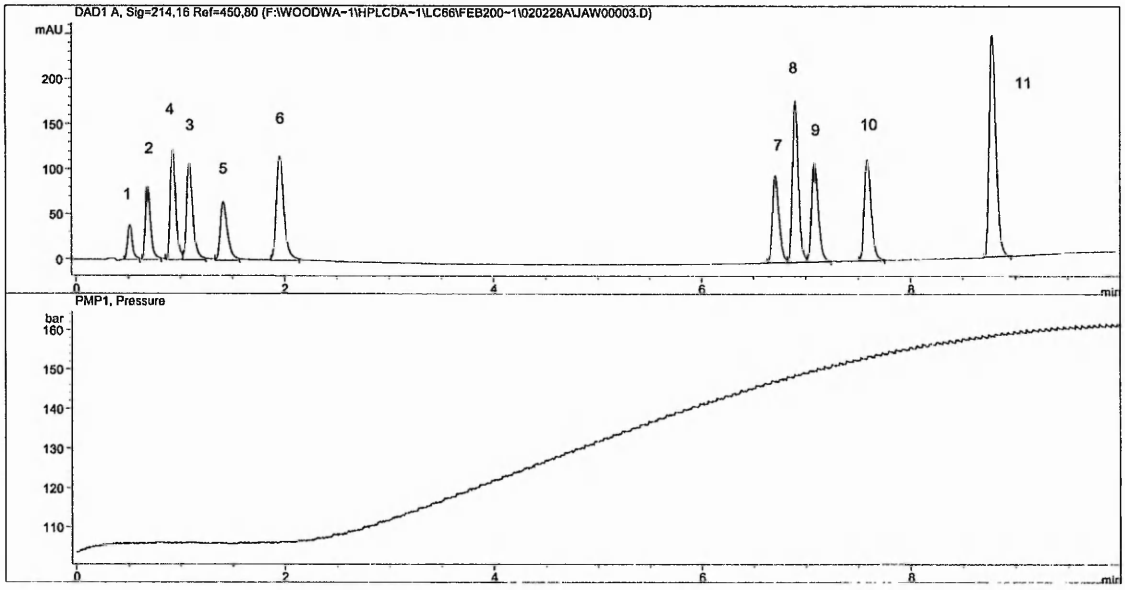

Figure 42. **Pressure profile for 3 µm HyPURITY C18 50 x 2.1 mm column at 75°C at flow rate of 0.5 ml/min**

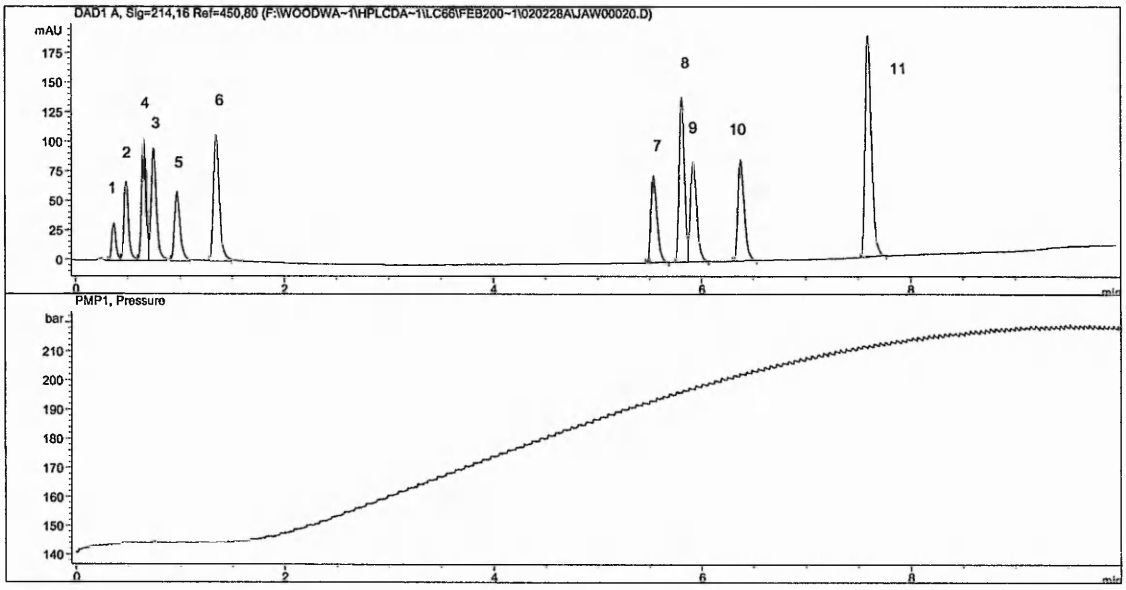

Figure 43. Pressure profile for 3 µm HyPURITY C18 50 x 2.1 mm column at 75°C at flow rate of 0.7 ml/min

The data in Table 4 show that operating a 3 µm column at 0.7 ml/min will produce a higher column pressure than operating a 5 µm column at 1.0 ml/min. This allows the development of a faster method on a 5 µm column. However, where extra efficiency is required, for example in separating two close eluting analytes, the use of a 3 µm column may be preferable.

5.1.3 Effect of Flow Gradients

The data from Drylab in section 5.1.2 showed that when analysing the 10 base mix on a linear gradient, two distinct groups of peaks were present. The hydrophilic peaks were early eluters with the lipophilic peaks eluting together much later. To try to reduce the time between the hydrophilic and lipophilic analytes flow gradients were used. By using a flow gradient it is possible to have a low flow rate during a critical separation with a higher flow rate between peaks which are well resolved to reduce the dead time of the separation. The chromatogram of the 10 base mix obtained using the 5 µm

HyPURITY C18 50 x 2.1 mm column at 75°C with a linear gradient of 5 to 100% mobile phase B over 10 minutes at a flow rate of 0.7 ml/min is shown in Figure 44.

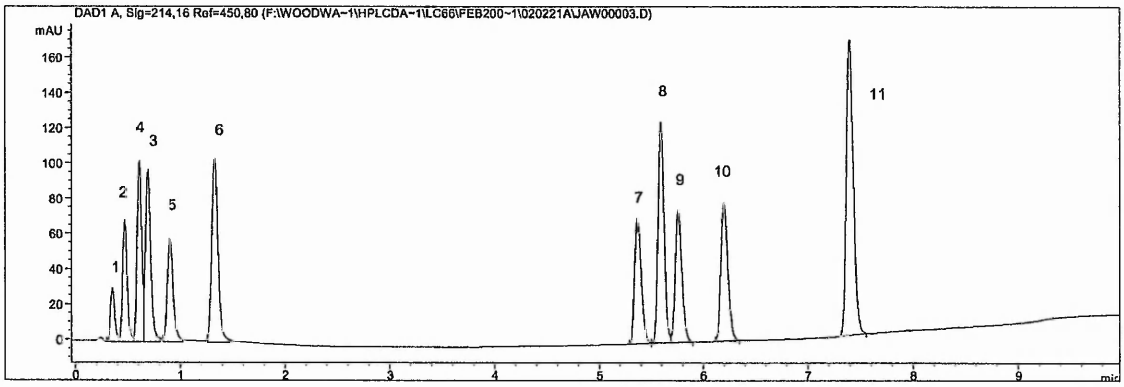

Figure 44. Chromatogram of 10 base mix with linear gradient at 0.7 ml/min

The vast time difference between peaks 6 and 7 can clearly be seen in Figure 44. It can also be seen that peaks 4 and 3 are not baseline resolved and the separation could be improved upon with the use of a lower flow rate during the elution of the hydrophilic bases, peaks 1 – 5.

To try to improve upon the separation above the gradient was altered as shown in Table 5.

Table 5. Modified Gradient Conditions 1

Time (mins)	% Mobile Phase B	Flow rate (ml/min)
0.00	5.0	0.5
1.50	19.5	0.5
3.00	33.5	0.7
10.00	100.0	1.0

The chromatogram obtained using these amended flow rates is shown in Figure 45.

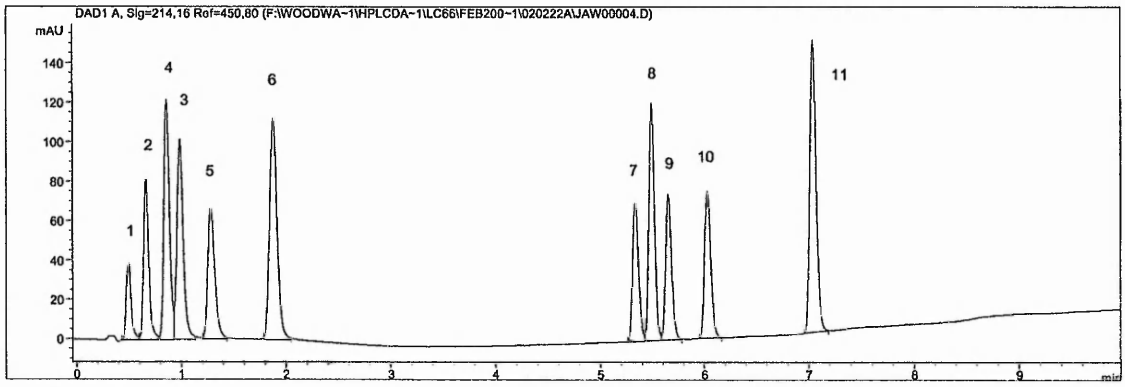

Figure 45. Flow gradient optimisation chromatogram 1

The chromatogram in Figure 45 shows that the separation between peaks 4 and 3 has improved, although they are not baseline resolved. Only a slight deterioration in separation between peaks 7, 8 and 9 was seen. The time between peaks 6 and 7 was not greatly reduced. Using this gradient the retention time of peak 11 has reduced by 0.3 minutes.

To try to improve upon the separation above and reduce the analysis time the gradient was altered as shown in Table 6.

Table 6. Modified Gradient Conditions 2

Time (mins)	% Mobile Phase B	Flow rate (ml/min)
0.00	5.0	0.5
1.00	14.5	0.5
1.01	14.6	1.0
3.00	33.5	1.2
4.00	43.0	1.5
10.00	100.0	1.5

The chromatogram obtained using these amended flow rates is shown in Figure 46.

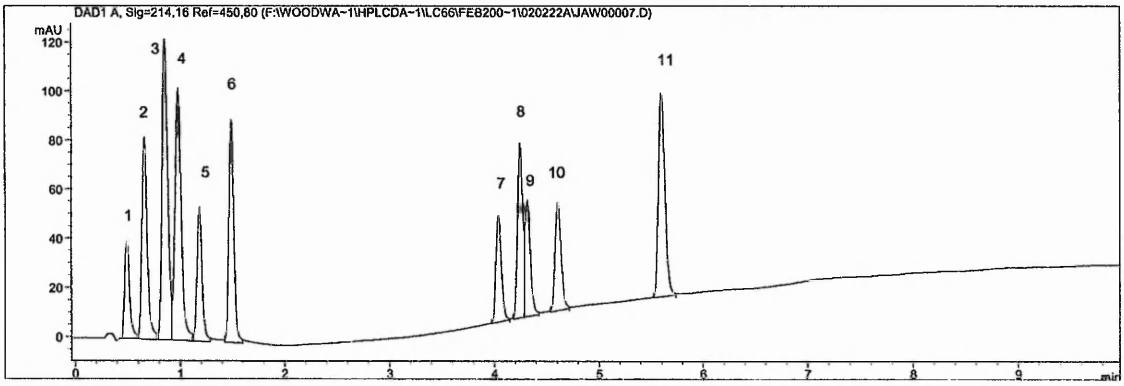

Figure 46. Flow gradient optimisation chromatogram 2

The chromatogram in Figure 46 shows that whilst the retention time of peak 11 has reduced by 1.7 minutes from that initially see in Figure 44, the separation of peaks 8 and 9 has deteriorated significantly.

The gradient was modified as shown in Table 7 to try to improve upon the separation of peaks 8 and 9 without significantly increasing the retention time of peak 11.

Table 7. Modified Gradient Conditions 3

Time (mins)	% Mobile Phase B	Flow rate (ml/min)
0.00	5.0	0.5
1.00	14.5	0.5
1.01	14.6	1.0
4.00	43.0	1.0
5.00	52.5	1.2
6.00	62.0	1.5
10.00	100.0	1.5

The chromatogram obtained using these amended flow rates is shown in Figure 47.

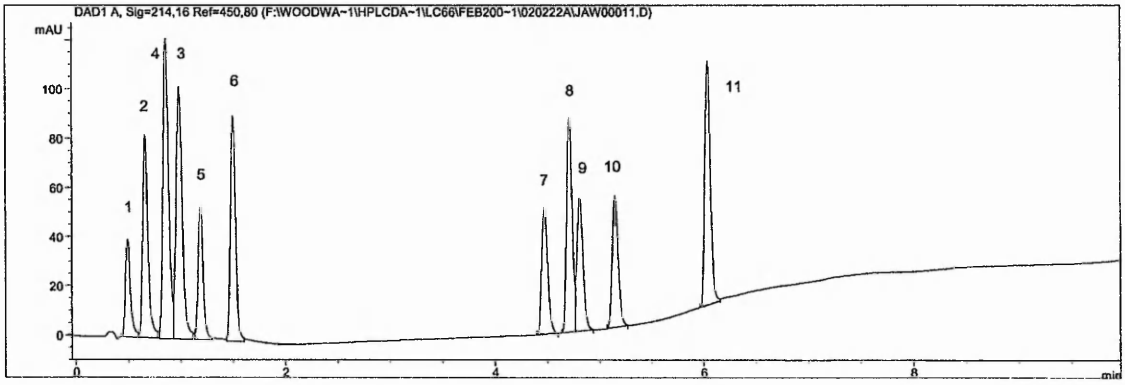

Figure 47. Flow gradient optimisation chromatogram 3

Figure 47 shows that whilst the separation between peaks 8 and 9 has improved, they are not well resolved. For compounds that differ widely in hydrophobicity it may not always be possible to remove the dead time in the chromatogram by the use of flow gradients without a compromise on resolution.

The example above used a linear gradient. By using a non-linear gradient and a flow gradient it may be possible to further improve the separation of the 10 base mix. The optimised gradient from DryLab for the analysis of the 10 base mix on the 5 µm HyPURITY C18 50 x 2.1 mm column at 75°C is shown in Table 8.

Table 8. Optimised Gradient from DryLab for Separation of 10 base mix

Time (mins)	% Mobile Phase B
0.00	5.0
0.50	30.0
1.20	30.0
2.20	30.0
3.18	41.0
10.00	100.0

The chromatogram obtained using this gradient is shown in Figure 48.

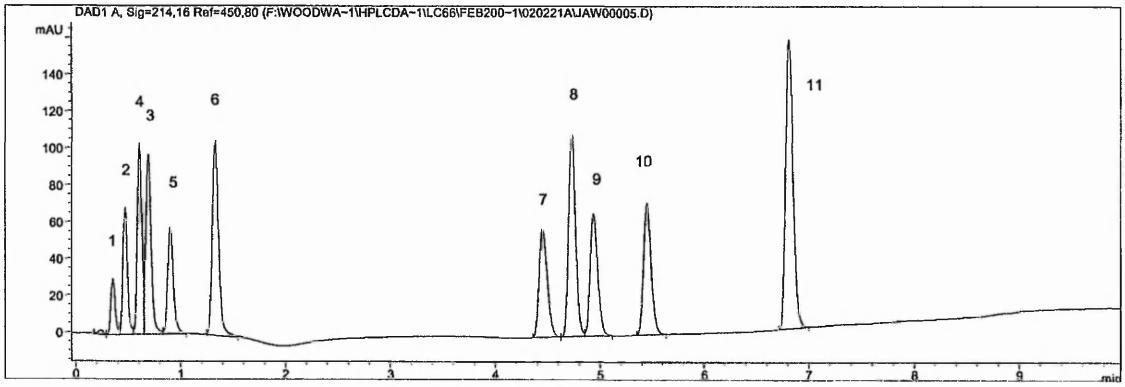

Figure 48. Gradient optimisation chromatogram

The optimised gradient alone does not reduce the dead time between the hydrophilic and lipophilic bases. By combining the power of gradient and flow optimisation the chromatogram may be improved. The new method conditions are shown in the Table 9.

Table 9. Method Conditions for Gradient and Flow Optimisation

Time (mins)	% Mobile Phase B	Flow rate (ml/min)
0.00	5.0	0.5
1.00	19.5	0.5
3.00	33.5	1.0
10.00	100.0	1.0

The chromatogram obtained using the optimised gradient and flow rate conditions is shown in Figure 49.

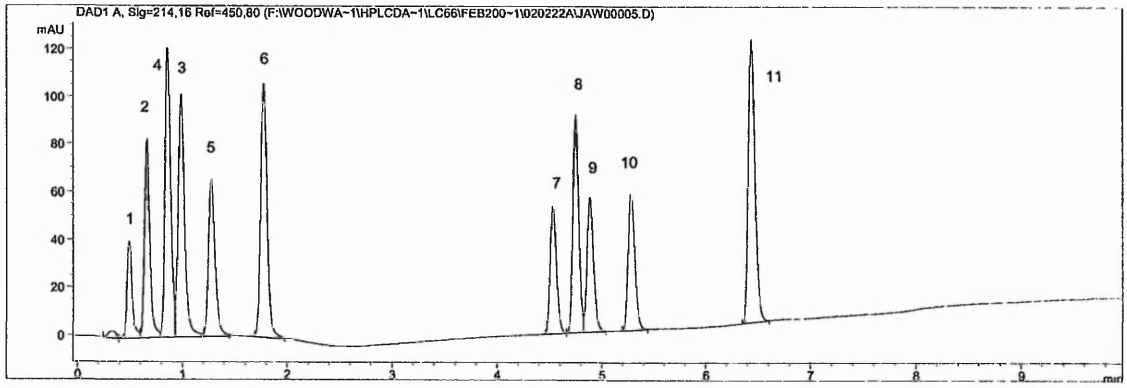

Figure 49. Flow and gradient optimisation chromatogram

The chromatogram above shows that whilst the power of gradient optimisation and flow gradients can be combined to achieve optimum peak separation, they are not always sufficient to reduce dead time in a chromatogram between compounds of widely different hydrophobicities.

5.1.4 Optimisation of LC hardware

The effect of detector flow cell dimensions, peak tubing dimensions and detector response times on retention time and peak shape characteristics was investigated.

5.1.4.1 Detector flow cells

For the Agilent Technologies 1100 diode array detector there are three types of flow cell that can be used. These have the following properties:

Standard flow cell – 10 mm path length, 13 µl volume, 120 bar pressure
Semi-micro flow cell – 6 mm path length, 4.5 µl volume, 120 bar pressure
High pressure micro flow cell – 6 mm path length, 1.7 µl volume, 400 bar pressure

The effect of flow cell dimensions on peak shape characteristics was investigated for a range of dimensions of the HyPURITY C18 column. Isocratic analysis of the hydrophilic and lipophilic base mixes were performed using 5% mobile phase B at linear velocity for the hydrophilic base mix and 70% mobile phase B at linear velocity for the lipophilic base mix. Injection volumes and flow rates were scaled appropriately depending on the dimensions of the column used as follows:

For 4.6 mm i.d. column: Injection volume = 85 µl, flow rate = 1.0 ml/min
For 3.0 mm i.d. column: Injection volume = 36 µl, flow rate = 0.425 ml/min
For 2.1 mm i.d. column: Injection volume = 18 µl, flow rate = 0.205 ml/min
For 1.0 mm i.d. column: Injection volume = 4 µl, flow rate = 0.047 ml/min

The injection scaling was performed to give the same detector response for all columns. This is due to the sensitivity increase obtained with a decrease in column diameter as the same sample mass is eluted in a smaller volume and therefore the concentration of the eluting peak is higher. All capillary tubing was kept the same throughout the detector flow cell optimisation.

The data are displayed in Tables 11-21 in the appendix and summarised in Figure 50 which shows the change in efficiency of terbutaline for each type of flow cell on a selection of column dimensions.

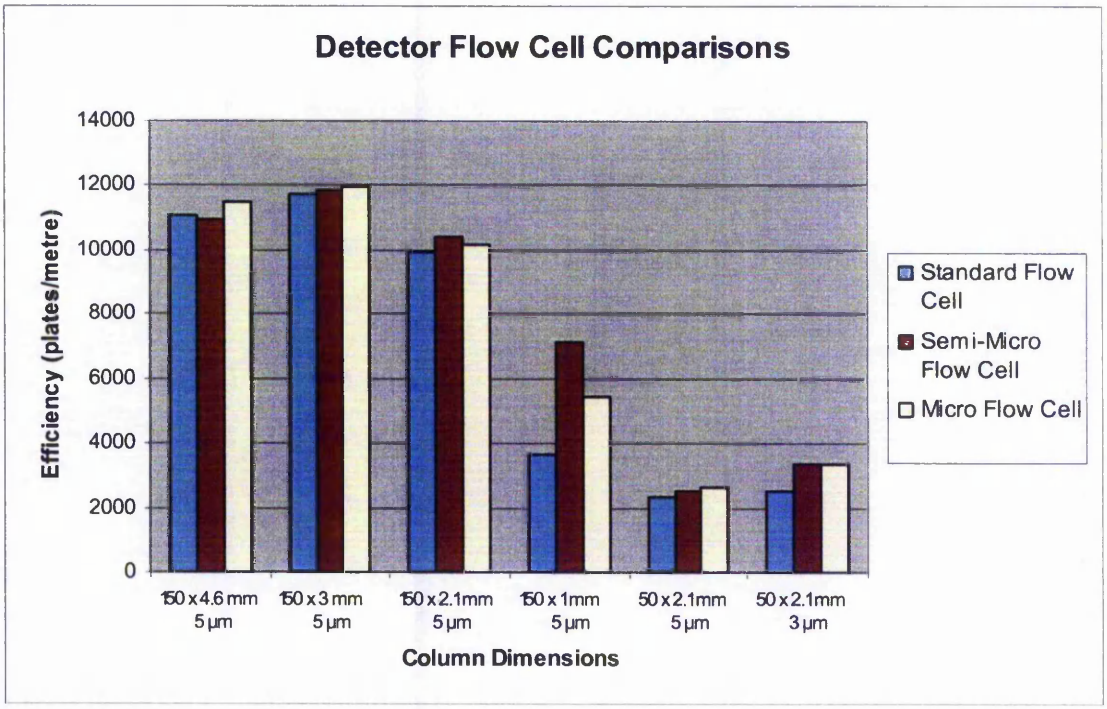

Figure 50. Change in efficiency with column dimension for different flow cells

The decrease in efficiency observed with a decrease in internal diameter of the 150 mm length column is a function of the extra column band broadening effects becoming more significant. The reduced volume flow cells were shown to offer greatest improvement in efficiency with short and narrow columns. Figure 51 shows the effect of changing

flow rate on the efficiency of terbutaline for each of the detector flow cells using short narrow columns.

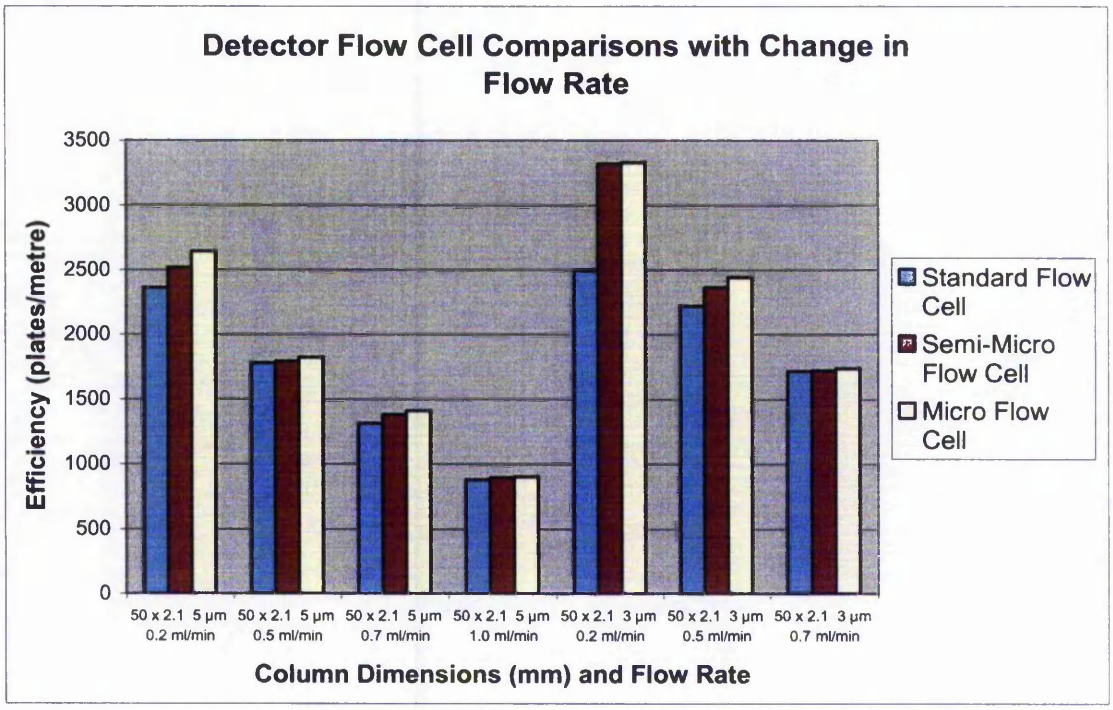

Figure 51. Change in efficiency with flow rate for different flow cells

The data show that the improvement in efficiency achieved by using a reduced volume flow cell is reduced with an increase in flow rate. The drop off in efficiency is more pronounced with the 3 µm column. These results above were all obtained using the default settings for the response time of the detector of 2 seconds, which may explain the drop off in efficiency with increasing flow rate. This is discussed in more detail in section 5.1.4.4.

As the micro and semi-micro flow cells have a reduced path length of 6 mm, the response obtained is only 60% of that obtained using the standard flow cell. Hence it is not always beneficial to use flow cells of reduced volume, especially where sensitivity is an issue. The choice of flow cell to use is often a compromise between sensitivity and efficiency.

5.1.4.2 Detector flow cell linearity

The linearity of each of the detector flow cells was assessed by injecting 100 µl terbutaline sulphate at concentrations of 50 – 1000 µg/ml on a 5 µm HyPURITY C18 150 x 4.6 mm column. Isocratic analysis was performed using 5% mobile phase B at a flow rate of 1.0 ml/min. This was to determine whether the detector saturation changes with a change in path length. The linearity plot obtained for each of the flow cells is shown in Figure 52.

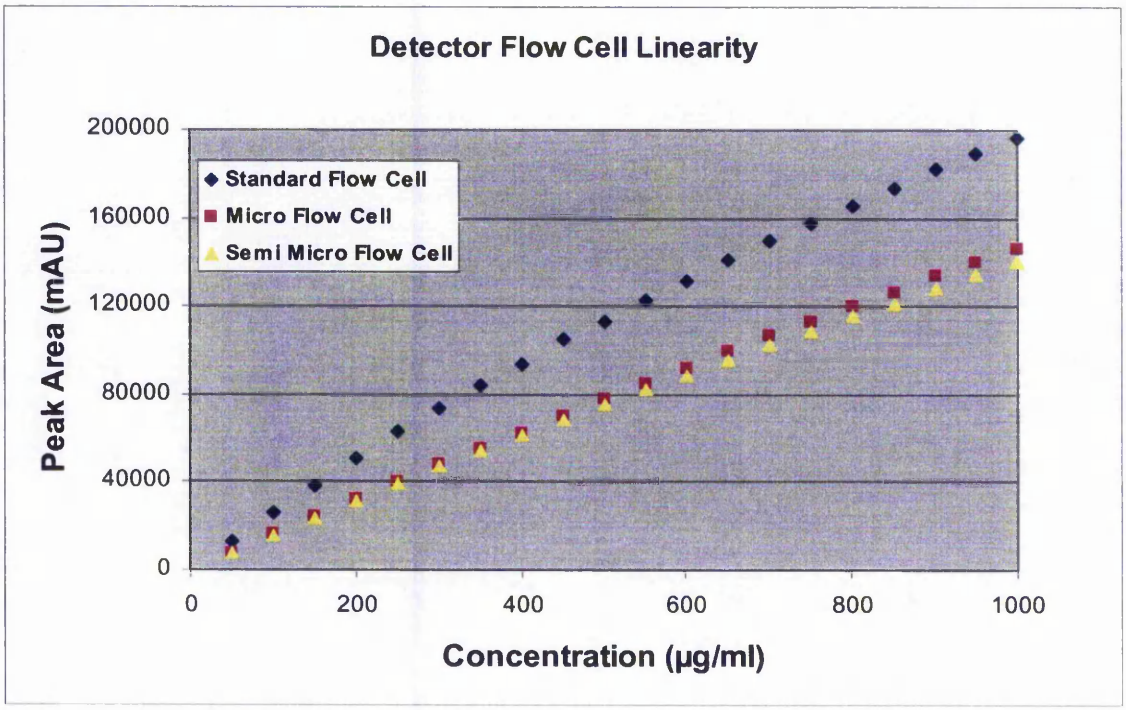

Figure 52. Linearity of detector flow cells

The results show that all flow cells are linear up to a response of approximately 80000 mAU. For the standard flow cell the linear range is 50 - 350 µg/ml, where as for the semi-micro and micro flow cells the linear range is 50 - 550 µg/ml. This shows that linearity is based on response and not concentration, showing that detector saturation does change with a change in path length.

5.1.4.3 PEEK Tubing

The effect of post column PEEK tubing dimensions on peak shape characteristics was investigated. Isocratic analysis of the hydrophilic base mix at 1.65 µg/ml was performed on the 3 µm HyPURITY C18 50 x 2.1 mm column using 5% mobile phase B, an injection volume of 18 µl and a micro flow cell with a volume of 1.7 µl in the diode array detector. The length and internal diameter of the PEEK tubing was altered and peak shape assessed for the hydrophilic bases and phenol. The internal diameter tubing tested was 0.127 and 0.254 mm at lengths of 115, 230 and 690 mm. Figure 53 shows the effect of PEEK tubing dimensions (and volume) on column efficiency at linear and high linear velocities for terbutaline. The data obtained for the hydrophilic bases and phenol is displayed in Tables 22 – 23 in the appendix.

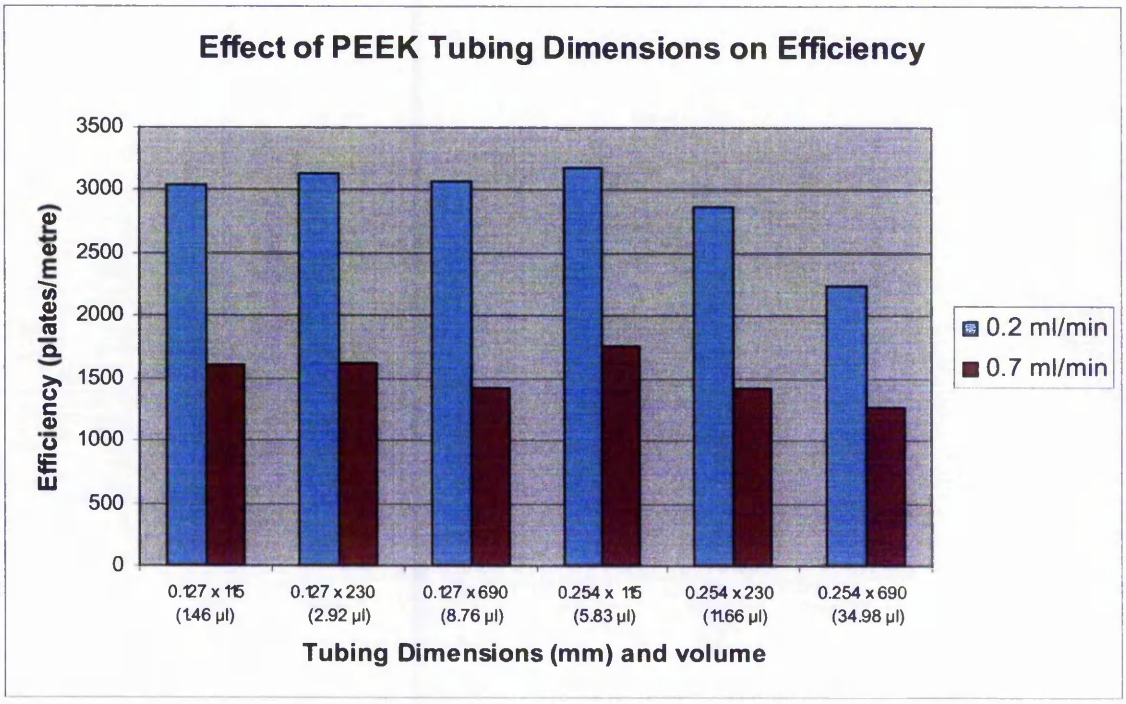

Figure 53. Effect of PEEK tubing dimensions on column efficiency

The results show that the decrease in efficiency with tubing length was more pronounced with the wider internal diameter tubing. Efficiency with the narrow internal diameter tubing was only seen to deteriorate with length of tubing at high linear velocity. These results show the importance of minimising post column tubing length and internal diameter for good efficiency.

5.1.4.4 Detector response times

The detector response time describes how fast the detector signal follows a sudden change in absorbance in the flow cell. The peak width is defined as the width of a peak, in minutes, at half the peak height. The peak width is set to the narrowest expected peak in the chromatogram. On an Agilent Technologies 1100 diode array detector the peak width sets the optimum response time. The peak detector ignores any peaks that are considerably narrower, or wider, than the peak width setting. The response time for a diode array detector is the time between 10% and 90% of the output signal.

For an Agilent Technologies 1100 diode array detector there are eight preset values for detector response time between 0.1 and 16 seconds. The effect of altering the response time on peak shape characteristics was investigated. Isocratic analysis of the hydrophilic base mix at 1.65 µg/ml was performed on the 3 µm HyPURITY C18 50 x 2.1 mm column using 5% mobile phase B, an injection volume of 18 µl and a micro flow cell in the diode array detector. Figure 54 shows the efficiency with change in response time at linear and high linear velocities. The data are displayed in Tables 24 – 25 in the appendix.

Choosing an appropriate detector response time is a balance between good efficiency and poor baseline due to over sampling. The results show that at 0.2 ml/min a response time of up to 2 seconds can be used before a rapid deterioration in efficiency is seen. However, when using high linear velocities it is important to select a more appropriate value. In this investigation, 0.5 seconds was optimum at 0.7 ml/min. This demonstrates the need to select an appropriate response time for the flow rate used and explains why a decrease in efficiency with increasing flow rate (Figure 51) was previously seen when assessing detector flow cells.

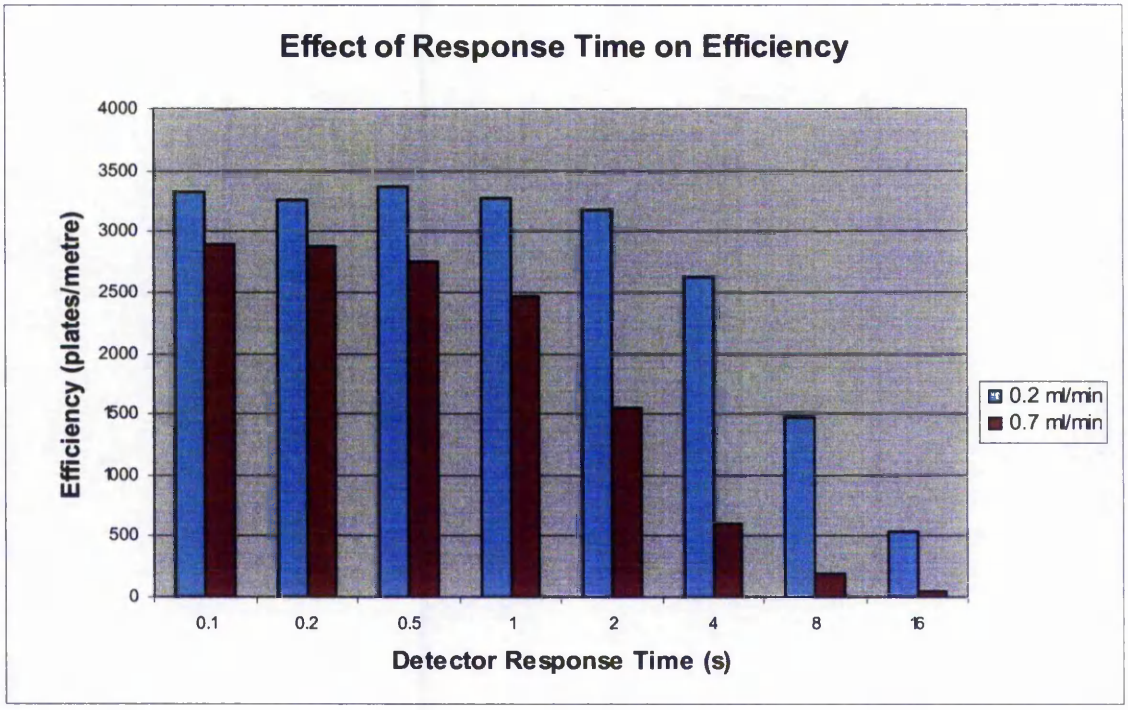

Figure 54. Change in efficiency with detector response time

5.1.5 Assessment of column format

To assess column format van Deemter type plots were constructed for the 3 µm HyPURITY 50 x 2.1 mm C18 column over the flow rate range 0.1 – 0.8 ml/min. Isocratic analysis was performed using 5% mobile phase B, injecting 18 µl terbutaline sulphate at 1.65 µg/ml. Figures 55 - 57 show efficiency, area and retention time plotted against flow rate at temperatures of 40, 60 and 80°C. The data are displayed in Table 26 in the appendix.

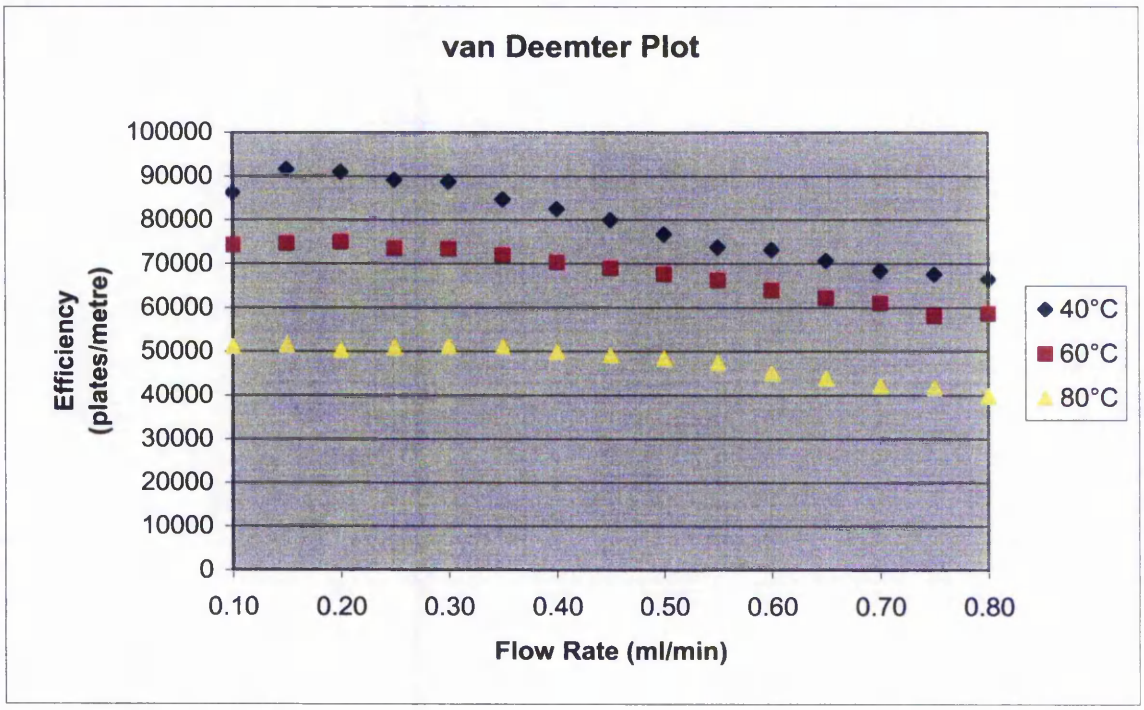

Figure 55. **van Deemter plot showing the effect of flow rate on efficiency**

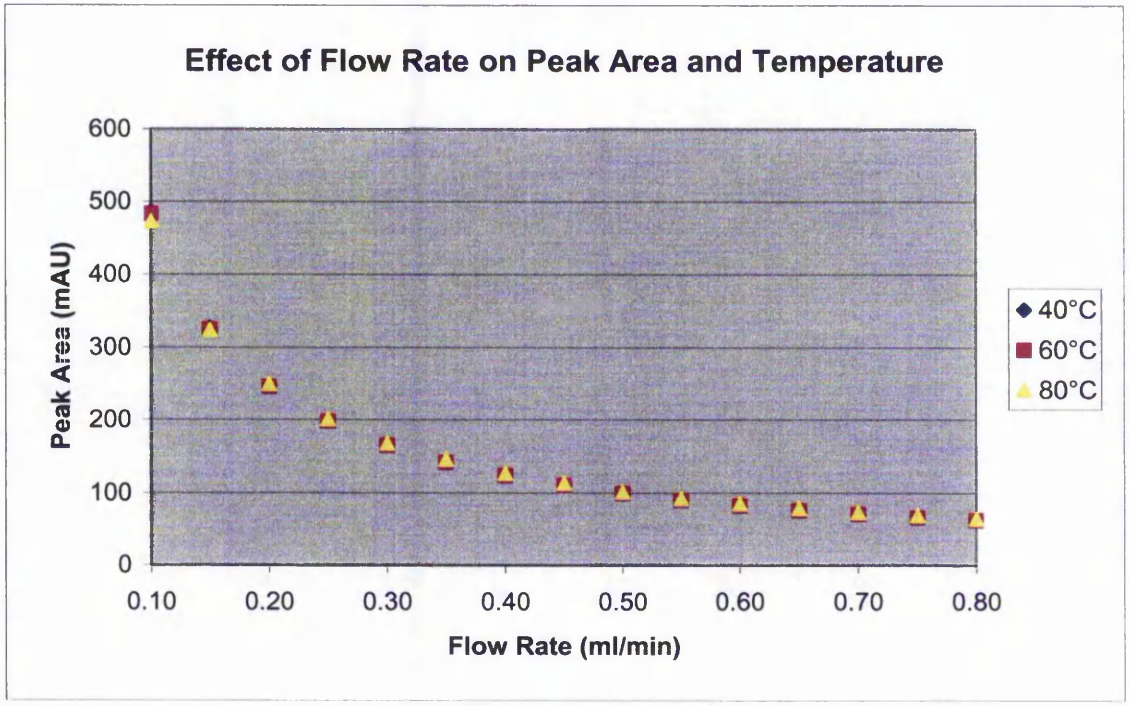

Figure 56. **Effect of flow rate on peak area and temperature**

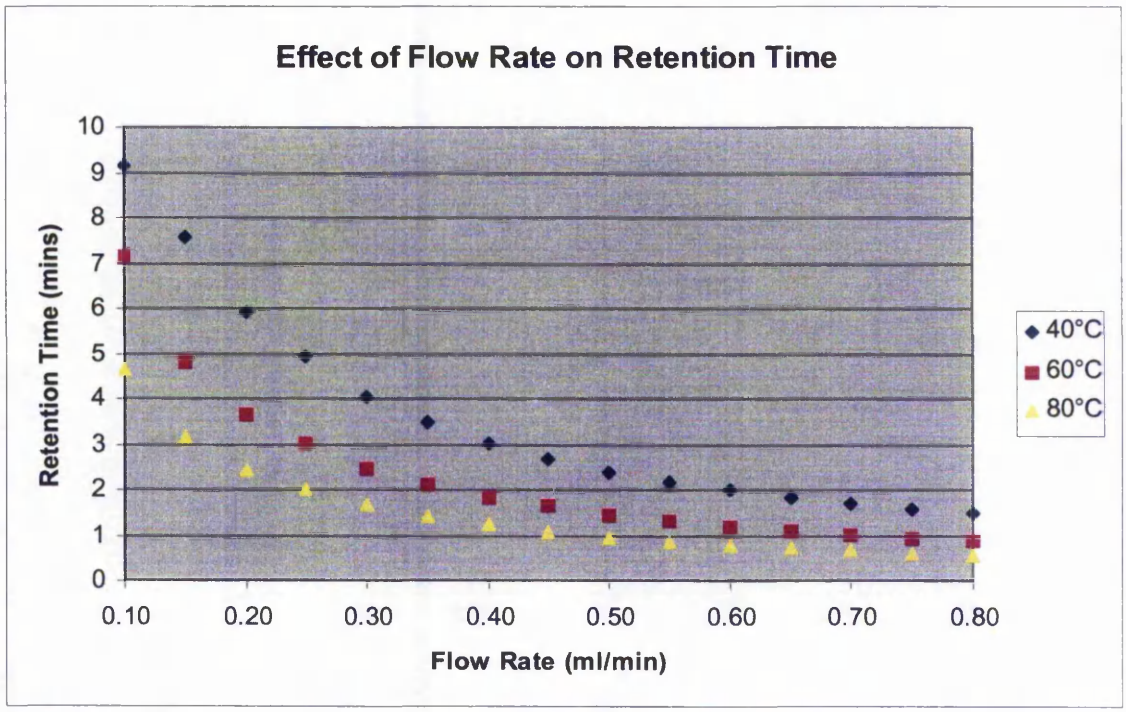

Figure 57. Effect of flow rate on retention time

The van Deemter plot in Figure 55 shows that for all temperatures the optimum flow rate for the 3 µm HyPURITY C18 50 x 2.1 mm column was 0.2 ml/min. At 60°C increasing the flow rate from 0.2 to 0.8 ml/min results in a decrease of approximately 19% in efficiency. An exponential decay in peak area with increasing flow rate is shown in Figure 56. However, increasing the temperature had no effect on peak area. Figure 57 shows an exponential decay in retention time with increasing flow rate. The decrease in retention time with increasing temperature represents approximately a 38.5% drop at 0.2 ml/min and 40.1% drop at 0.7 ml/min when going from 40°C to 60°C.

5.1.6 The use of overlap injection and CTC autosamplers

One of the time limiting steps in rapid analysis is the speed of the autosampler injection. In order to reduce the time taken to perform the injection we can either use an autosampler capable of performing fast injections or bury the injection time in the run time of the method. Three different autosamplers have been evaluated: CTC Analytics

HTC PAL autosampler, Agilent standard autosampler and the Agilent well-plate sampler as shown in sections 3.1.1.3 and 3.1.1.4.

Isocratic analysis was performed on the 3 µm HyPURITY C18 50 x 2.1 mm column using 5% mobile phase B, injecting 5 and 50 µl of terbutaline sulphate at injections speeds of 200 (default speed for Agilent Technologies autosamplers), 500 and 1000 µl/min (maximum speed for Agilent Technologies autosamplers). Concentrations were adjusted to ensure that the same amount was injected on column (6 µg/ml for 5 µl injections and 0.6 µg/ml for 50 µl injections). Injector timings and peak area percentage relative standard deviations (% RSDs) were determined for each of the three types of autosampler in standard mode and in overlap injection mode for the Agilent Technologies autosamplers. Injections in overlap mode were not performed on the CTC Analytics HTC PAL autosampler where the data shown are for the standard injection mode only. The results are shown in Figures 58 - 61.

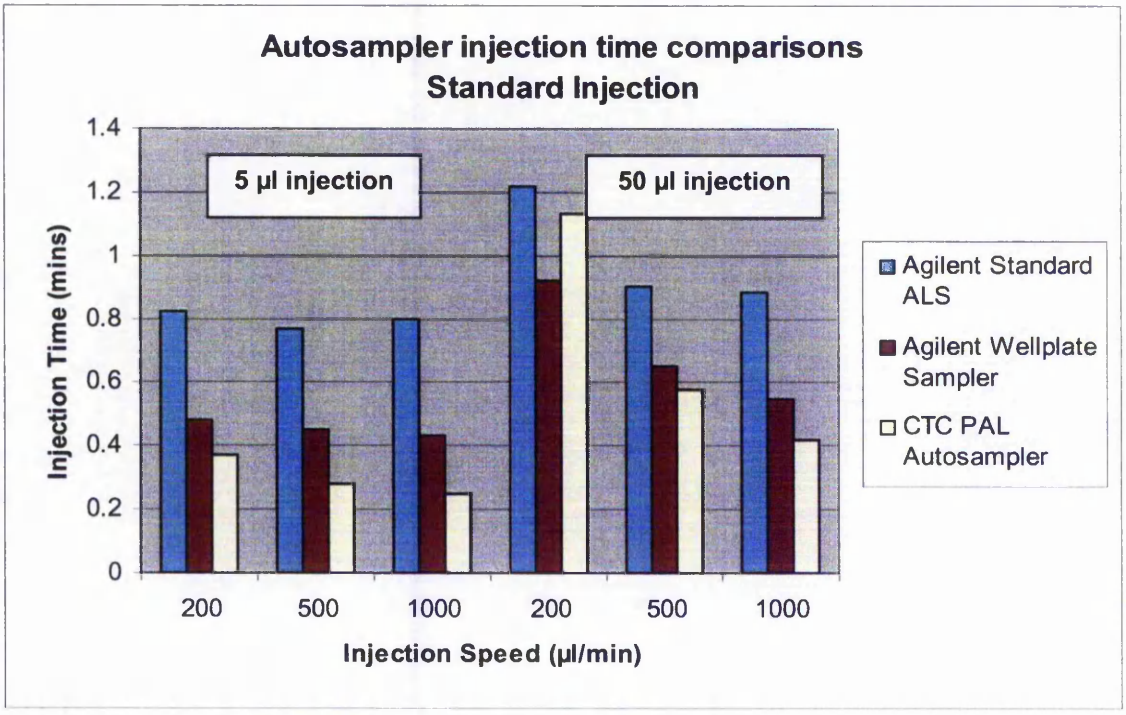

Figure 58. Autosampler injection time comparisons for standard injections

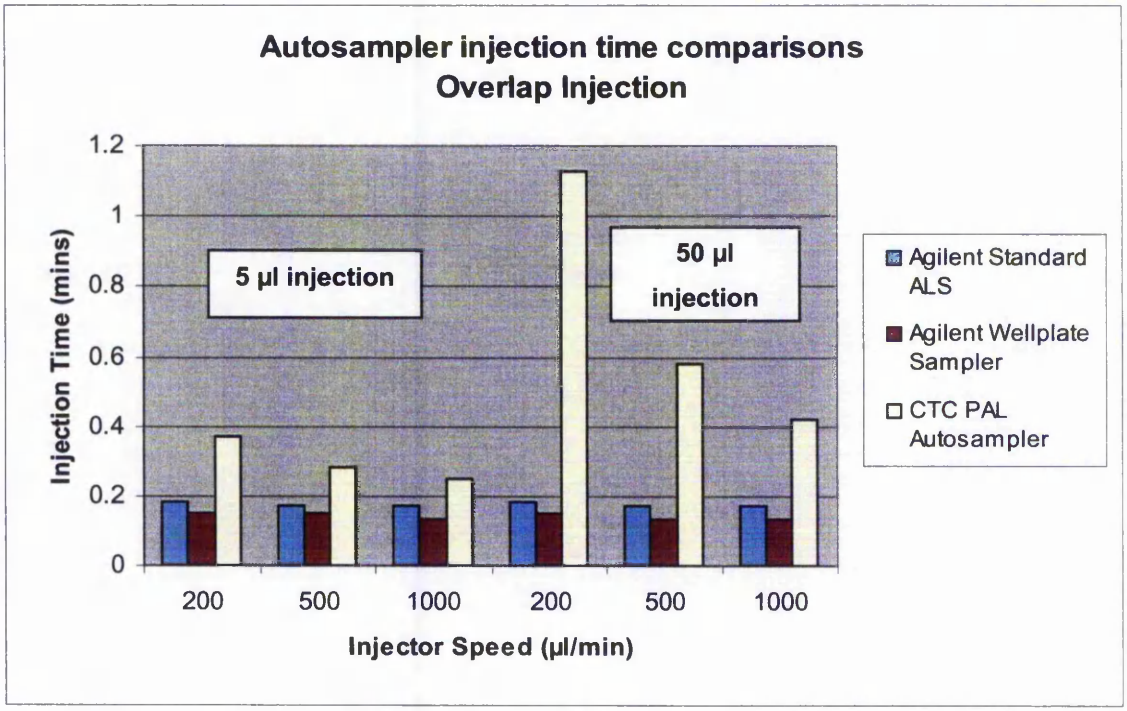

Figure 59. **Autosampler injection time comparisons for overlapped injections**

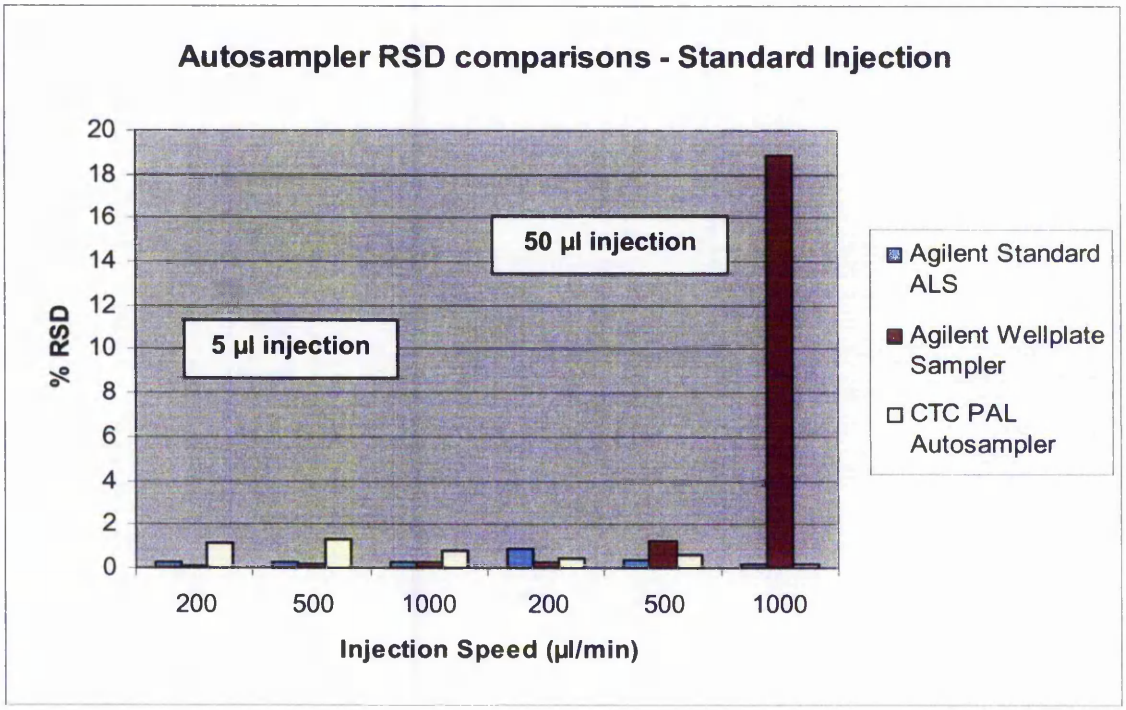

Figure 60. **Autosampler RSD comparisons for standard injections**

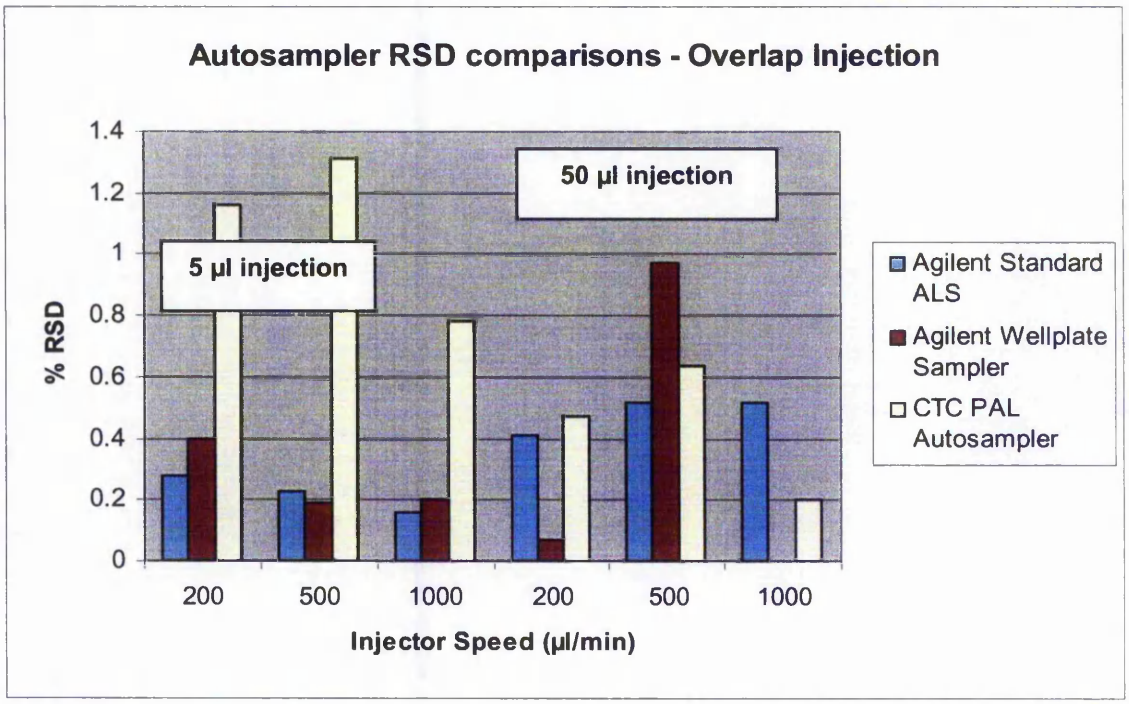

Figure 61. Autosampler RSD comparisons for overlapped injections

In standard injection mode for the 5 µl injection the CTC autosampler was the fastest at all injections speeds. For the 50 µl injections it was the fastest autosampler for speeds greater than the Agilent Technologies default. Using the overlap injection mode for the Agilent Technologies systems was shown to greatly reduce injection timings. The remaining time taken for the injection largely consisted of the time to balance the detector.

For the standard injection mode good RSDs were obtained for all injections except for large injection volumes at high injection speeds on the well plate sampler. This was due to air being drawn into the system which affected the chromatography. The use of the overlap injection mode did not deteriorate performance. However, at fast injections speeds of large injection volumes on the well plate sampler, an area RSD could not be obtained due to poor chromatography. The CTC Analytics HTC PAL autosampler gave the best performance at high injection speeds for large injection volumes. For high injection volumes the well plate sampler should be used at the low default injection speed setting of 200 µl/min only for good performance.

Using the overlap injection mode for the 50 µl injection on the standard Agilent Technologies autosampler at the default injection speed, had a time saving of 1 minute per injection when compared to the standard injection mode. For 100 injections this equates to a time saving of 100 minutes and a reduction in solvent consumption of 70 ml when performed at 0.7 ml/min, demonstrating the importance of reducing cycle times.

5.1.7 Column lifetime study

Using the 3 µm HyPURITY C18 50 x 2.1 mm column, 2000 injections of the hydrophilic base mix solution at 1.65 µg/ml were performed using isocratic analysis with 5% mobile phase B to assess how peak shape and retention time vary with increasing injection number. Figures 62 and 63 below show the chromatograms obtained initially and every 500 injections there after. The study was performed at 0.2 and 0.7 ml/min to see if a deterioration in performance is observed when operating at high linear velocities. The column oven was set to 60°C. A new column was used for each lifetime study.

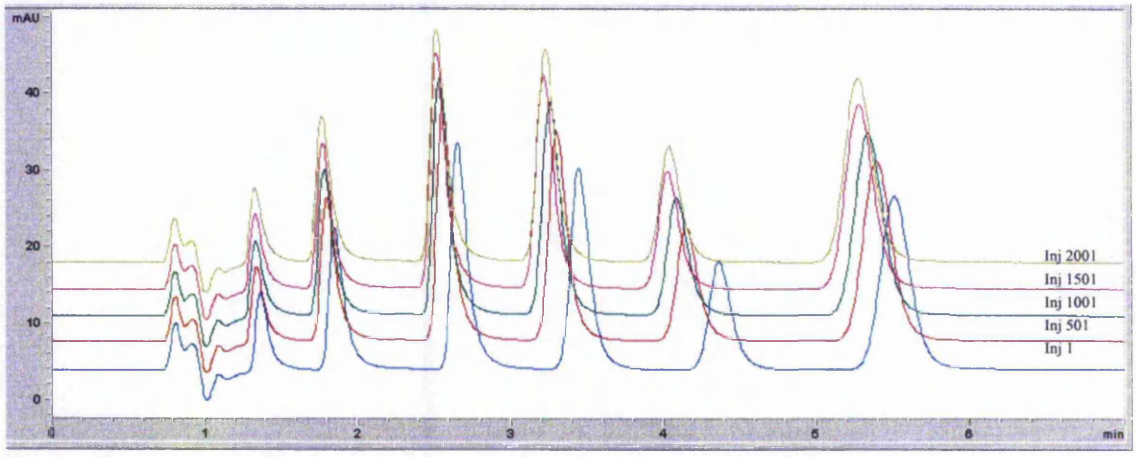

Figure 62. Column lifetime study at flow rate 0.2 ml/min

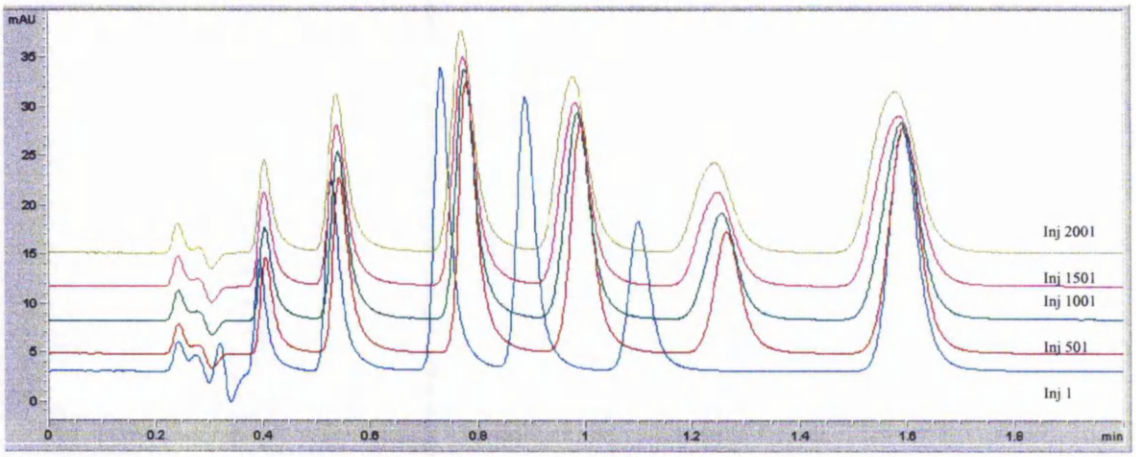

Figure 63. Column lifetime study at flow rate 0.7 ml/min

The column lifetime study at 0.2 ml/min showed a slight shift in retention time of the six components of the hydrophilic base mix. This stabilised after the first injection. No deterioration in peak shape was seen throughout the study. However, the column lifetime study performed at 0.7 ml/min showed that peak shape deteriorated quite badly throughout the run. Column efficiency, peak retention time and peak area have been looked at in more detail for the studies performed at 0.2 ml/min and 0.7 ml/min. The data are shown in Figures 64 – 69.

Figure 64 shows the drift in efficiency with increasing injection number for each of the components of the hydrophilic base mix at 0.2 ml/min. No significant change in efficiency was seen throughout the column lifetime study. Figure 65 shows the drift in retention time with increasing injection number for each of the components of the hydrophilic base mix at 0.2 ml/min. A slight decrease in retention time for all components of the hydrophilic base mix except nicotine was seen after the first injection. For subsequent injections the retention time remained stable. Figure 66 shows the drift in area with increasing injection number for each of the components of the hydrophilic base mix at 0.2 ml/min. No significant changes in area were seen throughout the column lifetime study. The relative standard deviation (RSD) across 2000 injections was 0.85% for terbutaline which represents good repeatability in area throughout the study. The RSD range for all components of the hydrophilic base mix was 0.33 – 1.5%.

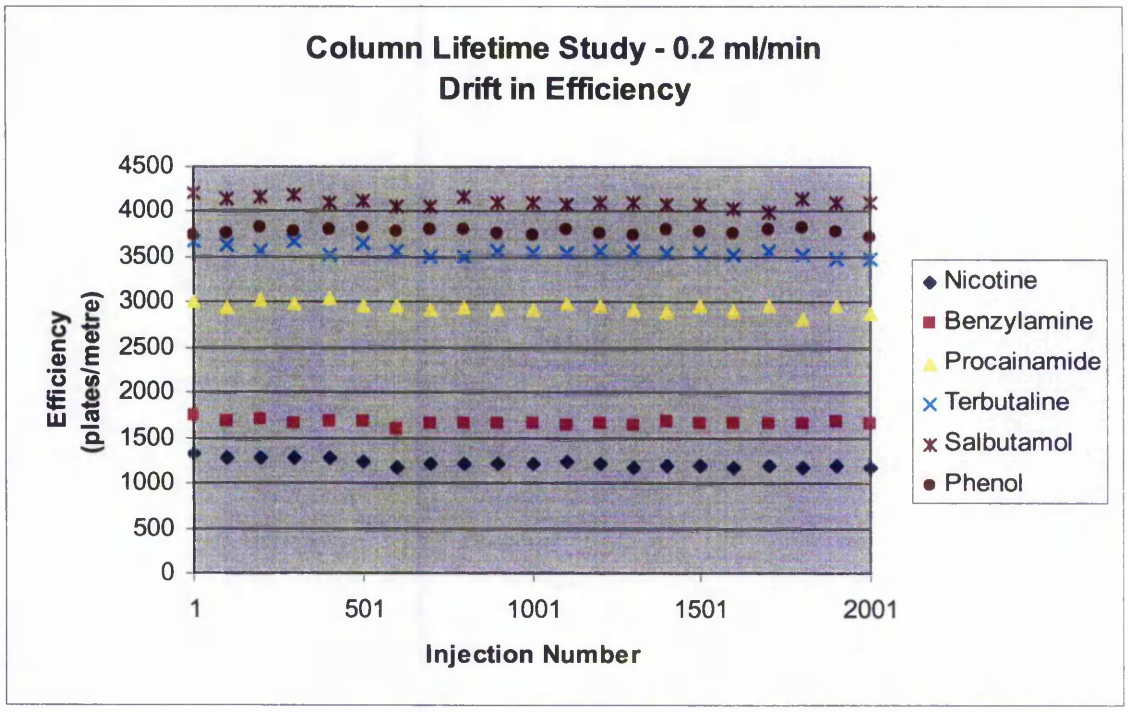

Figure 64. **Column lifetime study at 0.2 ml/min – drift in efficiency**

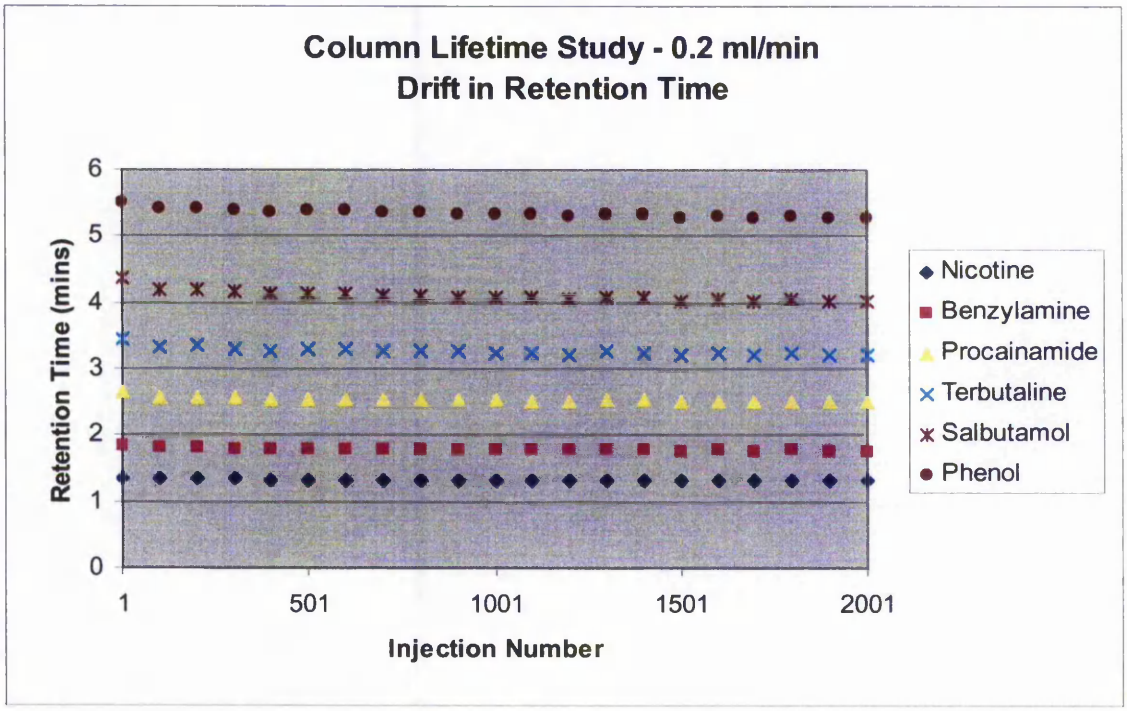

Figure 65. **Column lifetime study at 0.2 ml/min – drift in retention time**

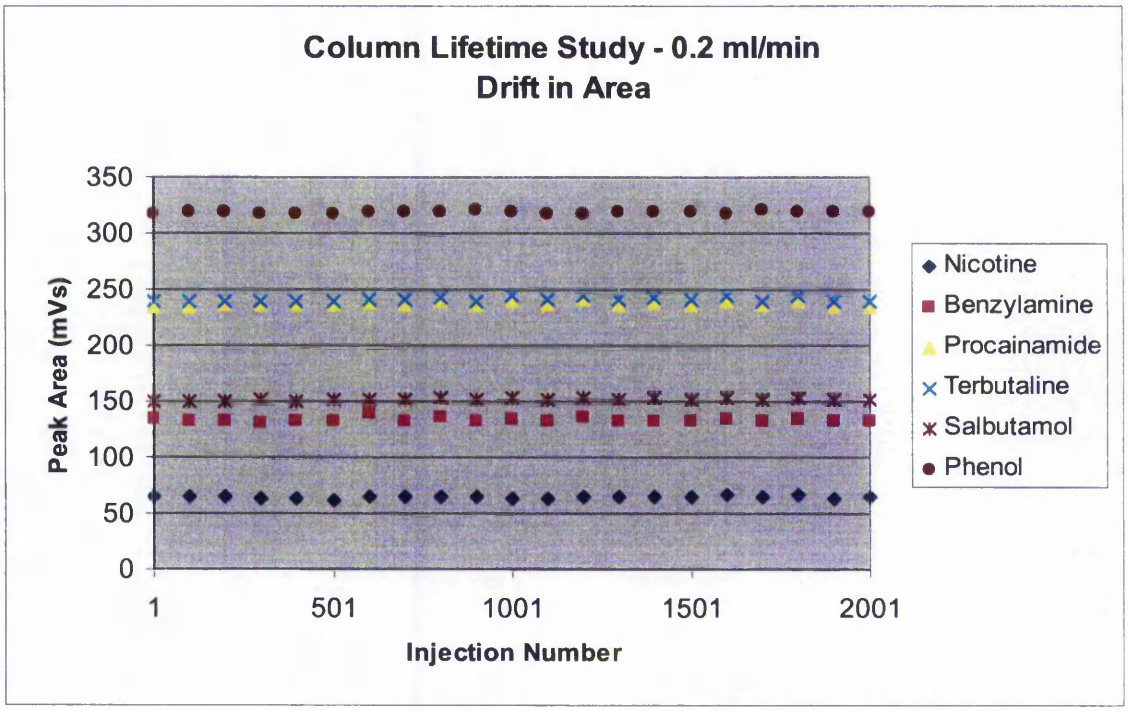

Figure 66. **Column lifetime study at 0.2 ml/min – drift in area**

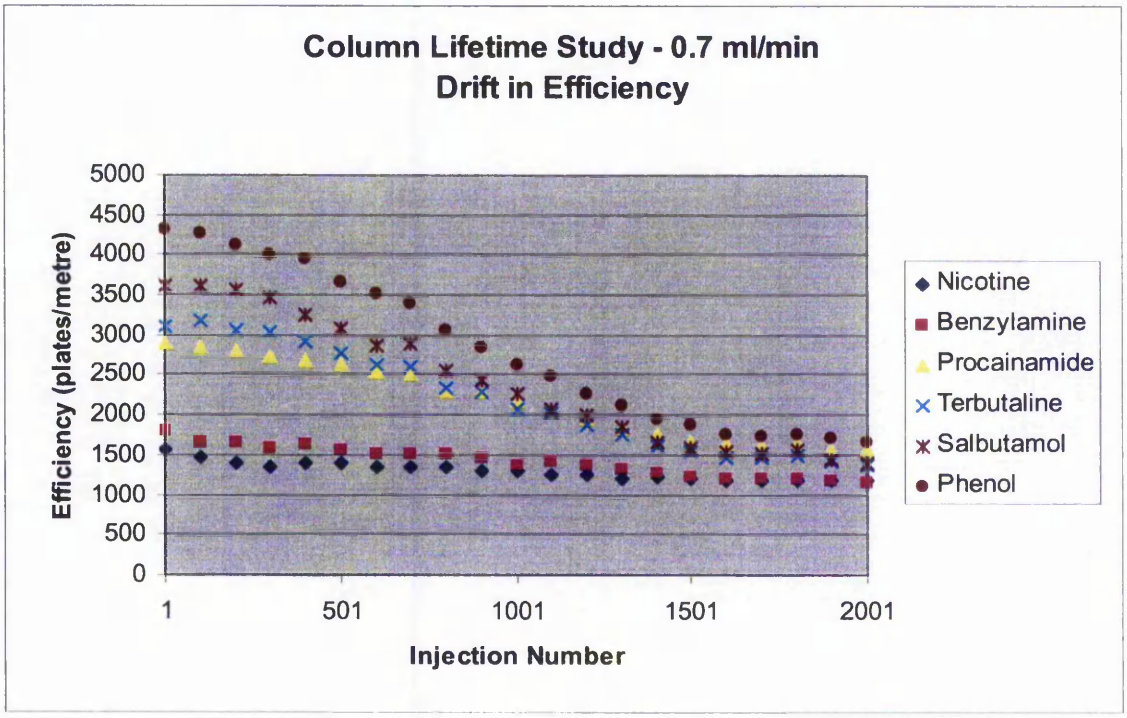

Figure 67. **Column lifetime study at 0.7 ml/min – drift in efficiency**

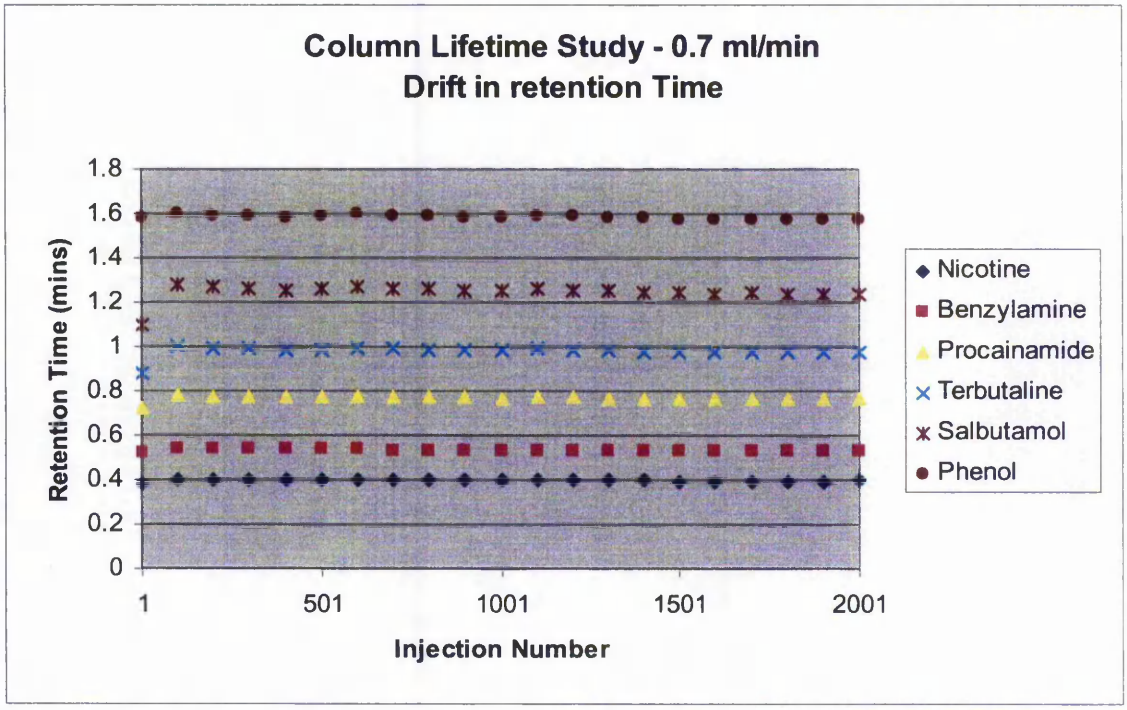

Figure 68. **Column lifetime study at 0.7 ml/min – drift in retention time**

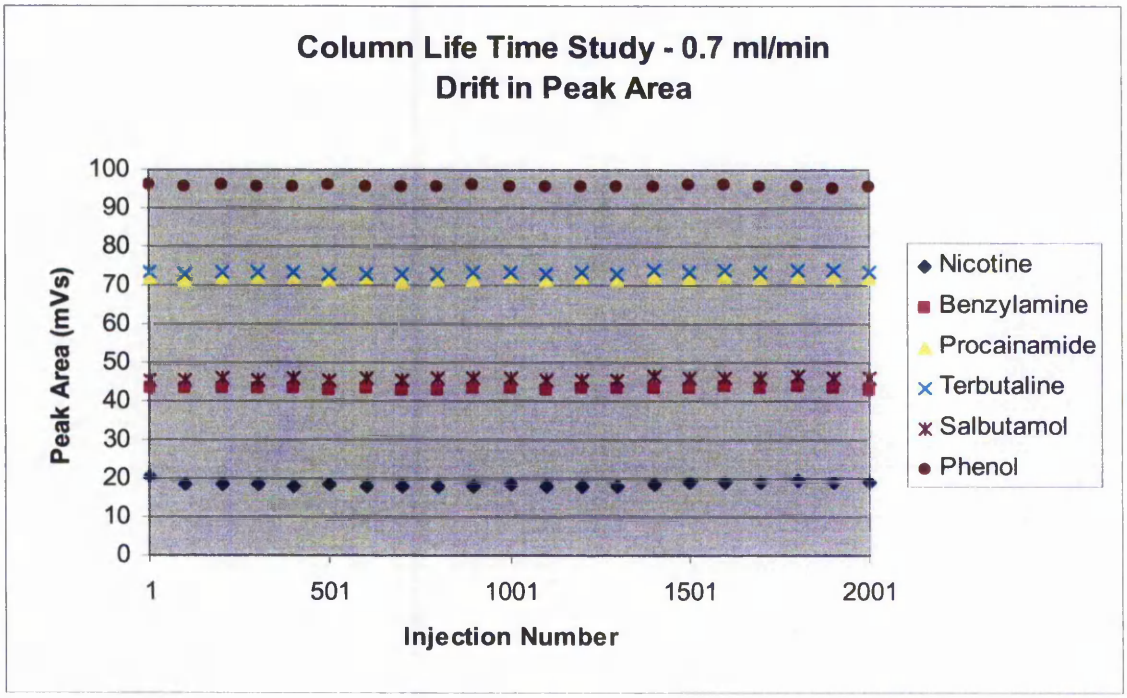

Figure 69. **Column lifetime study at 0.7 ml/min – drift in peak area**

Figure 67 shows the drift in efficiency with increasing injection number for each of the components of the hydrophilic base mix at 0.7 ml/min. After approximately 500 injections a rapid decrease in efficiency was seen. This drop off in efficiency was more pronounced for the later eluting components of the mix and had little effect on the early eluting nicotine and benzylamine. Figure 68 shows the drift in retention time with increasing injection number for each of the components of the hydrophilic base mix at 0.7 ml/min. An increase in retention time was seen after the first injection for procainamide, terbutaline and salbutamol. After this the retention time remained stable throughout the column lifetime study.

Figure 69 shows the drift in area with increasing injection number for each of the components of the hydrophilic base mix at 0.7 ml/min. No significant changes in area were seen throughout the column lifetime study. The relative standard deviation (RSD) across 2000 injections was only 0.53% for terbutaline which represents good repeatability in area throughout the study. The RSD range was 0.23 – 3.24%. The worst case being the early eluting nicotine peak. Excluding nicotine the range was 0.23-0.72%.

A column which exhibits good performance will have a lifetime of at least 10,000 column volumes. At 0.2 ml/min the column lifetime was greater than 36,000 column volumes (2000 injections), whereas at 0.7 ml/min only 9000 column volumes (500 injections) was achieved. This shows that the column lifetime of the 3 µm HyPURITY C18 50 x 2.1 mm column operating at a high linear velocity of 0.7 ml/min is at most only one quarter of that at linear velocity 0.2 ml/min.

However, this does not necessarily indicate poor column lifetime at high linear velocities but demonstrates the reduction in column lifetime achieved when operating at high flow rates. This study was performed at an elevated temperature of 60°C. Had the study been performed at 40°C the column lifetime at 0.7 ml/min may well have been in excess of the desired 10,000 column volumes.

5.2 MS Optimisation

5.2.1 Development of a stability indicating assay for terbutaline sulphate

Using the 5 μm HyPURITY C18 50 x 2.1 mm column, a rapid stability indicating LC/MS assay for the pharmaceutical terbutaline sulphate, an inhaled bronchodilator for the treatment of asthma [69, 70] was developed on the 'A' model Hewlett Packard 1100 LC/MSD. The method was required to separate terbutaline from the synthetic impurity (acetophenone) and degradant (isoquinoline). The structures of these compounds are shown in Figure 70. Table 10 shows the physicochemical data of these compounds.

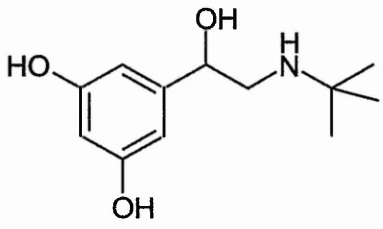

TERBUTALINE
M+H = 226

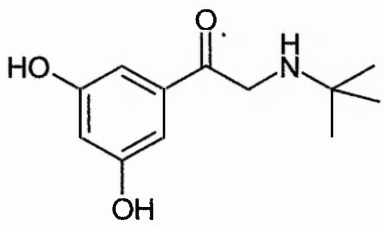

3,5-DIHYDROXY-*w*-*t*-BUTYLAMINO-ACETOPHENONE
M+H = 224

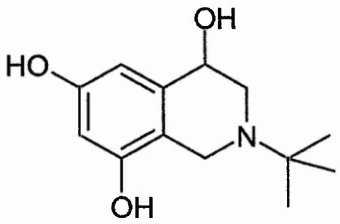

2-(1,1-DIMETHYLETHYL)-4,6,8-TRIHYDROXY-1,2,3,4-TETRAHYDROISOQUINOLINE
M+H = 238

Figure 70. **Structures of terbutaline, its acetophenone and isoquinoline derivatives**

Table 10. Physicochemical information for terbutaline and related compounds

Compound	log P	pK_a of basic functionality	pK_a of phenolic functionality	log D at pH 5.0	log D at pH 10.5
Terbutaline	0.48 ± 0.36	9.33 ± 0.47	9.12 ± 0.10 10.77 ± 0.10	-2.59	-0.99
Isoquinoline	0.59 ± 0.38	7.30 ± 0.50	9.69 ± 0.60 10.64 ± 0.60	-1.76	-0.75
Acetophenone	1.74 ± 0.39	7.11 ± 0.30	8.57 ± 0.10 10.09 ± 0.10	-0.85	-0.71

Data taken from ACD prediction software

Mass spectrometry conditions were optimised for terbutaline sulphate at 50 ng/ml using flow injection analysis to find a suitable fragmentor voltage, vaporiser temperature, drying gas and nebuliser pressure for the analysis. The mobile phase, optimised using HIPAC software was 0.025 M unadjusted ammonium acetate in acetonitrile - water (5:95 v/v) at a flow rate of 0.7 ml/min with injection volume of 100 µl.

The following optimised MS conditions were used for terbutaline suphate:

APCI positive ionisation at M+H 226

Fragmentor voltage:	40 V
Vaporiser temperature:	500°C
Gas temperature:	325°C
Drying gas:	5.0 L/min
Nebuliser pressure:	50 psig
Vcap:	4000 V
Corona current:	4.0 µA

Using these conditions the synthetic impurity (acetophenone) and degradant (isoquinoline) were separated from terbutaline sulphate in under 2 minutes. Figure 71 shows the chromatogram of this separation with the individual ions extracted out. The elution order was terbutaline, isoquinoline, acetophenone as predicted from the log D values for these analytes in Table 10, terbutaline having the lowest log D value and acetophenone the highest.

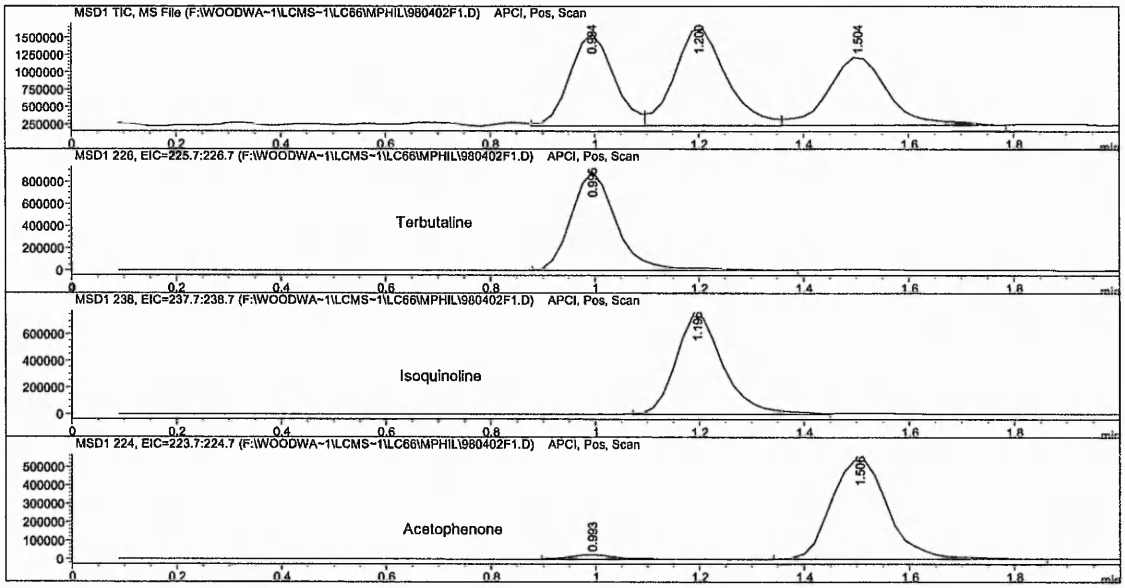

Figure 71. Chromatogram of terbutaline sulphate and its impurities

The response of terbutaline sulphate was shown to be linear over the concentration range 0.2 - 1000 ng/ml, with $R^2 = 0.99986$. This is shown in Figure 72. Table 11 shows the precision data obtained for 10 replicate injections over the concentration range 2 - 200 ng/ml.

Table 11. Precision data for terbutaline sulphate

Concentration (ng/ml)	% RSD
2	2.07
5	2.10
10	1.90
50	1.64
200	1.89

Precision was shown to be excellent at each of the concentrations tested. Concentrations below 10 ng/ml are classified as trace analysis. A precision limit of 5%

RSD would be acceptable at these concentrations. The above results are well within these limits.

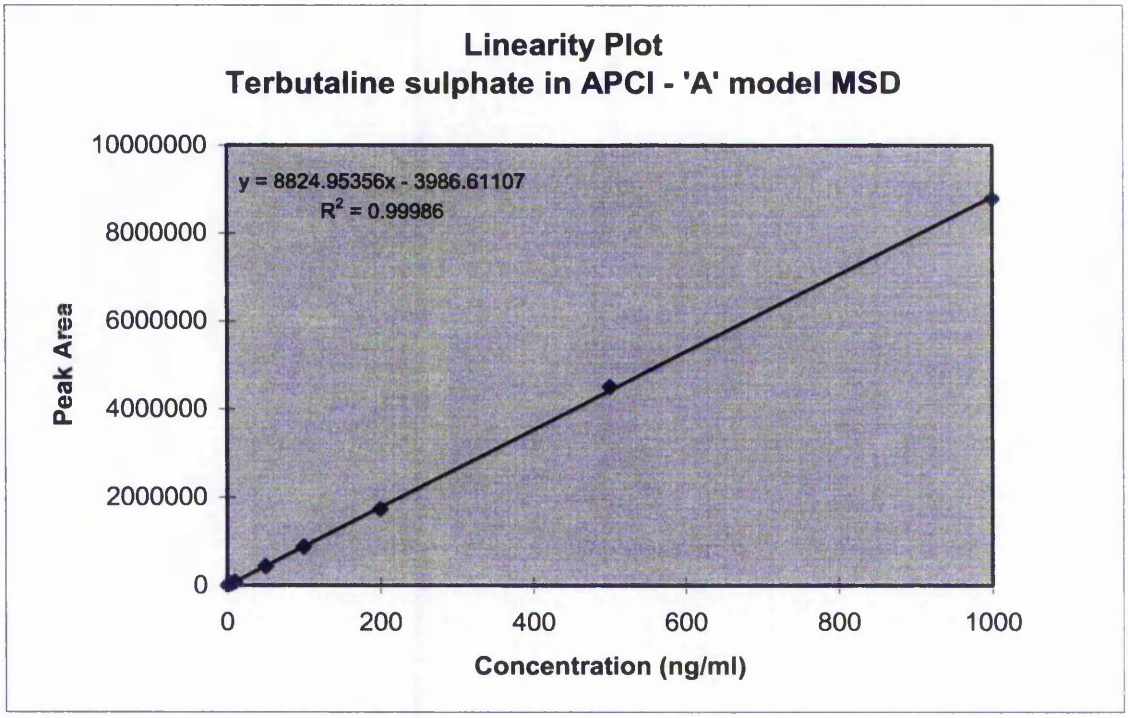

Figure 72. Linearity of terbutaline sulphate in APCI – 'A' model MSD

5.2.2 Mobile Phase Selection

5.2.2.1 Buffer Selection

Using the 'A' model 1100 MSD a selection of volatile buffers were investigated for the analysis of terbutaline sulphate using the LC/MS conditions as section 5.2.1. The analysis used a 5 µm HyPURITY C18 50 x 2.1 mm column with acetonitrile as the organic modifier. Ten injections of 50 ng/ml terbutaline sulphate were performed for each buffer type and concentration. The mean values for retention time, area, % area RSD and tailing factor are reported in the tables below. The pH of an equivalent aqueous mobile phase was measured. Table 12 below shows the results for unadjusted ammonium acetate.

Table 12. Unadjusted ammonium acetate as volatile buffer for the analysis of terbutaline sulphate

Ammonium Acetate Concentration (M)	pH	RT (mins)	Area Response	% Area RSD	Tailing Factor
0.01	6.76	0.747	356373	3.01	1.212
0.02	6.88	0.897	340133	6.67	1.331
0.025	6.92	0.954	368976	1.34	1.354
0.03	6.93	0.959	393199	0.87	1.338
0.04	6.98	0.968	394580	1.18	1.312
0.05	7.01	0.976	401056	1.47	1.307

Over the ionic strength range 0.01 – 0.05 M studied for ammonium acetate, the pH was 6.7 – 7.0. Over this pH range the % ionised for terbutaline would be the same, although the percentage of the silanols in the stationary phase that were ionised may be very different. It was expected that as the ionic strength was increased better peak shape would be obtained and the retention time would decrease but this was not observed. It is therefore assumed that the increase in retention time and tailing factor (USP) were due to the interactions of terbutaline with the ionised silanols in the stationary phase. A slight improvement in ionisation shown by an increase in response was obtained with increasing ionic strength. A concentration of 0.03 M was shown to give the lowest % area RSD whilst displaying a good response.

Table 13 below shows the results obtained for ammonium formate.

Table 13. Unadjusted ammonium formate as volatile buffer for the analysis of terbutaline sulphate

Ammonium Formate Concentration (M)	pH	RT (mins)	Area Response	% Area RSD	Tailing Factor
0.01	6.26	0.956	336047	8.96	1.495
0.02	6.38	0.944	327921	4.80	1.427
0.025	6.42	0.954	324803	5.58	1.435
0.03	6.43	0.968	326909	1.96	1.382
0.04	6.47	0.975	340395	4.59	1.370
0.05	6.52	0.985	309621	6.81	1.348

The results for ammonium formate showed a slight increase in retention time with increasing ionic strength. This was the opposite to that obtained for ammonium acetate and is due to little change in ionisation of the silanols in the stationary phase over the pH range 6.2 – 6.5. An ammonium formate concentration of 0.025 M gave a comparable retention time to that obtained using 0.025 M unadjusted ammonium acetate as the mobile phase buffer. Area response was shown not to alter significantly over the concentration range investigated.

Table 14 below shows the results obtained for TFA.

Table 14. TFA as volatile buffer for the analysis of terbutaline sulphate

TFA Concentration (%)	pH	RT (mins)	Area Response	% Area RSD	Tailing Factor
0.025	2.79	0.867	145406	4.35	1.145
0.05	2.59	0.959	159506	1.84	1.130
0.075	2.48	1.007	163274	1.15	1.128
0.10	2.38	1.038	126344	2.52	1.130
0.125	2.32	1.074	74710	5.62	1.187
0.15	2.25	1.094	89359	2.85	1.162
0.175	2.22	1.116	108503	3.58	1.166
0.2	2.18	1.114	128246	0.71	1.147

A TFA concentration of 0.075% gave the greatest response with a low % area RSD, whilst giving a comparable retention time to that obtained using 0.025 M unadjusted ammonium acetate as the mobile phase buffer.

Table 15 below shows the results obtained for formic acid.

Table 15. Formic acid as volatile buffer for the analysis of terbutaline sulphate

Formic Acid Concentration (%)	pH	RT (mins)	Area Response	% Area RSD	Tailing Factor
0.025	3.00	0.860	323756	35.8	1.476
0.05	2.86	0.769	178197	6.19	1.081
0.075	2.80	0.805	200837	4.78	1.104
0.10	2.77	0.770	209174	2.52	1.121
0.125	2.73	0.837	193342	3.75	1.123
0.15	2.69	0.852	187712	5.00	1.150
0.175	2.66	0.808	190559	4.56	1.152
0.2	2.64	0.716	199479	1.26	1.148

The use of formic acid in the mobile phase was shown to significantly reduce the retention time of terbutaline at all concentrations investigated. At concentrations of 0.05% and above the tailing factors obtained indicate good symmetrical peak shape.

The data from the four buffers above is summarised below in Table 16.

Table 16. Buffer comparison for the analysis of terbutaline sulphate

	Concentration	pH	Area	RT (mins)	% Area RSD	Tailing Factor
Ammonium Acetate	0.025 M	6.92	370000	0.954	1.34	1.354
Ammonium Formate	0.025 M	6.42	320000	0.954	5.58	1.435
TFA	0.05 %	2.59	160000	0.959	1.84	1.130
Formic Acid	0.05 %	2.86	180000	0.769	6.19	1.081

The LC/MS results for buffer optimisation show that the best ionisation of terbutaline was obtained with ammonium acetate and ammonium formate as both gave good responses, where as TFA and formic acid were poor by comparison. Although response was poor for TFA and formic acid, the peak shape was good, represented by a low tailing factor. Ammonium acetate and TFA were shown to give the most reproducible

peak areas, indicated by lower % area RSDs than for ammonium formate and formic acid. Using formic acid, a comparable retention time for terbutaline with that obtained using 0.025 M ammonium acetate could not be achieved. Based on the results above the preferred order of volatile buffers for the analysis of terbutaline sulphate in APCI is: Ammonium acetate > Ammonium formate >> TFA > Formic acid

The use of ammonium hydroxide pH 10.5 as an additive was compared to using ammonium acetate pH 5.0 for the analysis of terbutaline and its related impurities. The basic functionality of terbutaline has a pK_a of 9.33, where as its phenolic functionality has pK_as of 9.12 and 10.77 (section 5.2.1). Its related substance isoquinoline has pK_as of 7.30 for its basic functionality and 9.69 and 10.64 for its phenolic functionality, whilst acetophenone has pK_as of 7.11 for its basic functionality and 8.57 and 10.09 for its phenolic functionality. At pH 5.0 all the analytes are greater than 99% ionised. At pH 10.5 the basic functionalities of isoquinoline and acetophenone are fully unionised, where as terbutaline is only >90% unionised. However, for the phenolic functionalities terbutaline shows the greatest amount of ionisation. Plots of Log D versus pH for terbutaline and its isoquinoline and acetophenone derivatives are shown in Figure 73. The effect of changing the ionisation state of terbutaline on its analysis by LC/MS was investigated. The HyPURITY column used previously has a physical stability of pH 0.9 - 9, and hence is unsuitable for this investigation [71]. The column chosen for this study was a 5 µm Phenomenex Luna C18 50 x 2.0 mm which is claimed by the manufacturers to be stable over the pH range pH 1.5 – 10 [72]. The additional pH stability achieved with the Luna column is stated by the manufacturer to be due to a high purity silica that is nearly free of metal contaminates allowing for maximum bonded phase coverage of the silica surface. The dense bonded phase coverage creates a hydrophobic shield around the surface giving the extra stability.

An initial mobile phase of 0.025 M ammonium acetate pH 5.0 methanol-water (10:90 v/v) was used for the analysis of a terbutaline impurity mix solution containing 50 ng/ml terbutaline sulphate, and its isoquinoline and acetophenone derivatives. The LC/MS method conditions used are as for the 'D' model MSD in section 5.2.3.1. The obtained chromatogram from the analysis is shown in Figure 74.

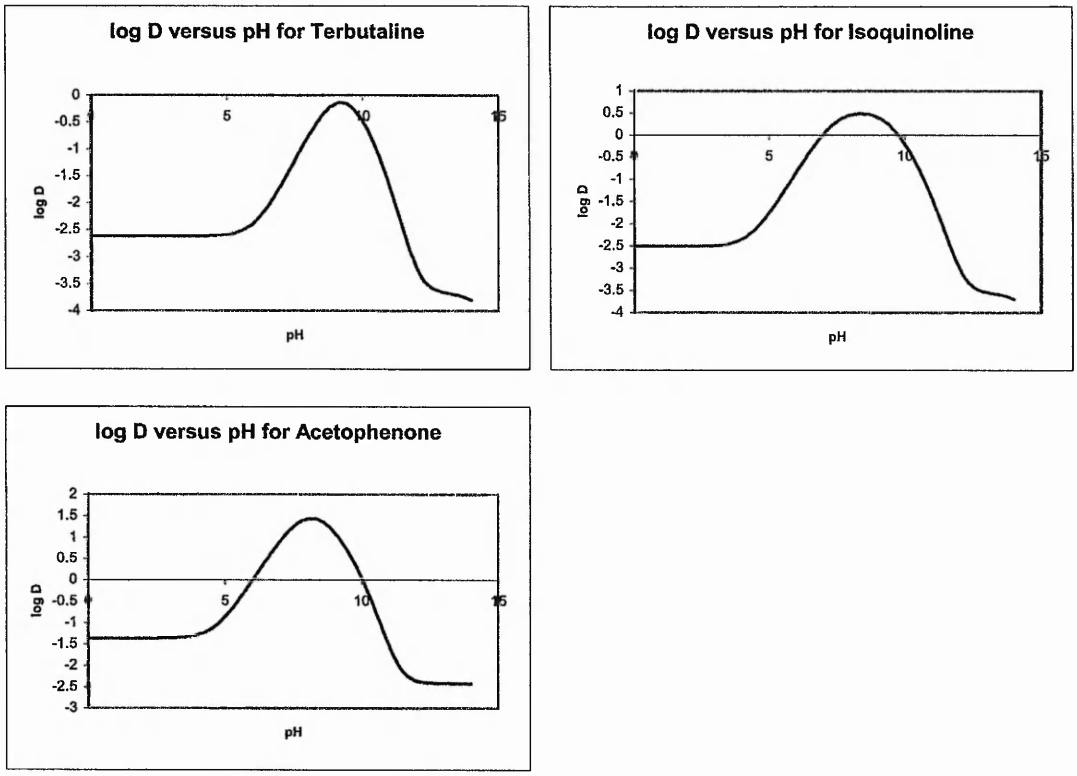

Figure 73. **log D versus pH plots for terbutaline and its isoquinoline and acetophenone derivatives**

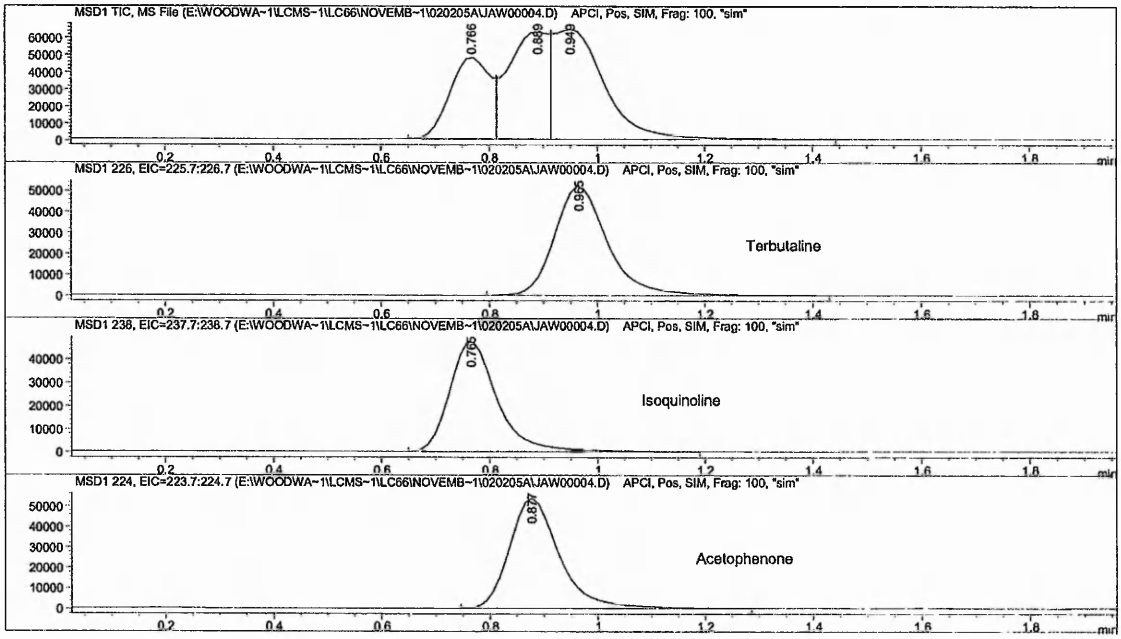

Figure 74. **Chromatogram of terbutaline impurity mix solution using ammonium acetate pH 5.0 buffer with a Luna column**

The chromatogram in Figure 74 shows that the three components of the terbutaline impurity mix solution were not completely resolved on the Luna column. The order of elution was the same as that seen on the HyPURITY column with the same mobile phase. The chromatogram obtained on the HyPURITY column is shown in Figure 75. The three components are not well separated but can be identified by the extracted ion chromatogram. The chromatogram obtained from the Luna column shows that terbutaline was retained on the column for longer than for the HyPURITY column, and the separation between isoquinoline and acetophenone was much improved. The separation mechanism on the Luna column is not simply a function of the analyte log D value but is also due to the interactions of the analytes with the stationary phase showing the difference in selectivity of the two columns.

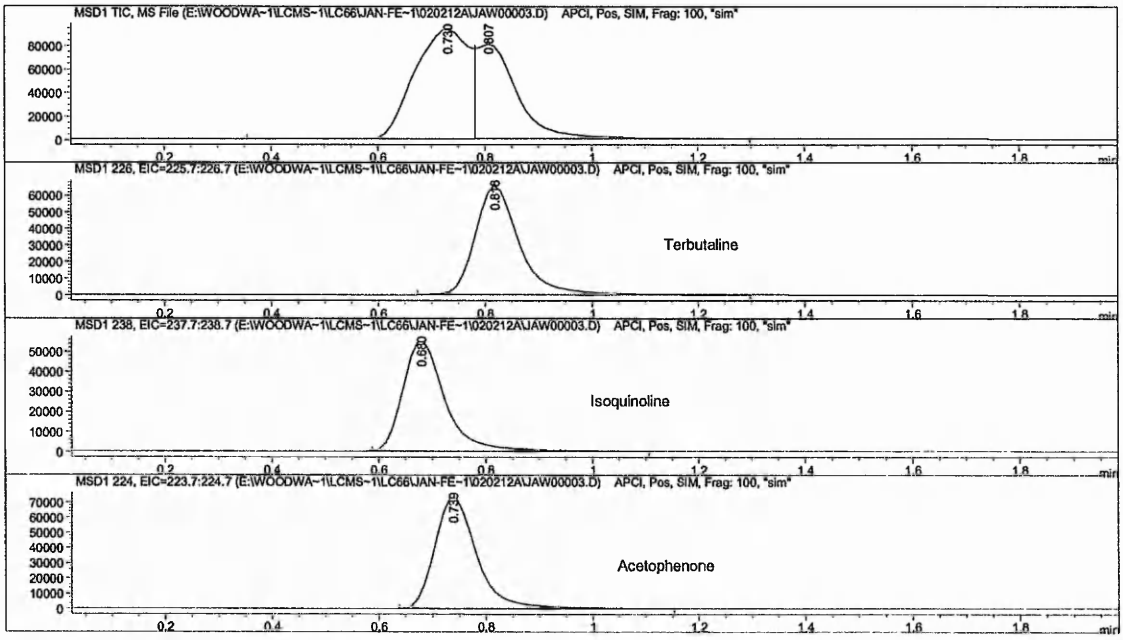

Figure 75. **Extracted ion chromatogram of terbutaline impurity mix solution using ammonium acetate pH 5.0 buffer with a HyPURITY column**

The analysis was repeated using a mobile phase of 0.1% w/v ammonium hydroxide pH 10.5 in methanol – water (10:90 v/v). The chromatogram obtained for the separation is shown in Figure 76.

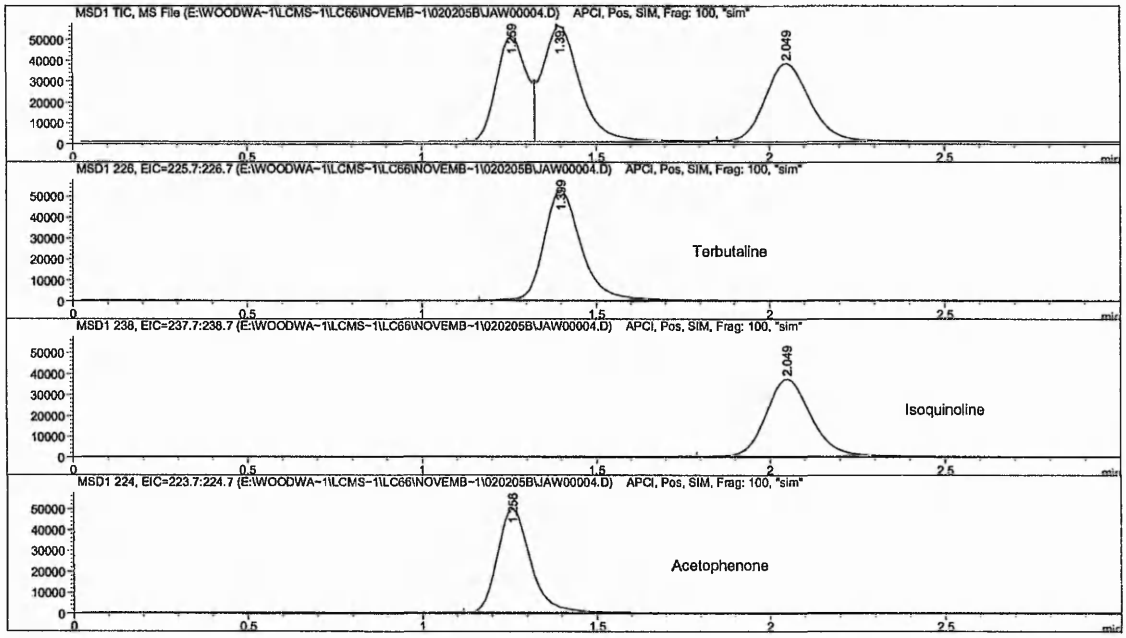

Figure 76. Chromatogram of terbutaline impurity mix solution using ammonium hydroxide pH 10.5 buffer with a Luna column

The elution order had changed to acetophenone, terbutaline, isoquinoline, with a later retention time observed for all peaks. This was due to the increased interactions of all three components with the stationary phase due to the components being largely in the unionised state (basic functionality unionised, phenolic functionality partially ionised). The log D values for acetophenone in Table 10 were shown to differ only slightly between pH 5.0 and pH 10.5, showing why there was little change in retention time. Isoquinoline; however, showed a larger increase in log D between pH 5.0 and 10.5 explaining the larger increase in retention time observed.

Analysing terbutaline in its unionised state showed an increase in its retention time. In order to have a comparable retention time to that obtained using a mobile phase of 0.025 M ammonium acetate pH 5.0 in methanol – water (10:90 v/v), it was shown necessary to increase the methanol content to 16%. A chromatogram of the separation is shown in Figure 77.

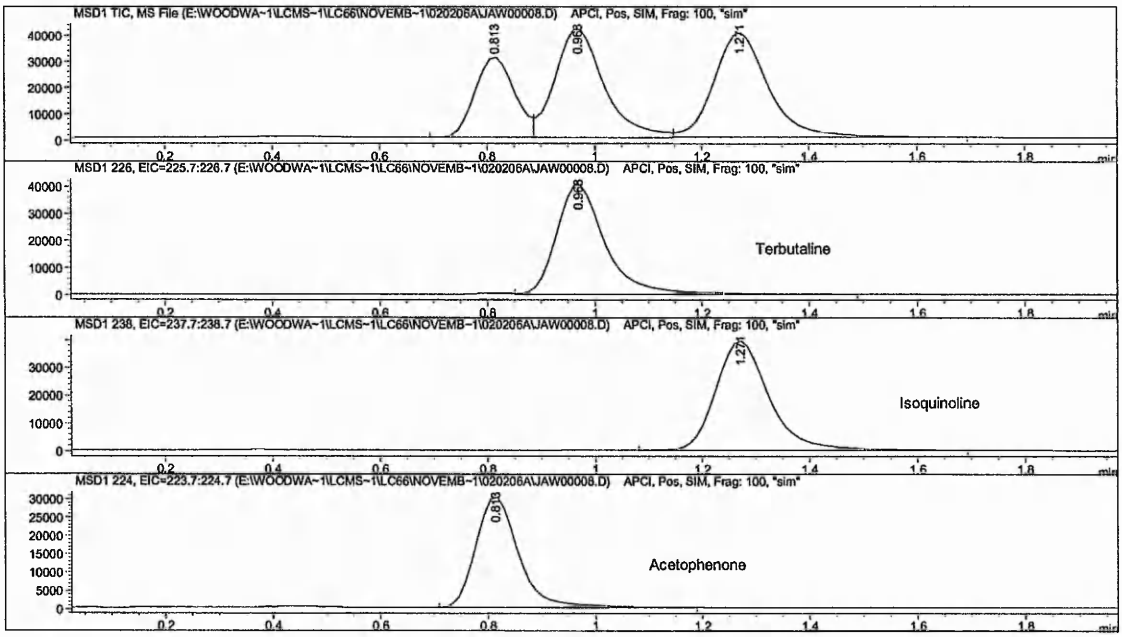

Figure 77. **Chromatogram of terbutaline sulphate system suitability solution using a mobile phase of 0.1% w/v ammonium hydroxide pH 10.5 in methanol – water (16:84 v/v) with a Luna column**

The chromatogram in Figure 77 shows the improved resolution obtained when using 0.1% w/v ammonium hydroxide pH 10.5 in methanol – water (16:84 v/v) over that obtained with 0.025 M ammonium acetate pH 5.0 in methanol – water (10:90 v/v) with the Luna column as shown in Figure 74. Using a pH 10.5 mobile phase has enabled enhanced selectivity for terbutaline and its related compounds due to differences in log D values increasing the interactions of the analytes with the stationary phase when in their unionised state.

A comparison of the analysis of the single component terbutaline sulphate using the two mobile phases on the Luna column is given below in Table 17.

Table 17. Comparison of the analysis of terbutaline sulphate using ammonium acetate pH 5 and ammonium hydroxide pH 10.5 as mobile phase additives

	Concentration of Buffer	Methanol %	pH	Area	RT (mins)	Tailing Factor
Ammonium Acetate	0.025 M	10	5.00	321118	0.967	1.328
Ammonium Hydroxide	0.1 %w/v	16	10.68	247828	0.969	1.420

These results show that the response for terbutaline was greater with the ammonium acetate buffer than with the ammonium hydroxide buffer. The peak obtained was also sharper with the ammonium acetate buffer than the ammonium hydroxide buffer demonstrated by a lower tailing factor for the ammonium acetate buffer. However, the results do demonstrate the suitability of ammonium hydroxide as an alternative buffer where enhanced specificity is required by analysing a compound in its unionised form.

The use of non-volatile buffers in the mobile phase or the sample solution can give rise to fouling of the spray chamber. An example of this is shown in Figure 78.

The buffer or salt deposits can lead to a blockage in the capillary which will result in a loss of signal. This can be quite rapid in onset depending on the concentration of buffer or salt used. When analysing solutions containing 4% bovine serum albumin (BSA) in Hank's balanced salt solution (HBSS) it was not possible to obtain a steady response from the MSD. The decrease in the response obtained is shown in Figure 79.

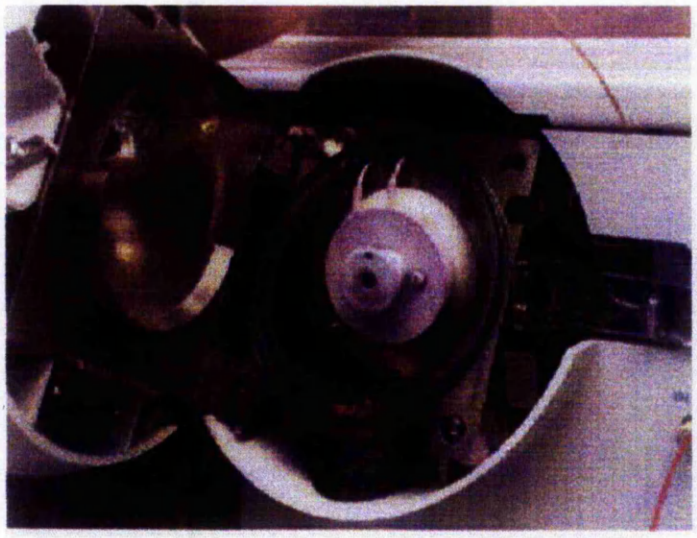

Figure 78. **Fouling of the spray chamber obtained when using non-volatile buffer**

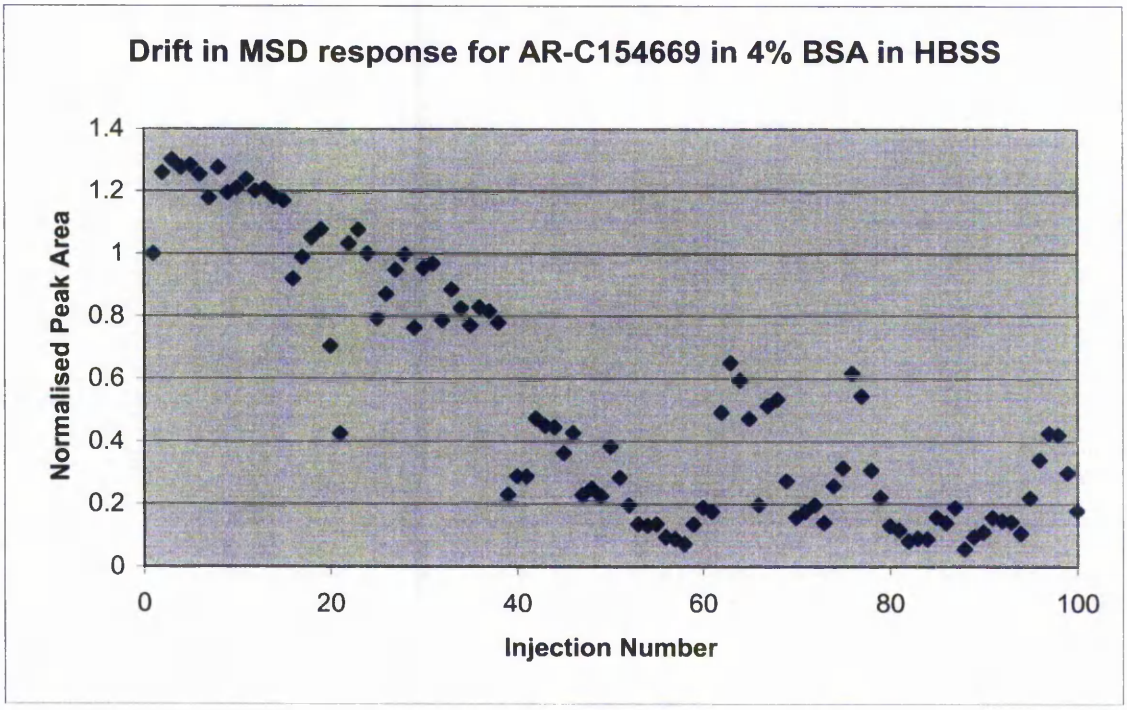

Figure 79. **Decrease in response obtained when analysing samples containing high levels of non-volatile material**

The results show the decrease in analyte response obtained when analysing multiple injections of a sample containing high concentrations of non-volatile material. Where it is necessary to analyse such samples the use of a column switching approach can be employed which would have the effect of removing the non-volatile component prior to the sample entering the MSD. An example of this is demonstrated in section 5.3.3.

5.2.2.2 Organic Modifier Selection

Methanol as an alternative organic solvent to acetonitrile was investigated for the analysis of terbutaline sulphate using the LC/MS conditions as section 5.2.1 on an 'A' model 1100 MSD. The analysis used a 5 µm HyPURITY C18 50 x 2.1 mm column with 0.025 M ammonium acetate, unadjusted pH as the volatile buffer in the mobile phase. Ten injections of 50 ng/ml terbutaline sulphate were performed for each organic solvent. The mean values for retention time, area, % area RSD and tailing factor are reported in Table 18 below.

Table 18. Organic solvent comparison for the analysis of terbutaline sulphate

	Concentration	Area	RT (mins)	% Area RSD	Tailing Factor
Methanol	10 %	472280	0.917	1.14	1.395
Acetonitrile	5 %	368976	0.954	1.34	1.354

Using the 'D' model 1100 MSD, additional organic solvents as alternatives to methanol were investigated for the analysis of terbutaline sulphate using the LC/MS conditions as section 5.2.3.1. The analysis used a 5 µm HyPURITY C18 50 x 2.1 mm column with 0.025 M ammonium acetate, pH 5.0 as the volatile buffer in the mobile phase. Ten injections of 50 ng/ml terbutaline sulphate were performed for each organic solvent. The mean values for retention time, area, % area RSD and tailing factor are reported in Table 19.

Table 19. Organic solvent comparison for the analysis of terbutaline sulphate

Solvent	Concentration	Area	RT (mins)	Column Pressure	% Area RSD	Tailing Factor
Methanol	10 %	375635	0.789	140	1.65	1.467
Ethanol	4 %	454094	0.792	129	0.52	1.481
Acetone	3 %	370279	0.754	123	0.68	1.465

As the data were obtained from both the 'A' and 'D' models of the MSD at pH 6.8 and 5.0 a direct comparison of all solvents is not possible. However, as methanol was used on both instruments, at both pHs a comparison of the alternative solvents to methanol can be made.

The differences in retention time between the two instruments were partly due to differences in the extra column volume. For the 'A' model MSD the post column capillary tubing went into the diode array detector and out into the MSD. For the 'D' model MSD the length of capillary tubing was kept to a minimum by by-passing the diode array detector, taking the post column capillary tubing directly into the MSD. Not only did this reduce the volume from the additional capillary tubing but also eliminated the volume from the diode array detector flow cell. The reduction in pH from 6.8 (0.025 M unadjusted ammonium acetate) to pH 5.0 also contributed to the reduction in retention due to a decrease in the interactions between terbutaline and the ionised silanols in the stationary phase. The concentration of organic modifier used was based on obtaining the same retention time for terbutaline for all modifiers and hence the concentration was not kept constant.

The improvement in ionisation for methanol compared to acetonitrile was due to a change in viscosity of the mobile phase. A decrease in the viscosity of the mobile phase obtained by an increase in organic content gave rise to an improvement in ionisation due to better spraying properties of the mobile phase. This increase in ionisation with increase in organic content was observed by Dams *et al* [73]. They showed that for a mobile phase of ammonium acetate (pH 4.5 or unadjusted) in water/methanol or water/acetonitrile, ionisation increased with increasing organic content up to around 60 % organic, thereafter any further increase in organic produced no increase in

response. Dams *et al* also showed that for APCI methanol gave a more extensive ionisation than acetonitrile, which was thought to be due to its better gas phase characteristics, especially its lower proton affinity. Based on area response, ethanol was shown to be the preferred solvent. % area RSDs for all solvents was shown to be good as all were less than 2%. Tailing factors obtained were comparable for all solvents. The differences in column pressures obtained for each solvent show that by switching from methanol to ethanol or acetone, a lower column pressure was obtained. This lower pressure allows the analysis to be performed at higher flow rates than could otherwise be achieved with methanol as the organic solvent.

Based on the results above the preferred order of solvents for the analysis of terbutaline sulphate is:
Ethanol > Methanol > Acetone > Acetonitrile

A reason why acetonitrile is a poor choice of solvent for analysis by APCI is due to deposits from the acetonitrile forming on the APCI corona needle, affecting the sample ionisation.

5.2.3 Method Transfer to 'D' Model MSD

The 'A' model MSD was upgraded to a 'D' model. The MS conditions for the analysis of terbutaline sulphate were optimised for the new model. For the differences between the two models of MSD see section 3.2.3.

5.2.3.1 Terbutaline sulphate in APCI

The method for terbutaline sulphate in APCI was optimised for the 'D' model MSD by flow injection analysis. The mobile phase used was 0.025 M ammonium acetate pH 5.0 in methanol - water (10:90 v/v) at a flow rate of 0.7 ml/min with an injection volume of 100 µl for a 50 ng/ml concentration of terbutaline sulphate. The following optimised MS conditions were determined for terbutaline sulphate:

APCI positive ionisation at M+H 226

Fragmentor voltage:	100 V
Vaporiser temperature:	400°C
Gas temperature:	350°C
Drying gas:	5.0 L/min
Nebuliser pressure:	35 psig
Vcap:	3500 V
Corona current:	4.0 µA

The linearity of this new method was determined between 0.01 – 5270 ng/ml.

The response of terbutaline sulphate was shown to be linear over the concentration range 0.01- 1581 ng/ml, with $R^2 = 0.99944$. A linearity plot is shown in Figure 80. Above this concentration a quadratic curve was obtained as the detector becomes saturated. This is shown in Figure 81. Table 20 shows the precision data obtained.

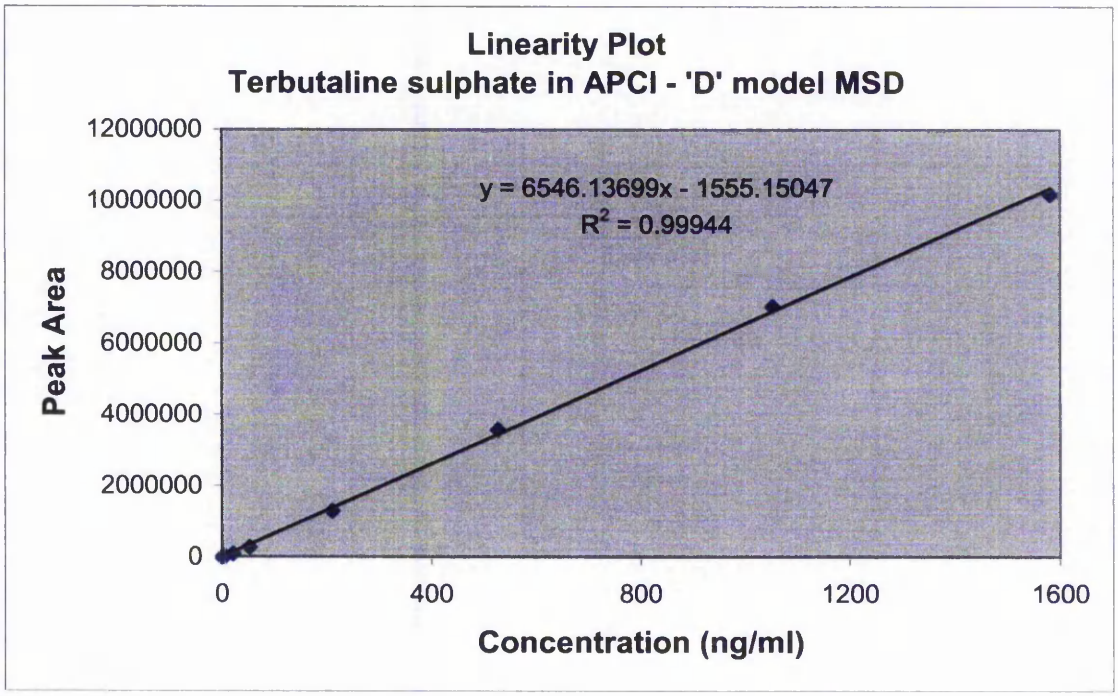

Figure 80. Linearity of terbutaline sulphate in APCI – 'D' model MSD

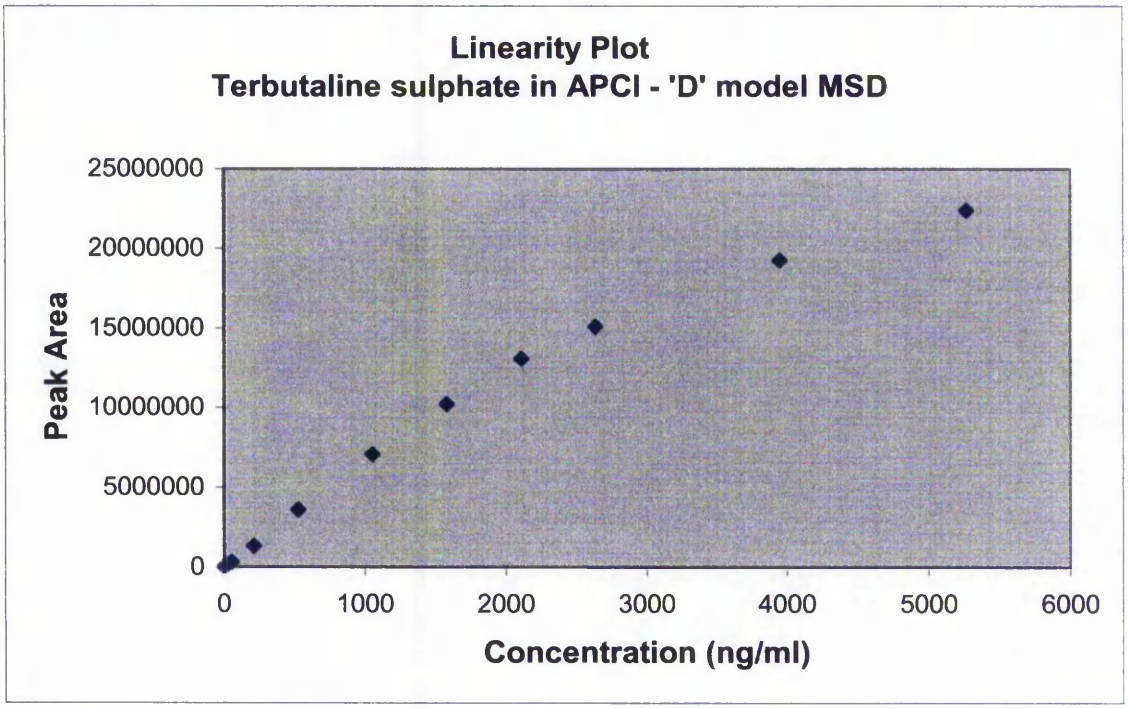

Figure 81. Linearity of terbutaline sulphate in APCI – 'D' model MSD

5.2.3.2 Terbutaline sulphate in ESI

The method for terbutaline sulphate in ESI was optimised for the 'D' model MSD by flow injection analysis. The mobile phase used was 0.025 M ammonium acetate pH 5.0 in methanol - water (10:90 v/v) at a flow rate of 0.7 ml/min with an injection volume of 100 µl for a 50 ng/ml concentration of terbutaline sulphate. The following optimised MS conditions were determined for terbutaline sulphate:

ESI positive ionisation at M+H 226

Fragmentor voltage:	100 V
Vaporiser temperature:	N/A
Gas temperature:	350°C
Drying gas:	12.9 L/min
Nebuliser pressure:	60 psig
Vcap:	2500 V
Corona current:	4.0 µA

The linearity of this new method was determined between 0.01 – 5270 ng/ml. The response of terbutaline sulphate was shown only to be linear over the concentration range 0.01- 21 ng/ml, with $R^2 = 0.99911$. A linearity plot is shown in Figure 82. Above this concentration a quadratic curve was obtained as the detector becomes saturated. This is shown in Figure 83.

The precision data obtained for 6 injections per concentration over the range 0.01 - 5270 ng/ml in APCI and ESI was compared. The data are shown in Table 20.

Table 20. Precision data of 'D' model MSD in APCI and ESI

Concentration (ng/ml)	% RSD	
	APCI	ESI
0.01054	20.86	8.30
0.02108	6.19	7.70
0.0527	3.93	3.55
0.1054	3.50	2.68
0.527	6.44	1.08
2.108	4.32	0.62
5.27	2.74	0.62
21.08	3.54	0.38
52.7	2.67	0.38
210.8	1.48	0.56
527	5.06	0.52
1054	ND	0.68
1581	6.52	0.92
2108	1.86	1.07
2635	2.10	1.52
3952.5	4.04	1.79
5270	3.64	2.08

ND – Not determined

These results show that the precision obtained was generally better for ESI than for APCI. Precision was shown to deteriorate at low concentrations. In ESI, concentrations 0.01 and 0.02 ng/ml were outside the desired limit of 5%. However, for all concentrations above this the precision was excellent, ranging from 0.38 to 3.55%. For APCI over the same concentration range the variation was 1.48 to 6.52%.

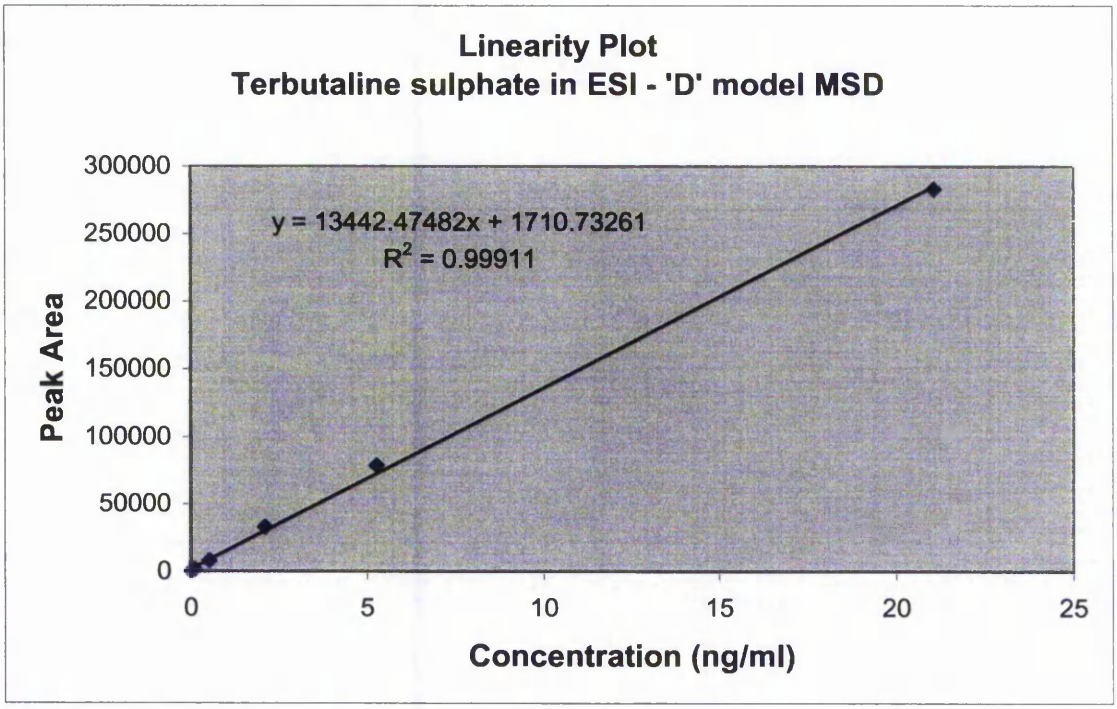

Figure 82. **Linearity of terbutaline sulphate in ESI – 'D' model MSD**

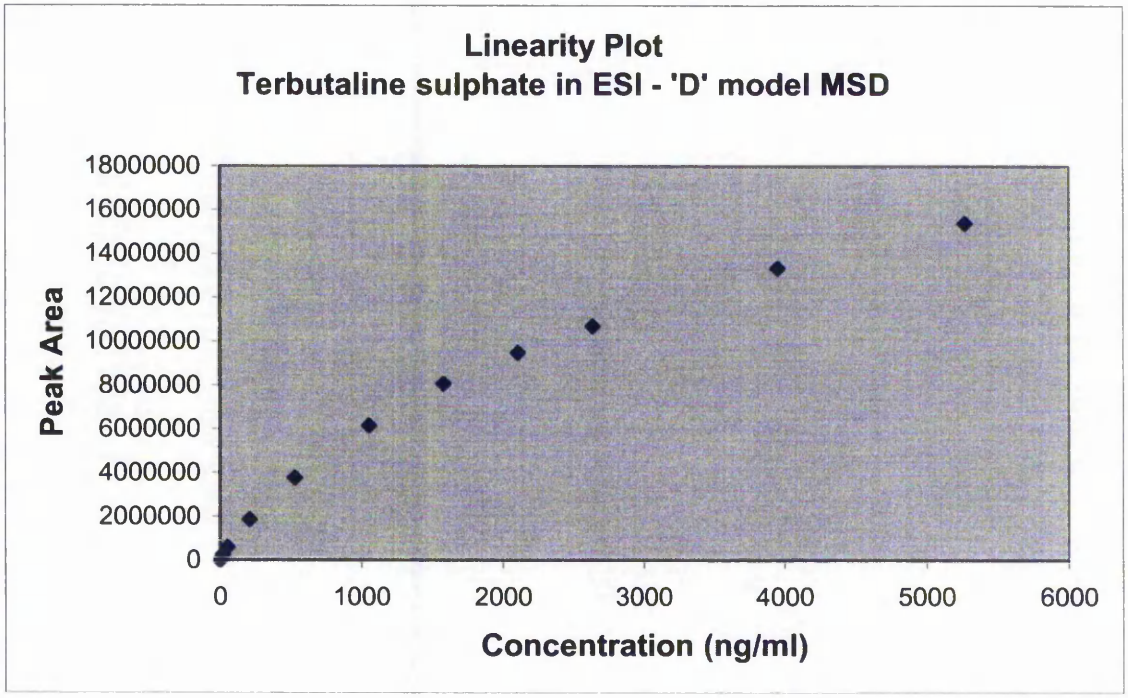

Figure 83. **Linearity of terbutaline sulphate in ESI – 'D' model MSD**

A comparison of the linear range for terbutaline sulphate in APCI and ESI showed that APCI was linear over 5 orders of magnitude where as linearity in ESI was only obtained over 3 orders of magnitude.

Chen *et al* [74] performed a detailed comparison of the repeatability of the retention times, peak efficiencies and peak areas of a dozen probe compounds in HPCL using UV and MS detection in APCI. Most compounds were basic, some were neutral. The repeatability in retention time was not influenced by the mode of detection; however, peak areas and column efficiencies were generally better with UV than MS detection. On average the precision for UV peak area detection was 2.5% versus 6.8% for MS detection. They found that although APCI responds to the mass flux of the analyte, its response factor was markedly affected by changes in the mobile phase and gas flow rates.

5.2.4 Daughter Ion Monitoring

Daughter ion monitoring can increase the specificity of an LC/MS method. Rather than collect data in single ion monitoring mode (SIM) of the M+H ion, a fragment ion is monitored instead. Daughter ion monitoring was investigated for terbutaline sulphate.

Analysis in scan mode was initially performed to assess the fragmentation of terbutaline. The fragmentation voltage was increased above the standard 100 V used previously to introduce fragmentation. Analysis was performed in SIM of the main fragment ion and the sensitivity monitored.

Using the 5 µm HyPURITY C18 50 x 2.1 mm column and a mobile phase of 0.025 M ammonium acetate, pH 5.0 in methanol - water (10:90 v/v), a 100 µl injection of 25 µg/ml terbutaline sulphate was performed. The initial mass spectrometry conditions used were:

APCI positive ionisation in scan over the range 50 – 250 amu.

Fragmentor voltage:	100 V
Vaporiser temperature:	400°C
Gas temperature:	350°C
Drying gas:	5.0 L/min
Nebuliser pressure:	35 psig
Vcap:	3500 V
Corona:	4.0 μA

The fragmentor voltage was increased step-wise from 100 – 260 V.

The relative abundances of the ions detected with increasing fragmentor voltage are shown in Table 21. The mass spectra obtained are shown in Figure 84.

Table 21. Relative abundances of terbutaline fragment ions

Fragmentor Voltage (V)	Relative Abundance (%) of Ions															
	226	208	170	152	135	125	110	107	105	84	81	79	77	74	69	57
100	100	4.9	-	0.6	-	-	-	-	-	-	-	-	-	4.0	-	-
120	100	9.5	1.5	3.1	-	-	-	-	-	-	-	-	-	1.0	-	-
140	100	8.5	8.8	21.2	-	-	-	-	-	-	-	-	-	0.7	-	0.7
160	69.5	5.8	18.8	100	0.7	1.6	-	0.8	-	-	-	-	-	-	-	1.7
180	12.3	0.7	6.7	100	2.5	5.0	0.9	3.7	-	-	-	-	-	-	-	2.3
190	5.3	0.6	3.7	100	4.1	8.7	1.4	7.7	0.7	1.0	-	0.5	-	-	0.6	2.3
200	2.1	-	1.8	100	7.6	15.0	3.3	17.4	2.1	2.1	0.5	1.5	-	-	1.7	2.4
220	-	-	-	100	13.1	32.0	15.2	61.6	13.6	5.7	2.2	6.9	0.9	-	6.0	4.2
240	-	-	-	37.8	11.6	27.4	29.7	100	52.1	5.9	5.7	15.8	4.7	-	15.4	8.8
260	-	-	-	11.6	7.6	16.4	44.4	100	99.7	3.8	11.6	19.9	13.5	-	24.7	13.9

Tentative assignments have been made for the ions produced on fragmenting terbutaline. These are shown in Figure 85.

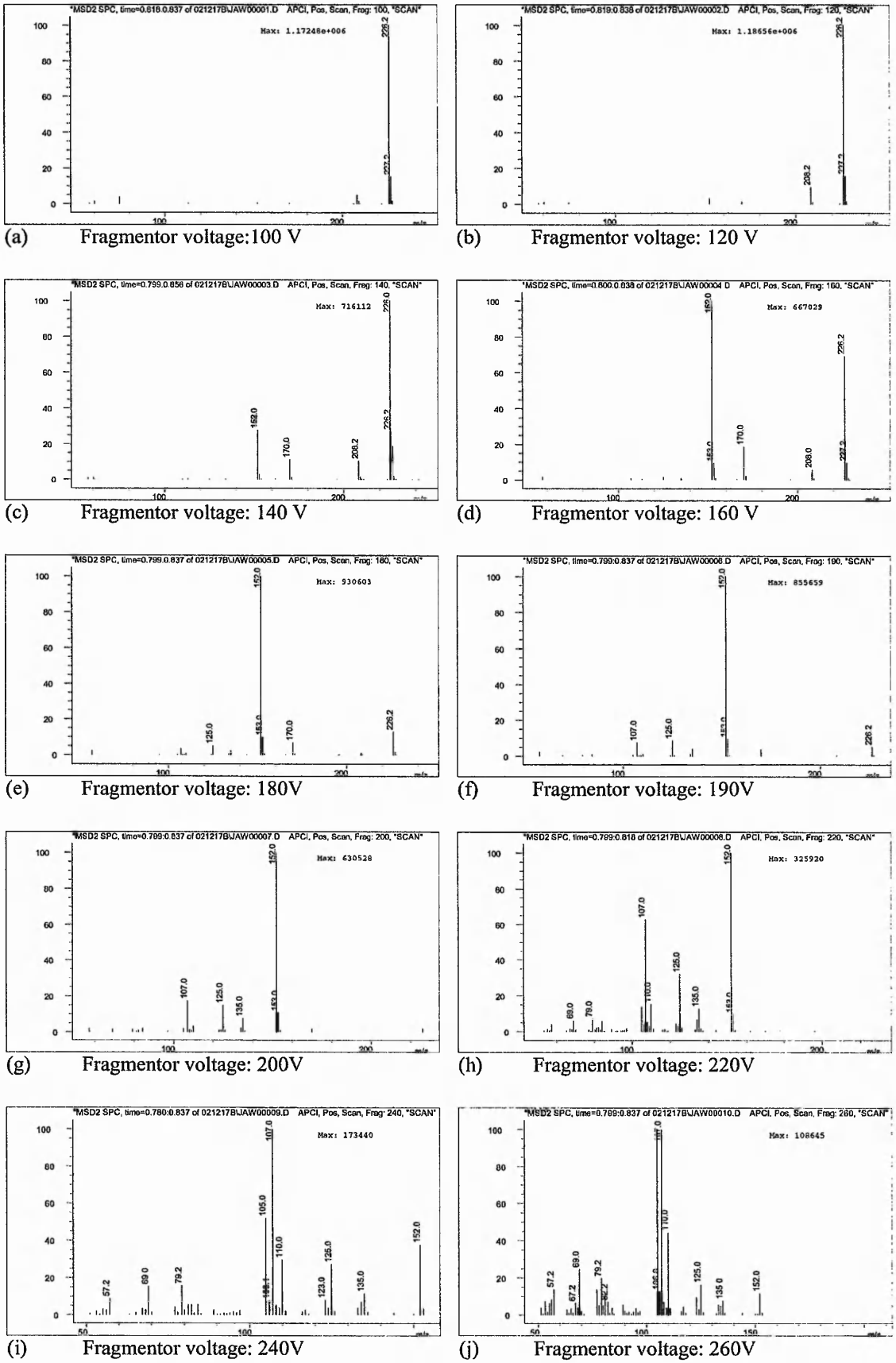

Figure 84. Mass spectra of terbutaline with increasing fragmentor voltage

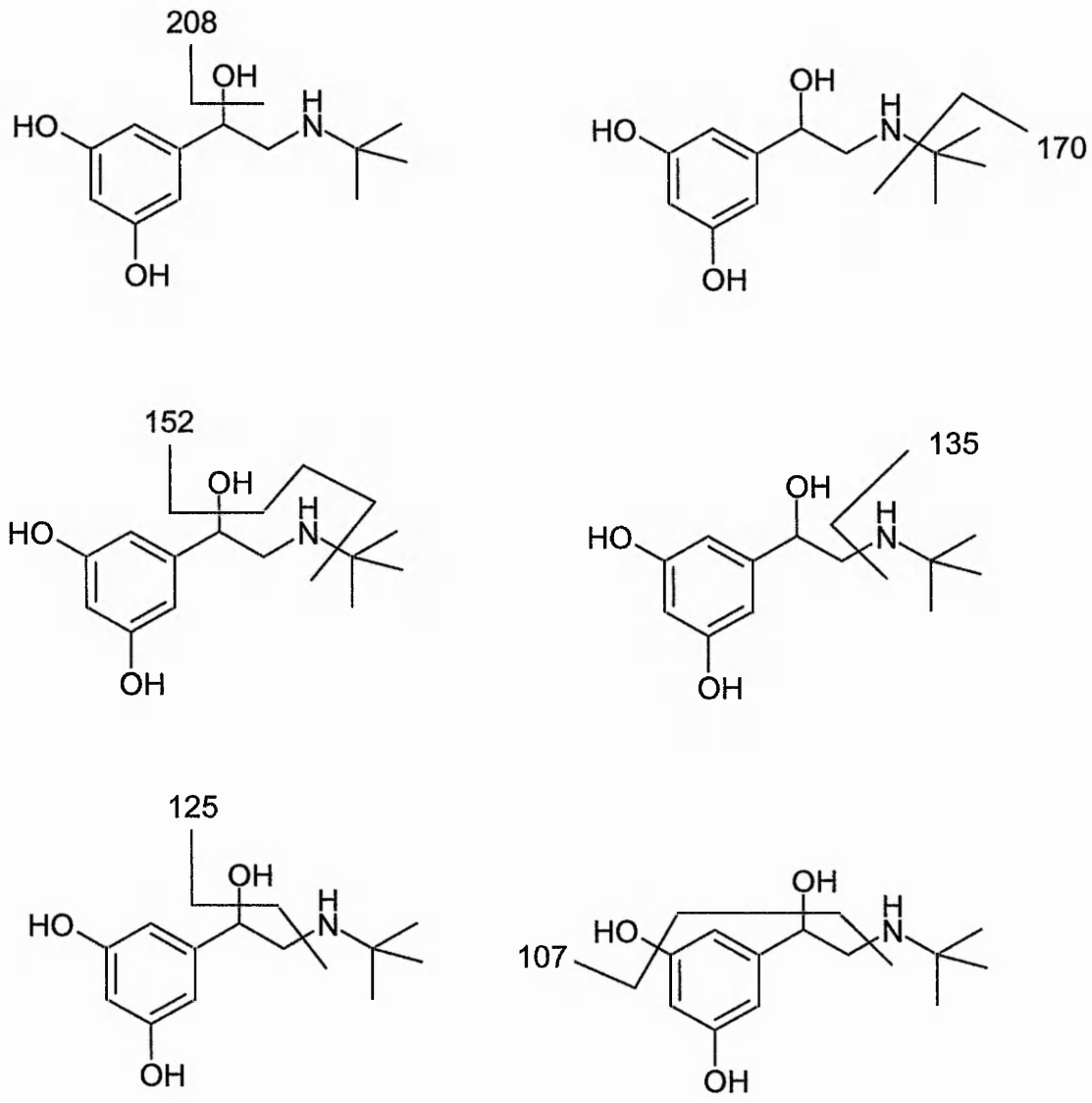

Figure 85. Tentative assignments of terbutaline fragments

The results above suggest that daughter ion monitoring could be performed at M+H 152 using a fragmentor voltage of 190 V. This voltage gave a clean spectrum, with little fragmentation other than the ion at 152. Linearity, precision and Limit of Detection (LOD) were performed using these new method parameters.

The response of terbutaline sulphate was shown to be linear over the concentration range 0.1 - 2105 ng/ml, with $R^2 = 0.99947$. This is shown in Figure 86. Above this concentration a quadratic curve was obtained as the detector becomes saturated. This is

shown in Figure 87. Table 22 shows the precision data obtained on a series of 6 injections at each concentration.

Table 22. Precision data for terbutaline fragment 152

Concentration (ng/ml)	%RSD
0.1053	4.83
0.5263	4.53
2.1052	2.08
5.263	0.76
21.052	4.29
52.63	1.65
210.52	1.31
526.3	2.21
1052.6	1.97
1578.9	0.50
2105.2	0.46
2631.5	0.73
3157.8	0.87
5263	1.56

Whilst daughter ion monitoring can increase the specificity of the method the sensitivity was shown to be reduced by a factor of 3 over that seen when monitoring at the M+H ion of 226, section 5.2.3.1. The precision data show that in general lower area %RSDs were obtained than when monitoring at 226.

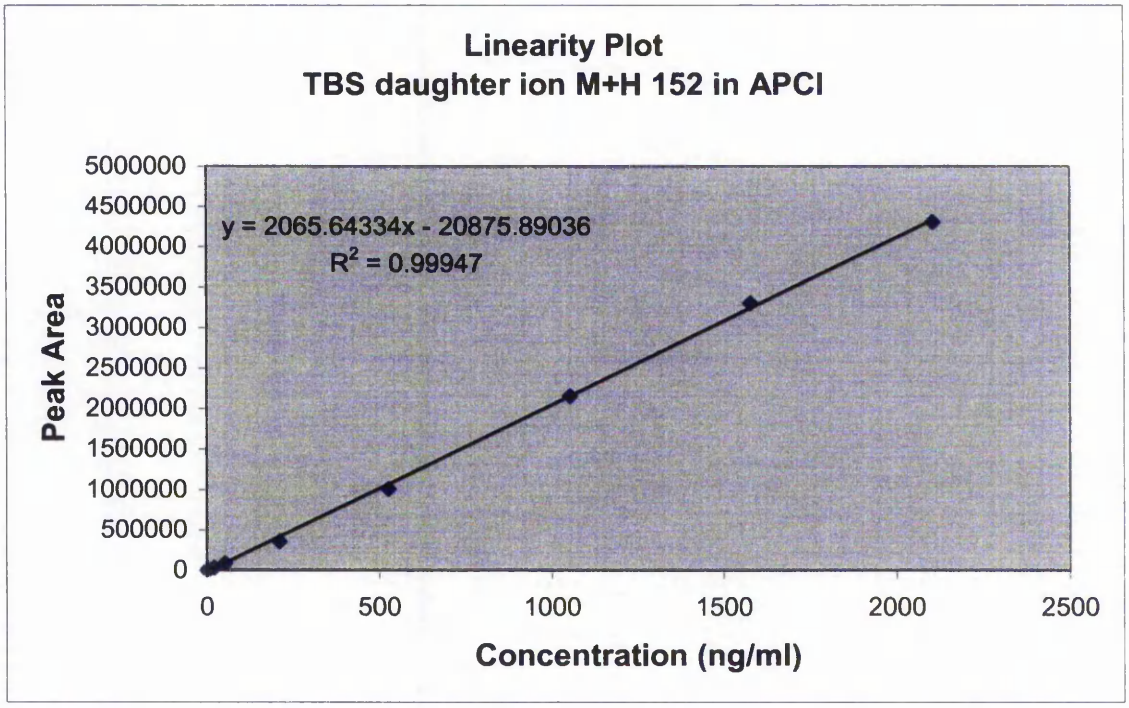

Figure 86. **Linearity of terbutaline sulphate daughter ion M+H 152 in APCI**

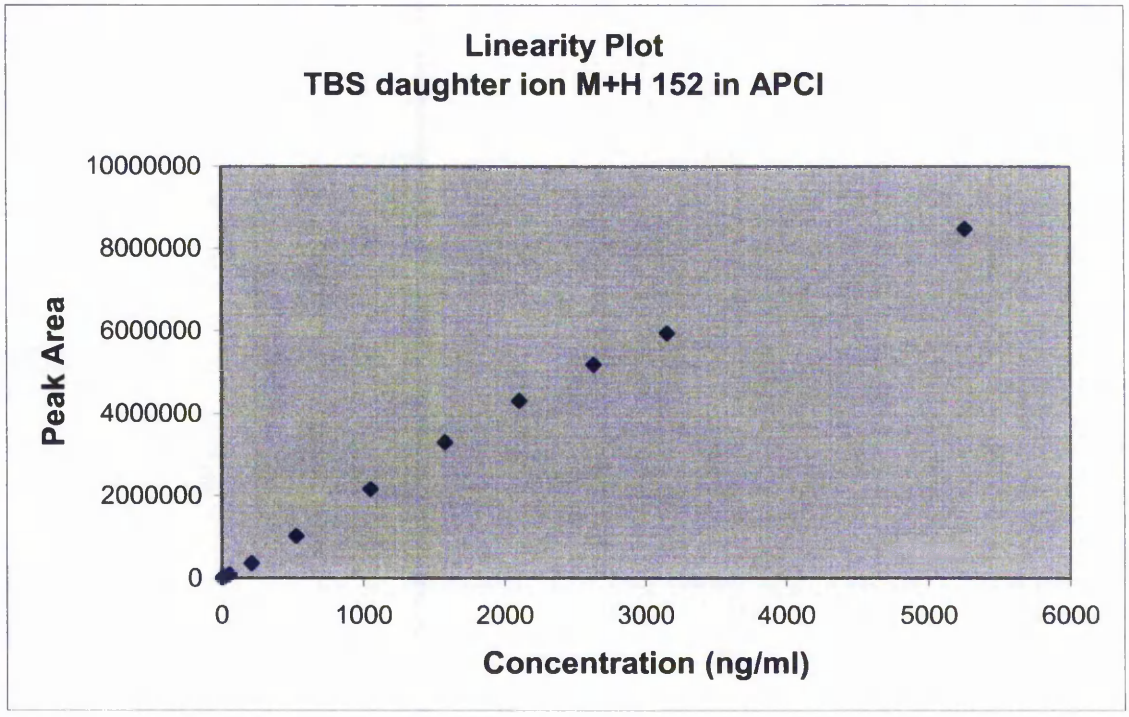

Figure 87. **Linearity of terbutaline sulphate daughter ion M+H 152 in APCI**

5.2.5 Flow Injection Analysis

The use of Flow Injection Analysis (FIA), where by the column is replaced with a zero dead volume connector was investigated for terbutaline sulphate. Using a mobile phase of 0.025 M ammonium acetate, pH 5.0 in methanol - water (10:90 v/v) a 100 µl injection of 50 ng/ml terbutaline sulphate was performed. LC/MS conditions were as section 5.2.3.1.

It was found that the LC conditions that were suitable for the analysis of terbutaline sulphate with a column in place were no longer suitable for FIA. A flow rate of 0.7 ml/min was found to be too rapid for FIA with the start of the peak eluting as data collection started at 0.05 mins. This is shown in Figure 88.

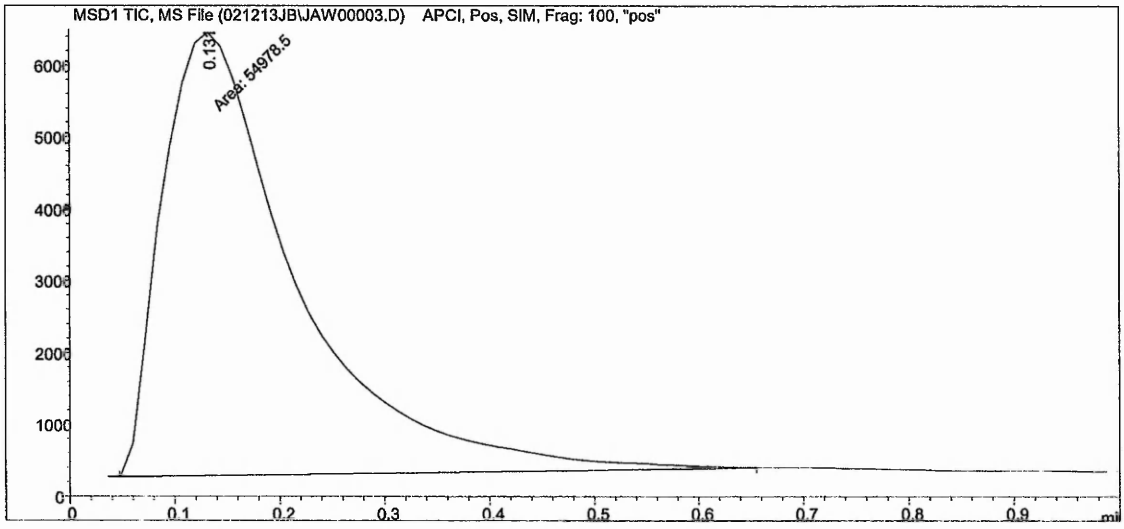

Figure 88. Chromatogram of terbutaline in FIA mode at 0.7 ml/min

Using the conditions above the peak width (half height) was 0.12 mins. The precision on 6 injections (RSD) was 2.84%. The flow rate was reduced by half to 0.35 ml/min in an attempt to delay the start of the peak elution. This is shown in Figure 89.

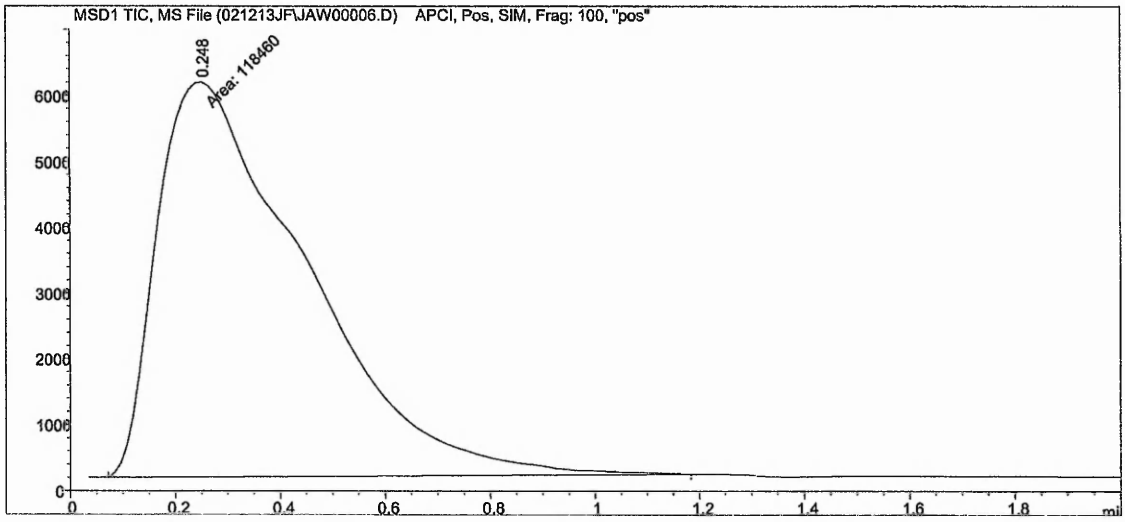

Figure 89. Chromatogram of terbutaline in FIA mode at 0.35 ml/min

Reducing the flow rate from 0.7 ml/min to 0.35 ml/min did not significantly delay the peak start as this occurred at 0.06 mins. However, the peak shape had deteriorated quite badly, with a peak width of 0.30 mins. A peak area % RSD determined on 6 injections was found to be 1.13%, showing that FIA with the above conditions was unsuitable. As reducing the flow rate was shown not to have an effect on the start of peak elution, the dead volume of the system was increased. This was achieved by replacing the zero dead volume connector with a length of PEEK tubing of dimensions 1880 x 0.254 mm, giving an increase in dead volume by 95 µl. The flow rate was set back to 0.7 ml/min. Figure 90 shows the chromatogram obtained using the peek tubing connector.

Using the PEEK tubing in place of the zero dead volume connector delayed the peak start to 0.08 mins. The peak width (half height) was 0.14 mins. However, the peak area RSD on 6 injections was 5.02%. It was noted that the area of the first injection was low. The analysis was repeated and again the first injection was low. The repeat analysis gave an area RSD of 4.22%. Omitting the first injection reduced this to a more acceptable 1.55%. One reason for the low first injection may be due to the formation of a coating on the inside of the PEEK tubing connector, and once this coating had been formed the areas were more reproducible.

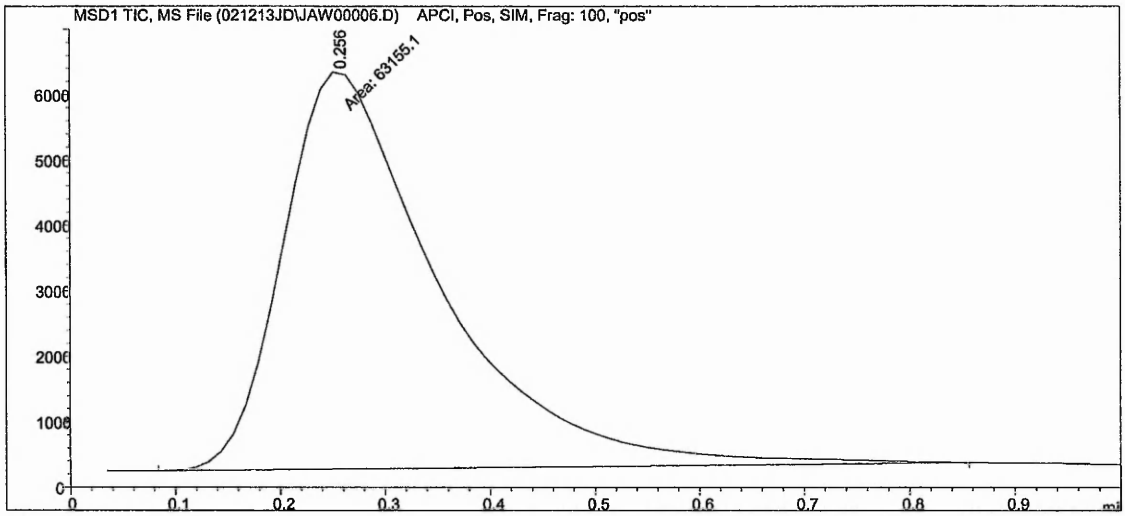

Figure 90. Chromatogram of terbutaline with PEEK tubing connector at 0.7 ml/min

Flow injection analysis has shown that whilst an acceptable retention time could be obtained, peak width and shape were poor. The default value for peak width, 0.12 mins had been used for this analysis. The peak width affects the data sampling rate. Optimisation of this value may have improved the peak shape; however, this was thought unlikely as the measured peak width at half height obtained at a flow rate of 0.7 ml/min varied between 0.12 - 0.15 mins. The data emphasise the need to use a column for the analysis to focus the analyte and hence improve peak shape and efficiency.

5.2.6 Mass Flow/Concentration Dependent Sensitivity

Mass spectrometry ion sources exhibit either mass flow or concentration dependent sensitivity. For a source to be mass flow sensitive the response obtained is a function of the amount of analyte in the detector. For a concentration sensitive source the response is a function of the analyte concentration in the detector.

Two ion sources for the Agilent MSD were evaluated to see whether they exhibit mass flow or concentration dependent sensitivity. The sources investigated were:

Atmospheric Pressure Chemical Ionisation (APCI)
Electrospray Ionisation (ESI)

To test the behaviour of each of the ion sources, the increase in intensity obtained from reducing the internal diameter of the column from 4.6 to 3.0, 2.1 and 1.0 mm was determined when operating at linear velocity with load on column kept constant.

Method Conditions

Mobile phase:	0.025 M ammonium acetate pH 5.0 in methanol – water (10:90 v/v)				
Column:	5 µm HyPURITY C18 150 mm length				
Run time:	10 minutes				
Injection volume:	20 µl				
Flow rates:	Column i.d. (mm)	4.6	3.0	2.1	1.0
	Flow Rate (ml/min)	1.0	0.425	0.208	0.047

MS conditions as sections 5.2.3.1 (APCI) and 5.2.3.2 (ESI)

When using the electrospray ion source at low flow rates (50 µl/min and below) a capillary electrospray nebuliser can be used. For the 1.0 mm internal diameter column operated at 50 µl/min (linear velocity) the standard and the capillary electrospray nebulisers were compared. The actual results obtained for the electrospray source are shown in Figures 91 and 92 along with the expected results for concentration dependent sensitivity.

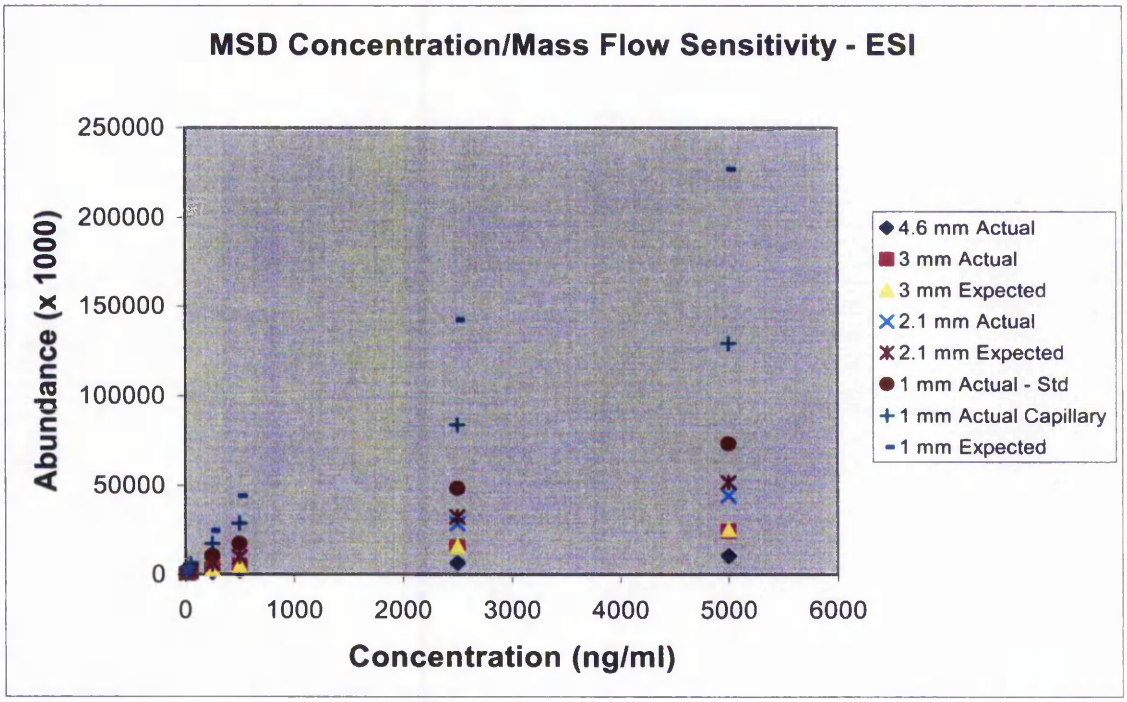

Figure 91. **MSD concentration versus mass flow sensitivity in ESI (1 – 4.6 mm i.d. columns)**

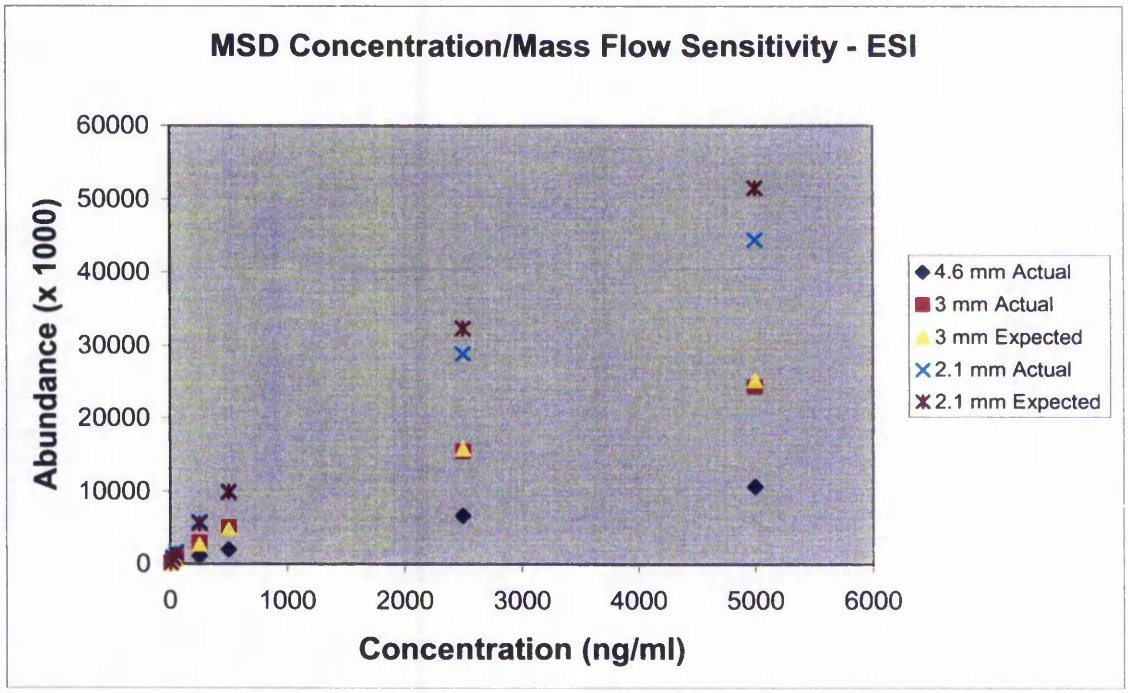

Figure 92. **MSD concentration versus mass flow sensitivity in ESI (2.1 – 4.6 mm i.d. columns)**

The results in Figures 91 and 92 show that the predicted data for electrospray correlate well with the actual data obtained for the 3.0 and 2.1 mm internal diameter columns. The data demonstrate the concentration dependent sensitivity of the electrospray source. The predicted data do not correlate well for the 1 mm internal diameter column with the standard electrospray nebuliser. It was thought that the standard electrospray nebuliser does not work well at low flow rates, due to poor droplet formation. A capillary electrospray nebiliser had been developed by Agilent Technologies for use at low flow rates. At low concentrations the correlation between predicted and actual results for this nebuliser were good but deteriorated with increasing concentration. This may be due to the source being non-linear above 50 ng/ml, i.e. the source is being overloaded.

The results obtained for the APCI source are shown in Figures 93 - 95 along with the expected results for concentration dependent sensitivity.

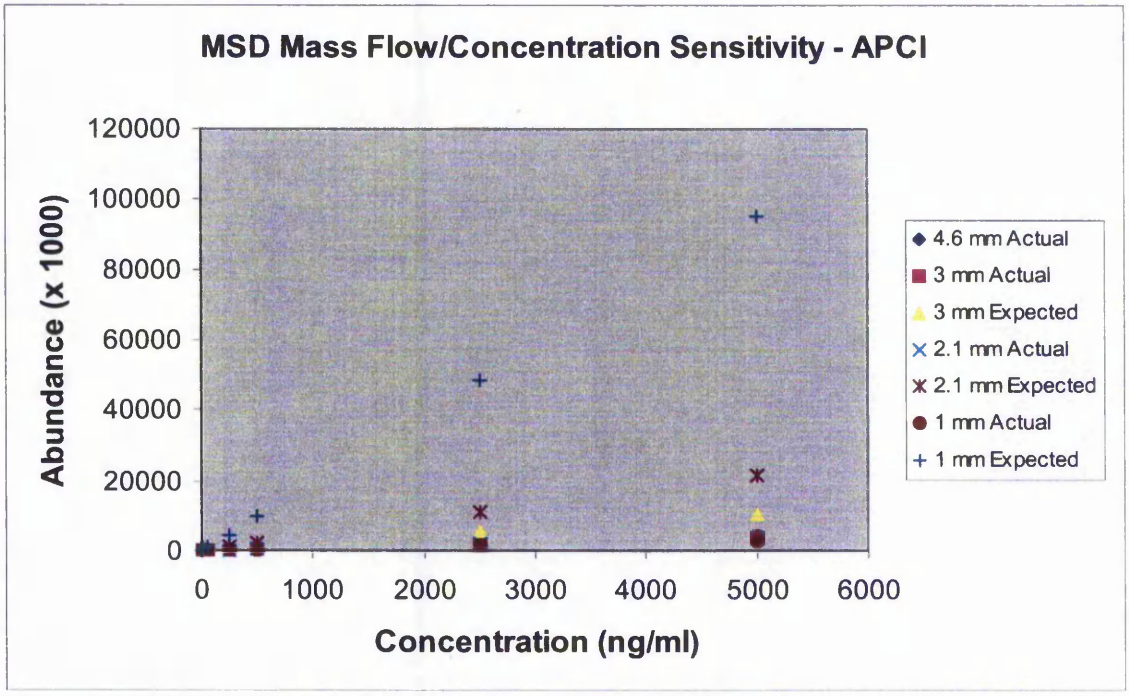

Figure 93. **MSD mass flow versus concentration sensitivity in APCI (1 – 4.6 mm i.d. columns)**

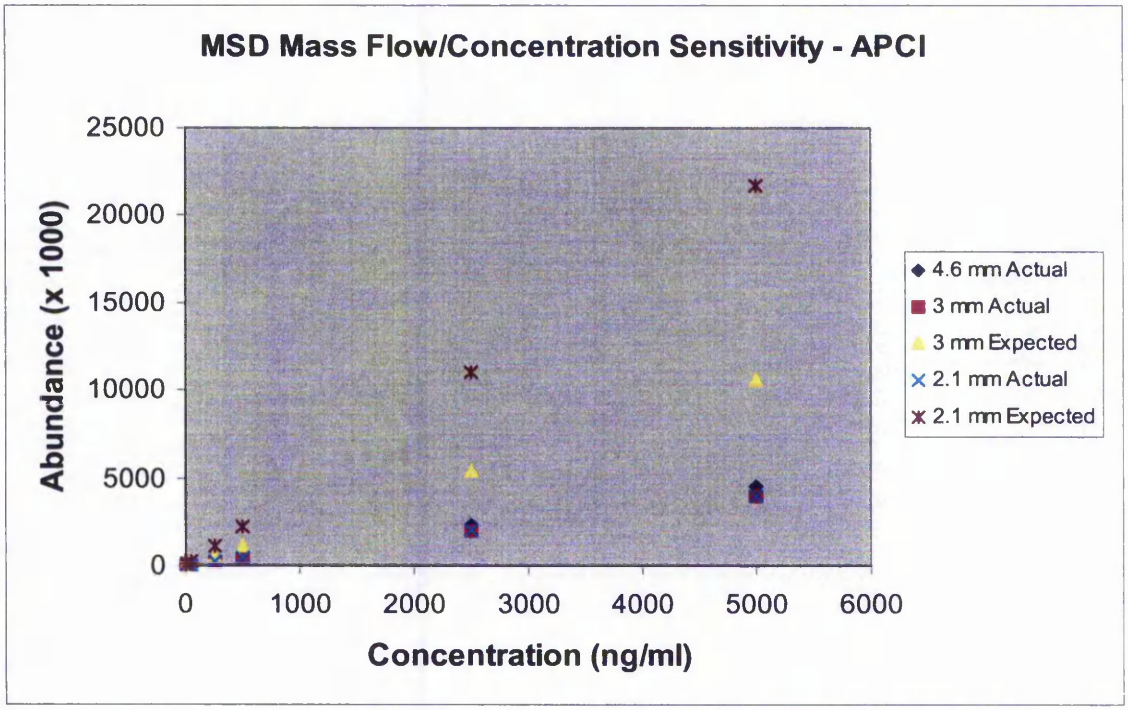

Figure 94. **MSD mass flow versus concentration sensitivity in APCI (2.1 – 4.6 mm i.d. columns)**

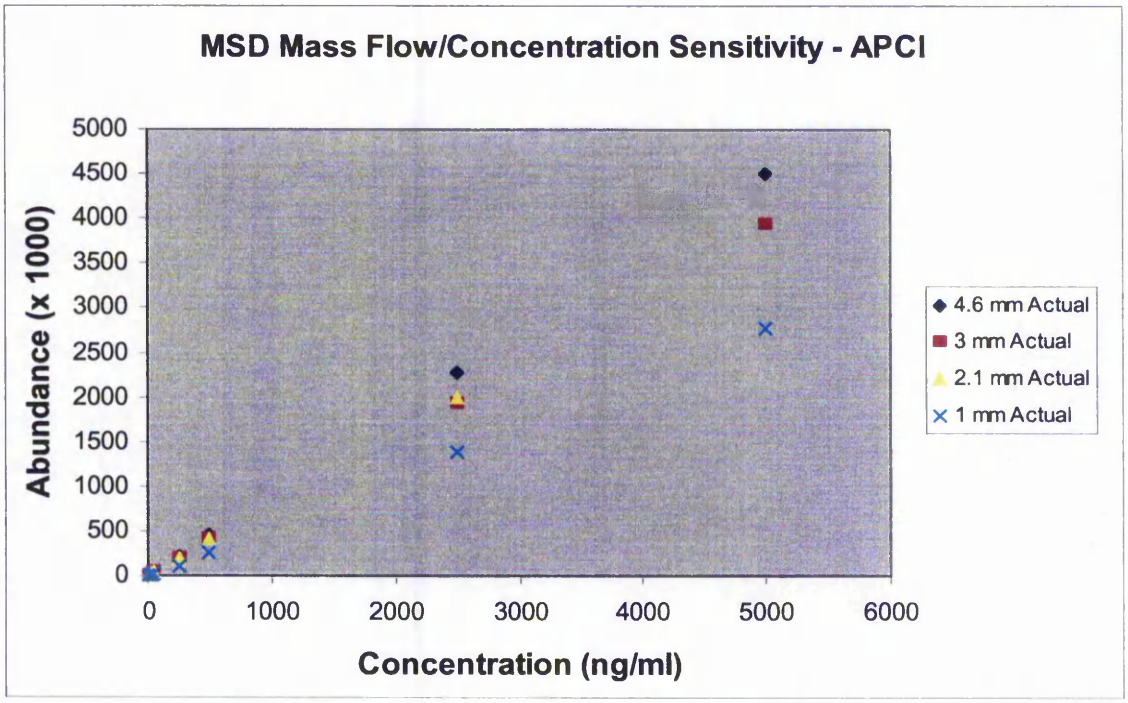

Figure 95. **MSD mass flow versus concentration sensitivity of APCI - Actual behaviour**

The expected abundances shown in Figures 93 and 94 represent the response expected for a concentration sensitive source. However, the data obtained do not match the expected values. The data for APCI show that at low concentrations the actual data obtained were comparable for 4.6, 3.0 and 2.1 mm internal diameter columns. There was slightly more variation for the 4.6 mm internal diameter column at high concentrations. The 1.0 mm internal diameter column showed lower abundances than the other three columns, suggesting that the source does not operate well at low flow rates. For APCI to be mass flow sensitive, it was expected that abundances obtained for all four columns would be the same. This was true with the exception of the 1.0 mm internal diameter column.

5.2.7 MS Drift in Response

An important consideration when performing a quantitative LC/MS assay is the instrument repeatability. The LC/MS needs to be able to give a stable response over the duration of the analysis.

Using the 'A' model 1100 MSD and the 5 µm HyPURITY C18 50 x 2.1 mm column, two hundred injections of terbutaline sulphate at a concentration of 50 ng/ml were performed with drift in peak area monitored over the length of the analysis. LC/MS analysis was performed in APCI and ESI for comparison.

5.2.7.1 APCI

The drift experiment was initially performed in APCI with a mobile phase of 0.025 M ammonium acetate unadjusted pH in methanol - water (10:90 v/v) at a flow rate of 0.7 ml/min with an injection volume of 100 µl and a run time of 2 minutes. The following optimised MS conditions were used for terbutaline sulphate:

APCI positive ionisation at M+H 226

Fragmentor voltage:	40 V
Vaporiser temperature:	500°C
Gas temperature:	325°C
Drying gas:	5.0 L/min
Nebuliser pressure:	50 psig
Vcap:	4000 V
Corona current:	4.0 µA

Figure 96 shows the drift in response of terbutaline with increasing injection number.

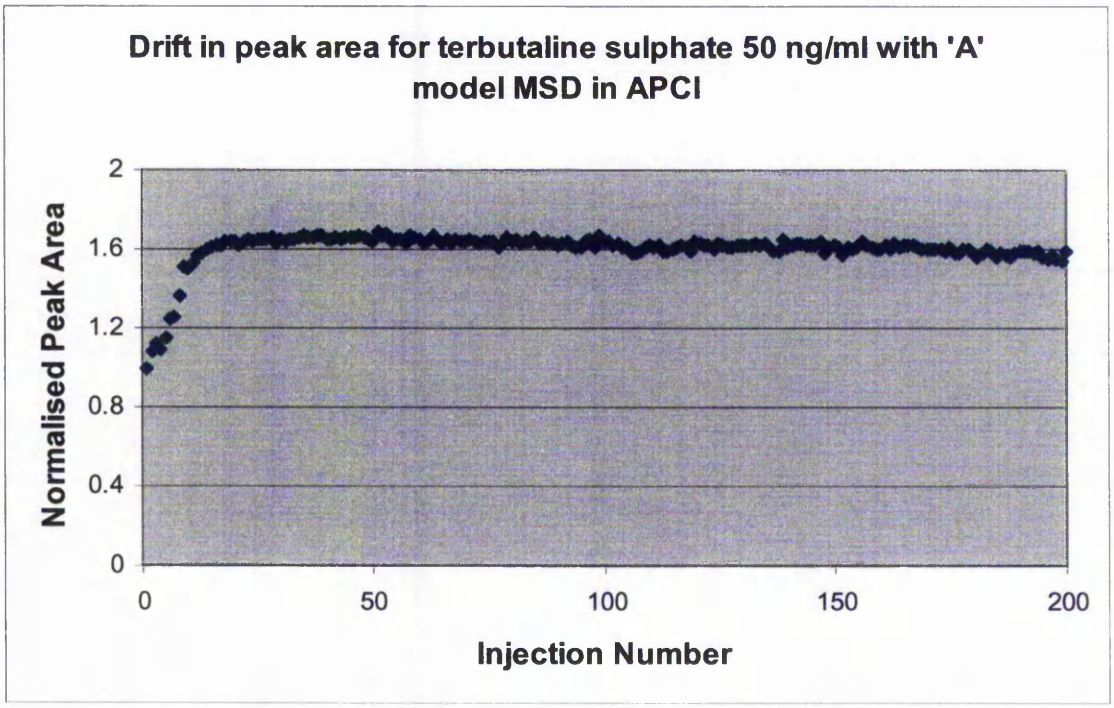

Figure 96. **Drift in response of terbutaline with time for the 'A' model MSD in APCI with ammonium acetate, unadjusted pH in the mobile phase**

The results show that a series of injections were required to stabilise the response from the MSD. During the first ten injections the response was shown to steadily increase. Thereafter it remained stable. The area % RSD over 200 injections was 6.04%. For injections 11-200 this had reduced to 1.77%. The requirement of a series of injections to stabilise the response may be due to the formation of a coating on either the corona needle or the spray plate from the mobile phase or sample solvent. Once this coating has formed the response stabilised.

The drift experiment above was repeated in APCI using a mobile phase of 0.025 M ammonium acetate pH 5.0 in methanol - water (10:90 v/v) at a flow rate of 0.7 ml/min with an injection volume of 100 µl. The pH adjustment was used to try to stabilise the response over the 200 injections. Figure 97 shows the drift in response for terbutaline with increasing injection number using a pH 5.0 mobile phase.

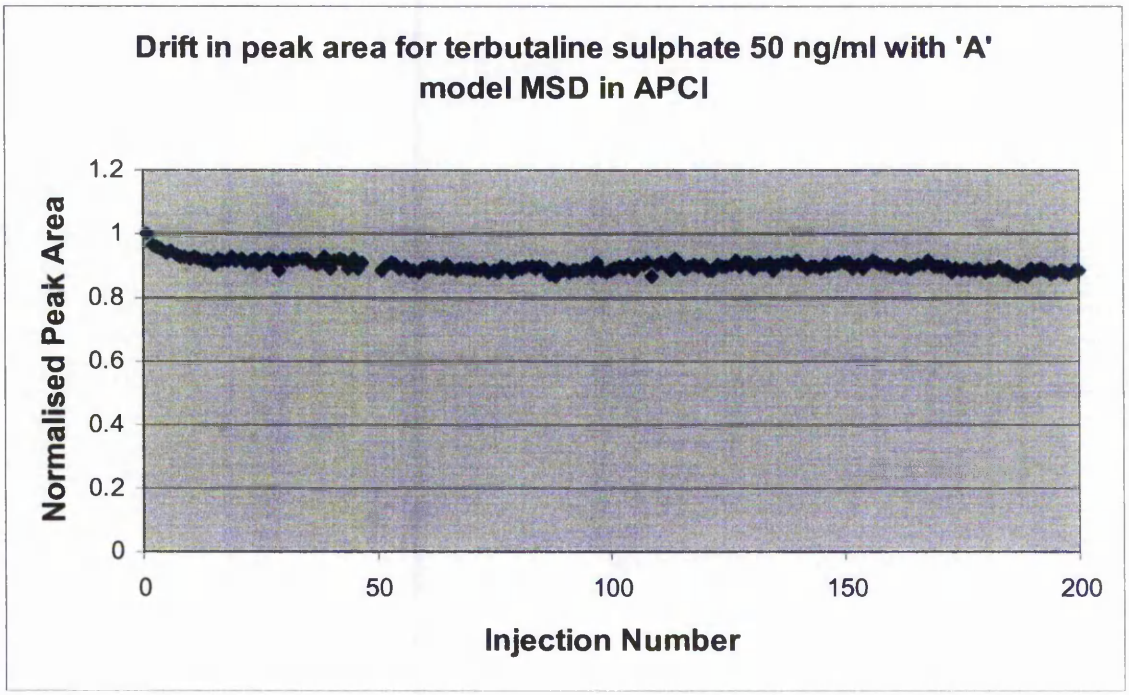

Figure 97. **Drift in response of terbutaline with time for the 'A' model MSD in APCI with ammonium acetate, pH 5.0 in the mobile phase**

The results show that again a series of injections are required to stabilise the response from the MSD. Here the response was shown to decrease slightly over the first 10 injections. Thereafter the response remained the stable. The change in response at the beginning of this study was much less than was seen in the previous study which used an unadjusted pH mobile phase. Here the area % RSD over 200 injections was 1.98%. For injections 11-200 this had reduced to 1.51%.

The drift experiment was repeated using the 'D' model MSD in APCI with a mobile phase of 0.025 M ammonium acetate pH 5.0 in methanol - water (10:90 v/v) at a flow rate of 0.7 ml/min with an injection volume of 100 µl. The following optimised MS conditions were used for terbutaline sulphate:

APCI positive ionisation at M+H 226

Fragmentor voltage:	100 V
Vaporiser temperature:	400°C
Gas temperature:	350°C
Drying gas:	5.0 L/min
Nebuliser pressure:	535 psig
Vcap:	3500 V
Corona current:	4.0 µA

Figure 98 shows the drift in response of terbutaline with increasing injection number for the 'D' model MSD.

The results show that with the 'D' model MSD an initial series of ten injections were not required to stabilise the response. The major difference between the two models of MSD is the wider bore capillary on the 'D' model. It is possible that on the 'A' model MSD with the narrower bore capillary a charging effect is seen, which requires a number of injections to stabilise this effect. Due to the larger surface area of the wider bore capillary charging is prevented from occurring and hence the response is stable. The response was shown to be stable over the 200 injections with an area % RSD of 1.92% over all injections and a high to low drift of 10%. This highlights the instruments excellent stability over a 16 hour run.

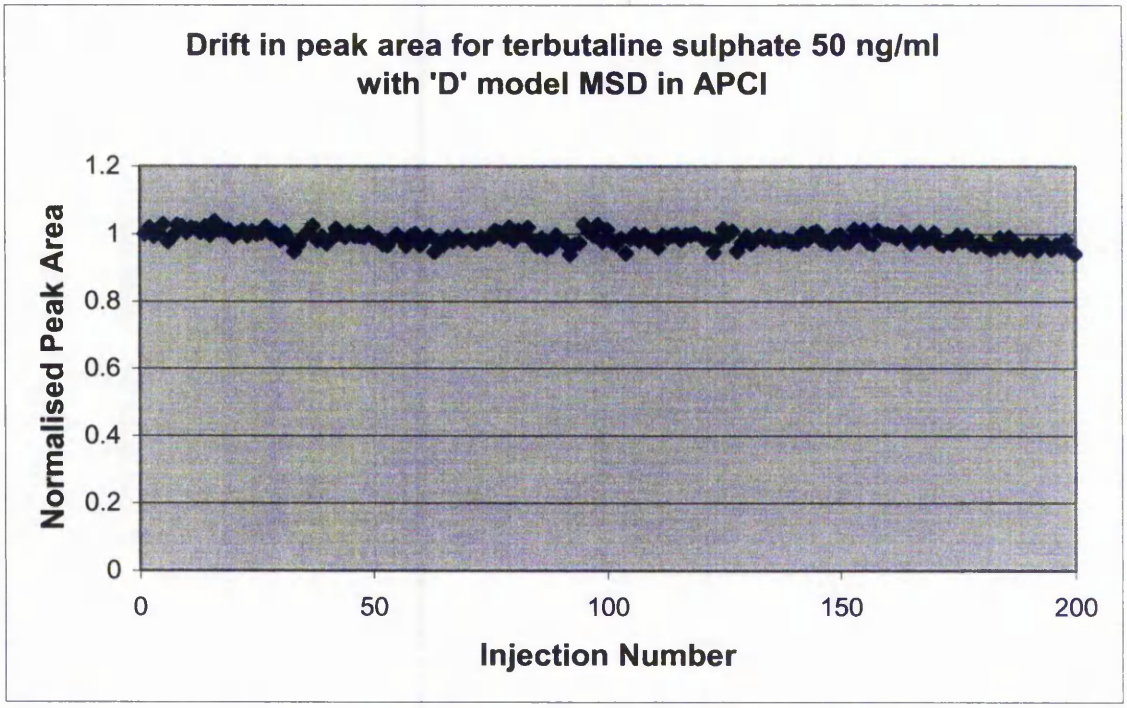

Figure 98. **Drift in response of terbutaline with time for the 'D' model MSD in APCI with ammonium acetate, pH 5.0 in the mobile phase**

5.2.7.2 ESI

The drift experiment was repeated in ESI with a mobile phase of 0.025 M ammonium acetate unadjusted pH in methanol - water (10:90 v/v) at a flow rate of 0.7 ml/min with an injection volume of 100 µl. The following optimised MS conditions were used for terbutaline sulphate:

ESI positive ionisation at M+H 226

Fragmentor voltage:	60 V
Vaporiser temperature:	N/A
Gas temperature:	350°C
Drying gas:	10.0 L/min
Nebuliser pressure:	40 psig
Vcap:	4000 V
Corona current:	4.0 µA

Figure 99 shows the drift in response of terbutaline with increasing injection number using the 'A' model MSD in electrospray.

The results for electrospray show that the response steadily increased in a step-wise manner throughout the duration of the study. Unlike the 'A' model MSD in APCI, a series of initial injections do not stabilise the response. The area % RSD for all injections was 6.03%.

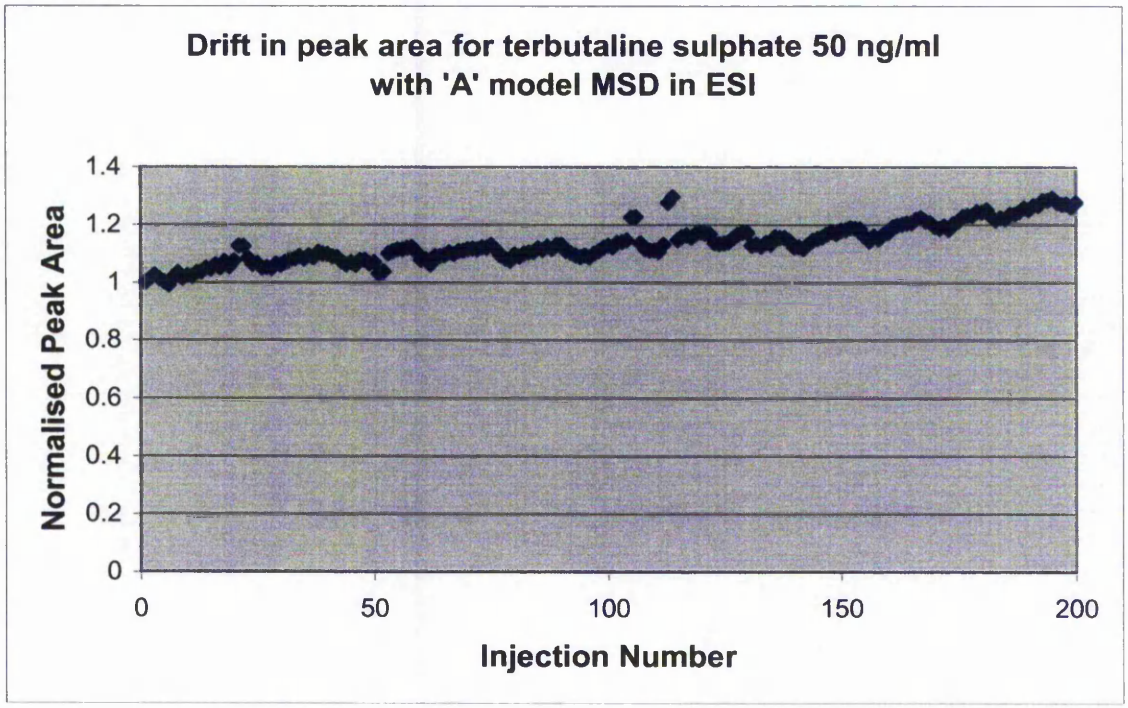

Figure 99. **Drift in response of terbutaline with time for the 'A' model MSD in ESI with ammonium acetate, unadjusted pH in the mobile phase**

The drift experiment was repeated using the 'D' model MSD in ESI with a mobile phase of 0.025 M ammonium acetate pH 5.0 in methanol - water (10:90 v/v) at a flow rate of 0.7 ml/min with an injection volume of 100 µl. The following optimised MS conditions were used for terbutaline sulphate:

ESI positive ionisation at M+H 226

Fragmentor voltage:	100 V
Vaporiser temperature:	N/A
Gas temperature:	350°C
Drying gas:	12.9 L/min
Nebuliser pressure:	60 psig
Vcap:	2500 V
Corona current:	4.0 µA

Figure 100 shows the drift in response of terbutaline with increasing injection number using the 'D' model MSD in electrospray.

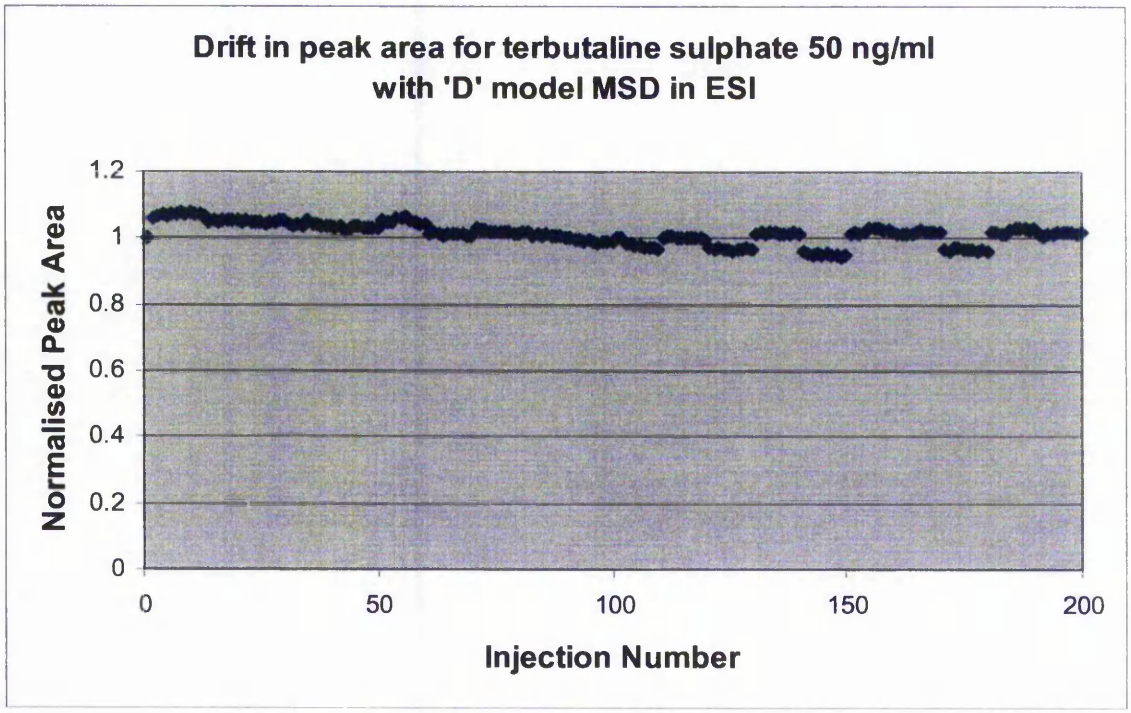

Figure 100. **Drift in response of terbutaline sulphate 50 ng/ml with time for the 'D' model MSD in ESI with ammonium acetate, pH 5.0 in the mobile phase**

The results above show that with the 'D' model MSD in ESI, after the first injection the response was stable for 50 injections. Thereafter the response was seen to vary with each set of 10 injections per vial. Over 200 injections the area % RSD was 3.06%, with a high to low drift of 14%.

To see if the phenomena of a change in response with a change a sample vial was due to the sample concentration, the analysis was repeated at a lower terbutaline sulphate concentration of 10 ng/ml as 50 ng/ml had previously been shown to be outside the linear range for the method (see section 5.2.3.2).

Figure 101 shows the drift in response of terbutaline sulphate 10 ng/ml with increasing injection number using the 'D' model MSD in electrospray.

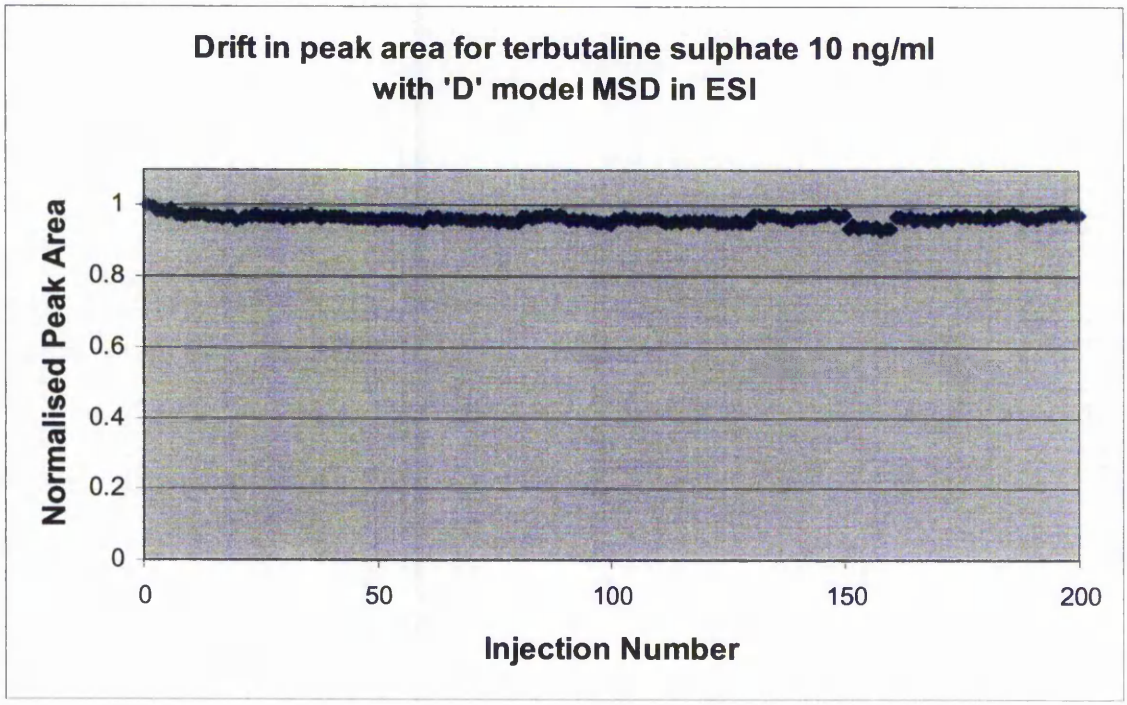

Figure 101. **Drift in response of terbutaline sulphate 10 ng/ml with time for the 'D' model MSD in ESI with ammonium acetate, pH 5.0 in the mobile phase**

The results in Figure 101 show that the response was reasonably stable throughout the 200 injections. The high to low drift was 7% with an area RSD of 1.05%. For some sample vials the response was seen to alter between vials, i.e. vial 16 (injections 151-160) where a decrease in response was obtained for all 10 injections from a single vial. The change in response with change in vial was not as dramatic as when injecting 50 ng/ml as shown in Figure 100.

It was thought that the change in response with change in vial observed at a terbutaline sulphate concentration of 50 ng/ml was due to adduct formation, with increasing adduct amount at higher concentrations. To confirm this, samples of terbutaline sulphate over the concentration range 10 ng/ml to 25 µg/ml were analysed in scan mode over the mass range 50 – 600 amu. Other LC/MS conditions were as above for analysis of terbutaline sulphate in electrospray. The spectra obtained at each of the concentrations tested are shown in Figure 102.

The spectra show the presence of an M+Na ion at 248.2. The relative intensity of the 248.2 ion increases with concentration until 2500 ng/ml. Thereafter no additional increase is seen. Other less dominant adduct ions present are M+K at 264.2 and 2M+Na at 473.2.

To see what affect the adduct ion 248.2 had on the drift in response of the terbutaline ion 226.2 in ESI, a drift experiment was performed by grouping together the ions 226.2 and 248.2 and extracting the individual ions out afterwards.

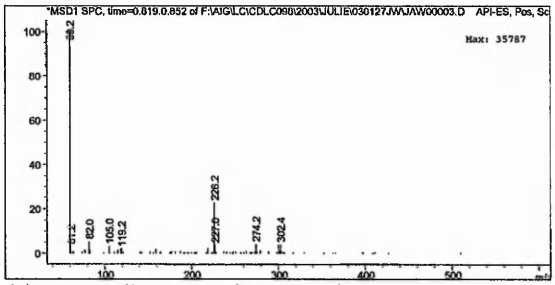

(a) Concentration 10 ng/ml

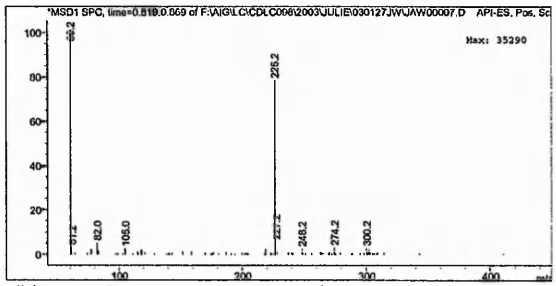

(b) Concentration 50 ng/ml

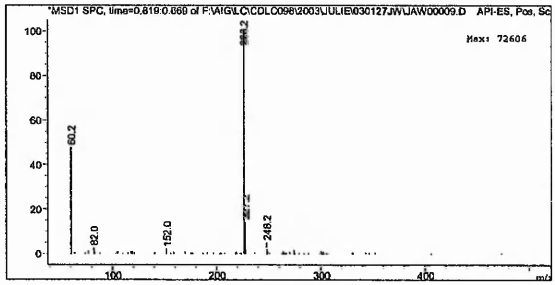

(c) Concentration 200 ng/ml

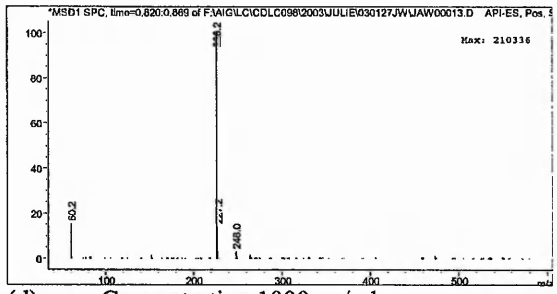

(d) Concentration 1000 ng/ml

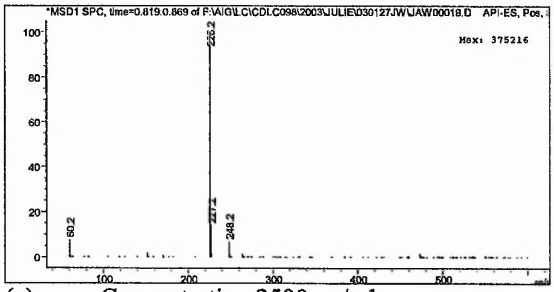

(e) Concentration 2500 ng/ml

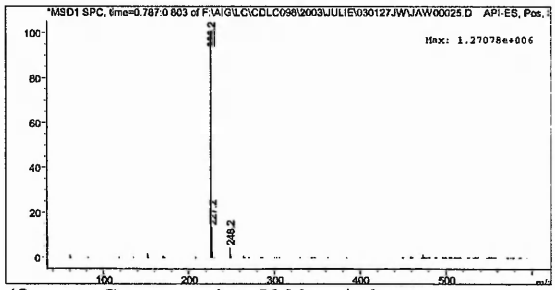

(f) Concentration 5000 ng/ml

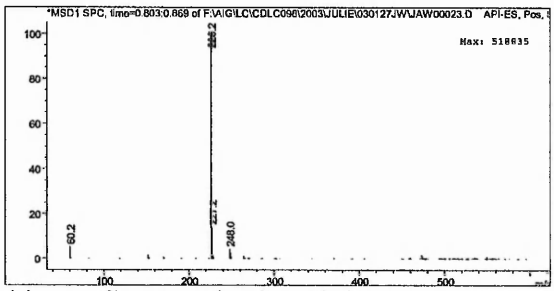

(g) Concentration 25 µg/ml

Figure 102. Spectra of terbutaline with increasing concentration showing adduct formation

The drift experiment used the 'D' model MSD in ESI with a mobile phase of 0.025 M ammonium acetate pH 5.0 in methanol - water (10:90 v/v) at a flow rate of 0.7 ml/min with an injection volume of 100 µl. The following optimised MS conditions were used for terbutaline sulphate:

ESI positive ionisation at M+H 226

Fragmentor voltage:	100 V
Vaporiser temperature:	N/A
Gas temperature:	350°C
Drying gas:	12.9 L/min
Nebuliser pressure:	60 psig
Vcap:	2500 V
Corona current:	4.0 µA

Figure 103 shows the drift in response of the ions 226.2 (M+H) and 248.2 (M+Na) with increasing injection number using the 'D' model MSD in electrospray. The same drift with enhanced scaling is shown in Figure 104.

Figures 103 and 104 show that after the first 10 injections where the response was shown to decrease for both M+H and M+Na, as the response for M+H increases the response for M+Na decreases and as the response for M+H decreases the response for M+Na increases. The change in response with vial is seen from vial 13, injection 122, though to a lesser extent than was previously seen. The responses from M+H and M+Na are combined and normalised and displayed in Figure 105.

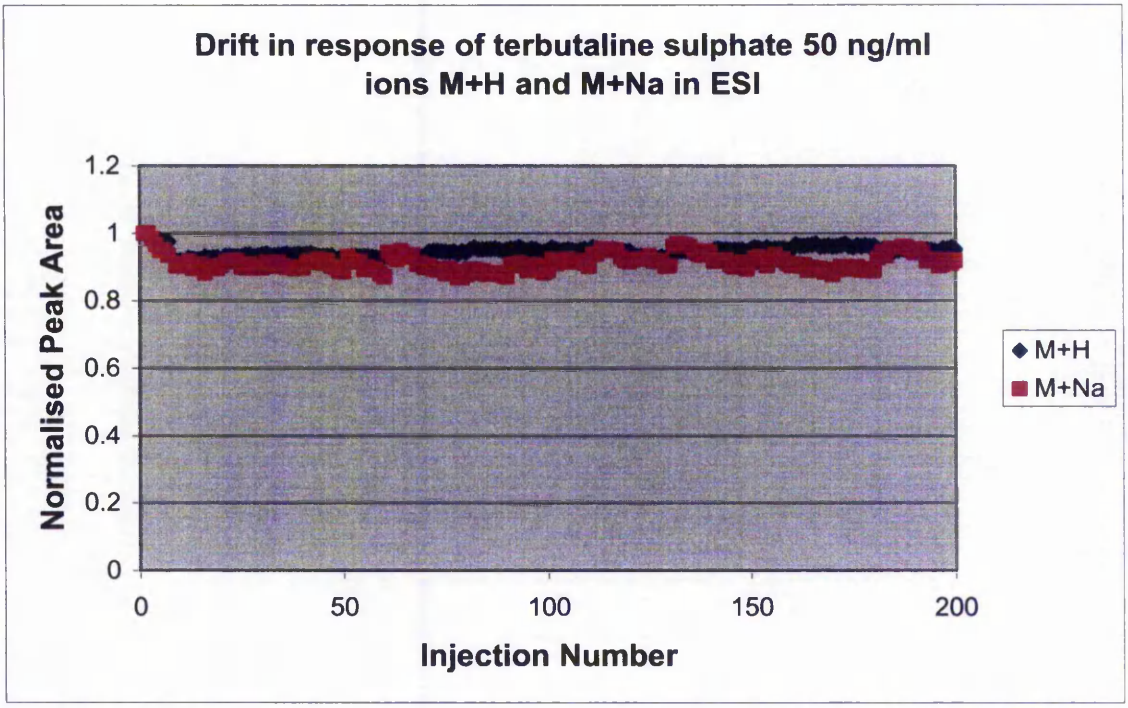

Figure 103. **Drift in response with time of ions M+H and M+Na from terbutaline sulphate 50 ng/ml for the 'D' model MSD in ESI**

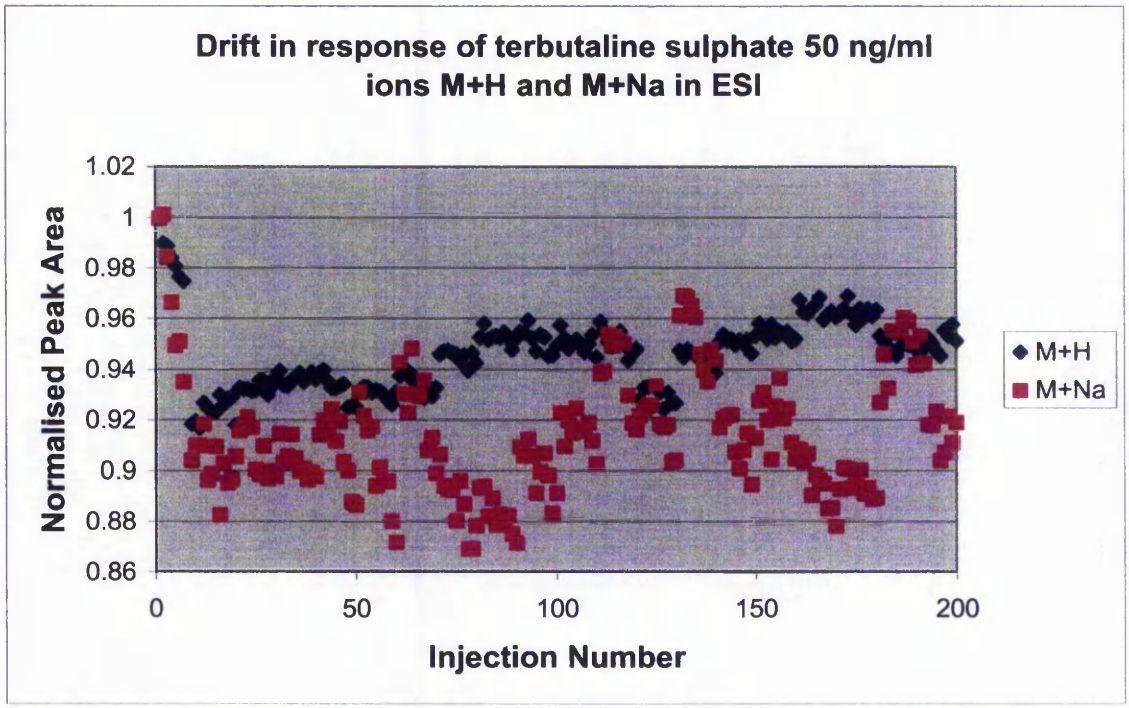

Figure 104. **Drift in response with time of ions M+H and M+Na from terbutaline sulphate 50 ng/ml for the 'D' model MSD in ESI**

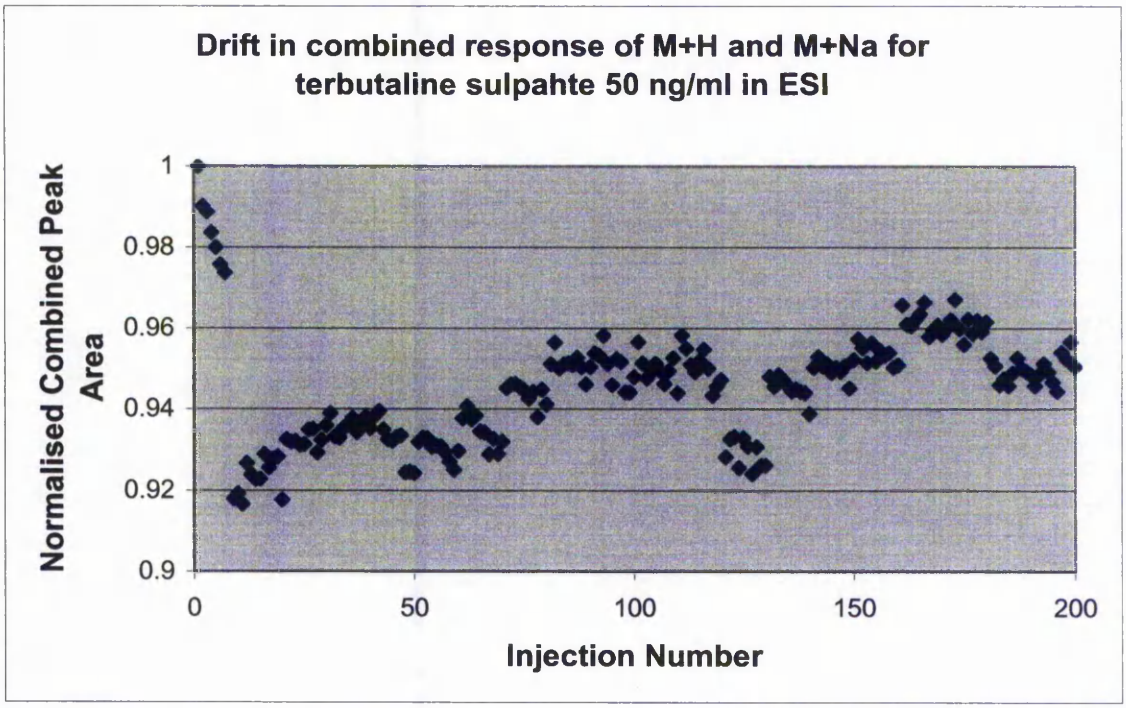

Figure 105. **Drift in combined response with time of ions M+H and M+Na from terbutaline sulphate 50 ng/ml for the 'D' model MSD in ESI**

The drift results are summarised below in Table 23.

Table 23. **Drift results for M+H and M+Na ions**

Ion	% Area RSD	% High to Low Drift
M+H	1.47	8
M+Na	2.65	13
(M+H) + (M+Na)	1.45	8

The combined response from M+H and M+Na showed that the response from M+Na was not sufficient to counteract the response pattern from M+H. This was because the response for M+Na was only 2.5% of that obtained for M+H. In order to overcome the response pattern observed for M+H it may be necessary to sum the response obtained for all adduct ions and not just M+Na, i.e. to also include M+K and 2M+Na.

5.2.8 Data Collection in Atlas

In order to facilitate rapid analysis a fast data processing package is required. It is not advantageous to have rapid optimised methods that take hours to process. The Agilent Technologies Chemstation data processing package, batch analysis, is both laborious and time consuming for quantitative analysis, particularly when performing multilevel calibration.

When the MSD was purchased from Hewlett Packard, the use of batch analysis software was the only way to process the data for a quantitative method. Unlike the Hewlett Packard UV detectors there were no analogue outputs to allow the collection of data into a chromatography data system, e.g. Multichrom or Atlas. Working with Agilent Technologies who appreciated the problems that had been encountered, a fraction collection box was developed which would allow a single signal from the MSD to be taken into the chromatography data system. The fraction collection box is shown in Figure 106.

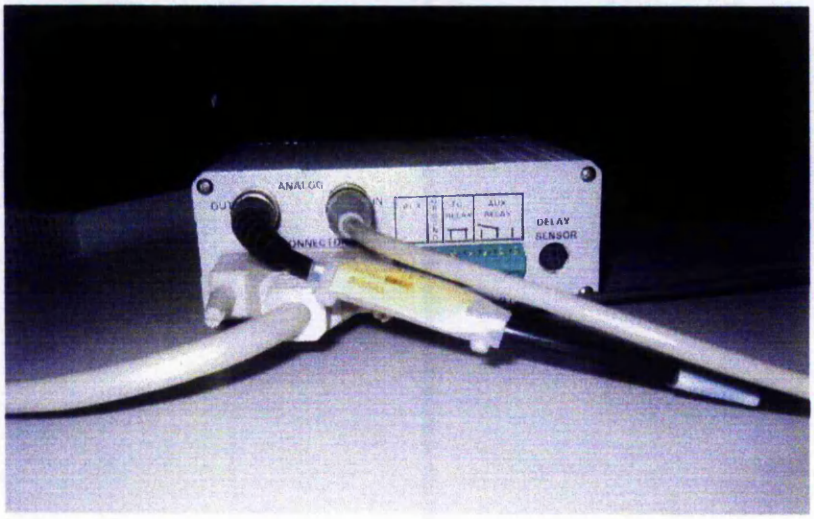

Figure 106. Agilent Technologies fraction collection box

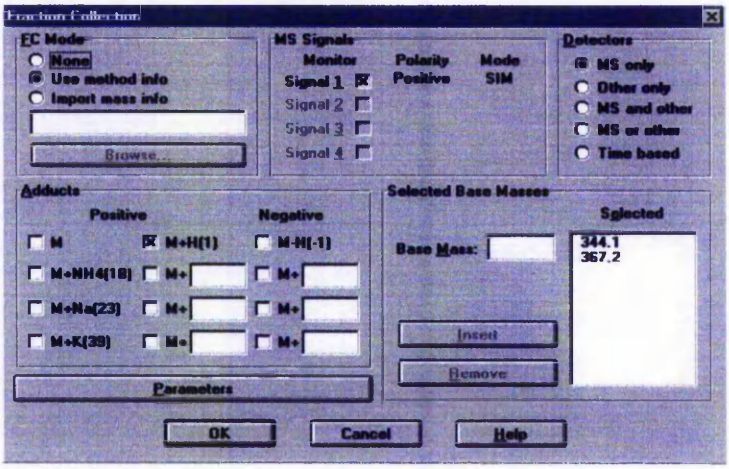

Figure 107. Fraction collection software in Chemstation

The fraction collection software as shown in Figure 107 allows the simultaneous collection of many ions. However, the software is unable to deconvolute the ions and instead sums up the response from each individual ion selected for output into the chromatography data system. Where multiple ions are required to be quantified in a single sample, the components need to be resolved chromatographically.

The dynamic range of data from the MSD often exceeds that of common chromatography data systems. To overcome this, the analogue output from the MSD can be scaled as shown in Figure 108 to provide a maximum of 1 volt on the chromatography data system scale. This has proven to be particularly useful when analysing samples of low concentrations which otherwise would not give a response on the chromatography data system.

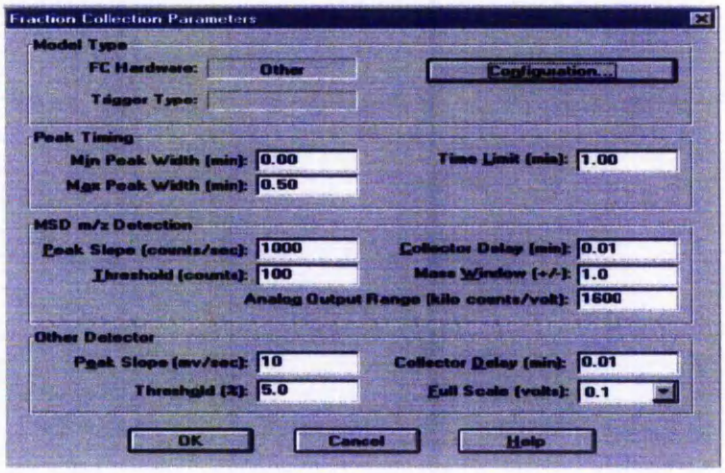

Figure 108. Fraction collection parameters in Chemstation

Quantitative LC/MS analysis was performed for a series of samples containing AR-C126925 using a column switching approach as described in section 5.3.3, with data collected on the Chemstation and through the chromatography data system Multichrom for comparison.

LC method conditions

Pre column: 5 µm Waters Sentry Symmetry C8 20 x 3.9 mm

Analytical column: 5 µm Waters Symmetry C8 150 x 4.6 mm

Loading pump mobile phases:

A: 1 % w/v ammonium acetate unadjusted pH

B: Acetonitrile

Analytical pump mobile phases:

A: 2.5 mM ammonium acetate pH 5.0

B: Methanol

Run time: 5 minutes

Loading pump gradient:

Time (mins)	% B	Flow Rate (ml/min)
0.00	5	1
1.00	5	1
1.10	95	3
2.50	95	3
2.51	5	3
3.40	5	1

Contact closure switch performed after 1 minute

Analytical pump gradient:

Time (mins)	%B
0.00	60
2.00	60
2.60	85
3.60	85
3.70	60

Flow rate for analytical pump: 1.0 ml/min
Injection volume: 20 µl
Column oven temperature: 40°C

The flow was diverted from the mass spectrometer to waste for the first one minute of the run time to prevent fouling.

Figure 109 shows the chromatogram obtained from the Chemstation. Figure 110 shows the chromatogram obtained from the chromatography data system Multichrom. The spike in the chromatogram at one minute represents the start of data collection as the first one minute the flow is directed to waste.

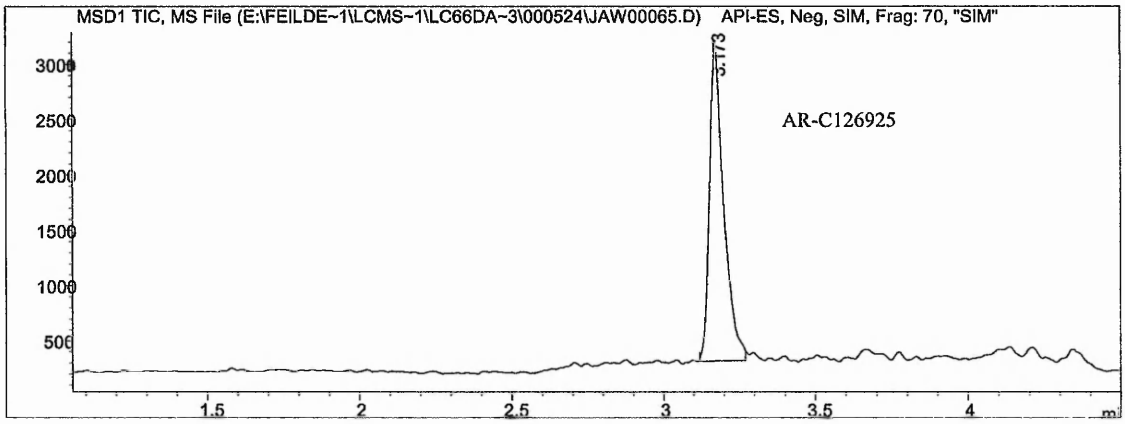

Figure 109. Chromatogram obtained in Chemstation for AR-C126925

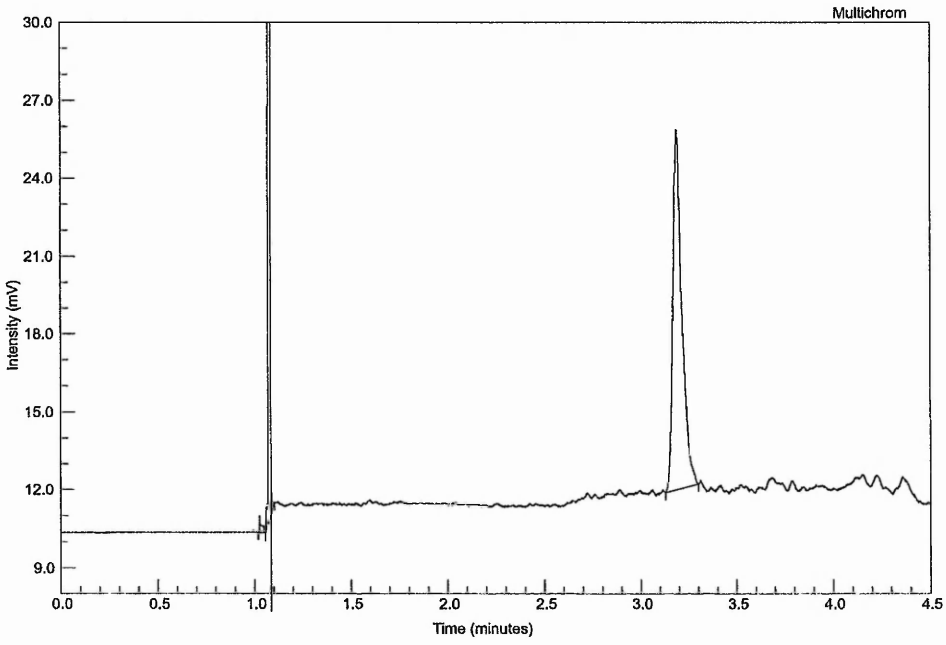

Figure 110. Chromatogram obtained in Multichrom for AR-C126925

The chromatogram of the analogue output signal was compared to that obtained in Chemstation. Data were processed using both software packages. The results are shown in Table 24.

Table 24. Comparison of Multichrom and Chemstation results

Sample	Multichrom Result (ng/ml)	Chemstation result (ng/ml)	Multichrom/Chemstation Variability (%)
Human-2 20hr	2.39	2.37	100.9
Human-2 28hr	4.02	3.97	101.1
Human-2 44hr	8.02	7.92	101.3
Human-2 52hr	9.82	9.75	100.7
Human-2 68hr	15.09	15.00	100.6
Human-2 75hr	18.41	18.24	100.9
Rat-7 20hr	3.48	3.45	100.9
Rat-7 28hr	5.82	5.74	101.3
Rat-7 44hr	12.24	10.53	116.3
Rat-7 52hr	15.32	12.48	122.7
Rat-7 68hr	24.35	21.00	115.9
Rat-7 75hr	28.62	25.42	112.6

The results above show good similarity between the Multichrom and Chemstation data. Where differences in results are seen this was largely due to integration differences between the two chromatograms, which occurred due to the low sample concentration analysed. Using Multichrom to process the data enabled a significant time saving, with processing time reduced from 3 hours for a typical overnight to run to under 30 minutes.

5.3 Rapid LC/MS Applications

Using the obtained results for the optimisation of LC and MS parameters for rapid analysis, applications have been developed for low level quantification by rapid LC/MS analysis.

5.3.1 Formoterol Swab Analysis

The first application was for the analysis of formoterol fumarate dihydrate (FFD) in cleaning verification samples. Following manufacture of FFD pressurised metered dose inhalers (pMDIs), the equipment is swabbed using a Kleenex Professional Wipe swab.

FFD is extracted from the swab and the resulting solution analysed to check for the absence of residual FFD. The original analytical method used LC/UV [75], but this was non-specific as a small interfering peak was seen in some batches of swabs. This method had a 10 minute run time. Figures 111 and 112 show chromatograms of a blank and a sample swab.

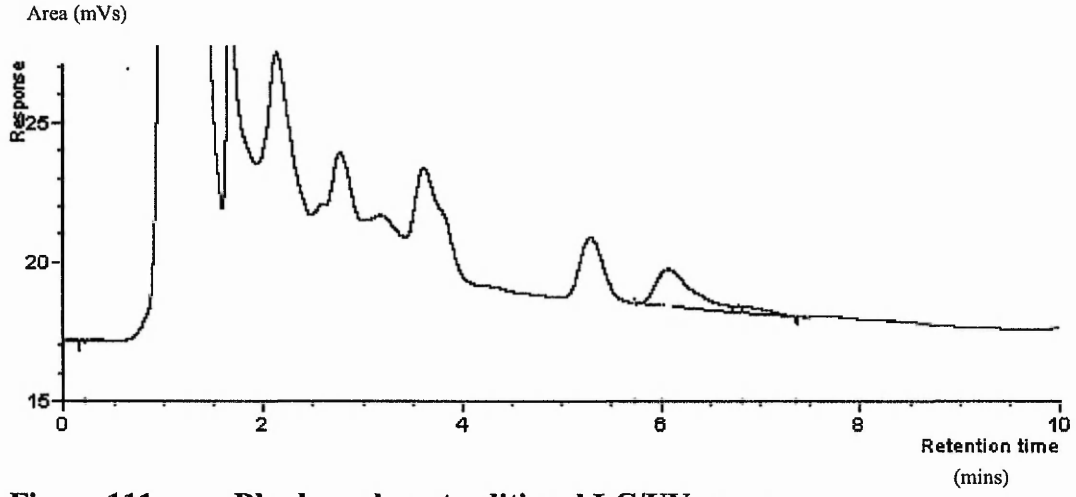

Figure 111. Blank swab on traditional LC/UV screen

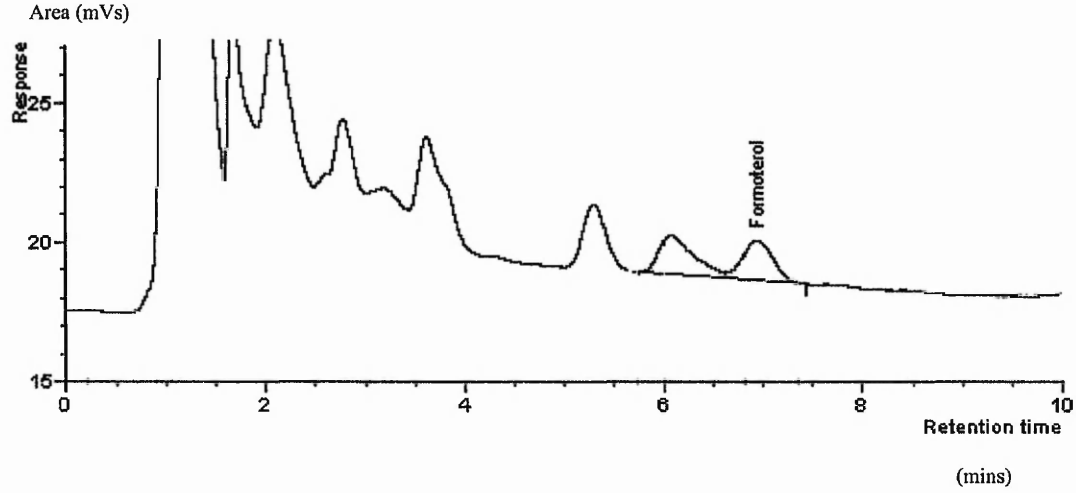

Figure 112. Typical chromatogram of swab sample with LC/UV analysis

An LC/MS method was required which separated formoterol from co-eluting impurities and had a significant reduction in run time. The method needed to be able to detect FFD at levels of 100 ng/ml. The LC/UV method used a sample solvent of 0.05 M phosphate buffer pH 6 in acetonitrile-water (16:84 v/v). This sample solvent had previously been shown to be suitable for the extraction of FFD from the swab material; however, as shown in section 5.2.2.1, it is necessary to restrict the amount of non-volatile materials entering the mass spectrometer to prevent fouling and loss of response.

Method Conditions

Mobile Phase:	0.025 M ammonium acetate pH 5.0 methanol-water (20:80 v/v)
Column:	5 µm HyPURITY C18 50 x 2.1 mm
Flow Rate:	0.7 ml/min
Injection Volume:	100 µl in overlap injection mode

Using flow injection analysis the following MS conditions were obtained:

APCI SIM at M+H 345 (Formoterol)

Fragmentor voltage:	40 V
Vaporiser temperature:	500°C
Gas temperature:	325°C
Drying gas:	5.0 l/min
Nebuliser pressure:	50 psig
Vcap:	4000 V
Corona current:	4.0 µA

The MSD was diverted to waste for 0.5 minutes at the start of the run to prevent any phosphate buffer in the sample solvent from entering the ion source. The use of 20% methanol in the mobile phase allowed the separation of an impurity in the blank swab at 1.65 minutes which was resolved from formoterol in the final method. The MS signal was exported into the chromatography data system Atlas to allow easy quantification of the data. A typical chromatogram of a blank swab with analysis by LC/MS is shown in Figure 113. A chromatogram of a formoterol swab sample with analysis by LC/MS is shown in Figure 114. The chromatograms show that it was possible to develop a rapid

LC/MS method which was specific for formoterol in cleaning verification samples. The run time for this method had been reduced from 10 minutes to 3 minutes, and used the overlap injection mode to bury the injection time in the run time of the method, allowing a significant reduction in analysis time for a series of samples compared to the original LC/UV method.

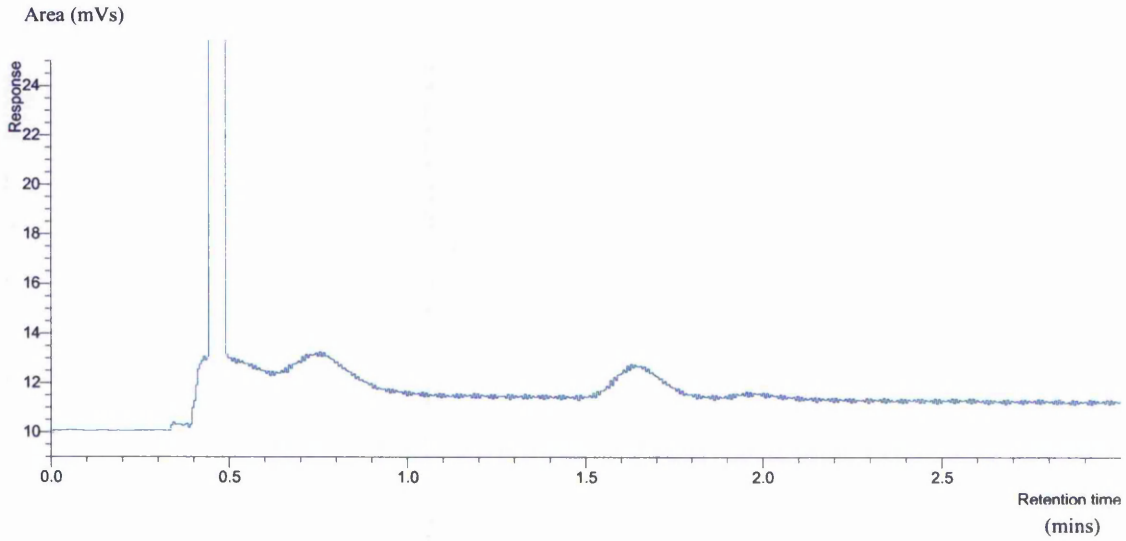

Figure 113. Typical chromatogram of blank swab with analysis by LC/MS

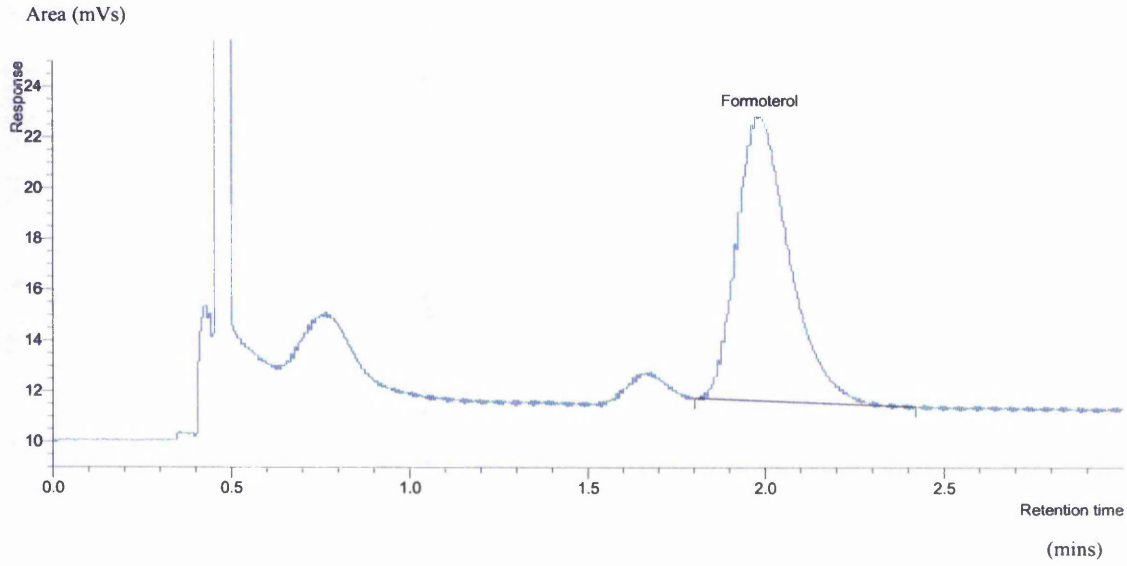

Figure 114. Typical chromatogram of formoterol swab sample with analysis by LC/MS

Linearity of FFD on the cleaning verification method was obtained between 10 and 1000 ng/ml as demonstrated in Figure 115, with a correlation coefficient of 0.9996. Precision on six injections of 1000 ng/ml FFD was 1.80%.

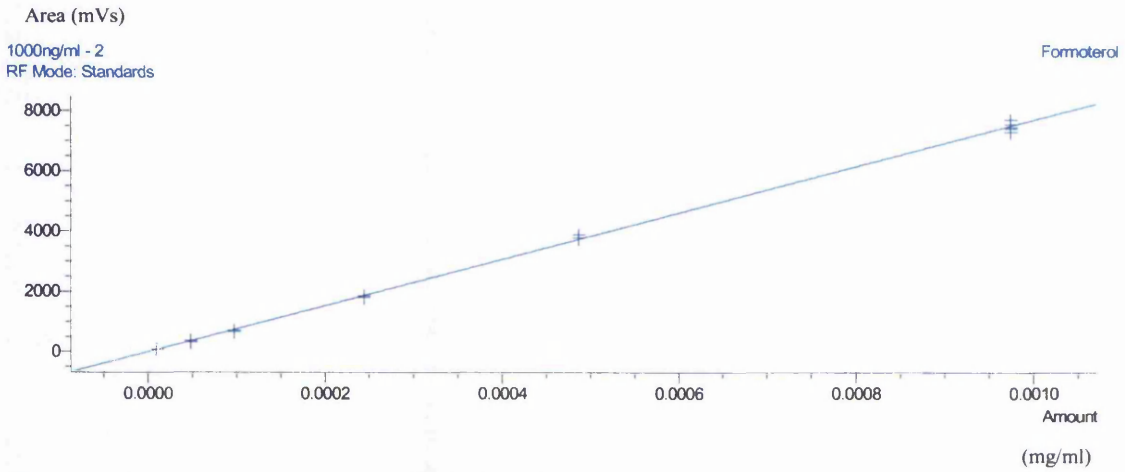

Figure 115. Linearity of FFD by LC/MS

The method was shown to be suitable for the analysis of FFD in cleaning verification samples with acceptable specificity, linearity and recoveries.

5.3.2 Formoterol Andersen Analysis

The second application was for the analysis of formoterol fumerate dihydrate (FFD) in Andersen impactor samples to determine particle size distribution. A diagram of the Andersen impactor is shown in Figure 116. Particles delivered from the pressurised metered dose inhaler (pMDI) spray are separated into different size fractions in the Andersen impactor. Very fine particles are collected on the filter and coarser particles in the throat and impaction stages 0 to 5. The particles deposited in each area of the impactor and on the actuator are dissolved in a solution of 14% methanol in purified water and collected quantitatively. The drug content of the resulting solutions is then determined. The traditional LC/UV method [76] required 15 shots of the 4.5 µg/actuation pMDI due to the detection limits of the method and had a 15 minute

run time due to the presence of late eluting impurities. Regulatory authorities had requested a method for the analysis of the dosed sample, i.e. one or two shots.

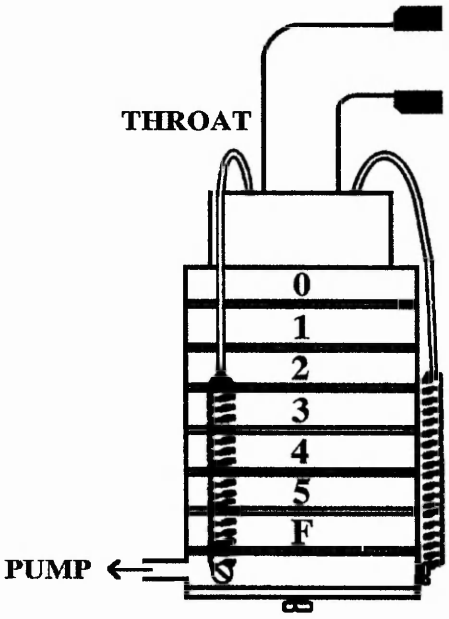

Stage	Cut-Off (μm)
0	9.0
1	5.8
2	4.7
3	3.3
4	2.1
5	1.1

Figure 116. Diagram of the Andersen Impactor and size cut-off for each stage

Single shot Andersen impaction samples were generated using the Novi Andersen robot as shown in Figure 117.

The Novi Andersen robot uses bambuterol hydrochloride as an internal dilution standard. The concentration of the samples generated were of the range 0.1 – 10 ng/ml. The Novi robot can generate 192 samples in a 24 hour period, i.e. one Andersen every hour. In order that the analytical method is not the bottle neck, a run time of under 3 minutes needed to be achieved which would allow the quantification of formoterol and bambuterol.

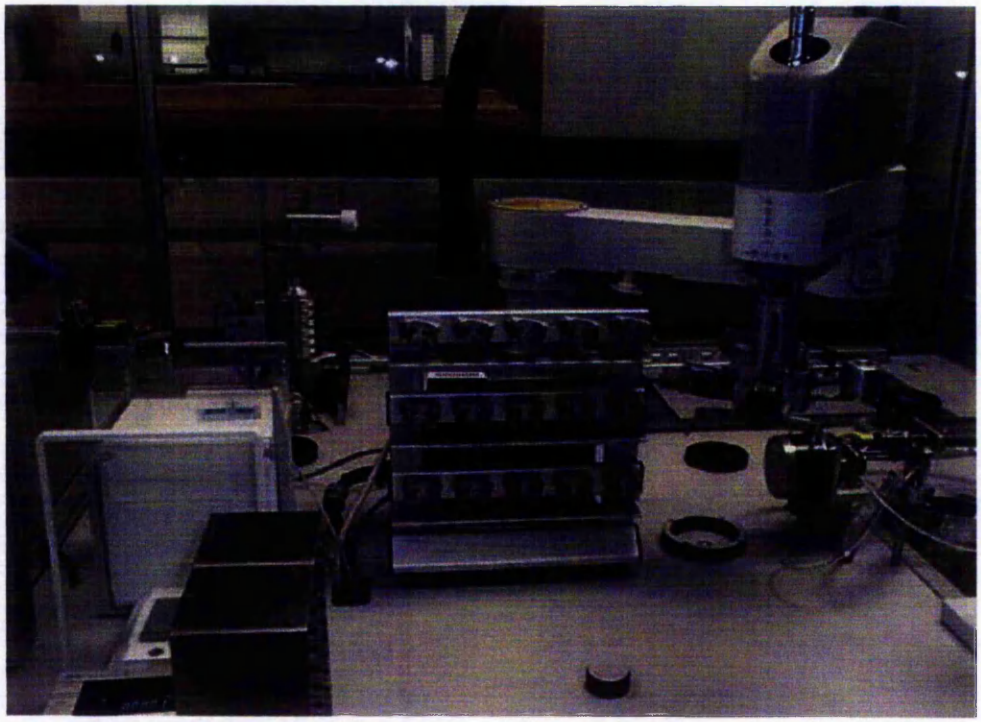

Figure 117. Novi Andersen robot

Method Conditions

Mobile Phase:	0.025 M ammonium acetate pH 5.0 in 28 % Methanol
Column:	5 µm HyPURITY C18 50 x 2.1 mm
Flow rate:	0.7 ml/min
Injection Volume:	100 µl in overlap injection mode

Using flow injection analysis the following MS conditions were obtained:

APCI SIM at M+H 345 (Formoterol) and 368 (Bambuterol)

Fragmentor voltage:	40 V
Vaporiser temperature:	500°C
Gas temperature:	325°C
Drying gas:	5.0 l/min
Nebuliser pressure:	50 psig
Vcap:	4000 V
Corona current:	4.0 µA

The MS signal was exported into the chromatography data system Atlas to allow easy quantification of the data. Figure 118 shows the chromatogram obtained for the separation of formoterol and bambuterol at a concentration of 0.5 ng/ml, representing a 50 pg column loading.

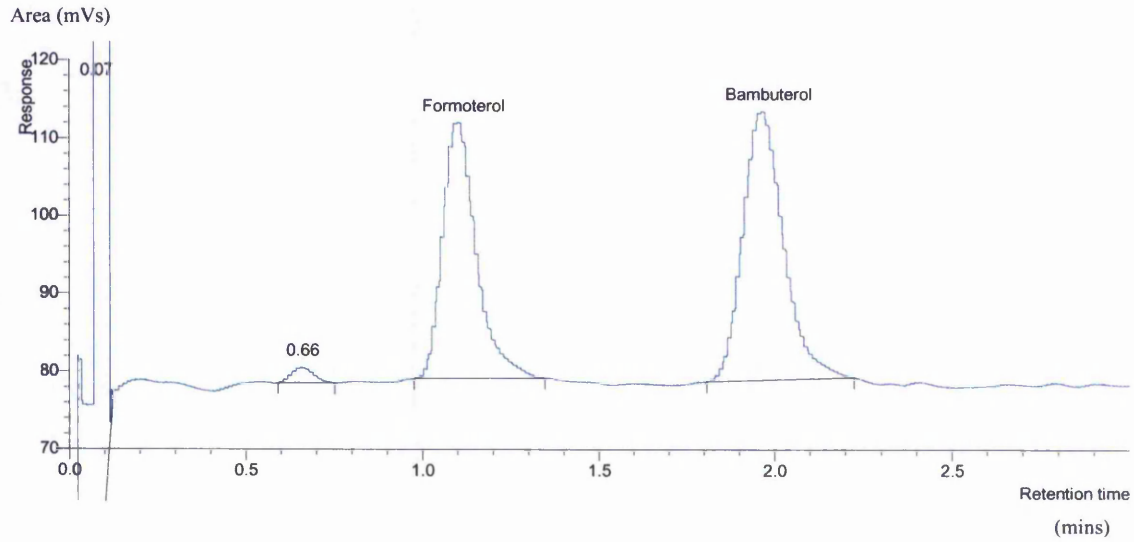

Figure 118. Chromatogram of formoterol and bambuterol standard at 0.5 ng/ml

The chromatogram in Figure 118 shows that the separation of formoterol and bambuterol is within the required 3 minutes and uses the overlap injection mode which buries the injection timing in the run time of the method to reduce cycle times. The LOQ for the method was 0.1 ng/ml, easily allowing detection of the single shot Andersen samples from the 4.5 µg/actuation pMDI. The 5 point calibration curve obtained for formoterol is shown in Figure 119. Linearity was achieved over the concentration range 0.1 - 10 ng/ml with a correlation coefficient of 0.9995. The 5 point calibration curve obtained for bambuterol is shown in Figure 120. Linearity was achieved over the concentration range 0.1 – 10 ng/ml with a correlation coefficient of 0.9982.

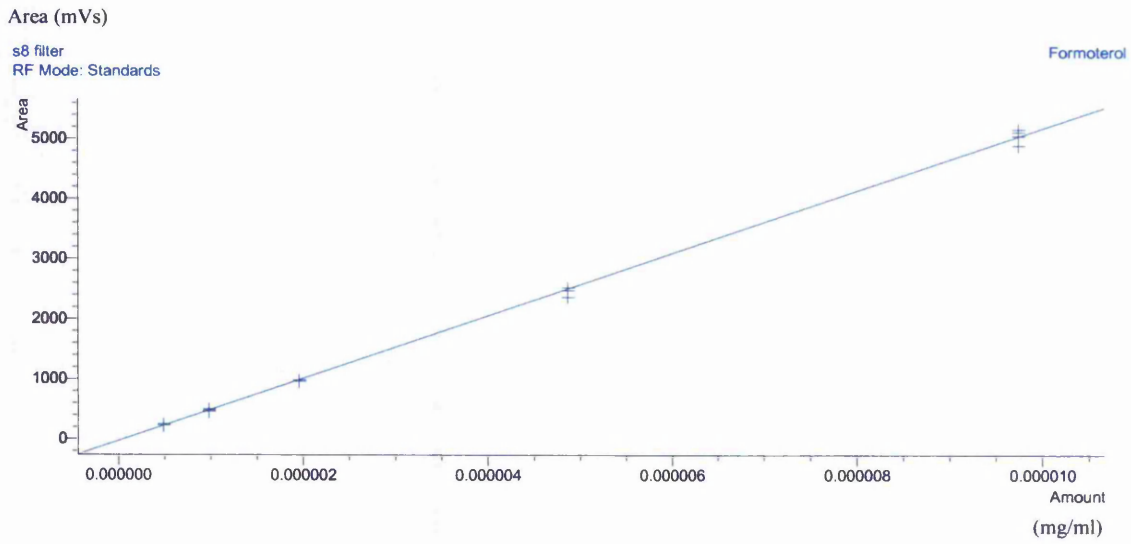

Figure 119. Calibration curve for formoterol

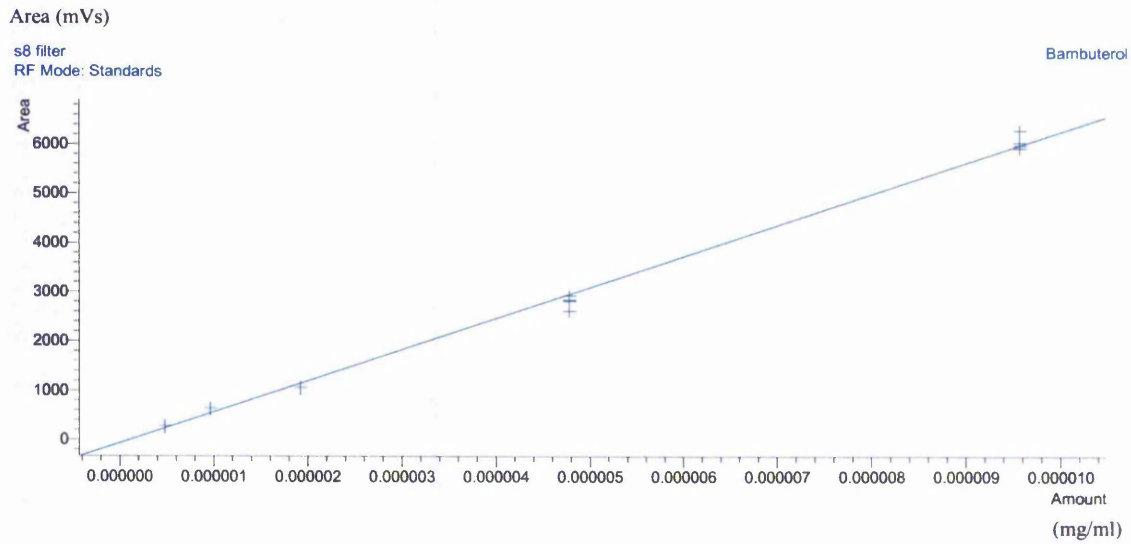

Figure 120. Calibration curve for bambuterol

Comparison of the single shot samples prepared on the Novi robot and analysed by LC/MS with the manually collected 15 shot samples analysed by LC/UV are shown in Table 25.

Table 25. Comparison of manual LC/UV Andersen data with robot LC/MS data

Andersen Sample	ng FFD Shot 8 (Robot)	ng FFD Shots 1-15 (Manual)
Throat	883	670
Stage 0	64	55
Stage 1	103	85
Stage 2	208	215
Stage 3	880	855
Stage 4	1504	1305
Stage 5	523	635
Filter	14	20
Total	4179	3840

The data show a good correlation between the 15 shot manual LC/UV data and the single shot Novi robot data. The use of mass spectrometry as the detector gave the increase in sensitivity required and the added specificity needed to reduce the run time. As the analysis was performed in single ion monitoring mode, the presence of late eluting impurities was no longer problematic.

The experimental drift in response of formoterol and bambuterol were investigated over 200 injections. The data are displayed in Figure 121. The drift results are summarised in Table 26.

Table 26. Summary of drift results for formoterol and bambuterol in APCI

Analyte	% Area RSD	% High to Low Drift
Formoterol	6.65	31
Bambuterol	5.61	27
Formoterol/Bambuterol	2.63	17

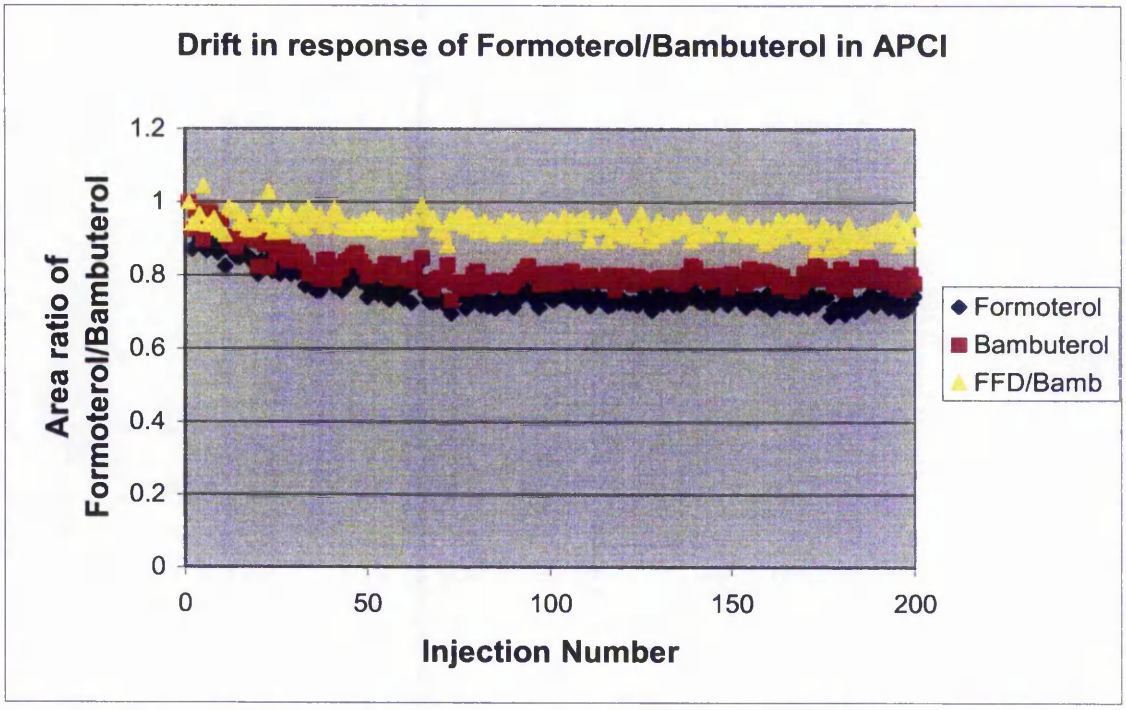

Figure 121. Drift in response of Formoterol/bambuterol in APCI

The results show that the response for both formoterol and bambuterol steadily decreased over the first 50 injections. There after it remained stable. This is also shown by the drift obtained when dividing the response of formoterol by that of bambuterol. Here the % area RSD and high to low drift are lower that that obtained from the individual responses. This shows that bambuterol is a good internal standard for formoterol, overcoming the drift in area observed.

5.3.3 Caco-2 cell sample analysis

During the pre-nomination phase of drug development, experiments are performed to assess the permeability of compounds through cell membranes. The caco-2 cell line is a well-differentiated intestinal cell line derived from human colorectal carcinoma. It is an established *in-vitro* model for oral drug absorption and evaluation of the mechanism of transport [77]. The different routes of transport across the cell membrane are shown in Figure 122.

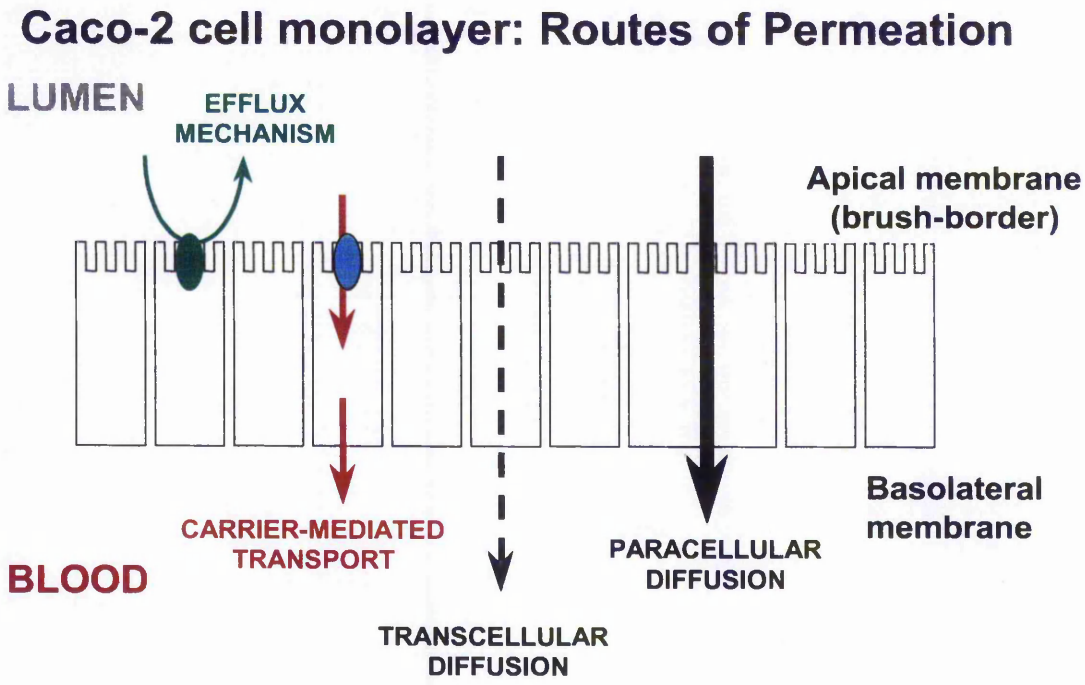

Figure 122. Routes of permeation through cell membranes

The cell monolayer sits on an insert in a well-plate. It has an area of 1.13 cm^2. A solution of the analyte in 0.1 % w/v bovine serum albumin (BSA) in Hanks Balanced Salt Solution (HBSS) containing radiolabelled mannitol is added to the apical side of the membrane. The HBSS provides pH control whilst the BSA prevents plastic binding. The mannitol is present as a marker for cell integrity and is quantified by liquid

scintillation counting. Solutions at the apical and basolateral sides of the membrane are sampled hourly over a four hour incubation time. By analysing these solutions for analyte concentration the permeability and mode of transport of the analyte across the cell membrane can be determined. For a compound displaying an efflux mechanism an efflux ratio (ER) can be determined. Each cell monolayer has a volume of 1.5 ml at the apical side and 0.6 ml at the basolateral side. Due to the low experimental volumes, only 100 µl is sampled at each time point for analysis.

Three compounds in the selective P_{2T}-receptor antagonist class for thromboatherosclerotic diseases, AR-C126583XX, AR-C133037XX and AR-C133541XX were assessed for permeability in the caco-2 cell line. The experiments were performed in triplicate at two concentrations, 2 and 10 µM. The developed analytical methods needed to fulfil the following criteria:

- be capable of providing a sample clean up step to remove the BSA, HBSS and radioactive mannitol, and prevent these from entering the mass spectrometer
- be suitable for the analysis over the concentration range 2 - 5000 ng/ml
- be generic in approach
- rapid methodology due to the large number of samples requiring analysis
- be specific for the compound analysed
- overcome the problem of low sample volumes

LC/MS methods with a column switching approach were developed for the analysis of the resulting solutions. A generic LC method was used for all compounds which consisted of a fast gradient for increased sensitivity, with a 6 minute cycle time.

LC method conditions

Pre column: 5 µm Waters Sentry Symmetry C8 20 x 3.9 mm

Analytical column: 5 µm Waters Symmetry C8 150 x 4.6 mm

Loading pump mobile phases:

A: 1% w/v ammonium acetate unadjusted pH

B: Acetonitrile

Analytical pump mobile phases:

A: 2.5 mM ammonium acetate pH 5.0

B: Methanol

Run time: 6 minutes

Loading pump gradient (all compounds):

Time (mins)	% B	Flow Rate (ml/min)
0.00	5	1
1.00	5	1
1.10	95	3
2.50	95	3
2.51	5	3
3.40	5	1

Contact closure switch performed after 1 minute

Analytical pump gradient:

AR-C133037XX		AR-C133541XX		AR-C126583XX	
Time (mins)	%B	Time (mins)	%B	Time (mins)	%B
0.00	60	0.00	60	0.00	60
2.00	60	2.00	60	2.50	60
2.60	85	2.60	90	2.60	95
3.60	85	3.60	90	3.60	95
3.70	60	3.70	60	3.70	60

Flow rate for analytical pump: 1.0 ml/min

Injection volume: 20 µl in overlap injection mode

Column oven temperature: 40°C

LC/MS methods with a column switching approach were developed for the analysis of the resulting solutions. The use of an additional binary pump and Knauer switching

valve allowed the removal of the BSA, HBSS and radiolabelled mannitol and so prevented fouling of the ion source in the mass spectrometer and reduced ion suppression where by matrix components in the sample are ionised preferentially to that of the analyte. A diagram of the column switching mechanism is shown in Figure 123.

Using an additional pump allowed the loading of the sample on to a 20 x 3.9 mm guard column with a high aqueous mobile phase, allowing the analyte to stick to the column and flush the none retained components to waste. The Knauer valve is switched after one minute and the analyte back flushed off the guard column with high organic mobile phase on to the analytical column for gradient elution. During the gradient elution, the Knauer valve switches back to its original position and mobile phase and equilibrates for the next injection.

Mass spectrometry detection was used due to the specificity of the detector and the increase in sensitivity obtained over the diode array detector. The mass spectrometry conditions were optimised for each compound. Although the compounds belonged to the same class and were structurally similar, their optimised ionisation parameters were very different. Due to the low levels of detection required a generic method for the ionisation conditions was not possible.

The optimised MS conditions for AR-C133037XX, AR-C133541XX and AR-C126583XX are shown in Table 27.

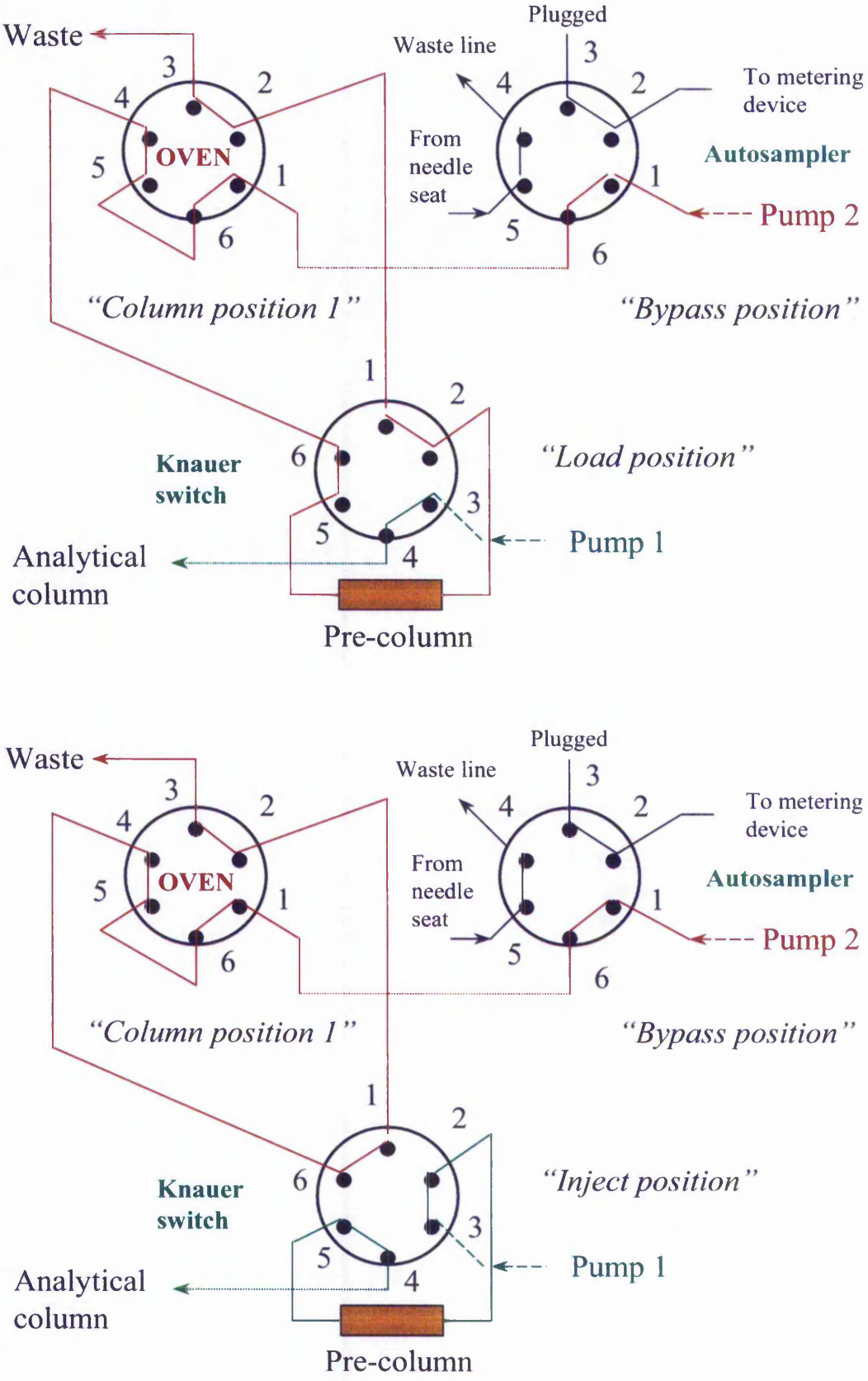

Figure 123. Column switching in load position and inject positions

Table 27. Optimised MS conditions for AR-C133037XX, AR-C133541XX and AR-C126583XX

	AR-C133037XX	AR-C133541XX	AR-C126583XX
Ionisation mode:	APCI	APCI	ESI
Polarity:	Positive	Positive	Negative
SIM ion:	541.5	501.4	545.5
Fragmentor voltage:	130 V	120 V	120 V
Vaporiser temperature:	500 °C	380 °C	N/A
Gas temperature:	350 °C	350 °C	350 °C
Drying gas:	5.0 L/min	5.0 L/min	13.0 L/min
Nebuliser pressure:	60 psig	60 psig	60 psig
Vcap:	4000 V	4000 V	4000 V
Corona:	4.0 µA	4.0 µA	N/A

The LC eluent was diverted to waste for the first 2 minutes of the run time to ensure that any remaining matrix components of the sample are flushed to waste and prevented from entering the mass spectrometer. Figure 124 shows the instrument set up used for the analysis. The permeability results obtained are shown in Figure 125.

Figure 124. Dual pump LC/MS instrument

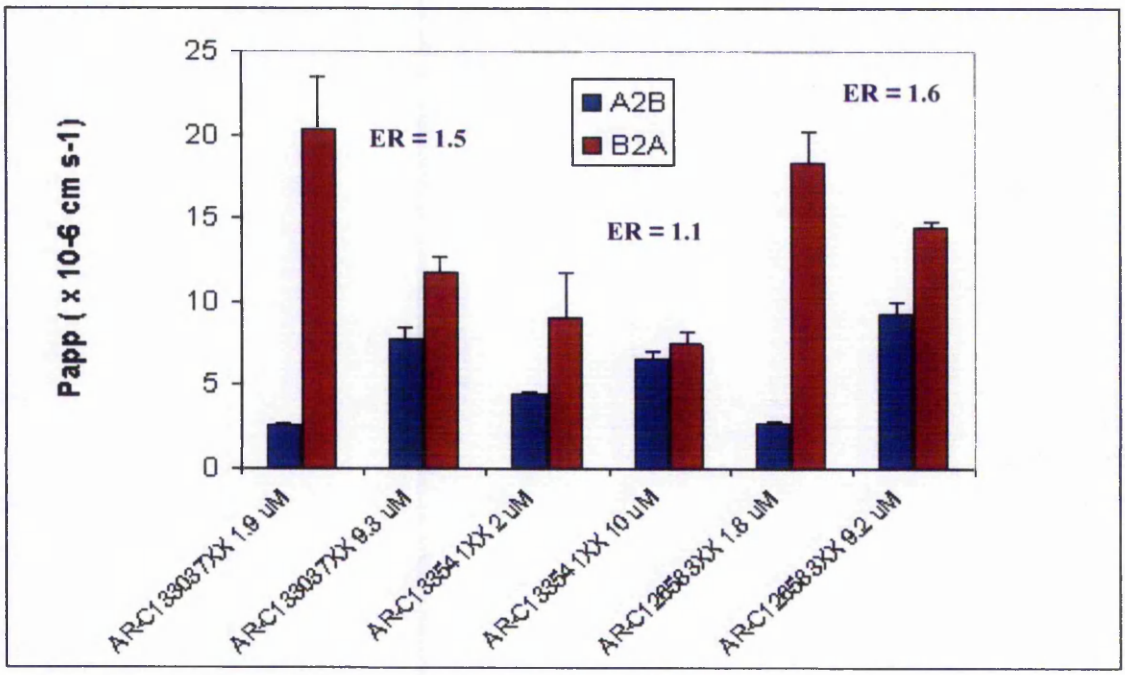

Figure 125. Permeability results

The permeability of a compound is assessed by its Papp value as shown in Table 28.

Table 28. Permeability assignments

Papp (x 10^{-6} cm s^{-1})	Permeability
< 1	Low
1 - 10	Medium
> 10	High

The Papp value is calculated from the following equation:

$$\text{Papp} = \frac{\text{(Flux x Volume)}}{\text{(Conc. x Area)}}$$

(flux is obtained from a plot of concentration versus time)

The mechanism for transport is assessed by the following:

Apical to Basolateral = Basolateral to Apical	Passive
Apical to Basolateral > Basolateral to Apical	Active
Apical to Basolateral < Basolateral to Apical	Efflux

An efflux ratio (EF) is calculated as follows:

$$ER = \frac{Papp\ B2A}{Papp\ A2B}$$

From the results above it is shown that at 2 µM Basolateral to Apical (B2A) is greater than Apical to Basolateral (A2B), representing an efflux mechanism. Efflux ratios (ER) were calculated for the 10 µM results and are displayed on Figure 125. At 10 µM the efflux mechanism becomes saturated as A2B approaches B2A with an efflux ratio approaching one and the analyte is entering the cell by passive diffusion. AR-C133541XX was shown to have a medium permeability where as AR-C126583XX and AR-C133037XX had a high permeability.

6. CONCLUSION

Stationary phase characterisation highlighted the importance of selecting a column with minimum acidic silanol content for high efficiencies for basic analytes. It was shown that it is not simply the pK_a of the analyte which affects its interaction with the stationary phase, but that the size, shape of the analyte and bonding chemistry are also important.

The use of computer simulation programs greatly reduces method development times. DryLab was used to predict separations on short narrow columns operating at high flow rates. The correlation between predicted and obtained chromatograms was excellent, although predicted peak shape was found to be highly dependent on accurate input values for column efficiency, t_0, system delay volume and extra column volume.

LC hardware was optimised for high throughput analysis. Micro flow cells were shown to give improved efficiency over standard flow cells for short narrow columns. This improvement in efficiency was reduced with increasing flow rate due to the use of default settings for detector response time. The choice of flow cell to use is often a compromise between increased sensitivity from the standard flow cell due to its larger path length and the increased efficiency obtained with the micro flow cell. Minimising the length and internal diameter of post column tubing was shown to improve efficiency. This improvement was more pronounced at high flow rates. The optimum detector response time was shown to be dependent on the flow rate used and should be optimised for good efficiencies for rapid analysis.

To prevent the injection timing becoming the rate limiting step in rapid analysis, high speed injections on the CTC Analytics HTC PAL autosampler, or the use of an overlap injection mode on the Agilent Technologies autosamplers which buries the injection time in the run time of the method can be used. The CTC Analytics HTC PAL autosampler was found to be the fastest autosampler in standard mode. The use of the overlap injection mode on the Agilent Technologies autosamplers was shown not to deteriorate performance when using the default injection speed.

The 3 µm HyPURITY C18 50 x 2.1 mm column was shown to have a lifetime in excess of 36,000 column volumes at linear velocity of 0.2 ml/min. At high flow rates of 0.7 ml/min the column lifetime had deteriorated to 9000 column volumes. This does not necessarily indicate poor column performance at high flow rates, due to the elevated temperature of 60°C being used, but demonstrates the reduction in lifetime achieved at high flow rates.

The sensitivity of an LC/MS analysis can be optimised by the selection of an appropriate buffer and buffer concentration. For the analysis of terbutaline sulphate the use of ammonium acetate or ammonium formate was shown to give double the response obtained when using TFA or formic acid. Ammonium hydroxide pH 10.5 was shown to be a suitable alternative buffer where high pH is needed to optimise a separation. The choice of organic modifier was shown to have less of an impact on sensitivity. However, the use of low viscosity organic solvents, e.g. ethanol gives rise to a lower column pressure than methanol or acetonitrile, allowing the analysis to be performed at higher flow rates than would normally be used.

A comparison between APCI and ESI showed that repeatability of injection was better for ESI. Repeatability was shown to deteriorate at low concentrations. In ESI, concentrations 0.01 and 0.02 ng/ml terbutaline sulphate were outside the desired limit of 5%. However, for all concentrations above this, 0.05 – 5000 ng/ml the precision was excellent, ranging from 0.38 to 3.55%. For APCI over the same concentration range the variation was 1.48 to 6.52%. The drift in response for both APCI and ESI was shown to improve when going from 'A' to 'D' model MSD. The response for APCI was shown to be stable over the 200 injections with an area RSD of 1.92% over all injections and a high to low drift of 10%. For ESI the area RSD was 1.05% with a high to low drift of 7%. This highlights the instruments excellent stability over a 16 hour run.

Daughter ion monitoring was shown to increase the specificity of the method; however, it led to a reduction in sensitivity by a factor of three over that seen when monitoring at the M+H ion. The precision data showed that in general lower area %RSDs were obtained than when monitoring at the M+H ion.

Flow injection analysis has demonstrated that whilst an acceptable retention time could be obtained, peak width and shape were poor, demonstrating the need to use a column for the analysis to focus the analyte and hence improve peak shape and efficiency.

The electrospray source was shown to exhibit concentration dependent sensitivity. However, the correlation was not as good at low flow rates due to poor droplet formation with the standard electrospray nebuliser. A capillary electrospray nebuliser showed an improvement in correlation at low flow rates, suggesting an improvement in droplet formation. The APCI source was shown to exhibit mass flow sensitivity. The data for APCI were comparable for all columns except the 1.0 mm internal diameter column which had a lower abundance than columns of larger internal diameter, suggesting that the APCI source does not operate well at low flow rates.

In order to facilitate rapid analysis a suitable data processing package was required to ensure that this was not the bottleneck of the analysis. Using an analogue output from the MSD it was possible to take a single SIM trace out from the MSD into a chromatography data system for processing using packages such as Multichrom and Atlas. Using the analogue output comparable data were obtained for both the internal Chemstation software and the external CDS software. The analogue output allowed the processing of data for a typical overnight run to be cut from 3 hours to under 30 minutes.

The developed high throughput methods have shown the importance of optimising both the LC and MS parameters. Using MS as a detection technique allowed the increased speed of analysis compared with UV detection due to complete separation of the analyte from its impurities not being necessary provided that ion suppression does not occur. Using MS can increase the sensitivity of the method by as much as 100 times over that of using UV detection. Combine this with the use of column switching approaches to remove non volatile materials and the scope of MS detection in pharmaceutical analysis is greatly increased.

7. FUTURE WORK

Further work to increase the scope and applicability of high throughput analysis would include the evaluation of the Twister, a high capacity autosampler from Agilent Technologies, the use of stagecoaching for sample introduction and the evaluation of a multi-analogue output signal box from Agilent Technologies. An alternative autosampler and sample introduction technique utilising chip technology is the Advion NanoMate.

7.1 The Twister

The Agilent 1100 series sample capacity extension shown in Figure 126 [78, 79] is a small footprint pick and place robot. It can extend the sample capacity to up to 80 well plates, allowing the unattended execution of up to 30,000 samples or 1292 x 2 ml vials. The system includes a barcode reader for positive plate identification allowing the capability to add and re-arrange plates and sample execution order whilst the system is running.

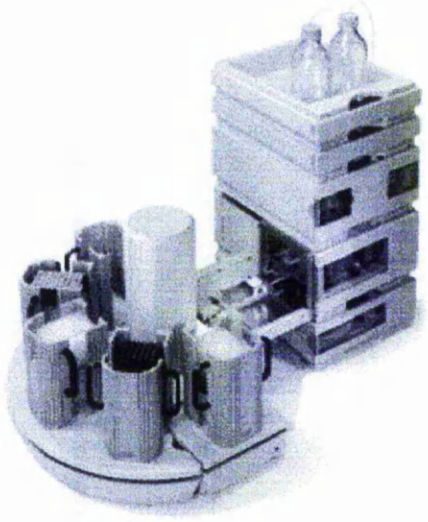

Figure 126. The Twister from Agilent Technologies

It would be useful to determine the time taken to exchange sample plates and investigate the robustness of the system, i.e. how reliable is the system at performing analysis on 30,000 unattended samples.

7.2 Stagecoaching

Stagecoaching is a sample introduction technique which removes the dead time from the cycle time of the method. As soon as the peak of interest has eluted, the peak from the next injection is starting to elute as demonstrated in Figure 127.

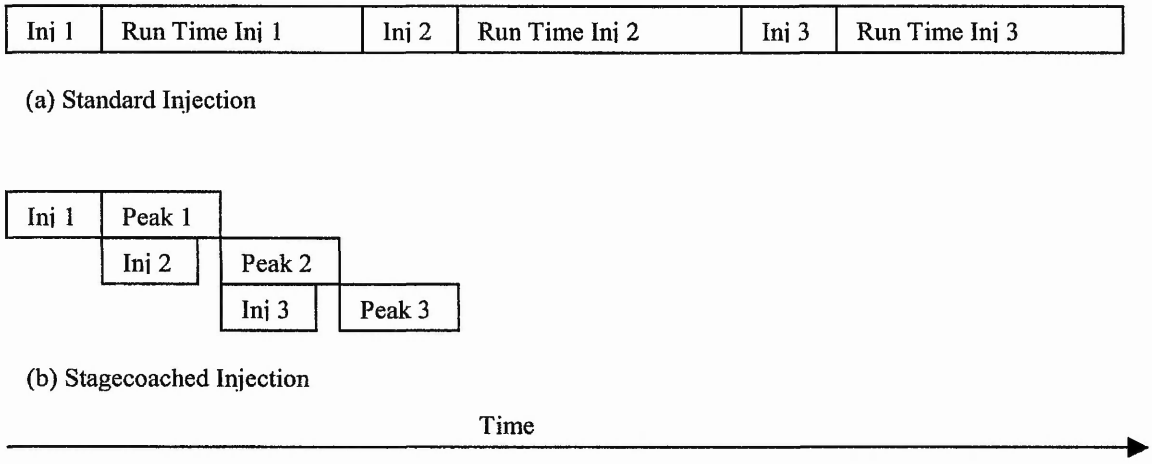

Figure 127. Comparison of standard and stagecoached injection

This type of injection may not be possible on current equipment configurations and may require working with the manufacturers to come up with a solution. It is also thought that the current CDS software would not be able to handle this type of analysis and may need a work around.

7.3 NanoMate chip sprayer

The NanoMate 100 [80, 81] is an alternative to the traditional autosampler. It is a unique, fully-automated nanoelectrospray system that easily mounts to triple quadrupole, ESI-TOF, QTOF, FT/MS, and ion trap mass spectrometers. Sample aliquots (1 to 25 μl) are drawn into disposable tips from a standard 96-well plate. The tips can be pre-filled with monolithic material to provide chromatography. Each sample is processed using a separate tip and nozzle, so there is no carryover between samples.

A sample-filled tip aligns with a chip nozzle, creating a tight seal. Nanoelectrospray initiates when head pressure and voltage are applied through the sample tip. The system infuses then moves to the next sample automatically. The 100-nozzle array of the disposable ESI Chip provides 96 nozzles for samples plus 4 additional nozzles for system testing and tuning. The system is shown in Figure 128.

The NanoMate 100 has the advantages of being automated, requiring reduced sample and reagent volume, having a high sample throughput and zero carryover between samples. It is said by the manufacturers to be a robust operation generating reproducible results.

It would be interesting to find out whether the instrument lives up to the manufacturers claim with respect to robustness, reproducibility and sample throughput and how this compares with standard LC/MS equipment as used in this study. Does the NanoMate 100 have a place within a busy Analytical Development laboratory within the pharmaceutical industry ?

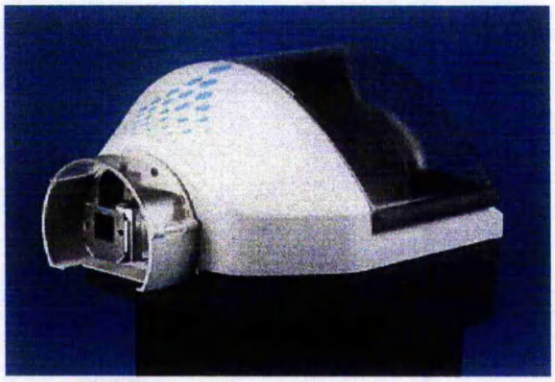

(a) NanoMate 100

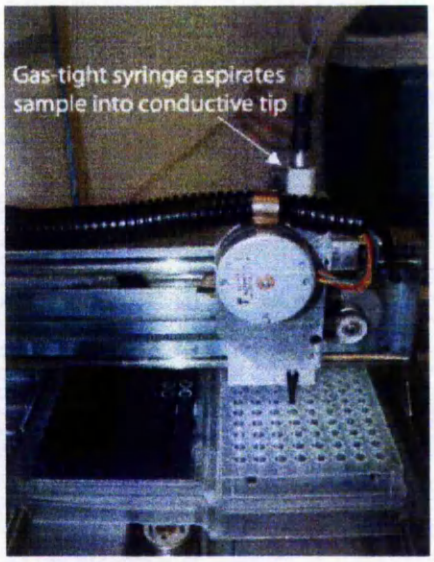

(b) Autosampler assembley

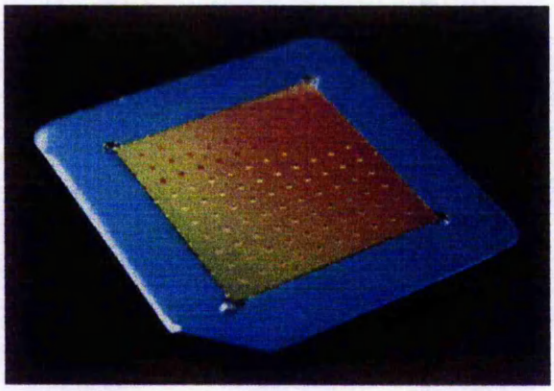

(c) The chip

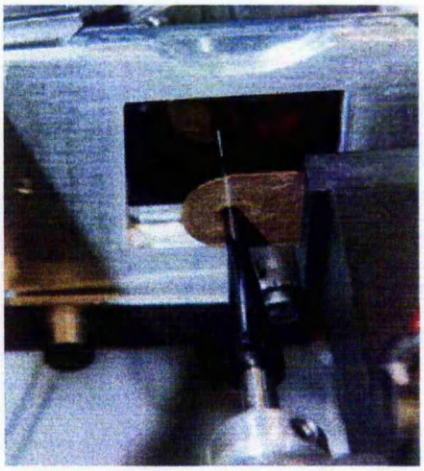

(d) Nozzle sprayer

Figure 128. The NanoMate 100 nanoelectrospray system

7.4 Multiple Analogue Output

The analogue output device used in this study for taking a signal from the MSD into a chromatography data system only allowed the output of a single signal from the MSD. This could be a single ion or a series of ions; however, where a series of ions are outputted they are not resolved in the chromatography data system. Any separation of the ions for quantitative analysis was required to take place chromatographically. Due to this limitation myself and others from AstraZeneca were instrumental in the

development of a multi signal output device by Agilent Technologies. The SIDE box (sprite information data extender) [82, 83] is capable of taking up to 12 signals from the MSD into the CDS. Front and rear views of the SIDE box are shown in Figure 129. This would be ideal for use with cassette dosing, where during toxicology studies multiple compounds are dosed simultaneously, or for those pharmaceuticals which contain more than one active ingredient. It would be useful to assess whether the time saved by not requiring separation of all analytes in the sample was greater than that required to process each individual signal.

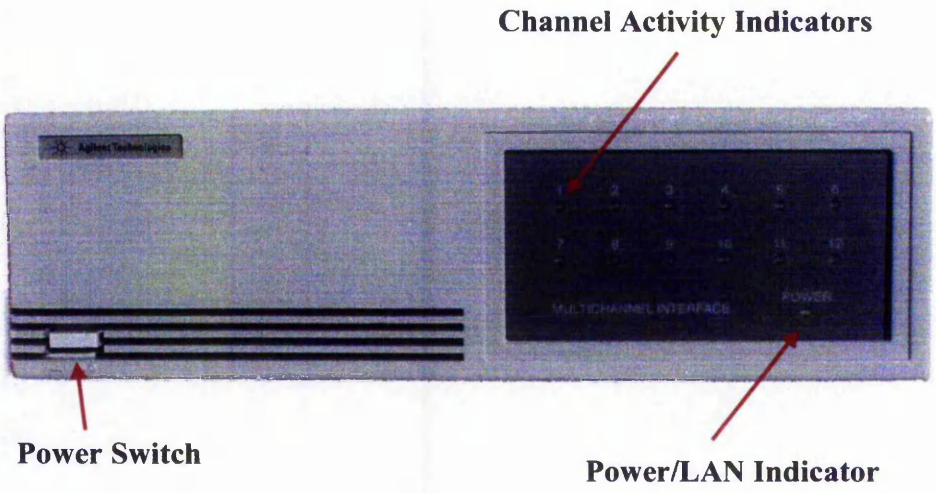

Figure 129. Front and rear view of multiple analogue output box (SIDE box)

8. REFERENCES

[1] www.laboratorytalk.com/books/chem/chrom/rs_5/contents.html
Liquid Chromatography Detectors
Chrom-Ed Book Series
R.P.W.Scott.

[2] DryLab chromatography reference guide
LC Resources inc.
Published 2000

[3] Ultrafast liquid chromatography/ultraviolet and liquid chromatography/tandem mass spectrometric analysis
Y-F Cheng, Z Lu, U. Neue.
Rapid Communications in Mass Spectrometry, **15** (2001) 141-151

[4] General equation for peak capacity in column chromatography
Y Shen, M.L. Lee.
Analytical Chemistry, **70** (1998) 3853-3856

[5] Fast gradient RP-HPLC for high-throughput quality control analysis of spatially addressable combinatorial libraries
W.K. Goetzinger, J.N. Kyranos.
American Laboratory, **30** (1998) 27-37

[6] Modern aspects of micro-bore column HPLC
T. Takeuchi.
Fresenius Journal of Analytical Chemistry, **337** (1990) 631-637

[7] HPLC method transfer to narrow bore columns : An evaluation
T.W. Ryan.
Journal of Liquid Chromatography, **18** (1995) 51-62

[8] Methacrylate monolithic columns of 320 μm I.D. for capillary liquid chromatography
P. Coufal, M. Čihák, J. Suchánková, E. Tesařová, Z. Bosáková, K. Štulík.
Journal of Chromatography A, **946** (2002) 99-106

[9] Comparison of the column performance of narrow bore and standard bore columns for chromatographic determination of alpha-, beta-, gamma- and delta-tocopherol
L. Ye, W.O. Landen, R.R Eitenmiller.
Journal of Chromatographic Science, **39** (2001) 1-6

[10] Reversed-phase HPLC of basic samples
M.A. Stadalius, J.S. Berus, L.R. Snyder.
LC.GC, **6** (1988) 494-500

[11] Characterisation of reversed-phase liquid chromatography stationary phases for the analysis of basic pharmaceuticals: eluent properties and comparison of empirical test methods
R.J.M. Vervoort, E. Ruyter, A.J.J. Debets, H.A. Claessens, C.A. Cramers, G.J. de Jong.
Journal of Chromatography A, **931** (2001) 67-79

[12] Characterisation and comparison of the chromatographic performance of conventional, polar-embedded, and polar-endcapped reversed-phase liquid chromatography stationary phases
J. Layne.
Journal of Chromatography A, **957** (2002) 149-164

[13] Chromatographic classification and comparison of commercially available reversed-phase liquid chromatographic columns using principle component analysis
M.R. Euerby, P. Petersson.
Journal of Chromatography A, **994** (2003) 13-36

[14] Comparative evaluation of bonded-silica reversed-phase columns for high-performance liquid chromatography using strongly basic compounds and alternative organic modifiers buffered at acid pH
D.V. McCalley.
Journal of Chromatography A, **769** (1997) 169-178

[15] Effect of organic solvent modifier and nature of solute on the performance of bonded silica reversed-phase columns for the analysis of strongly basic compounds by high-performance liquid chromatography.
D.V. McCalley.
Journal of Chromatography A, **738** (1996) 169-179

[16] Chromatographic classifications of commercially available reverse-phase HPLC columns
E. Cruz, M.R Euerby, C.M Johnson, C.A. Hackett.
Chromatographia, **44** (1997) 151 - 161

[17] Minimal number of chromatographic test parameters for the characterisation of reversed-phase liquid chromatographic stationary phases
T. Iványi, Y.V. Heyden, D. Visky, P. Baten, J. De Beer, I. Lázár, D.L. Massart, E. Roets, J. Hoogmartens.
Journal of Chromatography A, **954** (2002) 99-114

[18] Characterisation of reversed-phase liquid chromatographic columns by chromatographic tests. Rational column classification by a minimal number of column test parameters
D. Visky, Y.V. Heyden, T. Iványi, P. Baten, J. De Beer, Z. Kovács, B. Noszál, P. Dehouck, E. Roets, D.L. Massart, J. Hoogmartens.
Journal of Chromatography A, **1012** (2003) 11-29

[19] Application of a comparative evaluation of several reversed-phase columns to the automated analysis of candidate pharmaceuticals
I. Mutton.
Journal of Chromatography A, **697** (1995) 191-201

[20] Column switching in high-performance liquid chromatography with tandem mass spectrometric detection for high-throughput preclinical pharmacokinetic studies
V.C.X. Goa, W.C. Luo, Q. Ye, M. Thoolen.
Journal of Chromatography A, **828** (1998) 141-148

[21] Direct determination of Bisphenol A and Nonylphenol in river water by column-switching semi-microcolumn liquid chromatography/electrospray mass spectrometry
A. Motoyama, A. Suzuki, O. Shirota, R Namba.
Rapid Communications in Mass Spectrometry **13** (1999) 2204-2208

[22] Rapid pharmacokinetic screening of salbutamol in plasma samples by column-switching high-performance liquid chromatography-electrospray mass spectrometry
K. Schmeer, T. Sauter, J. Schmid.
Journal of Chromatography A, **777** (1997) 67-72

[23] Direct determination of estriol 3- and 16-glucuronides in pregnancy urine by column-switching high-performance liquid chromatography with fluorescence detection
T. Iwata, T. Hirose, M. Yamaguchi.
Journal of Chromatography B, **695** (1997) 201-207

[24] Rapid microbore liquid chromatographic analysis of biphenyldimethyl dicarboxylate in human plasma with on-line column switching
C.K. Jeong, S.B. Kim, S.J. Choi, D.H. Sohn, G.I. Ko, H.S. Lee.
Journal of Chromatography B, **738** (2000) 175-179

[25] Microbore high-performance liquid chromatographic determination of cisapride in rat serum samples using column switching
H.M. Lee, S.J. Choi, C.K. Jeong, Y.S. Kim, K.C. Lee, H.S. Lee.
Journal of Chromatography B, **727** (1999) 213-217

[26] www.Sepiatec.com/products/Sepimatrix.pdf

[27] Drug substance manufacture process control: application of flow injection analysis and HPLC for monitoring an enantiospecific synthesis.
K. Chong, T. Loughlin, C. Moeder, H.J. Perpall, R. Thompson, N. Grinberg, G.B. Smith, M. Bhupathy, G. Bicker.
Journal of Pharmaceutical and Biomedical Analysis, **15** (1996) 111-121

[28] Flow injection analysis of doxazosin mesylate using UV detection
G. Altiokka, Z. Atkosar.
Journal of Pharmaceutical and Biomedical Analysis, **27** (2001) 841-844

[29] A validated method development for ketoprofen by a flow-injection analysis with UV detection and its application to pharmaceutical formulations
H.Y. Aboul-Enein, A.G. Dal, M. Tuncel.
Il Farmaco, **58** (2003) 419-422

[30] Review. DryLab computer simulation for high-performance liquid chromatographic method development. I. Isocratic elution.
L.R. Snyder, J.W. Dolan, D.C. Lommen.
Journal of Chromatography, **485** (1989) 65-89

[31] Computer simulation for the convenient optimisation of isocratic reversed-phase liquid chromatographic separations by varying temperature and mobile phase strength.
R.G. Wolcott, J.W. Dolan, L.R. Snyder.
Journal of Chromatography A, **869** (2000) 3-25

[32] Computer-assisted method development and optimisation in high-performance liquid chromatography
T.H. Hoang, D. Cuerrier, S. McClintock, M. Di Maso.
Journal of Chromatography A, **991** (2003) 281-287

[33] Review. DryLab computer simulation for high-performance liquid chromatographic method development. II Gradient elution
J.W. Dolan, D.C. Lommen, L.R. Snyder.
Journal of Chromatography, **485** (1989) 91-112

[34] Reversed-phase liquid chromatographic separation of complex samples by optimising temperature and gradient time. III. Improving the accuracy of computer simulation.
J.W. Dolan, L.R. Snyder, RG. Wolcott, P. Haber, T. Baczek, R. Kaliszan, L.C. Sander.
Journal of Chromatography A, **857** (1999) 41-68

[35] Use of computer simulations in the development of gradient and isocratic high-performance liquid chromatography methods for analysis of drug compounds and synthetic intermediates.
Loren Wrisley.
Journal of Chromatography, **628** (1993) 191-198

[36] Computer-assisted rapid development of gradient high-performance liquid chromatographic methods for the analysis of antibiotics.
R. Bonfichi.
Journal of Chromatography A, **678** (1994) 213-221

[37] Simultaneous variation of temperature and gradient steepness for reversed-phase high-performance liquid chromatography method development.
I. Application to 14 different samples using computer simulation.
J.W. Dolan, L.R. Snyder, N.M. Djordjevic, D.W. Hill, D.L. Saunders, L. Van Heukelem, T.J. Waeghe.
Journal of Chromatography A, **803** (1998) 1-31

[38] The basics of LC/MS
Primer from Agilent Technologies
Published 2001

[39] New picogram detection system based on a mass spectrometer with an external ionization source at atmospheric pressure
E.C. Horning, M.G. Horning, D.I. Carroll, I. Dzidic, R.N. Stillwell.
Analytical Chemistry, **45** (1973) 936-943

[40] Atmospheric pressure ionisation (API) mass spectrometry. Solvent-mediated ionisation of samples introduced in solution and in a liquid chromatograph effluent stream
E.C. Horning, D.I. Carroll, I. Dzidic, K.D. Haegele, M.G. Horning, R.N. Stillwell.
Journal of Chromatographic Science, **12** (1974) 725-729

[41] Atmospheric pressure ionisation mass spectrometry: Corona discharge ion source for use in liquid chromatograph-mass spectrometer-computer analytical system
D.I. Carroll, I. Dzidic, R.N. Stillwell, K.D. Haegele, E.C. Horning.
Analytical Chemistry, **47** (1975) 2369-2373

[42] Terminal ions in weak atmospheric pressure plasmas. Applications of atmospheric pressure ionization to trace impurity analysis in gases
M.W. Siegel, W.L. Fite.
Journal of Physical Chemistry, **80** (1976) 2871-2881

[43] Determination of impurities in gases by atmospheric pressure ionization mass spectrometry
H. Kambara, I. Kanomata.
Analytical Chemistry, **49** (1977) 270-275

[44] Electrospray-Ion Spray: A Comparison of Mechanisms and Performance
Michael G. Ikonomou, Arthur T. Blades, and Paul Kebarle.
Analytical Chemistry, **63** (1991) 1989-1998

[45] Electrospray interface for liquid chromatographs and mass spectrometers
C.M. Whitehouse, R.N. Dreyer, M. Yamashita, J.B. Fenn.
Analytical Chemistry, **57** (1985) 675-679

[46] Multiple charging in electrospray ionization of poly(ethylene glycols)
S.F. Wong, C.K. Meng, J.B. Fenn.
Journal of Physical Chemistry, **92** (1988) 546-550

[47] Atmospheric pressure ionisation and liquid chromatography/mass spectrometry – together at last
B.A. Thomson.
Journal of the American Society for Mass Spectrometry, **9** (1998) 187-193

[48] Pharmaceutical application of LC-MS. 1. - Characterisation of a famotidine degradate in a package screening study by LC-APCI MS.
X-Z. Qin, D.P. Ip, K. H-C. Chang,P.M. Dradransky, M.A. Brooks and T. Sakuma.
Journal of Pharmaceutical & Biomedical Analysis, **12** (1994) 221-233.

[49] Characterisation of tepoxalin and its related compounds by high-performance liquid chromatography/mass spectrometry
D.J. Burinsky, B.L. Armstrong, A.R. Oyler, R. Dunphy.
Journal of Pharmaceutical Science, **85** (1996) 159-164

[50] Determination of 4-demethoxy-3'-deamino-3'-aziridinyl-4'-methylsulphonyldaunorubicin and its 13-hydroxy metabolite by direct injection of human plasma into a column-switching liquid chromatography system with mass spectrometric detection
M. Breda, G. Basileo, G. Fonte, J. Long, C.A James.
Journal of Chromatography A, **854** (1999) 81-92

[51] Determination of *n*-hexane metabolites by liquid chromatography/mass spectrometry 1. 2,5-hexanedione and other phase I metabolites in untreated and hydrolysed urine samples by atmospheric pressure chemical ionisation
R. Andreoli, P. Manini, A. Mutti, E. Bergamaschi, W.M.A. Niessen.
Rapid Communications in Mass Spectrometry, **12** (1998) 1410-1416

[52] Low level determination of a novel 4-azasteroid and its carboxylic acid metabolite in human plasma and semen using high-performance liquid chromatography with atmospheric pressure chemical tandem mass spectrometry
M.L. Constanzer, C.M. Chavez, B.K. Matuszewski, J. Carlin, D. Graham.
Journal of Chromatography B, **693** (1997) 117-129

[53] Determination of the β-adrenergic blocker timolol in plasma by liquid chromatography-atmospheric pressure chemical ionisation mass spectrometry.
T.V. Olah, J.D. Gilbert and A. Barrish.
Journal of Pharmaceutical and Biomedical Analysis, **11** (2) (1993) 157-163.

[54] Determination of ZD9583, a thromboxane receptor antagonist, in human plasma and urine by liquid chromatography atmospheric pressure chemical ionisation tandem mass spectrometry
C.X. Goa, K.H. Bui, A.S. Martz, N.C. LeDonne, M.C. Dyroff.
Journal of Chromatography B, **695** (1997) 299-307

[55] Determination of 1,4-benzodiazepines by high-performance liquid chromatography-electrospray tandem mass spectrometry.
M. Kleinschnitz, M. Herderich and P. Schreier.
Journal of Chromatography B, **676** (1996) 61-67.

[56] Quantitative determination of α-cyclodextrin in human plasma by liquid chromatography/positive ion electrospray mass spectrometry
W. Hammes, C. Bourscheidt, U. Büchsler, G. Stodt, H. Bökens.
Journal of Mass Spectrometry, **35** (2000) 378-384

[57] Picogram determination of a novel dopamine D4 receptor antagonist in human plasma and urine by liquid chromatography with atmospheric pressure chemical ionisation tandem mass spectrometry
C.M. Chavez-Eng, M.L. Constanzer, B.K. Matuszewski.
Journal of Chromatography B, **691** (1997) 77-85

[58] Rapid and automated determination of the β_2-agonist reproterol in human plasma by atmospheric pressure chemical ionisation high-performance liquid chromatography-tandem mass spectrometry
N.G. Knebel, M. Winkler.
Journal of Chromatography B, **702** (1997) 119-129

[59] A comparison of generic reversed phase and normal phase LC-MS in the pharmaceutical industry
M.A. Kelly, S. Grieb, J.V. Beaman.
Poster presentation at PSAG Cambridge, October 1998.

[60] Practical examination of a nonporous silica stationary phase for reversed-phase fast LC applications
D.R. Jenke.
Journal of Chromatographic Science, **34** (1996) 362-367

[61] Use of short high-performance liquid chromatography columns and tandem-mass spectrometry for the rapid analysis of a prostaglandin analog, fluprostenol, in rat plasma
T.H. Eichhold, D.L. Kuhlenbeck, T.R. Baker, M.E. Stells, J.S. Amburgey, M.A. deLong, J.R. Hartke, C.A. Cruze, S.A. Pierce, K.R. Wehmeyer.
Journal of Chromatography B, **741** (2000) 213-220

[62] Parallel ultra-high flow rate liquid chromatography with mass spectrometric detection using a multiplex electrospray source for direct, sensitive determination of pharmaceuticals in plasma at extremely high throughput
M.K. Bayliss, D. Little, D.N. Mallett, R.S. Plumb.
Rapid Communications in Mass Spectrometry, **14** (2000) 2039-2045

[63] Chromatographic aspects in high throughput liquid chromatography/mass spectrometry
L. Pereira, P Ross, M Woodruff.
Rapid Communications in Mass Spectrometry, **14** (2000) 357-360

[64] Optimisation and routine use of generic ultra-high flow-rate liquid chromatography with mass spectrometric detection for the direct on-line analysis of pharmaceuticals in plasma.
J. Ayrton, G.J. Dear, W.J. Leavens, D.N. Mallett, R.S. Plumb.
Journal of Chromatography A, **828** (1998) 199-207

[65] Simplified description of high-performance liquid chromatographic separation under overload conditions, based on the Craig distribution model: I. Computer simulations for a single elution band assuming a langmuir isotherm
J.E. Eble, R.L. Grob, P.E. Antle and L.R. Snyder.
Journal of Chromatography, **384** (1987) 45-79

[66] Determination of cisapride in plasma and animal tissues by high-performance liquid chromatography
R. Woestenborghs, W. Lorreyne, F.V. Rompaey, J. Heykants.
Journal of Chromatography, **424** (1988) 195

[67] Analysis of cisapride in neonatal plasma using high-performance liquid chromatography with a base-stable column and fluorescence detection
Y. Preechagoon, B.G. Charles.
Journal of Chromatography B, **670** (1995) 139-143

[68] Principles of Instrumental Analysis
Third Ed, 1985
Douglas A. Skoog.
Saunders College Publishing
Chapter 27, page 787

[69] Terbutaline: An effective bronchodilator by inhalation
M.B. Goldgraber.
Annals of Allergy, **38** (2) (1977) 127-128

[70] Terbutaline: A preliminary report of its pharmacological properties and therapeutic efficacy in asthma
R.N. Brogden, T.M. Speight, G.S. Avery.
Drugs, **6** (5) (1973) 324-332

[71] ThermoHypersil-Keystone
Column Technologies for HPLC and LC/MS
Catalogue 2002

[72] Phenomenex Chromatography columns and supplies
Catalogue 2002/2003

[73] Influence of the eluent composition on the ionisation efficiency for morphine of pneumatically assisted electrospray, atmospheric-pressure chemical ionization and sonic spray
R. Dams, T. Benijts, W. Günther, W. Lambert, A. De Leenheer.
Rapid Communications in Mass Spectrometry, **16** (2002) 1072-1077

[74] Comparison of the repeatability of quantitative data measured in high-performance liquid chromatography with UV and atmospheric pressure chemical ionisation mass spectrometric detection
Y. Chen, M. Kele, A.A. Tuinman, G. Guiochon.
Journal of Chromatography A, **873** (2000) 163-173

[75] AstraZeneca R&D Charnwood Standard Operating Procedure AS159.007/02

[76] AstraZeneca R&D Charnwood Standard Operating Procedure AS159.003/02

[77] Determination of *in vitro* permeability of drug candidates through a Caco-2 cell monolayer by liquid chromatography/tandem mass spectrometry
Z. Wang, C.E.C.A. Hop, K.H. Leung, J. Pang.
Journal of Mass Spectrometry, **35** (2000) 71-76

[78] www.chem.agilent.com/Scripts/PDS.asp?1Page=6257

[79] www.chem.agilent.com/temp/rad54207/00036961.pdf

[80] www.advion.com

[81] www.advion.com/R&D.html

[82] www.chem.agilent.com/Scripts/generic.asp?1Page=6608&indcol=Y&prodcol=Y

[83] www.chem.agilent.com/temp/radD7593/00038071.pdf
Review article
Use of a multisignal analog output device for MS data in a regulated laboratory
Application note
Douglas McIntyre and Wayne Duncan
Agilent Technologies

9. APPENDIX

Table 1. Effect of pH on peak symmetry for benzylamine

	Peak Symmetry					
pH	Hypersil Elite	Prodigy ODS(3)	Hypersil BDS	Hypersil HyPURITY	Hypersil 100	Hypersil ODS
2.72	0.44	0.50	0.47	0.55	0.41	0.16
2.92	0.44	0.50	0.50	0.55	0.41	0.21
3.23	0.47	0.50	0.51	0.58	0.42	0.15
3.96	0.46	0.50	0.49	0.55	0.29	0.17
4.76	0.46	0.47	0.52	0.55	0.41	0.20
5.35	0.46	0.47	0.50	0.56	0.36	0.35
5.97	0.45	0.48	0.52	0.57	0.34	0.37
6.35	0.44	0.54	0.53	0.61	0.32	0.37
6.62	0.44	0.56	0.53	0.64	0.31	0.38
6.84	0.44	0.63	0.52	0.66	0.29	0.35
7.06	0.43	0.75	0.58	0.74	0.26	0.46
7.31	0.51	1.16	0.71	0.98	0.21	0.39
7.68	0.90	1.96	1.39	1.75	n/c	n/c

n/c: not calculated

Table 2. Effect of pH on peak symmetry for pyridine

	Peak Symmetry					
pH	Hypersil Elite	Prodigy ODS(3)	Hypersil BDS	Hypersil HyPURITY	Hypersil 100	Hypersil ODS
2.72	1.63	1.16	1.46	1.17	2.45	n/c
2.92	1.44	0.96	1.30	1.04	2.10	n/c
3.23	0.90	0.69	0.81	0.78	1.07	n/c
3.96	2.05	1.83	1.72	1.65	2.38	n/c
4.76	2.10	1.90	1.79	1.71	2.41	5.57
5.35	2.03	1.92	1.74	1.80	2.44	5.53
5.97	2.05	1.89	1.78	1.82	2.37	5.20
6.35	1.97	1.92	1.81	1.72	2.38	5.00
6.62	2.04	1.92	1.77	1.82	2.28	4.72
6.84	1.94	1.94	1.83	1.75	2.30	4.62
7.06	1.99	1.91	1.84	1.76	2.32	4.47
7.31	1.94	1.90	1.76	1.76	2.31	4.39
7.68	1.98	1.95	1.85	1.81	2.30	4.12

n/c: not calculated

Table 3. Effect of pH on peak symmetry for procainamide

	Peak Symmetry					
pH	Hypersil Elite	Prodigy ODS(3)	Hypersil BDS	Hypersil HyPURITY	Hypersil 100	Hypersil ODS
2.72	1.57	1.51	1.53	1.33	1.58	7.20
2.92	1.57	1.61	1.53	1.35	1.62	n/c
3.23	1.55	1.49	1.48	1.34	1.61	7.43
3.96	1.63	1.57	1.53	1.78	1.96	n/c
4.76	1.74	1.50	1.49	1.56	1.96	n/c
5.35	1.67	1.56	1.53	1.43	1.76	n/c
5.97	1.75	1.52	1.62	1.41	2.03	n/c
6.35	1.77	1.47	1.57	1.42	2.14	n/c
6.62	1.82	1.39	1.64	1.47	2.29	n/c
6.84	1.92	1.36	1.74	1.44	2.43	n/c
7.06	1.92	1.27	1.72	1.44	2.61	n/c
7.31	2.08	1.19	1.81	1.49	2.71	n/c
7.68	2.19	1.08	1.91	1.41	2.88	n/c

n/c: not calculated

Table 4. Effect of pH on peak symmetry for codeine

	Peak Symmetry					
pH	Hypersil Elite	Prodigy ODS(3)	Hypersil BDS	Hypersil HyPURITY	Hypersil 100	Hypersil ODS
2.72	1.93	1.72	1.76	1.55	1.82	13.21
2.92	1.91	1.65	1.73	1.57	1.82	12.64
3.23	1.82	1.68	1.73	1.51	1.79	12.93
3.96	0.79	0.68	0.86	1.01	0.80	12.88
4.76	0.79	0.68	0.92	0.93	0.77	12.12
5.35	0.79	0.63	0.87	0.87	0.81	n/c
5.97	0.87	0.68	0.93	0.92	1.09	11.94
6.35	1.07	0.83	1.20	1.15	1.44	10.57
6.62	1.26	0.98	1.47	1.38	1.69	8.61
6.84	1.40	1.10	1.69	1.57	1.78	7.72
7.06	1.50	1.20	1.88	1.71	n/c	n/c
7.31	1.52	n/c	2.03	1.77	n/c	n/c
7.68	1.49	n/c	2.10	1.75	n/c	n/c

n/c: not calculated

Table 5. Effect of pH on peak symmetry for nicotine

	Peak Symmetry					
pH	Hypersil Elite	Prodigy ODS(3)	Hypersil BDS	Hypersil HyPURITY	Hypersil 100	Hypersil ODS
2.72	1.80	1.65	1.67	1.47	1.94	9.08
2.92	1.77	1.58	1.62	1.48	1.86	9.41
3.23	1.76	1.67	1.58	1.49	1.89	n/c
3.96	0.97	n/c	1.58	2.53	n/c	n/c
4.76	0.98	n/c	1.72	n/c	n/c	9.73
5.35	1.04	0.69	1.58	0.79	0.91	9.97
5.97	1.21	0.76	1.83	1.46	2.66	n/c
6.35	1.71	0.97	2.82	2.25	3.83	7.11
6.62	2.13	1.21	3.65	2.91	4.52	10.11
6.84	2.50	1.47	3.92	3.31	4.55	n/c
7.06	2.66	1.66	4.31	3.47	4.60	12.07
7.31	2.80	1.72	4.56	3.52	4.66	11.12
7.68	2.69	1.75	4.80	3.54	4.46	11.02

n/c: not calculated

Table 6. Effect of pH on peak efficiency for benzylamine

	Peak Efficiency (plates/metre)					
pH	Hypersil Elite	Prodigy ODS(3)	Hypersil BDS	Hypersil HyPURITY	Hypersil 100	Hypersil ODS
2.72	13827	13767	13107	18067	12316	288
2.92	13907	14453	13413	17140	12688	284
3.23	13960	14607	13420	17267	13444	136
3.96	14447	14413	14067	18220	5148	152
4.76	13773	14887	14120	18487	14084	196
5.35	14747	15820	13840	18020	12316	340
5.97	15153	16533	14640	18567	10812	368
6.35	14747	18560	16233	18433	9616	360
6.62	16800	19807	17627	20247	9092	396
6.84	18200	21673	17727	19707	8732	428
7.06	20327	21847	20053	20060	8324	560
7.31	25667	21507	21233	18293	9600	976
7.68	23900	14507	16940	12073	n/c	n/c

n/c: not calculated

Table 7. Effect of pH on peak efficiency for pyridine

	Peak Efficiency (plates/metre)					
pH	Hypersil Elite	Prodigy ODS(3)	Hypersil BDS	Hypersil HyPURITY	Hypersil 100	Hypersil ODS
2.72	15673	13060	16667	16680	15076	n/c
2.92	13187	9767	12920	11673	14576	n/c
3.23	5453	4253	5113	4313	5288	n/c
3.96	24200	25507	23460	22320	17892	2816
4.76	26327	28640	27280	26033	18628	3784
5.35	26887	29140	28527	27480	18940	4524
5.97	27113	29460	28740	27780	19312	6388
6.35	27140	29807	29420	27727	19472	7732
6.62	26673	29967	28820	28053	19280	8600
6.84	26747	30167	28520	28120	18876	9416
7.06	26707	29660	28527	27727	19260	10016
7.31	26593	29920	28953	27647	19132	10436
7.68	26093	30587	29180	27920	19352	10900

n/c: not calculated

Table 8. Effect of pH on peak efficiency for procainamide

	Peak Efficiency (plates/metre)					
pH	Hypersil Elite	Prodigy ODS(3)	Hypersil BDS	Hypersil HyPURITY	Hypersil 100	Hypersil ODS
2.72	13940	12893	14087	15967	15196	536
2.92	13667	12520	13260	15567	15392	544
3.23	13827	11880	13653	14947	14772	540
3.96	11987	10440	12780	14173	8144	500
4.76	11793	11020	12440	10167	8208	500
5.35	11373	11393	12520	10920	9684	504
5.97	10733	11407	11540	11660	11192	516
6.35	9980	11560	11013	11847	11068	528
6.62	9387	11640	10127	11447	10056	552
6.84	9213	12140	9333	11047	9744	588
7.06	8780	12880	8567	10787	9496	696
7.31	8553	13660	7733	9720	9048	672
7.68	8107	14767	6520	8287	8852	n/c

n/c: not calculated

Table 9. Effect of pH on peak efficiency for codeine

	Peak Efficiency (plates/metre)					
pH	Hypersil Elite	Prodigy ODS(3)	Hypersil BDS	Hypersil HyPURITY	Hypersil 100	Hypersil ODS
2.72	81511	67111	88489	100933	59088	n/c
2.92	10800	4311	15644	62844	15616	n/c
3.23	32800	n/c	22000	204222	4688	n/c
3.96	51689	35600	41200	27867	28224	1424
4.76	142222	148667	147778	102222	118816	2208
5.35	244711	287289	231244	187911	129440	3168
5.97	304089	385244	249822	212133	112272	7152
6.35	328356	432356	246622	212800	106368	8080
6.62	331956	453333	239911	208756	105392	11984
6.84	326933	459467	244356	207911	106672	18880
7.06	322133	458711	244933	210711	n/c	n/c
7.31	n/c	n/c	n/c	n/c	n/c	n/c
7.68	n/c	n/c	n/c	n/c	n/c	n/c

n/c: not calculated

Table 10. Effect of pH on peak efficiency for nicotine

	Peak Efficiency (plates/metre)					
pH	Hypersil Elite	Prodigy ODS(3)	Hypersil BDS	Hypersil HyPURITY	Hypersil 100	Hypersil ODS
2.72	13633	12887	14280	15420	16672	244
2.92	13053	11687	13747	14807	16184	244
3.23	12227	10067	13273	15140	14772	252
3.96	1620	647	2347	9427	3904	280
4.76	4920	n/c	3300	30633	1172	312
5.35	7753	5340	6180	4180	7056	356
5.97	21333	22300	22167	15333	29704	552
6.35	36707	43093	34687	28187	32360	792
6.62	45613	57787	37473	31820	28068	1788
6.84	49253	64853	36993	31920	26592	2020
7.06	49793	68000	35987	31313	26348	2996
7.31	49040	68920	36653	31187	26668	4720
7.68	48320	68807	36740	31607	27616	7364

n/c: not calculated

Table 11. Effect of flow cell dimensions on peak shape characteristics

HyPURITY C18 150 X 4.6 mm 5u column

Hydrophilic bases

Compound	Nicotine	Benzylamine	Procainamide	Terbutaline	Salbutamol	Phenol
Retention Time (mins) (std)	3.031	4.593	6.576	8.936	11.752	16.221
Retention Time (mins) (semi-micro)	3.016	4.592	6.542	8.789	11.494	16.272
Retention Time (mins) (micro)	3.051	4.646	6.686	9.117	12.010	16.434
Area (std)	99.0	237.1	372.4	374.4	247.5	464.2
Area (semi-micro)	61.9	140.6	223.8	222.6	147.6	298.4
Area (micro)	62.6	145.7	227.9	228.7	151.7	285.3
Height (std)	19.18	30.61	37.43	27.51	14.15	19.02
Height (semi-micro)	12.19	18.61	22.38	16.56	8.53	11.87
Height (micro)	12.18	18.82	22.86	16.71	8.56	11.59
Efficiency (Tan) (std)	8556	8361	10758	10366	10726	9977
Efficiency (Tan) (semi-micro)	8744	8635	10595	10275	10611	9395
Efficiency (Tan) (micro)	8921	8529	10998	10608	10976	10061
Efficiency (1/2 width) (std)	9185	8839	11484	11060	11615	10648
Efficiency (1/2 width) (semi-micro)	9663	9312	11723	10940	11404	9983
Efficiency (1/2 width) (micro)	9593	9309	11778	11512	11821	10546
Tailing Factor (std)	1.462	1.350	1.414	1.295	1.301	1.129
Tailing Factor (semi-micro)	1.458	1.351	1.407	1.293	1.298	1.015
Tailing Factor (micro)	1.475	1.367	1.411	1.318	1.303	1.129
T_o (std)	1.857					
T_o (semi-micro)	1.846					
T_o (micro)	1.851					

Lipophilic bases

Compound	Phenol	AR-C68397	AR-R12495	Diphenhydramine	Remacemide	Nortriptyline
Retention Time (mins) (std)	2.983	3.612	4.047	4.461	6.067	10.238
Retention Time (mins) (semi-micro)	2.968	3.608	4.046	4.462	6.067	10.280
Retention Time (mins) (micro)	2.980	3.627	4.065	4.485	6.107	10.348
Area (std)	473.7	532.9	389.6	411.1	414.6	821.8
Area (semi-micro)	281.4	321.6	237.5	251.5	247.5	497.2
Area (micro)	289.4	323.2	241.0	257.0	252.5	502.5
Height (std)	105.73	88.76	60.19	58.60	44.67	50.91
Height (semi-micro)	62.98	53.29	35.78	34.78	26.51	30.19
Height (micro)	64.92	53.32	36.83	35.69	27.26	30.69
Efficiency (Tan) (std)	10709	9059	10224	10397	10361	9669
Efficiency (Tan) (semi-micro)	10574	8929	9865	10079	10176	9417
Efficiency (Tan) (micro)	10712	8992	10167	10299	10508	9672
Efficiency (1/2 width) (std)	11468	9622	10933	11400	11188	10368
Efficiency (1/2 width) (semi-micro)	11354	9855	10663	11031	10917	10164
Efficiency (1/2 width) (micro)	11449	10010	11027	11525	11338	10300
Tailing Factor (std)	1.282	1.337	1.456	1.347	1.295	1.301
Tailing Factor (semi-micro)	1.272	1.334	1.480	1.325	1.272	1.302
Tailing Factor (micro)	1.291	1.350	1.450	1.337	1.278	1.318
T_o (std)	1.808					
T_o (semi-micro)	1.785					
T_o (micro)	1.770					

Table 12. Effect of flow cell dimensions on peak shape characteristics

HyPURITY C18 150 X 3.0 mm 5u column

Hydrophilic bases

Compound	Nicotine	Benzylamine	Procainamide	Terbutaline	Salbutamol	Phenol
Retention Time (mins) (std)	3.224	4.889	7.051	9.924	12.931	16.759
Retention Time (mins) (semi-micro)	3.220	4.899	7.115	10.077	13.172	16.843
Retention Time (mins) (micro)	3.233	4.927	7.159	10.116	13.237	16.828
Area (std)	95.1	208.1	320.5	374.0	253.5	484.4
Area (semi-micro)	55.7	124.3	190.3	222.5	150.9	289.3
Area (micro)	59.3	126.9	195.4	226.9	153.8	295.8
Height (std)	9.28	25.47	24.73	26.37	14.13	20.24
Height (semi-micro)	5.48	15.37	14.51	15.52	8.27	16.843
Height (micro)	5.71	15.63	14.78	15.80	8.38	12.25
Efficiency (Tan) (std)	3373	8549	7798	11160	11558	10907
Efficiency (Tan) (semi-micro)	3422	8769	7792	11101	11585	10889
Efficiency (Tan) (micro)	3456	8877	7827	11177	11603	10825
Efficiency (1/2 width) (std)	3718	9194	8501	11743	12399	11574
Efficiency (1/2 width) (semi-micro)	3708	9497	8656	11862	12557	11277
Efficiency (1/2 width) (micro)	3807	9605	8763	11954	12382	11460
Tailing Factor (std)	2.646	1.324	1.567	1.153	1.140	1.048
Tailing Factor (semi-micro)	2.793	1.328	1.596	1.144	1.128	1.048
Tailing Factor (micro)	2.850	1.329	1.602	1.149	1.135	1.046
T_o (std)	1.962					
T_o (semi-micro)	1.934					
T_o (micro)	1.937					

Lipophilic bases

Compound	Phenol	AR-C68397	AR-R12495	Diphenhydramine	Remacemide	Nortriptyline
Retention Time (mins) (std)	3.110	3.867	4.357	4.795	6.557	11.172
Retention Time (mins) (semi-micro)	3.080	3.843	4.335	4.775	6.545	11.202
Retention Time (mins) (micro)	3.078	3.856	4.356	4.798	6.574	11.261
Area (std)	489.8	554.3	337.3	395.0	415.9	847.1
Area (semi-micro)	292.4	331.2	200.5	237.1	247.6	501.6
Area (micro)	300.0	338.1	202.8	236.1	252.4	512.8
Height (std)	93.66	75.52	45.15	50.64	42.76	53.90
Height (semi-micro)	59.00	46.66	27.69	30.96	25.78	31.87
Height (micro)	60.58	47.96	28.20	31.43	26.24	32.55
Efficiency (Tan) (std)	8318	6987	8615	9353	10422	11463
Efficiency (Tan) (semi-micro)	9133	7475	9143	9741	10554	11421
Efficiency (Tan) (micro)	9214	7607	9245	9914	10729	11488
Efficiency (1/2 width) (std)	8858	7467	9242	10217	11072	12346
Efficiency (1/2 width) (semi-micro)	9770	7968	9748	10652	11286	12411
Efficiency (1/2 width) (micro)	10060	8236	10061	10541	11387	12196
Tailing Factor (std)	1.247	1.333	1.255	1.193	1.138	1.123
Tailing Factor (semi-micro)	1.235	1.335	1.251	1.197	1.136	1.128
Tailing Factor (micro)	1.249	1.355	1.231	1.197	1.136	1.133
T_o (std)	1.881					
T_o (semi-micro)	1.868					
T_o (micro)	1.854					

Table 13. Effect of flow cell dimensions on peak shape characteristics

HyPURITY C18 150 X 2.1 mm 5µ column

Hydrophilic bases

Compound	Nicotine	Benzylamine	Procainamide	Terbutaline	Salbutamol	Phenol
Retention Time (mins) (std)	3.472	5.172	7.479	10.714	13.682	17.894
Retention Time (mins) (semi-micro)	3.468	5.190	7.637	10.992	14.114	17.917
Retention Time (mins) (micro)	3.450	5.171	7.618	10.991	14.125	17.948
Area (std)	98.8	210.3	322.0	378.9	357.0	488.9
Area (semi-micro)	56.5	124.3	190.2	224.9	152.3	290.0
Area (micro)	65.9	127.2	185.3	237.4	156.4	301.2
Height (std)	6.04	20.78	17.74	22.70	12.60	18.75
Height (semi-micro)	3.83	12.80	10.66	13.51	7.41	11.23
Height (micro)	3.79	13.09	10.62	13.79	7.52	11.55
Efficiency (Tan) (std)	1396	6254	4459	9298	10035	10654
Efficiency (Tan) (semi-micro)	1574	6761	4783	9809	10488	10793
Efficiency (Tan) (micro)	1319	6714	4731	9596	10248	10624
Efficiency (1/2 width) (std)	1467	6684	4829	9909	10563	11274
Efficiency (1/2 width) (semi-micro)	1594	7096	5035	10431	11005	11302
Efficiency (1/2 width) (micro)	1362	7045	5010	10159	11023	11154
Tailing Factor (std)	2.587	1.358	1.770	1.197	1.173	1.087
Tailing Factor (semi-micro)	2.287	1.377	1.736	1.193	1.187	1.077
Tailing Factor (micro)	3.371	1.372	1.709	1.272	1.176	1.101
T_o (std)	2.166					
T_o (semi-micro)	2.105					
T_o (micro)	2.103					

Lipophilic bases

Compound	Phenol	AR-C68397	AR-R12495	Diphenhydramine	Remacemide	Nortriptyline
Retention Time (mins) (std)	3.374	4.221	4.698	5.163	7.066	12.107
Retention Time (mins) (semi-micro)	3.317	4.163	4.665	5.122	7.054	12.124
Retention Time (mins) (micro)	3.320	4.174	4.677	5.142	7.094	12.242
Area (std)	490.0	534.7	332.5	383.3	416.0	833.5
Area (semi-micro)	295.4	320.2	195.1	231.4	247.1	498.9
Area (micro)	299.9	323.6	200.7	232.7	250.6	509.1
Height (std)	66.61	51.00	32.93	37.52	33.57	44.67
Height (semi-micro)	43.76	33.57	21.12	24.06	21.06	27.28
Height (micro)	45.25	33.76	21.67	24.44	21.28	27.25
Efficiency (Tan) (std)	4813	3881	5255	6023	7379	9447
Efficiency (Tan) (semi-micro)	5699	4665	6182	6867	8282	9906
Efficiency (Tan) (micro)	5914	4718	6260	6991	8309	9779
Efficiency (1/2 width) (std)	5150	4021	5516	6421	7938	10115
Efficiency (1/2 width) (semi-micro)	6095	5018	6560	7242	8722	10388
Efficiency (1/2 width) (micro)	6272	5044	6703	7297	8606	10590
Tailing Factor (std)	1.299	1.711	1.360	1.243	1.223	1.167
Tailing Factor (semi-micro)	1.329	1.471	1.262	1.247	1.197	1.197
Tailing Factor (micro)	1.312	1.555	1.260	1.245	1.211	1.189
T_o (std)	2.048					
T_o (semi-micro)	1.990					
T_o (micro)	1.986					

Table 14. Effect of flow cell dimensions on peak shape characteristics

HyPURITY C18 150 X 1.0 mm 5µ column

Hydrophilic bases

Compound	Nicotine	Benzylamine	Procainamide	Terbutaline	Salbutamol	Phenol
Retention Time (mins) (std)	4.384	5.961	7.017	8.983	10.550	18.485
Retention Time (mins) (semi-micro)	4.707	6.639	9.783	13.476	16.972	21.136
Retention Time (mins) (micro)	4.310	6.024	8.129	10.234	12.205	20.308
Area (std)	81.7	228.0	349.9	367.3	237.4	452.0
Area (semi-micro)	57.0	135.5	196.7	212.3	137.0	270.9
Area (micro)	55.0	138.1	201.6	216.9	138.4	275.5
Height (std)	4.36	11.19	15.10	14.79	9.15	13.36
Height (semi-micro)	3.12	7.29	8.96	8.35	4.76	7.62
Height (micro)	3.30	7.83	9.77	9.58	5.76	7.96
Peak width 1/2 height (std)	0.264	0.287	0.323	0.350	0.370	0.487
Peak width 1/2 height (semi-micro)	0.250	0.263	0.317	0.377	0.433	0.520
Peak width 1/2 height (micro)	0.223	0.243	0.290	0.327	0.350	0.513
Efficiency (Tan) (std)	1589	2205	2447	3423	4218	7436
Efficiency (Tan) (semi-micro)	1791	3278	4921	6755	8107	8549
Efficiency (Tan) (micro)	1944	3089	4019	5173	6293	8230
Efficiency (1/2 width) (std)	1523	2395	2609	3649	4504	7993
Efficiency (1/2 width) (semi-micro)	1964	3521	5288	7091	8499	9153
Efficiency (1/2 width) (micro)	2063	3396	4353	5438	6736	8671
Tailing Factor (std)	2.692	1.809	1.507	1.516	1.429	1.386
Tailing Factor (semi-micro)	2.059	1.572	1.456	1.337	1.276	1.288
Tailing Factor (micro)	2.935	1.709	1.623	1.464	1.407	1.317
T_o (std)	3.387					
T_o (semi-micro)	3.206					
T_o (micro)	3.179					

Table 15. Effect of flow cell dimensions on peak shape characteristics

HyPURITY C18 50 X 2.1 mm 5µ column

Hydrophilic bases **0.208 ml/min**

Compound	Nicotine	Benzylamine	Procainamide	Terbutaline	Salbutamol	Phenol
Retention Time (mins) (std)	1.362	1.848	2.518	3.300	4.181	5.564
Retention Time (mins) (semi-micro)	1.306	1.795	2.476	3.267	4.158	5.525
Retention Time (mins) (micro)	1.311	1.817	2.496	3.276	4.153	5.648
Area (std)	97.6	244.8	374.1	388.4	248.4	485.6
Area (semi-micro)	61.1	150.4	226.9	234.1	148.5	288.2
Area (micro)	60.3	126.6	198.9	230.2	154.9	297.1
Height (std)	12.38	27.89	37.70	34.96	19.56	30.74
Height (semi-micro)	8.10	17.72	23.63	21.77	12.02	18.52
Height (micro)	8.42	15.86	21.51	22.41	13.01	18.78
Width 1/2 height (std)	0.111	0.123	0.140	0.160	0.187	0.233
Width 1/2 height (semi-micro)	0.101	0.117	0.132	0.153	0.180	0.233
Width 1/2 height (micro)	0.099	0.113	0.129	0.150	0.176	0.237
Efficiency (Tan) (std)	780	1132	1696	2199	2643	2908
Efficiency (Tan) (semi-micro)	865	1198	1804	2317	2763	2937
Efficiency (Tan) (micro)	910	1309	1918	2487	2906	2963
Efficiency (1/2 width) (std)	839	1243	1792	2357	2780	3150
Efficiency (1/2 width) (semi-micro)	921	1312	1959	2515	2957	3106
Efficiency (1/2 width) (micro)	978	1424	2078	2642	3100	3155
Tailing Factor (std)	1.837	1.596	1.623	1.370	1.305	1.194
Tailing Factor (semi-micro)	2.687	1.673	1.709	1.376	1.313	1.184
Tailing Factor (micro)	2.908	1.635	1.666	1.378	1.319	1.185
T_o (std)	0.946					
T_o (semi-micro)	0.885					
T_o (micro)	0.888					

Table 16. Effect of flow cell dimensions on peak shape characteristics

HyPURITY C18 50 X 2.1 mm 5u column

Hydrophilic bases **0.5 ml/min**

Compound	Nicotine	Benzylamine	Procainamide	Terbutaline	Salbutamol	Phenol
Retention Time (mins) (std)	0.582	0.789	1.086	1.400	1.793	2.361
Retention Time (mins) (semi-micro)	0.556	0.764	1.053	1.353	1.728	2.355
Retention Time (mins) (micro)	0.560	0.772	1.076	1.400	1.804	2.360
Area (std)	42.0	103.0	156.0	162.6	104.2	211.4
Area (semi-micro)	25.0	62.9	93.8	96.6	61.9	121.2
Area (micro)	26.3	57.5	86.0	99.0	66.5	125.1
Height (std)	10.30	23.69	32.17	30.13	16.84	30.08
Height (semi-micro)	6.56	14.99	20.15	18.84	10.53	17.82
Height (micro)	6.54	13.12	17.86	18.59	10.85	18.18
Width 1/2 height (std)	0.059	0.062	0.069	0.078	0.091	0.104
Width 1/2 height (semi-micro)	0.054	0.059	0.066	0.075	0.085	0.101
Width 1/2 height (micro)	0.056	0.060	0.068	0.077	0.090	0.102
Efficiency (Tan) (std)	507	826	1249	1632	2014	2671
Efficiency (Tan) (semi-micro)	539	872	1313	1715	2086	2800
Efficiency (Tan) (micro)	521	852	1291	1700	2100	2790
Efficiency (1/2 width) (std)	543	892	1365	1780	2167	2856
Efficiency (1/2 width) (semi-micro)	588	922	1417	1793	2272	2993
Efficiency (1/2 width) (micro)	553	918	1407	1824	2226	2986
Tailing Factor (std)	1.582	1.436	1.459	1.318	1.271	1.164
Tailing Factor (semi-micro)	1.325	1.532	1.486	1.315	1.272	1.189
Tailing Factor (micro)	1.826	1.626	1.532	1.339	1.293	1.208
T_o (std)	0.398					
T_o (semi-micro)	0.373					
T_o (micro)	0.372					

Table 17. Effect of flow cell dimensions on peak shape characteristics

HyPURITY C18 50 X 2.1 mm 5µ column

Hydrophilic bases **0.7 ml/min**

Compound	Nicotine	Benzylamine	Procainamide	Terbutaline	Salbutamol	Phenol
Retention Time (mins) (std)	0.415	0.559	0.762	0.970	1.244	1.654
Retention Time (mins) (semi-micro)	0.400	0.548	0.757	0.971	1.250	1.655
Retention Time (mins) (micro)	0.401	0.551	0.764	0.982	1.269	1.668
Area (std)	29.6	75.0	113.6	116.1	74.2	146.3
Area (semi-micro)	17.8	45.0	66.8	68.9	43.8	87.0
Area (micro)	17.0	40.1	60.3	70.1	47.0	89.5
Height (std)	8.86	21.00	29.24	27.57	15.58	28.27
Height (semi-micro)	5.51	12.89	17.71	16.73	9.42	16.97
Height (micro)	5.28	11.25	15.75	16.73	9.89	17.23
Width 1/2 height (std)	0.050	0.053	0.058	0.063	0.070	0.077
Width 1/2 height (semi-micro)	0.049	0.051	0.056	0.061	0.069	0.077
Width 1/2 height (micro)	0.049	0.052	0.056	0.061	0.071	0.077
Efficiency (Tan) (std)	369	594	929	1266	1600	2375
Efficiency (Tan) (semi-micro)	372	603	963	1319	1678	2409
Efficiency (Tan) (micro)	371	605	983	1314	1693	2375
Efficiency (1/2 width) (std)	381	621	971	1315	1725	2534
Efficiency (1/2 width) (semi-micro)	376	641	1021	1381	1811	2581
Efficiency (1/2 width) (micro)	378	633	1041	1413	1779	2621
Tailing Factor (std)	1.150	1.781	1.704	1.231	1.215	1.175
Tailing Factor (semi-micro)	1.206	1.930	1.787	1.237	1.217	1.179
Tailing Factor (micro)	1.381	1.979	1.791	1.264	1.232	1.186
T_o (std)	0.284					
T_o (semi-micro)	0.267					
T_o (micro)	0.267					

Table 18. Effect of flow cell dimensions on peak shape characteristics

HyPURITY C18 50 X 2.1 mm 5u column

Hydrophilic bases **1.0 ml/min**

Compound	Nicotine	Benzylamine	Procainamide	Terbutaline	Salbutamol	Phenol
Retention Time (mins) (std)	0.291	0.390	0.530	0.665	0.853	1.140
Retention Time (mins) (semi-micro)	0.281	0.382	0.526	0.665	0.859	1.141
Retention Time (mins) (micro)	0.283	0.385	0.532	0.674	0.872	1.153
Area (std)	20.5	53.0	79.2	81.7	52.2	102.7
Area (semi-micro)	12.5	31.9	46.7	48.4	30.8	60.9
Area (micro)	11.7	29.2	43.0	50.0	33.5	62.7
Height (std)	7.10	17.14	24.52	23.56	13.69	25.42
Height (semi-micro)	4.37	10.41	14.67	14.16	8.19	15.21
Height (micro)	4.16	9.30	13.23	14.45	8.75	15.59
Width 1/2 height (std)	0.046	0.047	0.050	0.053	0.058	0.062
Width 1/2 height (semi-micro)	0.046	0.047	0.049	0.052	0.057	0.062
Width 1/2 height (micro)	0.045	0.048	0.050	0.053	0.058	0.062
Efficiency (Tan) (std)	226	371	611	848	1147	1819
Efficiency (Tan) (semi-micro)	209	364	621	868	1181	1827
Efficiency (Tan) (micro)	223	359	619	873	1190	1854
Efficiency (1/2 width) (std)	222	376	632	878	1209	1877
Efficiency (1/2 width) (semi-micro)	210	365	634	896	1257	1897
Efficiency (1/2 width) (micro)	219	360	632	902	1262	1936
Tailing Factor (std)	0.788	1.138	1.261	1.045	1.160	1.143
Tailing Factor (semi-micro)	0.896	1.129	1.323	1.032	1.155	1.139
Tailing Factor (micro)	0.912	1.204	1.346	1.146	1.173	1.147
T_o (std)	0.200					
T_o (semi-micro)	0.189					
T_o (micro)	0.189					

Table 19. Effect of flow cell dimensions on peak shape characteristics

HyPURITY C18 50 X 2.1 mm 3µ column

Hydrophilic bases **0.208 ml/min**

Compound	Nicotine	Benzylamine	Procainamide	Terbutaline	Salbutamol	Phenol
Retention Time (mins) (std)	1.352	1.810	2.376	2.935	3.587	5.454
Retention Time (mins) (semi-micro)	1.381	1.889	2.744	3.591	4.573	5.703
Retention Time (mins) (micro)	1.373	1.875	2.698	3.541	4.513	5.655
Area (std)	96.6	246.1	379.4	385.0	247.9	484.2
Area (semi-micro)	60.8	153.7	222.4	228.5	146.5	286.9
Area (micro)	61.1	152.9	226.4	231.7	148.5	294.3
Height (std)	13.74	29.62	42.76	39.87	23.18	31.84
Height (semi-micro)	8.45	18.14	24.35	22.15	12.26	18.91
Height (micro)	8.63	18.57	25.51	22.87	12.65	19.41
Width 1/2 height (std)	0.101	0.117	0.125	0.138	0.153	0.227
Width 1/2 height (semi-micro)	0.099	0.113	0.128	0.147	0.173	0.227
Width 1/2 height (micro)	0.099	0.113	0.123	0.144	0.171	0.227
Efficiency (Tan) (std)	928	1232	1836	2324	2811	3035
Efficiency (Tan) (semi-micro)	1009	1360	2356	3044	3591	3300
Efficiency (Tan) (micro)	992	1382	2378	3045	3626	3277
Efficiency (1/2 width) (std)	986	1319	1991	2495	3031	3207
Efficiency (1/2 width) (semi-micro)	1086	1540	2533	3322	3857	3507
Efficiency (1/2 width) (micro)	1072	1516	2651	3330	3854	3448
Tailing Factor (std)	1.800	1.642	1.610	1.519	1.504	1.276
Tailing Factor (semi-micro)	1.909	1.685	1.617	1.523	1.476	1.233
Tailing Factor (micro)	2.191	1.679	1.620	1.508	1.462	1.242
T_o (std)	0.973					
T_o (semi-micro)	0.914					
T_o (micro)	0.913					

Table 20. Effect of flow cell dimensions on peak shape characteristics

HyPURITY C18 50 X 2.1 mm 3u column

Hydrophilic bases **0.5 ml/min**

Compound	Nicotine	Benzylamine	Procainamide	Terbutaline	Salbutamol	Phenol
Retention Time (mins) (std)	0.604	0.808	1.152	1.467	1.875	2.334
Retention Time (mins) (semi-micro)	0.575	0.779	1.122	1.436	1.840	2.306
Retention Time (mins) (micro)	0.576	0.779	1.127	1.446	1.857	2.311
Area (std)	42.0	108.0	156.8	161.8	102.6	202.8
Area (semi-micro)	24.9	64.3	93.3	98.0	61.7	121.3
Area (micro)	25.9	66.3	95.5	99.8	63.5	125.2
Height (std)	10.68	24.38	34.18	31.84	18.23	31.99
Height (semi-micro)	6.70	15.33	21.07	19.75	11.10	19.43
Height (micro)	6.87	15.73	21.78	20.27	11.39	19.99
Width 1/2 height (std)	0.058	0.062	0.066	0.073	0.081	0.093
Width 1/2 height (semi-micro)	0.053	0.059	0.062	0.070	0.079	0.091
Width 1/2 height (micro)	0.054	0.058	0.062	0.069	0.079	0.091
Efficiency (Tan) (std)	580	867	1577	2075	2723	3217
Efficiency (Tan) (semi-micro)	612	890	1673	2147	2739	3286
Efficiency (Tan) (micro)	607	893	1731	2228	2770	3318
Efficiency (1/2 width) (std)	609	926	1697	2218	2959	3463
Efficiency (1/2 width) (semi-micro)	645	960	1785	2363	3014	3584
Efficiency (1/2 width) (micro)	631	989	1850	2442	3071	3600
Tailing Factor (std)	1.552	1.544	1.478	1.441	1.411	1.320
Tailing Factor (semi-micro)	1.350	1.568	1.540	1.505	1.473	1.350
Tailing Factor (micro)	1.680	1.587	1.543	1.490	1.463	1.350
T_o (std)	0.408					
T_o (semi-micro)	0.382					
T_o (micro)	0.380					

Table 21. Effect of flow cell dimensions on peak shape characteristics

HyPURITY C18 50 X 2.1 mm 3u column

Hydrophilic bases **0.7 ml/min**

Compound	Nicotine	Benzylamine	Procainamide	Terbutaline	Salbutamol	Phenol
Retention Time (mins) (std)	0.431	0.574	0.818	1.030	1.321	1.639
Retention Time (mins) (semi-micro)	0.412	0.554	0.795	1.006	1.294	1.619
Retention Time (mins) (micro)	0.412	0.554	0.798	1.011	1.300	1.622
Area (std)	31.4	80.0	113.7	118.2	75.2	145.0
Area (semi-micro)	17.9	46.0	66.2	67.8	43.4	86.8
Area (micro)	16.9	45.9	66.9	69.1	44.0	88.8
Height (std)	9.33	21.70	30.54	28.99	16.80	30.54
Height (semi-micro)	5.65	13.38	18.60	17.64	10.12	18.61
Height (micro)	5.50	13.40	18.78	17.87	10.23	18.86
Width 1/2 height (std)	0.050	0.053	0.055	0.059	0.065	0.070
Width 1/2 height (semi-micro)	0.048	0.051	0.053	0.057	0.062	0.069
Width 1/2 height (micro)	0.047	0.050	0.053	0.057	0.063	0.069
Efficiency (Tan) (std)	394	616	1191	1615	2122	2778
Efficiency (Tan) (semi-micro)	403	641	1211	1637	2178	2849
Efficiency (Tan) (micro)	418	642	1205	1668	2211	2863
Efficiency (1/2 width) (std)	412	658	1246	1717	2288	2995
Efficiency (1/2 width) (semi-micro)	414	661	1259	1722	2375	3059
Efficiency (1/2 width) (micro)	423	681	1270	1740	2333	3073
Tailing Factor (std)	1.088	1.862	1.875	1.374	1.352	1.319
Tailing Factor (semi-micro)	1.209	2.311	1.939	1.351	1.389	1.317
Tailing Factor (micro)	1.292	1.381	1.969	1.366	1.391	1.328
T_o (std)	0.292					
T_o (semi-micro)	0.274					
T_o (micro)	0.272					

Table 22. Effect of post column tubing dimensions on peak shape characteristics

HyPURITY C18 50 X 2.1 mm 3u column
Hydrophilic bases **0.208 ml/min**

Compound	Nicotine	Benzylamine	Procainamide	Terbutaline	Salbutamol	Phenol
Retention Time (mins) (0.127 x 115 mm)	1.322	1.788	2.518	3.213	4.073	5.365
Retention Time (mins) (0.127 x 230 mm)	1.344	1.829	2.589	3.331	4.206	5.554
Retention Time (mins) (0.127 x 690 mm)	1.387	1.874	2.642	3.374	4.251	5.596
Retention Time (mins) (0.254 x 115 mm)	1.366	1.861	2.653	3.461	4.379	5.630
Retention Time (mins) (0.254 x 230 mm)	1.386	1.855	2.603	3.319	4.199	5.444
Retention Time (mins) (0.254 x 690 mm)	1.496	1.977	2.729	3.463	4.324	5.684
Area (0.127 x 115 mm)	61.4	143.8	214.9	227.3	148.8	288.3
Area (0.127 x 230 mm)	61.8	146.1	215.0	227.1	148.9	289.1
Area (0.127 x 690 mm)	59.0	144.5	210.9	223.1	145.2	289.2
Area (0.254 x 115 mm)	61.5	147.4	213.0	226.1	148.0	285.3
Area (0.254 x 230 mm)	58.2	145.2	218.4	228.7	149.1	287.9
Area (0.254 x 690 mm)	69.0	145.0	215.2	227.5	149.0	291.1
Height (0.127 x 115 mm)	8.90	18.75	25.48	23.85	13.54	19.92
Height (0.127 x 230 mm)	8.96	18.70	25.17	23.55	13.42	19.53
Height (0.127 x 690 mm)	8.19	17.39	23.41	22.18	12.66	18.48
Height (0.254 x 115 mm)	8.48	17.97	23.99	22.48	12.80	18.95
Height (0.254 x 230 mm)	7.60	16.58	22.79	21.52	12.40	18.74
Height (0.254 x 690 mm)	7.11	15.15	20.10	19.54	11.55	18.43
Peak width 1/2 height (0.127 x 115 mm)	0.096	0.111	0.122	0.138	0.160	0.216
Peak width 1/2 height (0.127 x 230 mm)	0.097	0.112	0.122	0.140	0.160	0.222
Peak width 1/2 height (0.127 x 690 mm)	0.101	0.117	0.127	0.145	0.164	0.230
Peak width 1/2 height (0.254 x 115 mm)	0.101	0.117	0.127	0.147	0.169	0.227
Peak width 1/2 height (0.254 x 230 mm)	0.108	0.122	0.132	0.149	0.171	0.227
Peak width 1/2 height (0.254 x 690 mm)	0.143	0.142	0.160	0.173	0.191	0.233
Efficiency (Tan) (0.127 x 115 mm)	997	1324	2251	2832	3363	3216
Efficiency (Tan) (0.127 x 230 mm)	992	1363	2324	2938	3512	3289
Efficiency (Tan) (0.127 x 690 mm)	977	1321	2237	2846	3419	3122
Efficiency (Tan) (0.254 x 115 mm)	927	1305	2236	2901	3464	3260
Efficiency (Tan) (0.254 x 230 mm)	885	1193	2000	2542	3133	3026
Efficiency (Tan) (0.254 x 690 mm)	579	1015	1551	2093	2667	3037
Efficiency (1/2 width) (0.127 x 115 mm)	1050	1446	2374	2988	3591	3432
Efficiency (1/2 width) (0.127 x 230 mm)	1056	1478	2508	3135	3828	3461
Efficiency (1/2 width) (0.127 x 690 mm)	1038	1429	2410	2999	3703	3280
Efficiency (1/2 width) (0.254 x 115 mm)	1006	1410	2431	3086	3725	3417
Efficiency (1/2 width) (0.254 x 230 mm)	912	1288	2164	2753	3337	3195
Efficiency (1/2 width) (0.254 x 690 mm)	603	1079	1612	2211	2837	3288
Tailing Factor (0.127 x 115 mm)	2.729	1.620	1.627	1.529	1.495	1.248
Tailing Factor (0.127 x 230 mm)	2.216	1.637	1.614	1.522	1.488	1.240
Tailing Factor (0.127 x 690 mm)	2.762	1.749	1.703	1.571	1.534	1.340
Tailing Factor (0.254 x 115 mm)	2.709	1.654	1.606	1.497	1.464	1.238
Tailing Factor (0.254 x 230 mm)	2.471	1.765	1.831	1.693	1.634	1.346
Tailing Factor (0.254 x 690 mm)	1.309	1.436	1.442	1.415	1.401	1.233

Table 23. Effect of post column tubing dimensions on peak shape characteristics

HyPURITY C18 50 X 2.1 mm 3µ column
Hydrophilic bases **0.7 ml/min**

Compound	Nicotine	Benzylamine	Procainamide	Terbutaline	Salbutamol	Phenol
Retention Time (mins) (0.127 x 115 mm)	0.398	0.533	0.759	0.950	1.214	1.559
Retention Time (mins) (0.127 x 230 mm)	0.402	0.539	0.764	0.952	1.210	1.586
Retention Time (mins) (0.127 x 690 mm)	0.413	0.551	0.774	0.959	1.216	1.596
Retention Time (mins) (0.254 x 115 mm)	0.410	0.553	0.794	1.014	1.293	1.633
Retention Time (mins) (0.254 x 230 mm)	0.414	0.548	0.771	0.958	1.220	1.565
Retention Time (mins) (0.254 x 690 mm)	0.443	0.578	0.796	0.976	1.228	1.609
Area (0.127 x 115 mm)	18.0	46.5	66.5	69.6	45.4	87.8
Area (0.127 x 230 mm)	18.6	47.3	66.3	69.7	44.9	86.2
Area (0.127 x 690 mm)	18.1	47.1	66.2	69.7	44.7	86.1
Area (0.254 x 115 mm)	18.9	47.1	66.3	69.2	44.8	86.6
Area (0.254 x 230 mm)	18.0	46.8	66.4	70.3	45.6	87.7
Area (0.254 x 690 mm)	17.7	46.3	66.1	69.8	44.9	86.2
Height (0.127 x 115 mm)	5.77	13.39	18.68	18.06	10.66	18.82
Height (0.127 x 230 mm)	5.95	13.56	18.66	18.18	10.68	18.63
Height (0.127 x 690 mm)	5.25	12.19	16.92	16.59	9.86	17.29
Height (0.254 x 115 mm)	5.81	13.24	18.08	17.46	10.21	18.14
Height (0.254 x 230 mm)	5.16	12.03	16.78	16.44	9.80	17.54
Height (0.254 x 690 mm)	4.90	11.64	15.88	15.70	9.45	17.26
Peak width 1/2 height (0.127 x 115 mm)	0.047	0.050	0.053	0.056	0.062	0.068
Peak width 1/2 height (0.127 x 230 mm)	0.048	0.051	0.053	0.056	0.061	0.069
Peak width 1/2 height (0.127 x 690 mm)	0.051	0.055	0.057	0.061	0.067	0.072
Peak width 1/2 height (0.254 x 115 mm)	0.049	0.051	0.053	0.058	0.064	0.069
Peak width 1/2 height (0.254 x 230 mm)	0.052	0.055	0.057	0.061	0.066	0.072
Peak width 1/2 height (0.254 x 690 mm)	0.056	0.058	0.063	0.066	0.070	0.074
Efficiency (Tan) (0.127 x 115 mm)	386	597	1108	1484	1975	2687
Efficiency (Tan) (0.127 x 230 mm)	389	604	1134	1507	1987	2774
Efficiency (Tan) (0.127 x 690 mm)	346	516	968	1275	1770	2423
Efficiency (Tan) (0.254 x 115 mm)	381	620	1154	1598	2115	2843
Efficiency (Tan) (0.254 x 230 mm)	333	515	965	1270	1766	2391
Efficiency (Tan) (0.254 x 690 mm)	336	514	865	1138	1560	2411
Efficiency (1/2 width) (0.127 x 115 mm)	389	630	1147	1578	2146	2910
Efficiency (1/2 width) (0.127 x 230 mm)	396	631	1160	1601	2147	2963
Efficiency (1/2 width) (0.127 x 690 mm)	358	552	1014	1355	1844	2706
Efficiency (1/2 width) (0.254 x 115 mm)	395	642	1227	1707	2230	3072
Efficiency (1/2 width) (0.254 x 230 mm)	353	547	1006	1345	1902	2601
Efficiency (1/2 width) (0.254 x 690 mm)	344	547	892	1213	1705	2589
Tailing Factor (0.127 x 115 mm)	1.228	1.439	1.772	1.360	1.386	1.315
Tailing Factor (0.127 x 230 mm)	1.095	1.446	1.757	1.357	1.406	1.308
Tailing Factor (0.127 x 690 mm)	1.103	1.813	1.683	1.427	1.467	1.374
Tailing Factor (0.254 x 115 mm)	1.187	2.216	2.002	1.373	1.377	1.309
Tailing Factor (0.254 x 230 mm)	1.079	1.799	1.670	1.286	1.506	1.407
Tailing Factor (0.254 x 690 mm)	1.106	1.625	1.493	1.210	1.389	1.305

Table 24. Effect of detector response times on peak shape characteristics

HyPURITY C18 50 X 2.1 mm 3u column

Hydrophilic bases			**0.208 ml/min**			
Compound	**Nicotine**	**Benzylamine**	**Procainamide**	**Terbutaline**	**Salbutamol**	**Phenol**
Retention Time (mins) (0.1 s)	1.368	1.856	2.657	3.405	4.357	5.485
Retention Time (mins) (0.2 s)	1.362	1.846	2.633	3.370	4.311	5.471
Retention Time (mins) (0.5 s)	1.359	1.844	2.630	3.370	4.308	5.471
Retention Time (mins) (1.0 s)	1.359	1.843	2.626	3.363	4.298	5.467
Retention Time (mins) (2 s)	1.358	1.840	2.620	3.354	4.285	5.460
Retention Time (mins) (4 s)	1.356	1.836	2.612	3.342	4.270	5.451
Retention Time (mins) (8 s)	1.351	1.829	2.605	3.332	4.257	5.437
Retention Time (mins) (16 s)	1.343	1.810				
Area (0.1 s)	63.3	137.4	223.5	243.3	146.1	307.6
Area (0.2 s)	63.2	136.9	224.2	243.6	144.2	309.8
Area (0.5 s)	63.8	137.1	224.0	247.4	145.0	307.8
Area (1.0 s)	62.8	137.0	224.6	244.1	144.4	305.1
Area (2 s)	63.0	137.0	225.1	245.0	146.6	309.9
Area (4 s)	63.3	135.2	223.6	242.5	143.6	310.8
Area (8 s)	60.8	130.5	221.0	241.2	145.1	310.8
Area (16 s)	67.9	149.1				
Height (0.1 s)	9.70	17.03	25.96	24.69	12.78	20.60
Height (0.2 s)	9.67	17.06	26.09	24.83	12.82	20.65
Height (0.5 s)	9.65	17.01	26.03	25.15	12.85	20.64
Height (1.0 s)	9.47	16.86	25.89	24.78	12.80	20.59
Height (2 s)	9.03	16.28	25.20	24.22	12.66	20.45
Height (4 s)	7.82	14.52	22.89	22.50	11.95	19.88
Height (8 s)	5.43	10.66	17.45	17.96	10.03	17.87
Height (16 s)	3.33	6.90				
Width 1/2 height (0.1 s)	0.091	0.110	0.120	0.141	0.166	0.221
Width 1/2 height (0.2 s)	0.091	0.109	0.121	0.139	0.163	0.222
Width 1/2 height (0.5 s)	0.092	0.108	0.120	0.140	0.163	0.220
Width 1/2 height (1.0 s)	0.092	0.108	0.120	0.140	0.163	0.220
Width 1/2 height (2 s)	0.097	0.115	0.125	0.142	0.167	0.220
Width 1/2 height (4 s)	0.119	0.131	0.141	0.156	0.176	0.230
Width 1/2 height (8 s)	0.181	0.189	0.196	0.205	0.219	0.258
Width 1/2 height (16 s)	0.323	0.361				
Efficiency (Tan) (0.1 s)	1183	1488	2534	3102	3678	3254
Efficiency (Tan) (0.2 s)	1182	1490	2516	3069	3644	3234
Efficiency (Tan) (0.5 s)	1155	1475	2489	3050	3645	3258
Efficiency (Tan) (1.0 s)	1123	1443	2433	3016	3605	3237
Efficiency (Tan) (2 s)	999	1323	2829	2829	3431	3146
Efficiency (Tan) (4 s)	684	1009	1821	2373	3024	2939
Efficiency (Tan) (8 s)	316	524	971	1425	1994	2296
Efficiency (Tan) (16 s)	83	144				
Efficiency (1/2 width) (0.1 s)	1257	1577	2716	3238	3825	3417
Efficiency (1/2 width) (0.2 s)	1246	1583	2631	3249	3859	3374
Efficiency (1/2 width) (0.5 s)	1218	1605	2661	3210	3854	3426
Efficiency (1/2 width) (1.0 s)	1204	1603	2654	3198	3836	3421
Efficiency (1/2 width) (2 s)	1078	1418	3080	3080	3662	3413
Efficiency (1/2 width) (4 s)	725	1081	1903	2557	3278	3111
Efficiency (1/2 width) (8 s)	308	521	893	1459	2100	2464
Efficiency (1/2 width) (16 s)	96	139				
Tailing Factor (0.1 s)	2.252	1.778	1.755	1.618	1.546	1.267
Tailing Factor (0.2 s)	2.322	1.820	1.759	1.616	1.526	1.285
Tailing Factor (0.5 s)	2.420	1.817	1.778	1.626	1.540	1.297
Tailing Factor (1.0 s)	2.278	1.788	1.746	1.611	1.532	1.292
Tailing Factor (2 s)	2.787	1.724	1.575	1.575	1.518	1.295
Tailing Factor (4 s)	2.075	1.516	1.513	1.462	1.429	1.270
Tailing Factor (8 s)	1.114	1.223	1.796	2.211	1.250	1.220
Tailing Factor (16 s)	0.581	1.018				

Table 25. Effect of detector response times on peak shape characteristics

HyPURITY C18 50 X 2.1 mm 3u column

Hydrophilic bases			**0.7 ml/min**			
Compound	**Nicotine**	**Benzylamine**	**Procainamide**	**Terbutaline**	**Salbutamol**	**Phenol**
Retention Time (mins) (0.1 s)	0.395	0.527	0.749	0.932	1.191	1.536
Retention Time (mins) (0.2 s)	0.395	0.526	0.748	0.930	1.187	1.534
Retention Time (mins) (0.5 s)	0.395	0.526	0.747	0.930	1.187	1.534
Retention Time (mins) (1.0 s)	0.397	0.528	0.750	0.932	1.189	1.536
Retention Time (mins) (2 s)	0.398	0.528	0.748	0.929	1.186	1.534
Retention Time (mins) (4 s)	0.395	0.526	0.746	0.926	1.184	1.530
Retention Time (mins) (8 s)						
Retention Time (mins) (16 s)						
Area (0.1 s)	18.2	41.2	68.3	74.1	44.8	93.2
Area (0.2 s)	18.1	41.2	68.3	74.7	45.1	93.3
Area (0.5 s)	17.8	40.3	67.4	73.0	43.6	93.0
Area (1.0 s)	18.0	41.0	67.9	74.0	44.7	93.3
Area (2 s)	17.5	40.3	67.7	73.9	45.2	94.1
Area (4 s)	18.0	40.8	68.5	74.7	45.7	94.5
Area (8 s)						
Area (16 s)						
Height (0.1 s)	9.82	17.11	26.20	24.15	12.46	22.77
Height (0.2 s)	9.78	17.14	26.25	24.37	12.46	22.87
Height (0.5 s)	9.35	16.59	25.59	23.86	12.26	22.65
Height (1.0 s)	8.13	15.18	23.69	22.61	11.85	22.03
Height (2 s)	5.80	11.69	18.94	18.92	10.32	19.89
Height (4 s)	3.51	7.41	12.40	12.94	7.46	15.04
Height (8 s)						
Height (16 s)						
Width 1/2 height (0.1 s)	0.025	0.031	0.035	0.042	0.049	0.058
Width 1/2 height (0.2 s)	0.024	0.032	0.035	0.041	0.049	0.057
Width 1/2 height (0.5 s)	0.026	0.032	0.036	0.042	0.049	0.057
Width 1/2 height (1.0 s)	0.031	0.036	0.040	0.045	0.052	0.060
Width 1/2 height (2 s)	0.047	0.050	0.052	0.057	0.062	0.068
Width 1/2 height (4 s)	0.066	0.088	0.088	0.091	0.094	0.096
Width 1/2 height (8 s)						
Width 1/2 height (16 s)						
Efficiency (Tan) (0.1 s)	1345	1462	2348	2563	3019	3678
Efficiency (Tan) (0.2 s)	1287	1414	2337	2579	2970	3677
Efficiency (Tan) (0.5 s)	1193	1370	2281	2503	2960	3609
Efficiency (Tan) (1.0 s)	852	1073	1865	2212	2637	3364
Efficiency (Tan) (2 s)	399	590	1071	1402	1860	2621
Efficiency (Tan) (4 s)	126	205	408	577	887	1393
Efficiency (Tan) (8 s)						
Efficiency (Tan) (16 s)						
Efficiency (1/2 width) (0.1 s)	1411	1574	2598	2775	3250	3954
Efficiency (1/2 width) (0.2 s)	1446	1531	2592	2872	3231	3944
Efficiency (1/2 width) (0.5 s)	1293	1477	2410	2759	3229	3945
Efficiency (1/2 width) (1.0 s)	919	1185	1993	2375	2934	3632
Efficiency (1/2 width) (2 s)	396	619	1138	1488	1994	2818
Efficiency (1/2 width) (4 s)	201	198	397	574	876	1399
Efficiency (1/2 width) (8 s)						
Efficiency (1/2 width) (16 s)						
Tailing Factor (0.1 s)	2.158	1.956	1.908	1.697	1.642	1.520
Tailing Factor (0.2 s)	2.122	1.955	1.851	1.706	1.648	1.487
Tailing Factor (0.5 s)	2.878	1.841	1.804	1.659	1.601	1.483
Tailing Factor (1.0 s)	2.201	1.681	1.665	1.574	1.553	1.447
Tailing Factor (2 s)	1.209	1.372	1.684	1.379	1.413	1.369
Tailing Factor (4 s)	0.626	1.101	0.912	1.406	1.164	1.174
Tailing Factor (8 s)						
Tailing Factor (16 s)						

Table 26. Effect of flow rate on efficency, retention time and peak area

HvPURITY C18 50 x 2.1 mm 3u column

Terbutaline sulphate 1.6 µg/ml 18µl injection

	EFFICIENCY (plates/m)			RT (mins)			AREA (mAUs)		
FLOW RATE (ml/min)	40°C	60°C	80°C	40°C	60°C	80°C	40°C	60°C	80°C
0.10	86220	74260	51020	9.159	7.163	4.650	486.7	483.4	473.2
0.15	91620	74580	51380	7.572	4.800	3.158	326.6	324.4	323.7
0.20	90980	74980	50160	5.922	3.642	2.411	246.8	245.2	249.2
0.25	89140	73460	50760	4.916	3.004	1.980	198.0	197.0	200.5
0.30	88680	73340	51060	4.055	2.487	1.646	165.4	164.5	167.4
0.35	84660	71940	50960	3.501	2.123	1.394	142.2	141.2	145.2
0.40	82480	70300	49760	3.024	1.847	1.218	123.5	123.3	126.7
0.45	79980	68960	49080	2.687	1.642	1.070	110.2	109.9	113.2
0.50	76740	67620	48320	2.390	1.462	0.957	99.0	98.9	101.3
0.55	73780	66180	47260	2.172	1.324	0.861	90.1	89.5	92.0
0.60	73160	63960	45020	1.991	1.201	0.784	82.2	81.8	84.8
0.65	70700	62140	43760	1.831	1.105	0.718	75.7	75.7	78.4
0.70	68380	61000	41960	1.698	1.017	0.660	70.7	70.5	73.0
0.75	67600	58060	41620	1.564	0.941	0.614	66.1	65.8	68.7
0.80	66500	58620	39720	1.470	0.882	0.568	62.0	61.9	64.2